Universidad Zaragoza
1542

Tesis Doctoral

Contribución al diseño optimizado de sistemas de posicionamiento Ultra-Wideband e integración en redes y servicios móviles

Autor

Juan Chóliz Muniesa

Director/es

Ángela Hernández Solana
Antonio Valdovinos Bardají

Centro Politécnico Superior.
Departamento de Ingeniería Electrónica y de Comunicaciones

2011

DOCTORADO EN TECNOLOGÍAS DE LA INFORMACIÓN Y COMUNICACIONES EN REDES MÓVILES (TICRM)

Universidad de Zaragoza

Tesis Doctoral

Contribución al diseño optimizado de sistemas de posicionamiento Ultra-Wideband e integración en redes y servicios móviles

Autor: Juan Chóliz Muniesa

Directores: Ángela Hernández Solana

Antonio Valdovinos Bardají

"Creativity is not the finding of a thing, but the making something out of it after it is found"

(James Russell Lowell)

Agradecimientos

A mis directores Ángela y Toni, por su orientación y apoyo continuo durante la realización de esta tesis.

A los miembros del equipo investigador, becarios y proyectistas que en mayor o menor medida han colaborado en las distintas tareas asociadas a los proyectos PULSERS PHASE II y EUWB, contribuyendo con ello al desarrollo de esta tesis.

A los socios de los proyectos PULSERS PHASE II y EUWB, por el conocimiento e ideas aportadas en los distintos temas abordados en esta tesis.

A mi familia y amigos por su apoyo incondicional y sus muestras de cariño.

Abstract

Ultra-wideband (UWB) radio technology has positioned recently as one of the most promising for the deployment of indoor location and tracking systems. High bandwidth of UWB entails a high temporal resolution, which allows estimating the time of arrival of the signal and consequently the distance between two devices with high precision. In the last few years, extensive research has focused on the design of algorithms for distance estimation and for position calculation given the estimated distances. Nevertheless, these studies generally focus on algorithm optimization, omitting practical aspects such as the design of the functional architecture, the procedure for the transmission of the associated information between the different elements involved or the amount of resources associated to the positioning service. On the other hand, although a few UWB-location systems are already commercially available, these systems only use UWB for distance estimation and other technologies, generally wired, are used to communicate the different elements of the system. However, the future trend is the design of UWB systems combining data transmission and location tracking, for instance in the framework of the IEEE 802.15.4 standard, aiming to increase the flexibility of the deployment and to reduce the cost and complexity of the systems. In this scenario it becomes clear that accuracy is not the only criteria in order to evaluate the location system, but also the amount of resources used, as it will impact on the transmission and location tracking capacity of the system.

Within this context, this thesis contributes to the global development of novel UWB-based positioning systems considering all the aspects previously mentioned, including distance estimation, position calculation, system functional architecture, the procedures for the exchange of signaling information and the allocation of resources for these exchanges.

Besides the immediate application of location tracking systems for the deployment of positioning services in various sectors such as industrial, medical or entertainment, 3G/4G networks and particularly systems such as LTE-Advanced or UMTS have the support of positioning services as an advanced objective aiming to improve the services offered to the user and even to improve the resource management of their networks, being these research areas topics of interest nowadays. In this thesis, the potential applications of location awareness for the enhancement of user services and for the improvement of radio resource management are analyzed. However, the integration of UWB with other radio technologies requires that interference-free coexistence is guaranteed. This has been subject of several studies and resulted in a restrictive regulation by the regulatory bodies. However, in some cases such as the collocation of UWB and other radio technology in the same device

additional studies are required. In this thesis is to analyze the regulatory framework of UWB and the coexistence with other radio technologies are analyzed, complementing the existing studies with studies related to the most interesting technologies, with a special focus on UMTS as the technology providing access to location based services.

Resumen

La tecnología Ultra-Wideband (UWB) se está posicionando en los últimos años como una de las más prometedoras de cara al despliegue de sistemas de localización en interiores. Su gran ancho de banda conlleva una alta resolución temporal, lo que permite estimar el tiempo de llegada de una señal y con ello la distancia entre dos dispositivos con una elevada precisión. El diseño de algoritmos para la estimación de distancias y para el cálculo de la posición en base a las distancias estimadas ha centrado un gran esfuerzo investigador en los últimos años. No obstante, en general estos estudios se centran casi exclusivamente en la optimización de los algoritmos, eludiendo aspectos prácticos como el diseño de la arquitectura funcional, el procedimiento de envío de la información asociada entre los distintos elementos del sistema o el consumo de recursos asociado al servicio de posicionamiento. Por otra parte, aunque existen algunos sistemas de localización basados en UWB en el mercado, éstos utilizan UWB únicamente para la estimación de distancias, realizándose la comunicación entre los distintos elementos del sistema mediante otras tecnologías, generalmente cableadas. Sin embargo, la evolución futura tiende hacia el diseño de sistemas UWB que combinan transmisión de datos y localización (por ejemplo, en el marco del estándar IEEE 802.15.4), con el objetivo de ganar flexibilidad en el despliegue y reducir los costes y complejidad de estos sistemas. En este escenario está todavía más claro que la precisión no será el único criterio para evaluar el sistema de localización, sino también la cantidad de recursos utilizados, ya que va a tener un impacto en la capacidad de transmisión y localización del sistema.

En este contexto, esta tesis contribuye al desarrollo global de nuevos sistemas de posicionamiento basados en UWB, incorporando todos los aspectos mencionados anteriormente: desde la estimación de las distancias y posiciones hasta el impacto de la arquitectura funcional del sistema y de los correspondientes procedimientos de intercambio de señalización y mapeado de la misma sobre los recursos disponibles.

Además de la aplicación directa de los sistemas de localización para el despliegue de servicios de posicionamiento en sectores como el industrial, sanitario o de ocio, las redes 3G/4G, y en particular sistemas como LTE-Advanced o UMTS, plantean como objetivos avanzados el soporte extensivo de servicios de posicionamiento, con el propósito de mejorar los servicios ofrecidos a los usuarios, e incluso mejorar la gestión de recursos de la propia red, estando estas áreas de investigación en auge en los últimos años. En esta tesis se analizan las potenciales aplicaciones del conocimiento de la localización en la mejora de los servicios ofrecidos a los usuarios y de la gestión de los recursos radio. Sin embargo, la

integración de UWB con otras tecnologías radio exige garantizar la coexistencia libre de interferencias. Ello ha sido objeto de múltiples estudios y ha resultado en una normativa restrictiva por parte de los organismos reguladores, aunque en algunos casos, como la colocación de UWB y otra tecnología en un mismo dispositivo, es necesario realizar estudios adicionales. En la presente tesis se analiza tanto el marco regulatorio de UWB como la coexistencia con otras tecnologías radio, complementando los estudios existentes en la literatura con estudios propios relativos a las tecnologías que presentan un mayor interés, con especial atención a UMTS como tecnología de acceso a servicios basados en localización.

Table of Contents

List of Figures

List of Tables

Abbreviations

3GPP	3rd Generation Partnership Project
AC	Access Category
ACR	Adaptive Channel Reservation
AD	Analog to Digital
AI	Anchor Initiated
AIC	Active Interference Cancellation
AmI	Ambient Intelligence
ANC	Adaptive Noise cancellation
AOA	Angle of Arrival
APD	Amplitude Probability Distribution
API	Application Programming Interface
AWGN	Additive White Gaussian Noise
B-ACK	Block Acknowledgement
BAN	Body Area Network
BCA	Borrowing Channel Assignment
BER	Bit Error Rate
BFWA	Broadband Fixed Wireless Access
BLER	Block Error Rate
BP	Beacon Period
BPM	Burst Position Modulation
BPPM	Binary Pulse Amplitude Modulation
BPSK	Binary Phase Shift Keying
BS	Base Station
BWA	Broadband Wireless Access
CAP	Contention Access Period
CDMA	Code Division Multiple Access
CEPT	European Conference of Postal and Telecommunications Administrations
CFP	Contention Free period
CQI	Channel Quality Indication
CSMA	Carrier Sense Multiple Access
CSMA-CA	Carrier Sense Multiple Access with Collision Avoidance
CSS	Chirp Spread Spectrum
CTS	Clear To Send
DA	Data Aided

DA	Data Aggregation
DAA	Detect and Avoid
DBPSK	Differential Binary Phase Shift Keying
DC	Distance Contraction
DCA	Dynamic Channel Allocation
DCS1800	Digital Cellular System-1800
DD	Delay Dependent
DFS	Dynamic Frequency Selective
DL	Downlink
DOP	Dilution Of Precision
DRP	Distributed Reservation Protocol
DS	Direct Sequence
DS-SS	Direct Sequence-Spread Spectrum
DT	Dirty Templates
ECC	Electronic Communications Committee
ECMA	European Computers Manufacturers Association
ED	Energy Detection
EDM	Euclidean Distance Matrix
EIRP	Effective Isotropic Radiated Power
EKF	Extended Kalman Filter
EP	Estimated Position
EP-PB	Estimated Position with Periodic Broadcast
FCA	Fixed Channel Allocation
FCC	Federal Communications Commission
FCS	Frame Check Sequence
FDS	Frequency Domain Spreading
FEC	Forward Error Correction
FER	Frame Error Rate
FFI	Fixed Frequency Interleaving
FFR	Fractional Frequency Reuse
FFT	Fast Fourier Transform
FIR	Finite Impulse Response
FWA	Fixed Wireless Access
GA	Gaussian Approximation
GC	Guarded Channel
GIS	Geographic Information System
GoS	Grade of Service

GPRS	General Packet Radio Service
GPS	Global Positioning System
GSM	Global System for Mobile Communications
GTS	Guaranteed Time Slot
GUI	Graphical User Interface
HC	Handover Control
HCA	Hybrid Channel Allocation
HCS	Header Check Sequence
HDMI	High-Definition Multimedia Interface
HDR	High Data Rate
HPCR	Hybrid Predictive Channel Reservation
HS	High Speed
HSPA	High Speed Packet Access
ICI	Inter-Cell Interference
IEEE	Institute of Electrical and Electronics Engineers
IGA	Impulsive Gaussian Approximation
Imm-ACK	Immediate Acknowledgement
IMT-2000	International Mobile Telecommunications–2000
IP	Internet Protocol
IR-UWB	Impulse Radio Ultra-Wideband
ITU-R	International Telecommunications Union - Radiocommunication Sector
JBSF	Jump Back and Search Forward
LBS	Location Based Services
LC	Location Controller
LC	Load control
LDC	Low Duty Cycle
LDR	Low Data Rate
LDR-LT	Low Data Rate with Location Tracking
LLOP	Linear Lines Of Position
LLR	Log-Likelihood Ratio
LMS	Least Mean Square
LOP	Line Of Position
LOS	Line-Of-Sight
LPL	Lower Prediction Limit
LQI	Link Quality Indicator
LR	Low Rate
LS	Least Squares

LT	Location and Tracking
LTE	3GPP Long Term Evolution
MA	Multi-user Access
MAC	Medium Access Control
MAE	Mean Absolute Error
MAS	Medium Access Slot
MB-OFDM	Multi-Band Orthogonal Frequency Division Multiplexing
MDS	MultiDimensional Scaling
MEP	Multiscale Energy Product
MEP-SB	Multiscale Energy Product with Search Back
MES	Maximum energy Signal
MESS	Maximum Energy Sum Selection
MES-SB	Maximum Energy Selection with Search-Back
MF	Matched filtering
MIC	Message Integrity Code
ML	Maximum Likelihood
MP	Multiscale Product
MR	Measurement Report
MRp	Multicast Response
MRq	Multicast Request
MS	Mobile Station
MZ DWT	Mallat-Zhong Discrete Wavelet Transform
NAT	Network Access Translation
NB	Narrow-Band
NDA	Non Data Aided
NDA	Non Data Aggregation
NICTS	New information and Communication Technologies
NL-LS	Non-Linear Least Squares
NLOS	Non Line of Sight
No-ACK	No Acknowledgement
OEM	Original Equipment Manufacturer
OFDM	Orthogonal Frequency Division Multiplexing
OFDMA	Orthogonal Frequency-Division Multiple Access
OLOS	Obstructed Line Of Sight
PAM	Pulse Position Modulation
PAN	Personal Area Network
PAN	Personal Area Network

PB	Periodic Broadcast
PC	Personal Computer
PC	Personal Computer
PCA	Prioritized Contention Access
PCR	Predictive Channel Reservation
PDA	Personal Digital Assistant
PDF	Probability Density Function
PDP	Power Delay Profile
PF	Particle Filter
PHR	PHY Header
PHY	Physical layer
PLCP	Physical Layer Convergence Protocol
PN	Pseudo-Noise
PP	Point-to-Point
PPDU	PLCP Protocol Data Unit
PPM	Pulse Amplitude Modulation
PRF	Pulse Repetition Frequency
PRF	Pulse Repetition Frequency
PRP	Pulse Repetition Period
PSD	Power Spectral Density
PSDU	PHY Service Data Unit
PSK	Phase Shift Keying
PSNR	Peak Signal to Noise Ratio
PU	Position Update
QoS	Quality of Service
RD	Range Difference
RDEV	Ranging-capable Device
RF	Radio-Frequency
RFID	Radio-Frequency Identification
RFRAME	Ranging Frame
RMARKER	Ranging Marker
RRM	Radio Resource Management
RSA	Range-Scaling Algorithm
RSCP	Received Signal Code Power
RSS	Received Signal Strength
RSSI	Received Signal Strength Indication
RTB	Road Topology Based

RTCP	Real-Time Control Protocol
RTLS	Real Time Location System
RTP	Real-Time Transport Protocol
RTS	Request To Send
Rx	Reception
SBS	Serial Backward Search
SFD	Start of Frame Delimiter
SHR	Synchronization header
SI	Spherical Interpolation
SIG	Special Interest Group
SINR	Signal to Interference plus Noise Ratio
SIR	Signal-to-Interference Ratio
SMACOF	Scaling by MAjorizing a COmplicated Function
SMS	Short Message Service
SNR	Signal to Noise Ratio
SR	Stored Reference
SRp	Single Response
SRq	Single Request
SX	Spherical Intersection
TC	Threshold Comparison
TCP	Transmission Control Protocol
TD	Threshold Distance
TDD	Time Division Duplexing
TDMA	Time Division Multiple Access
TDOA	Time Difference of Arrival
TDS	Time Domain Spreading
TFC	Time-Frequency Code
TFI	Time-Frequency Interleaving
TG	Task Group
TH	Time Hopping
TI	Target Initiated
TOA	Time of Arrival
TP	Topology management Period
TPC	Transmit power Control
TR	Transmitted Reference
Tx	Transmission
UDP	User Datagram Protocol

UL	Uplink
UMTS	Universal Mobile Telecommunications System
UPL	Upper prediction Limit
USB	Universal Serial Bus
UWB	Ultra-Wideband
VGA	Video Graphics Array
VHDR	Very High Data Rate
WAN	Wide Area Network
WCDMA	Wideband Code-Division Multiple-Access
WiMAX	Worldwide Interoperability for Microwave Access
WLAN	Wireless Local Area Network
WLS	Weighted Least Squares
W-MESS	Weighted Maximum Energy Sum Selection
W-MP	Weighted Multiscale Product
WPAN	Wireless Personal Area Network
WSN	Wireless Sensor Network
WUSB	Wireless Universal Serial Bus

Chapter 1

Introduction

1.1 Introduction

Location-awareness is rapidly becoming an essential feature of many commercial, public service, and military wireless networks. Whereas in outdoor environments GPS is widely extended in applications such as vehicle navigation, fleet management or emergency calls localization, the potential application of location-awareness in indoor environments is not yet being exploited due to the inability of GPS system to operate indoors. Some examples of possible applications of location-awareness in indoor environments include locating medical equipment and personnel in a hospital, monitoring the assembly line in a factory, tracking the stocks in a warehouse or developing intelligent audio guides that select narration according to the position of the visitor in a museum. Shopping malls, train stations, airports, congress and exhibition centers and sports stadiums are some interesting scenarios for the deployment of indoor location & tracking systems.

There are multiple alternatives for the development of indoor location & tracking systems, including ultrasound, computer vision, optical, satellite and radio systems. Focusing on radio systems, coarse location information can be obtained from cellular networks (GSM, UMTS, etc.) but, especially in indoor environments, its accuracy is unsuitable for most of applications. Several works can be found in the literature proposing the use of widely extended short and medium range technologies such as WiFi, Bluetooth, ZigBee or RFID that, despite not being specifically design for that purpose, may provide location information with a suitable accuracy level for many applications and a relatively low complexity.

Within this group of short range radio systems, Ultra-Wideband (UWB) stands out as one of the most promising technologies for the development of indoor location & tracking systems. UWB combines remarkable features concerning size and power consumption, providing high accuracy on distance estimation and allowing simultaneous location and data

transmission with high data rates. Extensive research has focused on the design of distance estimation and position calculation algorithms in the last few years. Nevertheless, in general these studies focus on the algorithm optimization in a simple scenario with a single terminal and a few previously defined reference nodes. Practical aspects such as the design of the functional architecture, the procedure for the transmission of the associated information between the different elements of the system, and the need of tracking multiple terminals simultaneously in various application scenarios, are generally omitted. These aspects would lead to consider the amount of resources associated to the global location service as a quality parameter and a variable and dynamic scenario of mobile terminals and reference nodes for positioning.

On the other hand, although a few UWB-based location & tracking systems can already be found in the market, these systems only use UWB for distance estimation, while the communication between the different elements involved in the positioning systems is done using other technologies, generally wired. Nevertheless, the future trend is the design of UWB systems combining location and data transmission (for example in the framework of IEEE 802.15.4 standard) with the goal of increasing flexibility and reducing the cost and complexity of the system deployment. In this scenario, it becomes clear that accuracy is not the only evaluation criteria of location & tracking systems, but also the amount of resources associated to the location service, as it impacts not only on the location capacity of the system but also on the data transmission capacity.

Another important characteristic of UWB systems is the distribution of the transmitted energy over a broad frequency range, which results in a very low power spectral density. This allows radio spectrum reutilization, producing a low interference level on existing narrowband services. Nevertheless, the operation of UWB systems in frequency bands allocated to licensed services requires guaranteeing that these services are not disturbed in any way by UWB devices in their proximity. Consequently, regulatory bodies have defined restrictive limits to the transmission power of UWB devices, thus limiting their range and as a result their potential applications.

Besides the direct application of UWB for the deployment of indoor location & tracking services in the industrial, health or entertainment sectors, the integration of UWB with cellular access technologies would extend the scope of UWB services and allow the development of multiple and novel applications. 3G/4G networks and particularly systems such as UMTS and LTE-Advance consider as an advanced objective the extensive support of positioning services, with the purpose of enhancing the services offered to users and even improving the network resource management, areas. In this context, 4G networks consider the flexible support of positioning services whether based on the own cellular network and/or

on external positioning systems (satellite systems or systems based on medium/short range radio technologies). The support of UWB-based positioning can be included within the latest group in those scenarios where a previous UWB deployment exists.

1.2 Objectives

This thesis aims to analyze the feasibility of the deployment of combined communication and indoor location systems based on Ultra-Wideband technology, as well as the potential applications of location-awareness in addition to the inherent positioning service. A previous requirement for UWB technology deployment, and particularly its integration with existing radio technologies in a single device, is guaranteeing harmless coexistence between them. The first objective of this thesis is consequently to analyze the regulatory framework and the coexistence of UWB with other radio technologies, complementing the studies that can be found in the literature with new studies related to the most interesting technologies, focusing on UMTS as the technology providing access to location based services.

The main objective of this thesis is to analyze, design and evaluate a combined communication and indoor location system based on Ultra-Wideband technology. This includes the analysis of different techniques for the estimation of the time of arrival of a pulsed signal and consequently the distance between two nodes, as well as different algorithms for position calculation based on the estimated distances to multiple reference nodes, their evaluation on different conditions and the proposal of improvements to the techniques that can be found in the literature. Furthermore, a system level analysis will be carried out including aspects such as system architecture, distribution of the information related to the location function and latency of the position update process. These aspects are not usually considered on the existing studies, but have a great impact on the capacity of systems combining data transmission and location.

Last but not least, a final objective of this thesis is to analyze the potential applications of location-awareness for mobile users in indoor environments, in addition to the positioning service itself. Specifically, these applications can be grouped into user-oriented applications, for instance location based services development, and network-oriented applications, focusing in this study on the enhancement of radio resource management through location-awareness.

1.3 Structure

This thesis is structured as follows:

In Chapter 2, an introduction to Ultra-Wideband radio technology is provided. The fundamentals of UWB and its main applications in very high data rate systems and low data rate with location and tracking systems are explained, with a special focus on Impulse Radio Ultra-Wideband systems and their application for indoor positioning. An overview of the current regulatory framework in different regions is given, and the most important standards related to Ultra-Wideband radio technology, namely WiMedia and IEEE 802.15.4a are described.

Chapter 3 provides a review on the state-of-art of the different topics addressed in this thesis. First, the coexistence of Ultra-Wideband radio technology with other radio services is addressed for both Impulse Radio and Multiband-OFDM systems, with a special focus on mitigation techniques such as Low Duty Cycle and Detect and Avoid. Then an overview on location and tracking is given, covering receiver architectures and techniques for distance estimation, location and tracking algorithms for position calculation and other system-level issues.

Chapter 4 deals with the coexistence and interoperability of Ultra-Wideband and UMTS. A UWB/UMTS interoperability platform is proposed in order to extend the scope of UWB applications. On this platform, the coexistence between UWB and UMTS is evaluated. Finally, cooperative mitigation techniques are proposed as a solution to guarantee harmless coexistence when UWB and other radio services are collocated in the same device.

In Chapter 5, location and tracking techniques and algorithms are assessed. Concerning distance estimation, different receiver architectures and Time of Arrival estimation algorithms proposed in the literature are evaluated through simulations. Then, various location and tracking algorithms are evaluated on different scenarios using a realistic Ultra-Wideband ranging model. Finally, the enhancement of location and tracking algorithms through the use of geographic information is proposed and evaluated.

In Chapter 6, a combined data communication and location tracking system is proposed based on IEEE 802.15.4a UWB. The system is evaluated not only in terms of accuracy, but also on the amount of resources used for the location tracking functionality, as it determines the capacity of the system. In order to optimize the use of resources, different functional architectures and strategies for the acquisition and distribution of the location information are

proposed and evaluated. Furthermore, the impact of the MAC layer on location accuracy and system capacity is also assessed.

Chapter 7 deals with the application of location-awareness to improve the performance of radio access networks and enhance user experience. Focusing on the users, location based services leverage a user's physical location to provide enhanced services and experiences. From the network point of view, location information can be used to design and develop more efficient radio resource management strategies in order to increase system capacity.

In Chapter 8 the main conclusions are summarized, and future lines of work are identified.

Finally, Annex I provides further mathematical background on the location and tracking algorithms that have been evaluated in Chapter 5.

Chapter 2

Ultra-Wideband

2.1 Ultra-Wideband

Ultra-wideband radio technology is not a completely new topic; in the past, it has been alternatively referred to as baseband, carrier-free or impulse radio. Impulse Radio Ultra-Wideband (IR-UWB) was already used for military radar applications 50 years ago. However, it has gained strong interest recently as one of the most promising short-medium range wireless technologies, thanks to its low power consumption, low complexity, high data rates and accurate distance estimation.

Although UWB has been traditionally associated with pulse-based systems, but FCC (Federal Communications Commission) and ITU-R (International Telecommunications Union – Radiocommunication Sector) now define UWB as any transmission for which emitted signal bandwidth exceeds the lesser of 500 MHz or 20% of the center frequency, regardless of the modulation used. Consequently, systems based on the aggregation of narrow band carriers or spread spectrum systems can be also considered UWB provided that they meet the definition.

The use of unlicensed generic UWB devices in the frequency band between 3.1 GHz and 10.6 GHz was allowed by the FCC in 2002 [FCC, 2002]. In March 2006, a decision on the conditions for devices using UWB technology was adopted by the ECC (Electronic Communications Committee) [ECC, 2006a].

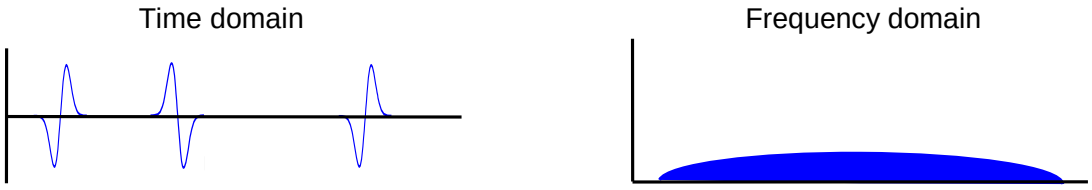

Figure 2.1. IR-UWB signal in time and frequency domain

As a result of the large bandwidth of the UWB signal, the transmitted energy is distributed over a broad frequency range, resulting in very low power spectral density. Consequently, the interference produced over narrowband systems is very low, thus allowing radio spectrum reutilization. However, the operation of UWB in licensed bands requires guaranteeing harmless coexistence between UWB and the other technologies sharing the radio spectrum. In order to guarantee that actual and future radio services are not interfered by UWB, regulatory bodies have proposed restrictive spectrum masks that limit the emitted power spectral density of UWB devices.

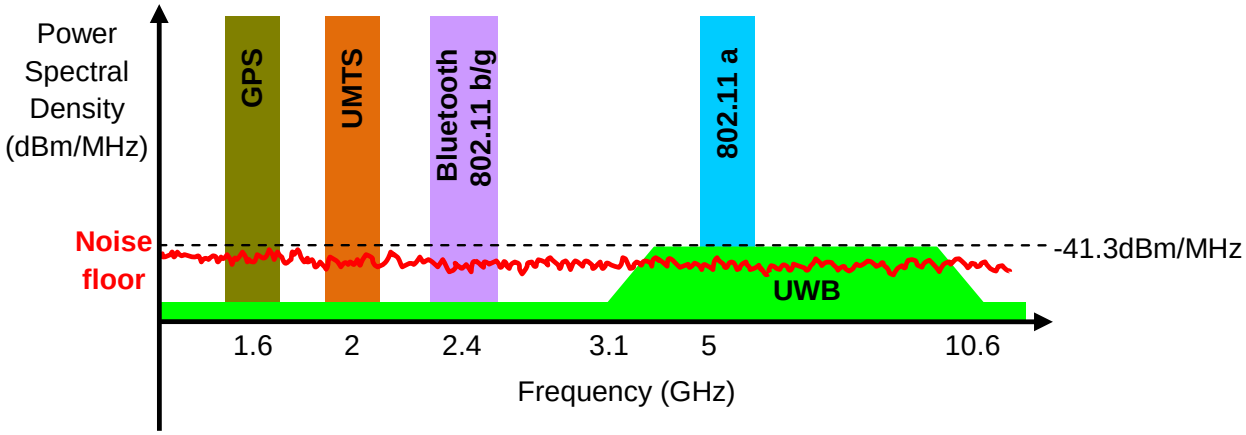

Figure 2.2. Radio spectrum reutilization

Some of the benefits of UWB technology are:

- High capacity
- High immunity to narrow band interference
- High immunity to multipath propagation and frequency selective fading
- In case of pulse-based systems, high precision in time of arrival estimation, low complexity and low cost

UWB applications are diverse, whether in scenarios demanding a very high data rate (HDR/VHDR: High/Very High Data Rate) or in scenarios requiring low power consumption combined with high location accuracy (LDR/LDR-LT: Low Data Rate with Location Tracking) [Porcino, 2003].

2.1.1 VHDR systems

VHDR UWB systems were studied within the Institute of Electrical and Electronics Engineers (IEEE) 802.15.3a group. Two proposals, using either a direct sequence pulse based (DS-UWB) modulation or frequency-hopped orthogonal frequency division multiplexing (OFDM), resulted of the work of this group. The group was finally dissolved without resulting in a standard, although the OFDM-based proposal was adopted by the WiMedia Alliance and is the only broadly supported system. European Computers Manufacturers Association (ECMA) standard ECMA-368 specifies UWB physical layer (PHY) and medium access control layer (MAC) for a high-speed short range wireless network, utilizing all or part of the spectrum between 3.1-10.6 GHz [ECMA, 2005]. It supports data rates of up to 480 Mb/s at 2 m. distance, although further enhancements of the data rates and ranges are planned.

VHDR systems are interesting for outdoor peer-to-peer networking in multimedia and gaming applications, particularly for high definition video transmission, and in order to replace wired technologies (Ethernet, USB, FireWire) for short range communications providing data rates over 100 Mbps in home and office environments. For instance, WiMedia UWB proposal has been adopted by the USB Implementers Forum as the physical and MAC layers of the Certified Wireless USB (WUSB) standard [USB IF, 2005]. A wide catalogue of WUSB products is already available in the market, including adapters, hubs and hard-drives from several manufactures such as Alereon, Staccato, Realtek and Wisair, and vendors such as Belkin, D-Link, Olidata or IOGEAR. Dell, Fujitsu and Lenovo already integrate WUSB technology in some of their notebooks. A particular application of WUSB is the wireless transmission of audio and high definition video from a laptop/PC to a display/TV as a replacement of VGA and HDMI cables. Alereon, Wisair, Cables-To-Go, Cables Unlimited, Olidata or Veebeam are some of the vendors commercializing this kind of solution. WiMedia UWB proposal was also considered by the Bluetooth Special Interest Group (Bluetooth SIG) for High Speed (HS) support in Bluetooth v3.0 + HS along with IEEE 802.11, but only 802.11 was adopted in the final specification.

2.1.2 LDR-LT systems

Concerning LDR-LT system, they are generally based on Impulse Radio modulations and provide lower transmission rates, between 1 and 10 Mbps, with a range in the order of tens of meters. IR-UWB signal consist of a burst of very short duration pulses sent at a certain pulse rate. The information can be imparted on UWB signals by encoding the phase

of the pulse (Phase Shift Keying modulation, PSK), the amplitude of the pulse (Pulse Amplitude Modulation, PAM), and/or the position of the pulse (Pulse Position Modulation, PPM). Due to simplicity of pulse-based modulations, LDR-LT UWB devices have low complexity, low cost and low power consumption. They also provide a very high resolution in the estimation of time of arrival and consequently of the distance between two nodes, so they are very well suited to location and tracking applications.

Consequently, LDR-LT UWB is interesting for systems with low communication needs combined with accurate location and tracking, such as intelligent wireless networks for home automation applications, wireless BAN (Body Area Network) sensor networks for medical applications, positioning and identification networks for logistic and industrial applications, wireless outdoor sensor and surveillance networks for environmental protection and radar and imaging applications.

In 2004, the IEEE established the 802.15.4a task group with the goal of defining an alternative physical layer concept based on UWB radio technology in order to provide the IEEE 802.15.4 standard [IEEE, 2006], which focuses on low-cost, low-speed Wireless Personal Area Networks (WPAN) with little to no underlying infrastructure, with extended range and location capabilities. These specification tasks were concluded with the IEEE 802.15.4a standard, approved in March 2007, which includes Direct Sequence UWB as one of the additional physical layers [IEEE, 2007]. UWB is also being considered as a potential physical layer for active RFID (Radio-Frequency Identification) systems within the IEEE 802.15.4f group.

Unlike for VHDR UWB systems, where companies involved in WiMedia Alliance have pushed the standardization and development of applications such as WUSB, there are very few LDR-LT UWB products available in the market. First IEEE 802.15.4a compliant chipsets are available since Q1 2010, although chipset manufacturers (DecaWave, Time Domain) are still looking for strategic OEM (Original Equipment Manufacturer) agreements with potential industrial partners aiming to develop products based on these chipsets, so 802.15.4a-based commercial products are not foreseen to hit the market in a short term. However, some UWB-based Real Time Location Systems (RTLS) are already available in the market (Time Domain PLUS, Zebra – Multispectral Solutions Shappire Dart, Ubisense), although they are proprietary solutions not compatible with 802.15.4a.

2.2 IR-UWB Location Systems

2.2.1 Indoor positioning systems

There are multiple alternatives for the development of location & tracking systems with different levels of accuracy and complexity, including ultrasound, computer vision, optical, satellite and radio systems. Whereas in outdoor environments GPS is widely extended, in indoor and mixed environments, there is no prevailing technology. Figure 2.3 shows a comparative of different solutions according to their precision and the level of market introduction.

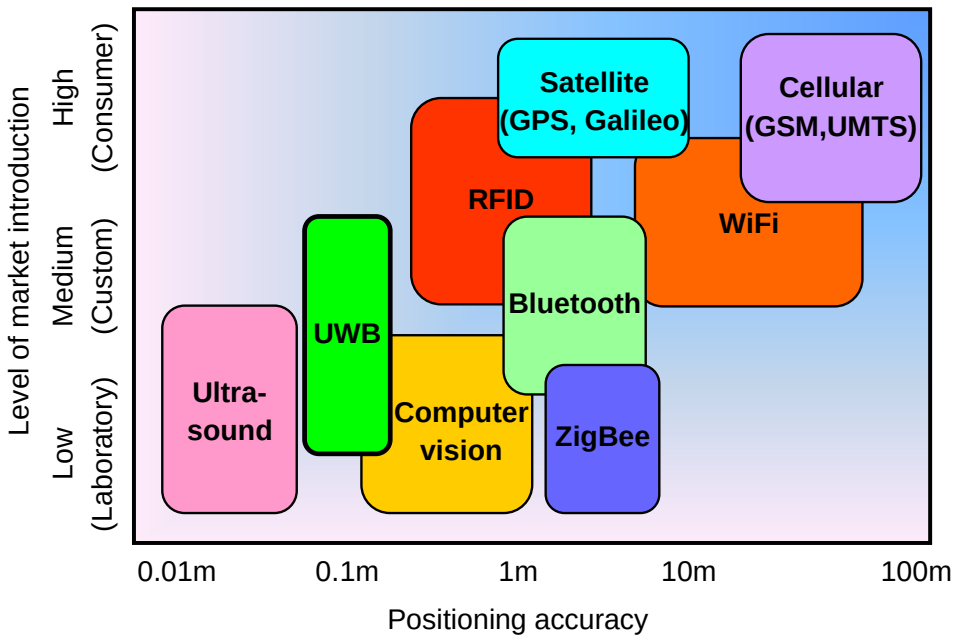

Figure 2.3. Comparative of positioning solutions (accuracy vs market introduction)

Ultrasound based systems provided the highest precision, but their range is very limited. Satellite navigation systems such as GPS and Galileo provide accuracy in the order of a few meters and are widely extended for outdoor applications, but their performance is severely degraded or completely disabled in indoor environments. Computer vision requires line-of-sight between the camera and the target and complex real-time image processing.

Focusing on radio systems, they are usually based on the estimation of the distance between the element to be located and some fixed reference nodes. Distance estimation can be based on the measurement of different parameters such as Received Signal Strength

Indication (RSSI) and Time of Arrival (TOA) of reference signals exchanged between the element to be located and the reference nodes. Also the relative angles between the element to be located and the reference nodes can be estimated based on the measurement of the Angle of Arrival (AOA) of the incident signal. Subsequently, several location & tracking algorithms can be used to combine the estimated angles or distances in order to compute the position of the node.

Positioning accuracy is highly dependent on the signal parameters and especially on the wireless technology used, since it determines the quality of the estimation of those parameters. In general RSSI estimation is not very suitable for indoor location, as RSSI is very sensitive to multipath propagation and non-line-of-sight (NLOS) conditions and the accuracy of the estimated distance is usually within a few meters [Bahl, 2000], [Kong, 2009]. On the other hand, TOA is less sensitive to multipath propagation and its resolution is inversely proportional to the signal bandwidth.

Concerning the wireless technology, coarse location information can be obtained from cellular networks (GSM, UMTS) but, especially in indoor environments, their accuracy is unsuitable for most of applications. Several works can be found in the literature proposing the use of widely extended short and medium range technologies such as WiFi, Bluetooth, ZigBee or RFID that, despite not being specifically design for that purpose, may provide location information with a suitable accuracy level for many applications and a relatively low complexity [Liu, 2007], [Gu, 2009].

Within this group of short-range technologies, UWB stands out as the most promising technology for indoor positioning systems as it combines remarkable features concerning size and power consumption, providing high accuracy on distance estimation and allowing simultaneous location and data transmission [Yang, 2004]. IR-UWB communication systems are based on the transmission of very short duration pulses, which originates very high bandwidth signals. The short duration of the pulses, in the order of a nanosecond, allows a high level of accuracy in TOA estimation and a centimeter-level ranging resolution [Gezici, 2005b]. For example, a pulse duration of 1 ns, which entails a bandwidth of 1 GHz, provides a TOA resolution of 30 cm.

The main advantages of UWB over other radio technologies for indoor positioning are:

- Unmatched resolution in TOA and distance estimation
- Good performance in indoor environments as, due to the short duration of the pulses, it is possible to differentiate the incoming pulses corresponding to the different multipath components.

- Low complexity and low power consumption, which are essential in order to design battery-powered sensors and to integrate them into handheld devices.
- High immunity to interference thanks to the high bandwidth, whereas WiFi, Bluetooth or ZigBee operate in the crowded 2.4 GHz band

In contrast, short range and limited data rate are the main drawbacks of IR-UWB systems.

2.2.2 Fundamentals of IR-UWB location systems

IR-UWB communication systems are based on transmission of very short duration pulses periodically repeated with a given Pulse Repetition Frequency, PRF. The base of the high level of accuracy in TOA estimation resides in this aspect. The inverse of PRF defines the frame duration T_f. As a pulse should be received within the frame duration in order to avoid interframe interference, frame duration limits maximum range to the distance that entails a delay equal to the frame duration.

The UWB signal is generated from a data sequence and the information is associated to different characteristics of the pulse, such as amplitude (Pulse Amplitude Modulation, PAM), phase (Phase Shift Keying, PSK) or pulse position (Pulse Position Modulation, PPM). Typically BPSK (Binary Phase Shift Keying) or BPPM (Binary PPM) are used. Each symbol is coded with N_s pulses, therefore symbol duration T_s and data rate R_b are defined. Typical values for LT applications lay between hundreds of Kbps and a few Mbps.

One of the advantages of UWB is the possibility to perform location and communication simultaneously. Anyway, the use of a training sequence for location is recommended, as knowledge of the transmitted signal is needed on correlation-based receivers and may be helpful to avoid TOA estimation errors when using PPM modulation. A key parameter concerning location accuracy is the number of pulses, K, used in TOA estimation. A higher number of pulses reduces the effect of noise, but increases the duration of location process, which limits the location update rate. Moreover, if a training sequence is used, a higher number of pulses increases the amount of time used on location, thus decreasing the amount of time available for communication and reducing data rate.

There are multiple options for the pulse shape, but Gaussian pulse and its derivates, Gaussian monocycle and Gaussian doublet, are widely used as they present minimum time-bandwidth product and are easy to generate. Pulse duration typically is in the range between 0.2 and 1.5 ns. This results in an uncertainty margin of 6 cm to 45 cm.

Aiming to allow Multi-user Access (MA) and to avoid collisions between the different transmissions, a Time Hopping (TH) code can be used. Moreover, the use of TH codes randomizes the transmitted signal, removing its periodicity and smoothing the shape of the transmitted signal spectrum. Each frame is divided into a number of slots or chips of T_c duration, which can be obtained from the frame duration and the TH sequence length. In order to avoid interframe interference when using TH codes, a guard interval may be defined between consecutive frames and therefore PRF and data rate is reduced.

Finally, the UWB signal is modulated with a given carrier frequency, although this does not have significant influence on TOA estimation. Another important parameter concerning TOA estimation is the sampling frequency of the receiver, as it defines the time granularity and therefore maximum achievable accuracy. Figure 2.4 illustrates in a simplified manner the main parameters of the UWB signal and the effect of multipath propagation for a BPPM modulation and the TH code sequence {1,2,2,1}.

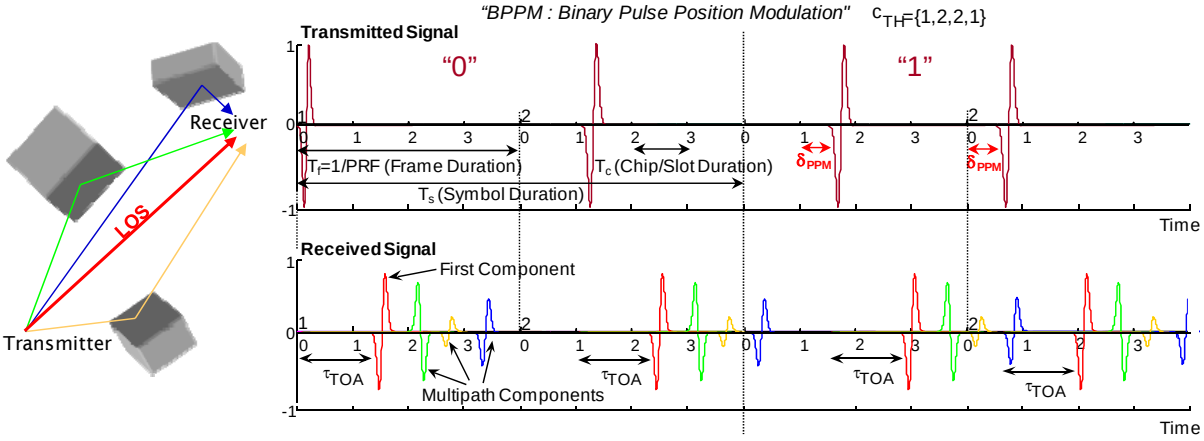

Figure 2.4. IR-UWB transmission parameters.

On the other hand, it must be taken into account that location implies a set of transmissions between the object to be located and the reference nodes whose positions are known. Three procedures are defined:

- One way ranging: The object to be located transmits to the reference nodes, which measure the time of arrival and estimate the distance. It requires very accurate synchronization or a common clock for all the devices. If TDOA (Time Difference Of Arrival) based technique is used, which measures the difference of the delay between two reference nodes, the common clock is just required for the reference nodes, thus eliminating the synchronization problem between transmitter and receiver.

- Two way ranging: The reference nodes query the object to be located, which answers subsequently after a predefined time. The reference nodes measure the time of arrival of the response and can estimate the transmission delay and the distance between the nodes. Synchronization between the involved devices is not required.

-Three way ranging: Similar to the two way ranging scheme, but in this case two responses are sent in order to compensate the clock drift, thus increasing accuracy.

2.3 Regulation and Standardization

2.3.1 Regulatory framework

The introduction of a new radio technology, especially when it is a wide band technology, has to take into account the existing regulatory frameworks in the different regions of the world. The existing traditional radio services have occupied the radio frequency resources since a relative long time. The national authorities (ministries, governments) control these physically limited radio spectrum resources to establish a harmonized access and usage.

As it was previously stated, transmitted energy of the UWB signal is distributed over a broad frequency range, which results in a very low power spectral density that allows radio spectrum reutilization. However, UWB operation in licensed bands requires that harmless coexistence between UWB and the other radio services sharing the spectrum is assured. In order to guarantee that actual and future radio services are not interfered by UWB, regulatory bodies have proposed restrictive spectrum masks that limit the maximum e.i.r.p. (Effective Isotropic Radiated Power) emitted by UWB devices, as shown in Figure 2.5.

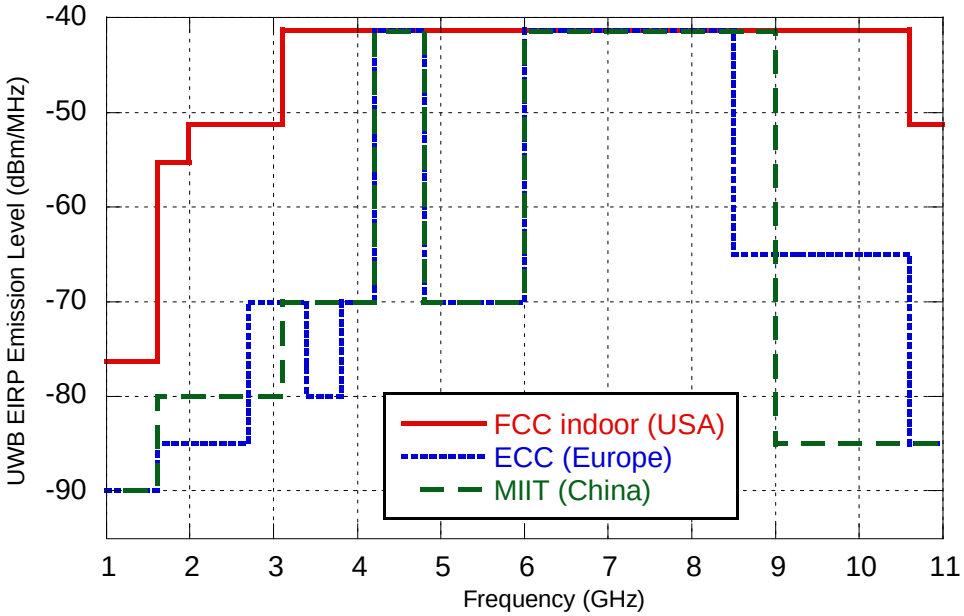

Figure 2.5. UWB spectrum mask in USA, Europe and China

2.3.1.1 Europe

The UWB radio regulatory process in Europe is mainly driven, under respective mandates issued to them by the European Commission, by Task Group 3 (TG3) of the Electronic Communications Committee (ECC) within the European Conference of Postal and Telecommunications Administrations (CEPT).

Decision ECC/DEC/(06)04 on the harmonized conditions for devices using UWB technology in bands below 10.6 GHz was adopted by the ECC in March 2006 [ECC, 2006a] and amended in July 2007 [ECC, 2007]. This ECC Decision is the baseline decision and provides a picture of the European spectrum mask for generic UWB devices without the requirement for additional mitigation, as shown in Table 2.1. A phased approach was applied to frequency band 4.2-4.8 GHz. Such a phased approach means that the first generation of UWB devices operating in the 4.2-4.8 GHz frequency band with a maximum mean e.i.r.p. spectral density of –41.3 dBm/MHz without additional mitigation is introduced earlier in Europe, and after a cut-off date (December 31, 2010) it will gradually be replaced with the second generation of UWB devices implementing a mandatory requirement for additional mitigation. This decision refers to UWB indoor and handheld devices and some categories of outdoor usage (road and rail vehicles, aviation and fixed outdoor installations) are explicitly excluded from the scope of this regulation as they could present a significant risk of interference to radio services deployed outdoor.

Table 2.1. European Power Spectral Density restrictions for UWB devices

Frequency band	Power spectral density (e.i.r.p.)
< 1.6 GHz	–90 dBm/MHz
1.6 - 2.7 GHz	-85 dBm/MHz
2.7 - 3.4 GHz	-70 dBm/MHz
3.4 - 3.8 GHz	-80 dBm/MHz
3.8 - 4.2 GHz	–70 dBm/MHz
4.2 - 4.8 GHz	–41.3 dBm/MHz (until December 31st, 2010) –70 dBm/MHz (beyond December 31st, 2010)
4.8 - 6 GHz	–70 dBm/MHz
6 - 8.5 GHz	–41.3 dBm/MHz
8.5 - 10.6 GHz	–65 dBm/MHz
> 10.6 GHz	–85 dBm/MHz

On the other hand, decision ECC/DEC/(06)12 on the harmonized conditions for devices using Ultra-Wideband technology with Low Duty Cycle (LDC) in the frequency band 3.4-4.8 GHz was adopted by the ECC in December 2006 [ECC, 2006b] and amended in October 2008 [ECC 2008a]. This decision defines conditions of use applicable to UWB technology with Low Duty Cycle and studies relating to further mitigation techniques, e.g. Detect and Avoid (DAA) in frequency band 3.4-4.8 GHz.

2.3.1.2 USA

In USA the Federal Communications Commission approved the rules allowing the use of UWB in 2002 [FCC, 2002]. Unlicensed use of generic UWB devices is authorized between 3.1 GHz and 10.6 GHz with a restriction on maximum mean e.i.r.p. spectral density of -41.3 dBm/MHz.

2.3.1.3 China

China's Ministry of Information Industry Technology approved spectrum use for UWB in 2009 [Xiaochen, 2008]. The UWB in-band transmission is restricted to the frequency range of 4.2-4.8 GHz and 6.0-9.0 GHz. UWB devices operating in the 4.2-4.8 GHz range are restricted to be used indoor, with a maximum mean e.i.r.p. spectral density of -41.3

dBm/MHz until December 31, 2010. After that, the UWB devices shall adopt the Interference Relief Technology, such as DAA. UWB devices operating in the 6.0-9.0 GHz range can be used both indoor and outdoor with a maximum mean e.i.r.p. spectral density of -41.3 dBm/MHz.

2.3.1.4 Japan

Japan's UWB emission mask was established on Dec. 12th, 2006 by the Ministry of Internal Affairs and Communications [Xiaochen, 2008]. Compared to FCC rules, Japan's regulation includes the following changes:

- The band 3.1-3.4 GHz is restricted.
- UWB devices operating in the 3.4-4.2 GHz band should incorporate interference mitigation techniques (DAA), as this band is licensed for satellite communication operators.
- The band 4.2-4.8 GHz is nationally reserved for the future 4G use, and requires DAA. Without DAA, the emission power is limited to -70 dBm/MHz or less. DAA is waived until December 31, 2008.
- The band 6.0-7.25 GHz is restricted

2.3.1.5 Korea

UWB regulation in the Republic of Korea was established by the Ministry of Information and Communication in July 2006 [Xiaochen, 2008]. Considering the importance of harmful interference avoidance to IMT-Advanced system and broadcasting relay system, Korea requires use of Detect and Avoid technology for the UWB devices operating in the 3.1-4.2 GHz band from April 2007, and for those operating in the 4.2-4.8 MHz band from July 2010. Without DAA, the emission power in the 3.1-4.8 GHz band is limited to -70 dBm/MHz. On the other hand, the 6.0-7.2 GHz band is protected for the licensed services.

2.3.2 WiMedia

The WiMedia Alliance is an industry association that promotes the adoption of High Data Rate UWB for wireless Personal Area Networks (PAN) and enables regulation, standardization and multi-vendor interoperability. ECMA-368 Standard [ECMA, 2005] specifies the WiMedia UWB physical layer and Medium Access Control sublayer for a high-speed short range wireless network, utilizing all or part of the spectrum between 3.1-10.6 GHz and supporting data rates of up to 480 Mbps.

WiMedia channelization scheme is based on the definition of band groups and the definition of Time-Frequency Codes (TFCs). The UWB spectrum is divided into 14 bands, each with a bandwidth of 528 MHz. As shown in Figure 2.6, five band groups are defined, consisting of four band groups of three bands each and one band group of two bands. The band allocation is summarized in Table 2.2.

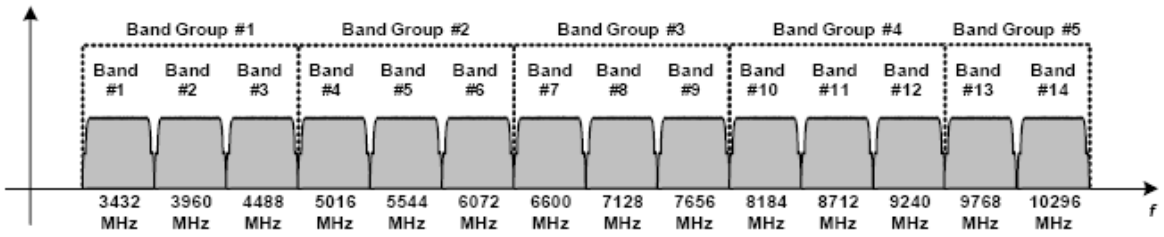

Figure 2.6. Diagram of the band group allocation

Table 2.2. Band group allocation

Band Group	Band_ID	Lower Frequency (MHz)	Centre Frequency (MHz)	Upper Frequency (MHz)
1	1	3168	3432	3696
	2	3696	3960	4224
	3	4224	4488	4752
2	4	4752	5016	5280
	5	5280	5544	5808
	6	5808	6072	6336
3	7	6336	6600	6864
	8	6864	7128	7392
	9	7392	7656	7920
4	10	7920	8184	8448
	11	8448	8712	8976
	12	8976	9240	9504
5	13	9504	9768	10032
	14	10032	10296	10560

Unique logical channels are defined by using a time-frequency code. The ECMA-368 standard specifies two types of time-frequency codes: one where the coded information is interleaved over three bands, referred to as Time-Frequency Interleaving (TFI); and, one where the coded information is transmitted on a single band, referred to as Fixed Frequency

Interleaving (FFI). Within each of the first four band groups, four time-frequency codes using TFI and three time-frequency codes using FFI are defined; thereby, providing support for up to seven channels per band. For the fifth band group, two time-frequency codes using FFI are defined. Therefore, 30 channels are specified in total. The TFCs for band group 1 are defined in Table 2.3 as a function of BAND_ID values. Similarly the TFCs for band groups 2, 3, 4, and 5 can be defined. For band group 5, only TFC 5 and 6 shall be defined.

Table 2.3. Time-Frequency Codes for Band Group 1

TFC Number	**Band_ID for TFC**					
1	1	2	3	1	2	3
2	1	3	2	1	3	2
3	1	1	2	2	3	3
4	1	1	3	3	2	2
5	1	1	1	1	1	1
6	2	2	2	2	2	2
7	3	3	3	3	3	3

The WiMedia Standard specifies a Multi-Band Orthogonal Frequency Division Modulation (MB-OFDM) scheme to transmit information. A total of 110 subcarriers (100 data carriers and 10 guard carriers) are used per band to transmit the information. In addition, 12 pilot subcarriers allow for coherent detection. All OFDM symbols are the same length and have an effective raw data rate of 640Mbps. Data is coded across the carriers of the OFDM symbol and also across blocks of 6 consecutive symbols. Consequently, symbols are always transmitted in blocks of 6.

As all symbols carry data at the same raw rate (640Mbps), the payload data rates are obtained by redundantly coding the data over the OFDM symbols. Coding of the inputs to the IFFT provides a range of coded data rates (53.3, 80, 106.7, 160, 200, 320, 400 and 480 Mbps). Frequency-domain spreading (FDS), time-domain spreading (TDS), and forward error correction (FEC) coding are used to vary the data rates. The FEC used is a convolutional code with coding rates of 1/3, 1/2, 5/8 and 3/4. Higher redundancy improves the probability of successfully decoding the data at the cost of a lower data rate. Table 2.4 shows the modulation, coding rate and spreading schemes used to produce each one of the available payload data rates, as well as the amount of information bits coded in each block of 6 OFDM symbols.

Table 2.4. PSDU rate-dependent parameters

Data Rate (Mbps)	Modulation	Coding Rate	FDS	TDS	Coded bits / 6 OFDM symbol	Info bits / 6 OFDM symbol
53.3	QPSK	1/3	YES	YES	300	100
80	QPSK	1/2	YES	YES	300	150
106.7	QPSK	1/3	NO	YES	600	200
160	QPSK	1/2	NO	YES	600	300
200	QPSK	5/8	NO	YES	600	375
320	DCM	1/2	NO	NO	1200	600
400	DCM	5/8	NO	NO	1200	750
480	DCM	3/4	NO	NO	1200	900

Information sent over the WiMedia PLCP (Physical Layer Convergence Protocol) is organized in sets of symbols forming frames called PPDU (PLCP Protocol Data Unit). Frames are made up of three parts:

- The PLCP preamble is the first component of the PPDU and can be further decomposed into a packet/frame synchronization sequence, and a channel estimation sequence. Instead of the standard preamble, burst preambles can be used in bandwidth-critical applications.
- The PLCP Header contains information about the nature of the frame and how to process it. The PLCP header can be further decomposed into a PHY header, MAC header, header check sequence (HCS), tail bits, and Reed-Solomon parity bits.
- The PSDU (PHY Service Data Unit) is the last major component of the PPDU and is formed by concatenating the frame payload with the frame check sequence (FCS), tail bits, and pad bits. Payload length can vary from 1 byte to 4095 bytes.

Concerning transmission power, a device must provide support for transmit power control (TPC) in order to minimize the transmit Power Spectral Density (PSD) while still providing a reliable link for the transfer of information. When the device is using time-frequency interleaving, the monotonic dynamic range for the attenuation of the transmit power shall be 0 – 12 dB, with a step size granularity of 2 dB. On the other hand, when the device is using fixed-frequency interleaving, the monotonic dynamic range for the attenuation of the transmit power shall be 0 – 8 dB, with a step size granularity of 2 dB.

WiMedia MAC sublayer is designed to enable mobility, such that a group of devices may continue communicating while merging or splitting from other groups of devices. To maximize flexibility, the functionality of the MAC is distributed among devices. These functions include distributed coordination to avoid interference between different groups of devices by appropriate use of channels and distributed medium reservations to ensure Quality of Service. The MAC sublayer provides prioritized schemes for isochronous and asynchronous data transfer. To do this, a combination of Carrier Sense Multiple Access (CSMA) and Time Division Multiple Access (TDMA) is used. A Distributed Reservation Protocol (DRP) is used to reserve the medium for TDMA access for isochronous and other traffic. For asynchronous transfers, Prioritized Contention Access (PCA) is provided using a CSMA scheme. PCA is a random access scheme with a backoff mechanism used to resolve contention for the channel. The PCA mechanism provides differentiated, distributed contention access to the medium for four access categories (ACs) of frames buffered in a device for transmission: voice, video, best effort and background.

The basic timing structure for frame exchange is a superframe. The superframe is composed of 256 medium access slots (MASs), where MAS duration is 256 μs. Each superframe starts with a Beacon Period, which extends over one or more contiguous MASs. The maximum length of the Beacon Period is 96 beacon slots and the duration of each beacon slot is 85 μs. Beacons are always transmitted at 53.3 Mbps.

MAC layer also provides the following functionalities:

- Request To Send (RTS) / Clear To Send (CTS): The RTS and CTS frames prevent the neighbours of the source and recipient devices from accessing the medium while the source and recipient are exchanging the following frames.
- Acknowledgement: No acknowledgement (No-ACK), immediate acknowledgement (Imm-ACK) and block acknowledgement (B-ACK) policies are defined.
- Security: Enabling security requires an exchange of keys and the addition of a Security Header and Message Integrity Code (MIC) in the payload of every secure frame.
- Power management: Two power management modes are defined, active and hibernation. Devices in active mode transmit and receive beacons in every superframe. Devices in hibernation mode hibernate for multiple superframes and do not transmit or receive in those superframes.

2.3.3 IEEE 802.15.4a

The IEEE 802.15.4-2006 standard defines wireless MAC and PHY specifications for Low-Rate Wireless Personal Area Networks (LR-WPAN) [IEEE, 2006]. IEEE 802.15.4a amends this standard with the addition of two alternate physical layers: Ultra-Wideband and Chirp Spread Spectrum (CSS) [IEEE, 2007]. The UWB PHY supports an over-the-air mandatory data rate of 851 kbps with optional data rates of 110kbps, 6.81 Mbps, and 27.24 Mbps at frequencies of 3 GHz to 5 GHz, 6 GHz to 10 GHz, and less than 1 GHz.

The UWB PHY supports three independent bands of operation:

- The sub-gigahertz band, which consists of a single channel and occupies the spectrum from 249.6 MHz to 749.6 MHz. Channel 0 is defined as the mandatory channel
- The low band, which consists of four channels and occupies the spectrum from 3.1 GHz to 4.8 GHz. Channel 3 is the mandatory channel
- The high band, which consists of eleven channels and occupies the spectrum from 6.0 GHz to 10.6 GHz. Channel 9 is the mandatory channel

The set of operating frequency bands is defined in Table 2.5. Within each channel, there is support for at least two complex channels that have unique preamble codes. The combination of a channel and a preamble code is termed a complex channel. A total of 32 complex channels are assigned for operation, two channels in each of the 16 defined operating frequency bands. A compliant implementation shall support at least the two logical channels for one of the mandatory bands. Support for the other channels is optional.

UWB channels {4, 7, 11, 15} are differentiated from other UWB channels by the larger bandwidth (> 500 MHz) of the transmitted signals. These channels overlap the existing lower bandwidth channels. The larger bandwidth enables devices operating in these channels to transmit at a higher power (for fixed PSD constraints), and thus they may achieve longer communication range. The larger bandwidth pulses offer enhanced multipath resistance and leads to more accurate range estimates.

Table 2.5. 802.15.4a channel allocation

Band Group	Channel number	Center Frequency (MHz)	Bandwidth (MHz)	Mandatory/optional
0	0	499.2	499.2	Mandatory below 1 GHz
1	1	3494.4	499.2	Optional
	2	3993.6	499.2	Optional
	3	4492.8	499.2	Mandatory in low band
	4	3993.6	1331.2	Optional
2	5	6489.6	499.2	Optional
	6	6988.8	499.2	Optional
	7	6489.6	1081.6	Optional
	8	7488.0	499.2	Optional
	9	7987.2	499.2	Mandatory in high band
	10	8486.4	499.2	Optional
	11	7987.2	1331.2	Optional
	12	8985.6	499.2	Optional
	13	9484.8	499.2	Optional
	14	9984.0	499.2	Optional
	15	9484.8	1354.97	Optional

The UWB PHY waveform is based upon an impulse radio signaling scheme using band-limited data pulses. A combination of burst position modulation (BPM) and binary phase-shift keying (BPSK) is used to support both coherent and non-coherent receivers using a common signaling scheme. The combined BPM-BPSK is used to modulate the symbols, with each symbol being composed of an active burst of UWB pulses. In the BPM-BPSK modulation scheme, a UWB PHY symbol is capable of carrying two bits of information: one bit is used to determine the position of a burst of pulses while an additional bit is used to modulate the phase of this same burst. The various data rates are supported through the use of variable-length bursts.

The structure and timing of a UWB PHY symbol is illustrated in Figure 2.7. Each symbol consists of an integer number of possible chip positions, N_c, each with duration T_c. The overall symbol duration denoted by T_{dsym} is given by $T_{dsym} = N_c \cdot T_c$. Furthermore, each symbol is divided into two BPM intervals each with duration $T_{BPM} = T_{dsym}/2$, which enables binary position modulation. Pulse duration is the inverse of channel bandwidth, e.g. 2 ns for 500 MHz channels, while T_c is 2 ns for every channel.

A burst is formed by grouping N_{cpb} consecutive chips and has duration $T_{burst} = N_{cpb} \cdot T_c$. In each UWB PHY symbol interval, a single burst event is transmitted. The fact that burst duration is typically much shorter than the BPM duration provides for some multi-user access interference rejection in the form of time hopping. The total number of burst durations per symbol, N_{burst}, is given by $N_{burst} = T_{dsym}/T_{burst}$. In order to limit the amount of inter-symbol interference caused by multipath, only the first half of each T_{BPM} period shall contain a burst. Therefore, only the first $N_{hop} = N_{burst}/4$ possible burst positions are candidate hopping burst positions within each BPM interval. Each burst position can be varied on a symbol-to-symbol basis according to a time hopping code.

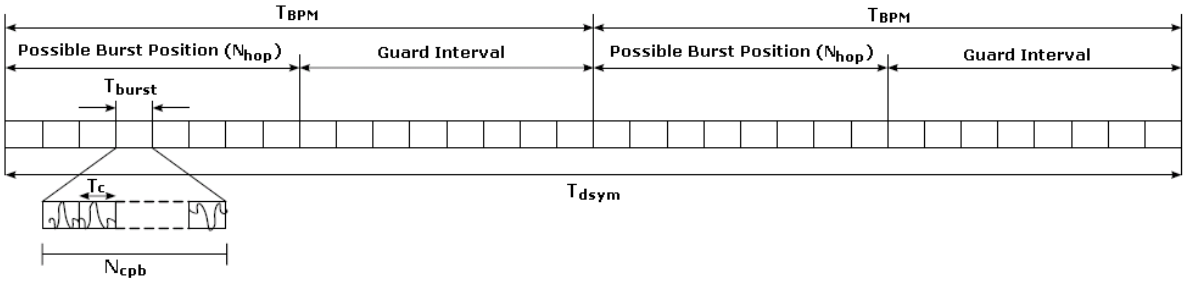

Figure 2.7. 802.15.4a UWB symbol structure and timing

The UWB PHY contains several optional data rates, preamble code lengths, and PRF (Pulse Repetition Frequency). Peak PRF is 499.2 MHz and corresponds to the highest frequency at which a compliant transmitter shall emit pulses. Additionally, the mean PRF is defined as the total number of pulses emitted during a symbol period divided by the length of the symbol duration. There are two possible preamble code lengths (31 or 127) and three possible mean PRFs (15.6 MHz, 3.90 MHz, and 62.4 MHz). Each UWB channel allows for several data rates (110kbps, 851 kbps, 6.81 Mbps, and 27.24 Mbps) that are obtained by modifying the number of chips within a burst, while the total number of possible burst positions remains constant. Therefore, the symbol duration, T_{dsym}, changes to obtain the stated symbol rate and bit rates.

The UWB frame (PPDU) is composed of three major components:

- SHR (Synchronization Header) preamble: The preamble can be subdivided into two distinct portions: SYNC (packet synchronization, channel estimation, and ranging sequence) and SFD (Start of Frame Delimiter). Four mandatory preambles are defined: default, short, medium and long preamble.
- PHY header (PHR): The PHR contains information about the data rate used to transmit the PSDU, the duration of the current frame's preamble, and the length of the

frame payload. Additionally, six parity check bits are used to further protect the PHR against channel errors.

- The PSDU contains data payload, coded concatenating an outer Reed-Solomon systematic block code and an inner half-rate systematic convolutional code.

Depending on the application requirements, an IEEE 802.15.4 LR-WPAN may operate in either of two topologies: the star topology or the peer-to-peer topology.

- In the star topology the communication is established between devices and a single central controller, called the PAN (Personal Area Network) coordinator. The PAN coordinator is the primary controller of the PAN.
- The peer-to-peer topology also has a PAN coordinator; however, it differs from the star topology in that any device may communicate with any other device as long as they are in range of one another. Peer-to-peer topology allows more complex network formations to be implemented, such as mesh networking topology. A peer-to-peer network may also allow multiple hops to route messages from any device to any other device on the network. Such functions can be added at the higher layer.

An example of the use of the peer-to-peer communications topology is the cluster tree. The cluster tree network is a special case of a peer-to-peer network in which multiple devices may act as a coordinator and provide synchronization services to other devices or other coordinators. Only one of these coordinators can be the overall PAN coordinator. The simplest form of a cluster tree network is a single cluster network, but larger networks are possible by forming a mesh of multiple neighboring clusters.

The PAN coordinator may optionally define a superframe structure. The superframe is bounded by network beacons sent by the coordinator and is divided into 16 equally sized slots. The beacon frame is transmitted in the first slot of each superframe and is used to synchronize the attached devices, to identify the PAN, and to describe the structure of the superframes. Any device wishing to communicate during the contention access period (CAP) between two beacons competes with other devices using a slotted CSMA-CA (Carrier Sense Multiple Access with Collision Avoidance) or ALOHA mechanism. For low-latency applications or applications requiring specific data bandwidth, the PAN coordinator may dedicate guaranteed time slots (GTSs) portions of the active superframe. The GTSs form the contention-free period (CFP), which always appears at the end of the active superframe following the CAP, as shown in Figure 2.8. The PAN coordinator may allocate up to seven of these GTSs, and a GTS may occupy more than one slot period. However, a sufficient

portion of the CAP remains for contention-based access of other networked devices or new devices wishing to join the network.

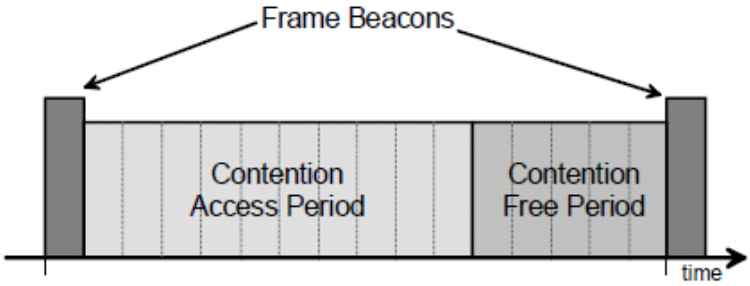

Figure 2.8. 802.15.4 superframe structure

Four frame types are defined:

- A beacon frame, used by a coordinator to transmit beacons
- A data frame, used for all transfers of data
- An acknowledgment frame, used for confirming successful frame reception
- A MAC command frame, used for handling all MAC peer entity control transfers

The UWB PHY also has the optional feature of precision ranging. UWB devices that have implemented optional ranging support are called ranging-capable devices (RDEVs). A UWB frame with the ranging bit set in the PHR is called a ranging frame (RFRAME). The fundamental measurements for ranging are achieved using a data-acknowledgment frame exchange. As far as ranging is concerned, the critical instant in a frame is the first pulse of the PHR or ranging marker (RMARKER). The standard primarily supports the two-way time-of-flight computation of distance between two RDEVs, although one-way ranging operation is allowed as well.

RDEVs produce results that are used by higher layers to compute the ranges between devices. These results comprise a set of five numbers (ranging counter start value, ranging counter stop value, ranging tracking interval, ranging tracking offset and ranging figure of merit) and the total collection is called a timestamp report. At the end of a two-way exchange, each device is in position of a timestamp report. The mandatory part of ranging is limited to the generation of timestamp reports during the period that ranging is enabled in an RDEV. The estimation of the time-of-arrival, the transmission of the timestamp reports and the subsequent computations to reconstruct the location of devices in a network are beyond the scope of the 802.15.4a standard.

Chapter 3

State of the Art

3.1 Coexistence and Mitigation Techniques

As it was already mentioned, the energy of the UWB signal is distributed over a broad frequency range, which results in a very low power spectral density that allows radio spectrum reutilization. However, UWB operation in licensed bands requires that harmless coexistence between UWB and the other radio services sharing the spectrum is guaranteed.

The level of interference caused by UWB in current radio services has been widely studied, both theoretically and with measurement campaigns. In order to guarantee that actual and future radio services are not interfered by UWB, regulatory bodies have proposed restrictive spectrum masks that limit the power spectral density of UWB, as it was shown in Section 2.3.1. However, these restrictions limit the range of UWB devices and as a result their potential applications. Extensive research is directed to the development of reliable mitigation techniques which allow coexistence with a minimum degradation in UWB performance. Two are the main techniques under study or already included in the current regulation: Low Duty Cycle and Detect and Avoid.

3.1.1 Coexistence

Within the framework of the regulation and standardization process of UWB several companies and organizations provided different coexistence studies to the regulatory bodies. Some of them are available in the official web page of ECC or ITU-R. A complete summary of the results of these simulations is available in [ITU-R, 2006], covering the coexistence between UWB and other radio services such as: land mobile service, IMT-2000 services, fixed service, fixed-satellite service, mobile satellite systems, radio navigation satellite services, Broadcasting Services, Earth exploration satellite, Space research and Radio

astronomy services. In January 2006, ITU-R Task Group 1/8 publicized the final version of a specific study.

The content of this section is based on the large number of contributions received from the private sector for ECC consultation about establishing a definitive UWB regulation in Europe. Companies such as Siemens, Texas Instruments, Intel, Ericsson, Alereon, France Telecom or Motorola sent several papers in response to the ECC TG3 request to find a definitive solution for the coexistence of UWB devices and existing radio systems. These contributions resulted in ECC Report 64 regarding the protection requirements of radio communications systems below 10.6 GHz from generic UWB applications [ECC, 2005a].

Several measurement campaigns have also been conducted to test the performance parameters of victim service allocated in the same environment when one or more UWB devices are active. In case of cellular services (GSM, GPRS, UMTS), field measurements have been performed by France Telecom, Nokia and Swisscom in response to the ECC TG3 request and can be found in [ECC,2005b]. This measurement campaigns provided similar results compared to the compatibility studies conducted in the ECC report 64, showed that an UWB out-of-band emission limit of -75.4 dBm/MHz produced insignificant amount of interference, if the separation distance was more than one meter, and recommending a maximum emission level of -85 dBm/MHz under 36 cm protection distance.

Both mentioned simulation studies and measurement campaigns were developed in order to support the UWB regulation process with the aim of finally define a spectral emission mask for UWB low enough to protect incumbent radio services but able to ensure an adequate UWB development. On the other hand, several works can be found in the literature addressing the coexistence of UWB with other radio services that are presented in the following subsections for both LDR-LT and VHDR UWB systems.

3.1.1.1 Pulse-based UWB coexistence

In the last decade, several authors have studied the coexistence of IR-UWB and different radios services, whether through analytical and simulation studies or through measurement campaigns. Here the most important ones are summarized.

One of the first works dates back to 2001. In [Swami, 2001] the interference caused by UWB signals on narrow-band (NB) systems is assessed via analysis and simulations. Analytical results include the aggregate effect of spatially distributed UWB radios on a receiver, and theoretical Bit Error Rate (BER) expressions. Simulation results of the effects of multiple UWB emitters on a narrow band BPSK receiver are also provided.

A very complete overview on the analytical study of interference and coexistence among UWB systems and other conventional narrow-band systems is presented in [Chiani, 2009]. Both point-to-point UWB under the interference generated by a finite number of NB radio transmitters and vice versa are considered. Channels including additive white Gaussian noise and multipath fading both for the victim and the interfering links, and different receiver architectures are also considered. Concerning UWB systems affected by NB interference, it is showed that the impact of the NB interference strongly depends, for a IR-UWB coherent receiver, on the carrier frequency of the interferer, the UWB pulse shape, and the spreading code adopted. In a realistic setting, there is no significant performance degradation in the UWB link for a Signal-to-Interference Ratio (SIR) on the order of -20 dB or greater. However, due to the low transmitted power level currently allowed for UWB systems, which is typically much lower than for NB transmitters, a scenario with strong NB interferers producing very small SIR at the UWB receiver is not unlikely. Similarly, for the dual case of NB systems affected by UWB interference, we have shown that the effects of a single UWB interferer are almost negligible, and the performance of the NB links is practically unchanged for sufficiently large SIR values (greater than -20 dB). However, situations where the NB receiver is much closer to the UWB transmitter than to the NB transmitter can produce very low SIR, with consequent performance degradation in the NB link. Moreover, while it is true that the effect of a single UWB interferer is in many cases negligible for NB links, this may not be the case when considering the aggregate effect of many UWB transmitting nodes.

In [Hämäläinen, 2002] the level of interference caused by different ultra-wideband (UWB) signals to other various radio systems, as well as the performance degradation of UWB systems in the presence of narrowband interference and pulsed jamming, are evaluated. The in-band interference caused by a selection of UWB signals is calculated at GSM900, UMTS/wideband code-division multiple-access (WCDMA), and GPS frequency bands. Since this work was carried out before the FCC approval, it was assumed that the frequency bands for the UWB transmission overlapped with the victim systems. Two UWB system concepts were analyzed: time hopping and direct sequence spread spectrum. Proper selection of pulse waveform and pulse width allows avoiding some rejected frequency bands up to a certain limit. An UWB system suffers most from narrowband systems if the narrowband interference and the nominal center frequency of the UWB signal overlap. This is proved by BER simulations in an additive white Gaussian noise (AWGN) channel with interference at global GSM and UMTS/WCDMA frequencies.

In [Giuliano, 2005], the coexistence between an UWB-based system and UMTS, GPS, DCS1800, fixed wireless access (FWA) systems and point-to-point (PP) links is analyzed. It

is showed that, especially when the carrier frequency of the UWB is selected to lie in the 3.1–10.6-GHz band, there is no risk for UMTS, GPS, and DCS receivers operations, even for very large UWB terminal densities. The coexistence issues of UWB with FWA and PP systems have been analyzed in detail, since they could be impaired when the UWB operates in the 3.1–10.6-GHz band. Even in this case, we showed that even in the extreme UWB devices densities proposed there is no practical risk for FWA and PP operations.

IEEE 802.15.4a-2007 standard also provides some coexistence studies for 802.15.4a UWB PHY and other standards operating in the bands allocated to UWB [IEEE, 2007]. The only other IEEE wireless standard that overlaps this same spectrum is IEEE 802.16 systems (WiMAX) occupying 3400–3800 MHz licensed frequency bands in some regions (Europe and Asia). Distances of 4-8 m and 2-4.5 m were identified for a 1 dB and a 3 dB rise in the effective operating noise floor of the IEEE 802.16 receiver respectively. Coexistence with the proposed standard IEEE P802.22 operating between 54 MHz and 862 MHz was also analyzed. Due to the power limitation of UWB in this band, it was concluded that a 802.15.4a device would not be able to operate at all at ranges where its emissions would impact the IEEE P802.22 device. In such a case, the IEEE 802.15.4a device could simply use a different channel. In addition, coexistence with WiMedia UWB as specified in ECMA-368 was also analyzed. For the coexistence analysis, it was assumed that the ECMA-368 device operates using frequency hopping in bands across the 3.1–4.8 GHz unlicensed UWB bands and the IEEE 802.15.4a device operates in band 3. Distances of 6 m and 3 m were identified for a 1 dB and a 3 dB rise in the effective operating noise floor of the ECMA-368 receiver respectively.

The effect of UWB interference on a WiMAX receiver is also addressed in [Sarfaraz, 2005]. The performance of a WiMAX receiver located in the vicinity of a DS-UWB hot spot has been evaluated. It is concluded that, for different values of receiver bandwidth and number of users, the aggregate UWB interference resulting from a realistic hot spot scenario will be maintained below the threshold levels specified the different modes of WiMAX. The two systems can coexist with the UWB system, posing no threat to the operation of the WiMAX receiver.

Another system operating in the same spectrum band where UWB operation was allowed by FCC is wireless local area network (WLAN) standard IEEE 802.11a. In [Bellorado, 2003] a physical layer based analysis of the coexistence issues of ultra-wideband (UWB) with 802.11a is provided. Results indicate that a UWB interferer operating at the peak allowable power density induces minimal interference into WLAN devices in line-of-sight (LOS) scenarios, even at close range. However, in the NLOS case, a UWB interferer can severely affect the data-rate sustainable by 802.11a systems. Moreover, 802.11a

interference into UWB systems is shown to reduce the SIR by as much as 36 dB when the interferer is within LOS of the UWB receiver.

Although UWB does not operate on UMTS bands, the coexistence with UMTS has been also a subject of interest, and some measurement campaigns can be found. In [Quijano, 2005] the impact of impulse radio UWB transmitters in UMTS (WCDMA) receivers is quantified. Through a measurement campaign it is concluded that a ratio, defined as total WCMA signal power to Ultra Wideband interference power level, of -8.9 dB is enough to protect UMTS handset operation at 12.2Kbps mode, and -3.3 dB at 64 Kbps operation mode, working at theoretical reference sensitivity levels and worst case conditions. Less strict protection criteria are proposed considering the low probability of worst case situations to be encountered.

In [Cassioli, 2005] results of experimental trials performed to assess the coexistence of the UMTS systems and the UWB emissions are presented. The maximum UWB power level in the UMTS channel tolerable by a UMTS receiver is found to be in the range around -110 / -95 dBm: beyond this value the BER of the UMTS receiver increases over 10^{-3}, which is the BER threshold specified for the conformance testing by the UMTS technical specifications. The emission mask issued by the FCC for UWB indoor communications gives a total maximum UWB allowed power of -45 dBm in the bandwidth of a single UMTS RF channel, compared to -79 dBm for ECC emission mask. Since the signal attenuation as given by the free-space theory, the maximum allowed UWB signal power in the UMTS channel at 1 m is -85 dBm for the FCC ruling and -119 dBm for the ECC regulation. Thus, the more restrictive limits imposed by the ECC regulation assure the protection of UMTS system against the UWB interference, while the FCC ruling may fail.

In [Hämäläinen, 2006] results of a coexistence measurement study between multiple UWB transmitters and a UMTS mobile phone are presented. A large number of FCC compatible UWB transmitters were used to generate interference for an active UMTS connection. The results clearly show that UMTS and high pulse repetition rate UWB devices can coexist at link level when a moderate number of simultaneously active UWB devices operate in close proximity of the UMTS victim receiver. The results also show that the activity factor of the UWB transmitter disproportionately impacts the effective interference. When using low activity factors, even with high pulse repetition rates and very large numbers of UWB devices, it is difficult to detect UMTS link performance degradation. As the activity factors grow beyond 5%, the impact of the UWB interference becomes visible.

3.1.1.2 MB-OFDM UWB coexistence

As UWB was historically identified with pulse-based modulations and MB-OFDM UWB is a more recent development, most of studies focus on IR-UWB. Nevertheless, some studies specifically focused on MB-OFDM coexistence can be found.

In [Nasri, 2007] this paper the effect of MB-OFDM UWB interference on narrowband receivers is investigated. Analytical expressions for the amplitude probability distribution (APD) and the bit error rate of a binary phase-shift keying NB receiver are derived. For NB signals with much smaller and much larger bandwidths than the MB-OFDM subcarrier spacing, a Gaussian approximation (GA) and an impulsive GA (IGA), respectively, of the MB-OFDM UWB interference lead to accurate performance predictions. However, for most NB channel models and signal bandwidths the exact BER analysis has to be used to obtain meaningful results. An exception is the Rayleigh fading NB channel where both GA and IGA yield tight approximations of the exact BER regardless of the NB signal bandwidth. In general, the BER of the NB receiver strongly depends on the carrier frequency offset between the NB signal and the MB-OFDM signal, the NB signal bandwidth, the number of MB-OFDM frequency bands, and the NB pulse shape.

Although it focuses on IR-UWB systems, in [Chiani, 2009] UWB systems employing carrier-based DS-SS and OFDM modulations are also considered on the study of interference and coexistence among UWB systems and conventional narrow-band systems. Main conclusions are that the effects of a single UWB interferer are almost negligible, except for situations where the NB receiver is much closer to the UWB transmitter than to the NB transmitter or when the aggregate effect of many UWB transmitting nodes is considered.

In [Cano, 2010] the performance of a 3.5 GHz WiMAX victim receiver under the presence of a single MB-OFDM UWB interferer is evaluated. A comprehensive analysis of these interference effects is provided by means of theoretical, simulation and measurement approaches. Analytical expressions of the BER for uncoded and coded WiMAX systems, impaired by a single MB-OFDM UWB interference signal, are provided for both AWGN and Rayleigh fading channel environments. The maximum permissible interference levels and the SIR values, which allow the UWB interference effects to be considered negligible, are estimated from simulation and measurement results.

An extensive simulation analysis is provided. Simulation results showed that the effect of the non-hopping UWB interference on the WiMAX link is 4.5 dB larger than the hopping one. This is due to the fact that the frequency hopped interference is only active one third of the time. BER values for analytical minimum permissible SIR showed that the BER degrades considerably with respect to the case of non-interference, especially when TFC5 is

employed, so more restrictive SIR levels are required in order to neglect the UWB interference effects. Measurements in a conducted modality were also carried out to analyze the effects of the UWB interference on the WiMAX link. It is concluded that the effects of the interference signal become negligible when the NIR is larger than 10 dB.

3.1.2 Mitigation techniques

Mitigation techniques arise as a promising solution to minimize the effect of UWB systems on the existing radio services. To permit uses of the low band (3.4 GHz to 4.8 GHz) to low-activity applications with the guarantee of an efficient protection of licensed services, the European regulator considered the use of two mitigation techniques in decision ECC/DEC(06)12 [ECC, 2008a]:

- LDC (Low Duty Cycle): Based on the establishment of temporal restrictions to UWB transmissions. It is especially suitable for UWB applications with a low activity factor, presenting a very low risk of interference as transmission is usually limited to a few seconds during long periods of time, for instance LDR-LT UWB systems.

- DAA (Detect And Avoid): Based on the detection of the presence of a victim service and the consequent application of a protection procedure on the UWB transmission in order to reduce the interference. DAA techniques present a higher complexity, as a mechanism to detect the presence of the victim service is required.

UWB devices implementing mitigation techniques are allowed to transmit at higher power (-41.3 dBm/MHz) than defined in Decision ECC/DEC(06)04 [ECC, 2006a] (-80 dBm/MHz between 3.4 GHz and 3.8 GHz and -70 dBm/MHz between 3.8 GHz and 4.8 GHz) on the condition that these mitigation techniques provide at least an equivalent protection.

3.1.2.1 Low Duty Cycle

Technical requirements for LDC UWB devices to protect FWA terminals are presented in ECC Report 94 [ECC, 2006c]. T_{on} is defined as the duration of a burst irrespective of the number of pulses contained. T_{off} is defined as the time interval between two consecutive bursts when the UWB emission is kept idle. The following restrictions are applied:

$T_{on}max = 5ms$

$T_{off}mean \geq 38ms$ (averaged over 1 s)

$\Sigma T_{off} > 950ms$ per second

$\Sigma T_{on} < 5\%$ per second and 0.5% per hour

In addition, results of measurements campaigns are reported by ECC-TG3 to give confidence that LDC is capable to protect the FWA services. These results were discussed internally in this ECC task group and there was an agreement on the efficiency of such technique. Accordingly, this technique was discussed in a plenary ECC meeting, where it was agreed on including the LDC technique in the ECC Decision [ECC, 2006b]. Results indicated that when the UWB activity factor was limited to 5%, the impact to WiMAX system might be acceptable while measurement at 10% activity factor showed some significant effect for few cases. All measurements were made with 0.5 meters distance, which will rarely occur, considering the target applications for UWB LDC, and when the distance increases, the situation is foreseen to get better. On the other hand, the impact reduction with respect to the distance between UWB transmitter and FWA receiver will likely prevent any aggregation effect.

In IEEE 802.15.4a the use of low duty cycle is proposed to reduce potential interference effects within a UWB piconet [IEEE, 2007]. The following low-duty-cycle piconet scenarios are considered:

- IEEE 802.15.4a devices are deployed in high density in a limited area, e.g., hot-spot deployment scenarios.
- Victim systems cover much larger area than the coverage of a typical IEEE 802.15.4a PANs (e.g., IEEE 802.16) or are closely located with a piconet coordinator (e.g., devices placed at the same desk or even within the same computer).

In these cases, transmissions from every device in the PAN can affect the victim receiver. The aggregate interference from the PAN increases with increment in number of PAN members. For reasons of less complexity, lower power consumption, as well as physical limitations, it is difficult for simple IEEE 802.15.4a devices to detect victim system reliably, so detect-and-avoid techniques are not suitable. The interference to victim systems could be limited by controlling the duty cycle of the PAN through general active/inactive periods. The UWB traffic can occur only in the active period, and victim systems would then be free of interference in the inactive period.

Considering the applications for which the UWB PHY is designed in application scenarios where a greater number of nodes can be expected (for example, a sensor network application), duty cycle (aggregate and individual) can be expected to be orders of magnitude less than 1%. Consequently, there is low impact on coexistence due to a large number of IEEE 802.15.4a nodes as the aggregate duty cycle remains very low.

In addition, the 802.15.4a UWB PHY provides support for optional data rates as high as 27 Mb/s. These rates are not designed to support high-rate applications, but instead are provided to allow devices in close proximity to shorten their transmission duty cycle to further reduce the likelihood that these devices will interfere with or be subject to interference by other devices when conditions allow.

Finally, in [Sodeyama, 2010] the coexistence environment between LDR UWB communication system such as wireless sensor network and an existing wideband system using OFDM such as 4th generation mobile cellular system (4G) and WiMAX is considered. In order to analyze the interference mitigation capability of LDC algorithm with impulse based UWB system, the frame error rate (FER) of the wideband OFDM system is examined. It is shown that LDC algorithm is an efficient interference mitigation technique for low data rate UWB communication via computer simulations regardless of the transmitted power of UWB communication system, provided that adequate PRF and duty-cycle of LDC-UWB system are chosen.

3.1.2.2 Detect and Avoid

DAA techniques comprise two phases: detect phase and avoid phase. Detect phase aims to detect if there is any possible interference between the different radio services. If any degradation on the victim service is detected, a protection mechanism will be applied on the interferer service in order to avoid any interference (avoid phase). The technical requirements for DAA UWB devices to ensure the protection of radiolocation services in the bands 3.1 - 3.4 GHz and 8.5 - 9 GHz and Broadband Wireless Access (BWA) terminals in the band 3.4 – 4.2 GHz are presented in ECC report 120 [ECC, 2008b].

DAA techniques can be classified into cooperative and non-cooperative depending on the participation of the victim service in the detection phase. Cooperative techniques are aimed to dual devices implementing both technologies, so the victim service itself can inform the UWB transceiver of its activity state. DAA implementations have mainly focused in non-cooperative strategies but cooperative techniques are very interesting solution for interoperability applications.

Concerning the detection of the victim service in non-cooperative DAA, two algorithms have been presented:

- Dynamic Frequency Selective (DFS) – Energy based detection: This detection algorithm consists of averaging the squared magnitudes of the Fast Fourier transform (FFT) coefficients over M successive FFT windows and comparing the resulting 128 points against a detection threshold. In [Intel, 2005] the particular case of indoor

Fixed System (FS) downlink detection, performed by a Wimedia MB-OFDM UWB receiver, is analyzed. The presented algorithm does not rely on any signal specific features in order to detect the FS, but performs non-coherent energy integration in order to discriminate between the background noise and the narrowband interferer representing the FS signal.

- BER based victim detection: This technique is based on the following idea: a Broadband Fixed Wireless Access (BFWA) signal is detectable when the received signal level affects the BER measured at the UWB receiver. This is a Texas Instruments proposal [Texas Instruments, 2005] that has been demonstrated for a particular worst case scenario. A scheme is proposed to detect the WiMAX downlink (multicast) and other radio by the BER counts of the OFDM subcarriers.

Concerning interference avoidance, there is a wide a range of options to satisfy the desired protection criteria with respect to the FS or other victim systems:

- Permanent avoidance of the conflicting band: The simplest UWB devices may permanently operate above 5 GHz, only using the upper band and dropping the potential conflictive 3.1-5 GHz band.
- Eventually ceasing operation in the whole band: UWB devices with a simple mitigation mechanism may operate below 5 GHz on the basis that in the event any victim service is detected, the device will cease operation below 5 GHz.
- Change of UWB emission band: UWB devices may operate in a different band group, or change the frequency band within a band group (for instance, through FFI TFC codes) in the event any victim service is detected.
- Suppression of UWB transmission in the conflicting band: Alternatively, a more sophisticated UWB device may first estimate the centre frequency/bandwidth, and use some heuristics to compute the minimum span of frequencies over which UWB emissions must be dynamically reduced. This is based on a priori information about parameters such as DL/UL frequency separation for the range of possible affected systems that operate below 5 GHz.
- Narrow-band RF notch filters: The design of narrow-band RF notch filters is, in general, a challenging problem, and achieving the desired filter attenuation may involve significant chip cost. Additionally, the notch frequency, the centre of the narrow-band RF filter, may need to be adjustable according to the regional (e.g. Europe and Japan) spectrum usage.

- FIR (Finite Impulse Response) filter: Alternatively, the use of an FIR filter is the most well known and the simplest solution, although it is a very power hungry solution.
- Turning off transmissions of the implied OFDM sub-carriers: Another approach, particularly suited to OFDM, is to turn off the transmission of the sub-carriers or tones located in the interference band. This option is potentially much more flexible because the narrow-band notch filtering is realized by digital signal processing and is more attractive from the chip implementation and cost point of view. However, simply turning off interference tones does not provide an adequately suppression of the interference.
- Active Interference Cancellation (AIC): Based on a concept of emitting, together with the transmitted data signal, the interference cancellation signal. Only a small number of tones are necessary to actively cancel the interference for the OFDM-based transmitters, and the required signal processing is in the frequency domain, so the power consumption is not too much. The interference cancelling tones are computed as a solution to an optimization problem, but the necessary numbers are provided as pre-computed coefficients. This technique also solves the problem of having and interference victim band spread over two bands; two separate notches could be applied over two neighbouring bands.

Multiple DAA mechanisms are proposed in the literature, most of them focused on improving coexistence between UWB and WiMAX. In [Somayazulu, 2006] some of the aspects of DAA solutions are discussed and the ongoing work in this area is presented, describing the elements of the DAA architecture being considered for adoption in order to mitigate UWB interference to WiMAX serving indoor subscriber stations (SS). Results demonstrate feasibility of the approach in many of the situations to be considered. In [Mishra, 2007] various options for detection and avoidance are discussed. The main obstacles faced in achieving robust detection and avoidance with an on-chip implementation of basic DAA functionality are described. Finally, measurement results for operation of a single UWB device with a WiMax system are presented, with encouraging results.

UWB manufacturer Wisair proposed a DAA mechanism addressed to protect a WiMAX service from UWB VHDR devices using MB-OFDM modulation type [Wisair, 2005]. The procedure is composed of: a DAA silent period for coexistence between UWB and victim services when avoid mechanisms is not yet active; a DAA detection period for victim service uplink (UL) detection; and a transmission period, when the UWB terminals to communicate themselves: in case a victim service is detected, avoid operation mode is set in order to protect the downlink (DL) signal, by changing the UWB operating frequency band.

Finally, in [Facchini, 2009] a DAA procedure is proposed that can be used to reduce the percentage of time the UWB interferes with victims operating in a time division duplexing (TDD) mode (e.g. WiMAX). The performance of the proposed DAA procedure is evaluated, analyzing its dependence on some key UWB transmission parameters, bit rate and the emitted power. It is shown that the DAA timeout parameters can be tuned so as to arbitrarily reduce the average percentage of time the UWB interferes with the considered victim systems even well below the limits imposed by regulatory bodies, at the expense of reduced performance of the UWB transmission. The proper selection of DAA timeouts for a desired percentage of UWB interference and UWB link efficiency is discussed.

3.2 Location and Tracking

In general, location comprises two phases, parameter measurement, and position calculation. Based on the measurement of different parameters, such as Received Signal Strength Indication and Time of Arrival, of reference signals exchanged between the element to be located and some reference nodes, distances can be estimated, which is commonly referred to as ranging. Also, based on the measurement of the Angle of Arrival of the incident signal, the relative angles between the element to be located and the reference nodes can be estimated. On the other hand, several algorithms can be used to compute the position according to the estimated angles or distances, from basic geometrical algorithms to tracking algorithms that take into account user's previous position information. Since the location and tracking algorithms are independent of the selected technology and the potential benefit of UWB lies on the possibility to obtain a high precision TOA estimation, we will focus on TOA-based distance estimation exclusively.

3.2.1 Distance estimation

As it has been exposed above, the accuracy of positioning on a UWB-based location system depends on the accuracy of the estimated distance derived from TOA. The potential high precision TOA estimation achieved with IR-UWB systems lies in the physical layer implementation, particularly in the short duration of the pulses and consequently the very high bandwidth. This estimation depends on the sampling frequency of the receiver, as it defines the time granularity and therefore maximum achievable accuracy, and on the correct detection of the first path of the reference signal at the receiver. In fact, the goal of the receiver architecture design must be to allow a good detection of this first component. However, several effects, including noise and multipath propagation, make this task difficult.

In general, most of the proposed receiver architectures have a common framework. The first step is to extract the energy of the signal during a time period called region of uncertainty. This region is defined as the time interval where the first component of the received signal is presumably located. Then, over the captured signal energy, several TOA estimation algorithms can be applied in order to decide which sample corresponds with the first component. A complete overview of TOA estimation techniques together with the primary sources of TOA error (including propagation effects, clock drift, and interference) and fundamental TOA bounds in both ideal and multipath environments can be found in [Dardari, 2009].

3.2.1.1 IR-UWB receiver structure

The receiver demodulates the received UWB signal in order to get the data sequence. Three basic receiver approaches are commonly used [Güvenç, 2006]:

- Energy Detection (ED)

The simplest method for detection is to collect the energy of the received signal in a determined integration interval defined as block duration, T_b, which corresponds to the sampling interval for the receiver. Then, the TOA estimation algorithm is applied on these samples of the RSS (Received Signal Strength). Figure 3.1 shows the block diagram of a typical ED receiver. In order to improve the performance of this method, measured energy is averaged over K consecutive pulses.

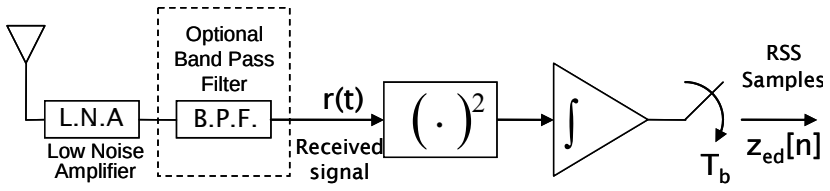

Figure 3.1. Block diagram of the Energy Detection receiver

The advantage of this method is the possibility to obtain an efficient energy detection using sampling frequencies under Nyquist frequency. Nevertheless, this method is very susceptible to noise and in low Signal-to-Noise Ratio (SNR) conditions, noise samples can prevail over signal samples, resulting in degradation of the receiver performance. In [Li, 2007] an adaptive noise cancellation (ANC) algorithm is proposed based on the least mean square (LMS) algorithm to decrease the effect of the noise in ED receivers.

- Stored Reference (SR)

Matched filtering (MF) is the optimal detection technique. The easiest way to implement matched filtering is to correlate the received signal with a stored reference template of the transmitted signal. Figure 3.2 shows the block diagram of the SR receiver. This method requires the knowledge of the transmitted waveform shape. It also requires a high sampling rate in the correlator so that perfect alignment with the template and received waveform can be obtained. Otherwise, the SR will not be able to collect sufficient energy from the received multipath arrivals due to timing mismatches. This requirement extremely increases the complexity of the receiver. In order to improve the performance of the receiver, correlation samples are averaged over *K* consecutive pulses, as in the ED receiver.

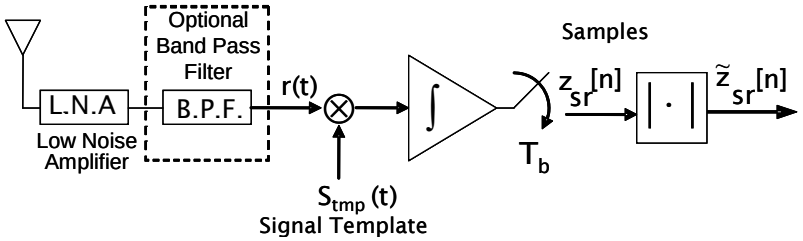

Figure 3.2. Block diagram of the Stored Reference receiver

- Transmitted Reference (TR)

In order to avoid timing and pulse-shape mismatch between the stored reference template and the received signal, in the TR scheme a template that matches the transmitted data signal is also transmitted with a certain known delay.

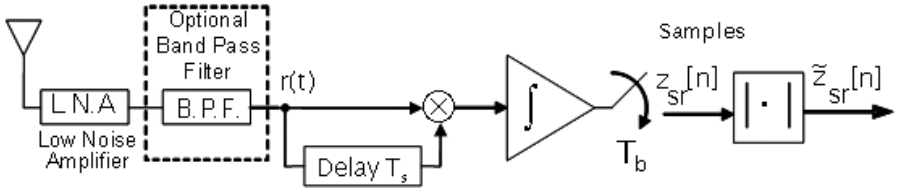

Figure 3.3. Block diagram of the Transmitted Reference receiver

Similar to the transmitted reference (TR) approaches for symbol demodulation, DT (Dirty Templates) based receivers were proposed in [Yang. 2004]. But different from TR, which relies on 50% training (pilot) symbols and requires timing to operate, DT algorithms entail none or a small number of training symbols and are designed in order to acquire timing synchronization. Correlation is performed with Dirty Templates extracted from the received waveform. The received signal is divided into segments composed by pairs of consecutive symbols. Overlap between segments is not allowed. Then, the portion of the segment corresponding to the first symbol (even symbol) is used as a template for the second symbol (odd symbol) correlation. This is known as double mode. An alternative proposal, named

single mode, is based on using each symbol as the template for the next symbol, allowing overlap between segments and halving the number of pulses needed. Cross correlation between two consecutive segments of the received signal reaches its maximum, in absence of noise, on $\tau=\tau_{TOA}$.

There are two possible operation modes. In the Non Data Aided (NDA) mode or blind mode the received signal corresponds to the transmission of a sequence of modulated data. In the Data Aided (DA) mode, a cyclic training sequence is used in order to reduce the number of pulses needed for each TOA estimation without performance degradation. Figure 3.4, Figure 3.5 and Figure 3.6 show the block diagrams of different proposals. On option 1, either for NDA and DA modes, the result of the correlation is squared and averaged. On option 2 the result of the estimation is averaged before being squared, which reduces the effect of noise. Performance is improved in Option 3 averaging both the signal and the template before the correlator, although complexity also increases.

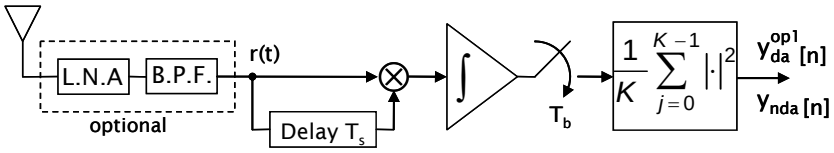

Figure 3.4. Dirty template receiver NDA/DA Option 1

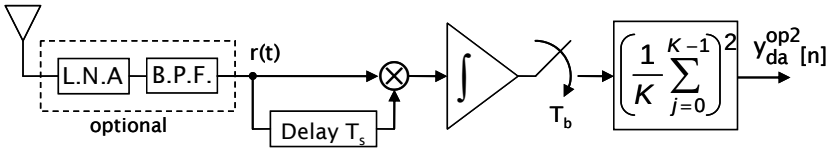

Figure 3.5. Dirty template receiver DA Option 2

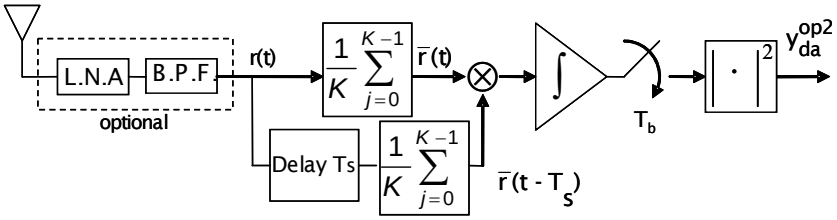

Figure 3.6. Dirty template receiver DA Option 3

Although MF is the optimal detection technique in LOS conditions, it requires a very high sampling rate. As a result, some alternative receiver designs have been proposed to reduce the complexity.

The ED&SR receiver was proposed in [Gezici, 2005] and combines both Energy Detection and Stored Reference receivers so that sampling frequencies lower than Nyquist

frequency can be used, offering a solution with a reasonable performance, low consumption and low complexity. In order to speed up the estimation process, a two step TOA estimation algorithm is proposed. The first step estimates the block in which the first signal path exists based on the received signal energy. As in the ED receiver, the signal is squared and integrated with a given block duration, T_b, in order to extract the energy. The result is averaged over N_1 consecutive frames in order to reduce the effect of noise. Finally, the block with more energy is selected and the uncertainty region is defined adding a number of chips prior to the selected block just in case the higher energy does not correspond to the first path. Then, in the second step, the chip position in which the first path resides is estimated from the low rate correlation output. With this purpose, Log-Likelihood Ratio (LLR) is computed at the output of a correlator with low sampling rate, 1 sample per chip. N_2 consecutive frames are used on this phase.

In [Mollfulleda, 2005] a receiver architecture based on a bank of analog filters, which allow for sub-Nyquist sampling rate, is introduced. The bank of filters are designed such that they form an orthogonal basis of the discrete time signal space which allows for an analog frequency-domain sampling of the receive signal. The sampled signal at the output of the bank of filters can be directly use, after Analog to Digital (AD) conversion, as the input observation signal to the TOA estimator. In [Navarro, 2006] the use of low complexity frequency-based TOA estimation techniques is proposed by estimating the autocorrelation matrix of the sampled signal in the frequency domain.

3.2.1.2 TOA estimation algorithms

Once we have the samples of the energy or the correlation, an algorithm must be applied in order to detect the leading edge of the signal and estimate the Time of Arrival.

ML estimators are known to be asymptotically efficient, that is, their performance achieves the Cramer-Rao Bound in high SNR region. However, it is difficult to implement this estimator since the received waveform must be estimated. When channel parameters are unknown, TOA estimation in multipath environments is closely related to channel estimation. In this case, path amplitudes and delays are jointly estimated using, for example, the ML approach [Win, 2002]. However, the computational complexity of ML estimators limits their implementation. To alleviate this problem, several practical suboptimal TOA estimators have been proposed in the literature. For instance, [Li, 2002] presents a generalized ML-based TOA estimation technique that estimates the relative delay of the first path by assuming that the strongest path is perfectly locked. The delay and ratio statistics between the first arriving path and strongest path are obtained from extensive IEEE

802.15.3a channel measurements. Nevertheless, very high sampling rates and computational complexity are still required.

In order to perform low-complexity TOA estimation, some simple algorithms were proposed in [Güvenç, 2005c]. Figure 3.7 summarizes in an intuitive way the operation of some of these algorithms.

- Maximum Energy Selection (MES): Choosing the maximum energy output to be the leading edge is the simplest way of achieving TOA estimation. However, the strongest energy block may not be the leading energy block in many cases, and the MES therefore hits an error-floor even in a high SNR region.

- Threshold Comparison (TC): Received samples can be compared to an appropriate threshold, and the first sample index exceeding the threshold corresponds to the TOA estimate. The normalized threshold value, ξ_{norm}, varies between 0 and 1. The major challenge is the selection of an appropriate threshold based on the received signal statistics. A low threshold can result in false detections, picking a noise sample, and a high threshold can result in missing the leading edge, so there is a trade-off.

  As discussed in [Guvenç, 2005a], the optimal threshold value depends on the SNR and the channel characteristics. However, calculation of the SNR without the knowledge of the TOA is an extremely challenging task, making it impractical to adapt the normalized threshold based on it. Same authors propose in [Güvenç, 2005d] a threshold selection technique using the Kurtosis of the received signal samples. In [Xu, 2008] a delay-dependent (DD) threshold selection method is introduced. DD sets the threshold as a function of propagation delay. The motivation of doing so is based on the fact the strength of the direct path increases with shorter transmitter-to-receiver (Tx-Rx) distance, so false alarm probability when the Tx-Rx distance is relatively large is reduced.

- Maximum Energy Selection with Search-Back (MES-SB): In order to improve the performance of the TC in low SNRs, the energy samples which will be compared to the threshold are limited to a search-back window prior to the maximum energy sample. Search-back window is denoted by W_{sb}, which is set based on the statistics of the channel.

  In [Guvenç, 2009] the same authors propose two search-back algorithms: jump back and search forward (JBSF) and serial backward search (SBS). In JBSF, the first sample within the window exceeding the threshold is selected. In SBS, the last sample exceeding the threshold and preceded by K samples below the threshold is selected.

- Maximum Energy Sum Selection (MESS): MES is susceptible to noise since the energy in a single sample is used, and it does not provide high timing resolution as there may be a large delay between the leading edge and the maximum energy block. In order to exploit the energy in the multipath components, energy samples can be summed within a window of N_w length. On the results obtained for the sliding window, the MES algorithm is applied to detect the leading edge. Since a very large window length captures a lot of noise and a small window length does not capture sufficient energy, there exists an optimum window length that depends on the channel characteristics, for instance its Delay Spread.

- Weighted-MESS (W-MESS): In order to improve the performance of the MESS algorithm, given that all the multipath components do not have the same energy, the sum can be weighted with an estimation of the channel PDP (Power Delay Profile). This is actually equivalent to correlating the received energy vector with the estimated PDP of the channel. Then, the MES algorithm is applied to select the sample corresponding to the leading edge.

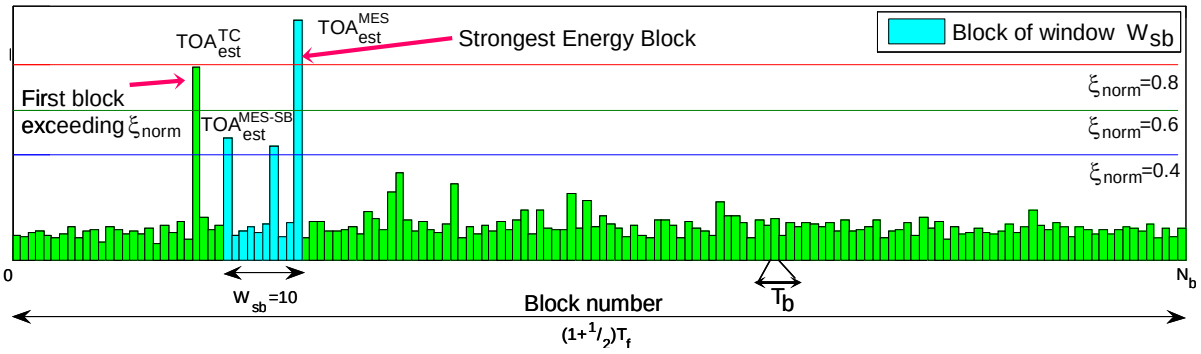

Figure 3.7. MES, TC (ξ_{norm}=0.6) and MES-SB (ξ_{norm}=0.4, W_{sb}=10) algorithms.

The performance of each algorithm depends on the observed SNR and the channel characteristics, such as the delay spread. More complex algorithms that perform different operations over the sampled signal have also been proposed in the literature.

Multiscale product (MP) based algorithms aim to improve the performance of the basic TOA estimation algorithms in order to reach a high accuracy even for low SNR without using the more complex SR receiver. Approximations of the Gaussian function derivate are commonly used for peak detection. MP based algorithms, such as W-MP (Weighted MP) MZ DWT (Mallat-Zhong Discrete Wavelet Transform) and MEP (Multiscale Energy Product), are valid for the ED receiver only. The W-MP MZ-DWT algorithm proposed in [Sadler, 1999] uses the Mallat-Zhong Discrete Wavelet Transform [Mallat, 1992] on the vector with the energy of the received signal collected with the ED receiver. The multiscalar

product is then computed on the MZ-DWT using a weight function in order to soften the peaks corresponding to noise. On the other hand, MEP algorithm was proposed in [Güvenç, 2005b] and is based on a multiscale filter bank which aims to exploit the signal energies from coarse to finer time scales in order to improve leading edge detection performance. Figure 3.8 shows the block diagram of MEP algorithm, with the scaled filter bank applied on the energy vector and the product computed on the filter output. Since the energy samples at different scales are correlated and the noise samples are uncorrelated, their product is expected to enhance the peaks due to signal existence. Then a search-back window can be used to detect the leading edge, as in MES-SB, in that case being called MEP-SB.

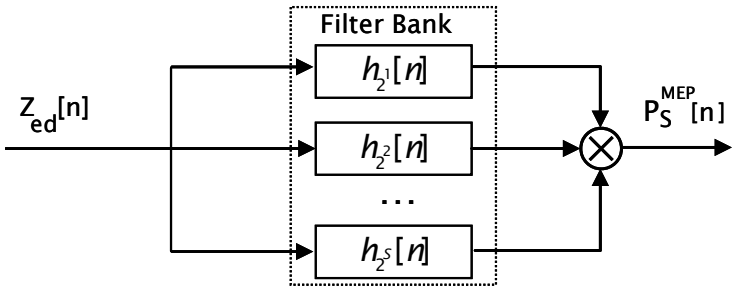

Figure 3.8. Block diagram of MEP algorithm

In [Dashti, 2008] an iterative algorithm is proposed to detect the first-arrival path. On each step, the strongest path is detected and the noise floor in the interval prior to the strongest path is computed. If the difference between the strongest path and the noise floor is below a certain threshold, the path is selected as first-arrival path; otherwise the process is repeated again in the interval prior to the strongest path.

3.2.2 Location and tracking algorithms

Several location & tracking algorithms have been proposed in the literature to compute user's position according to the estimated distances to some reference nodes. Algorithms can be classified into iterative and non-iterative. Non-iterative algorithms compute the estimated position as the closed-form solution of a set of equations, whereas in the iterative methods, the estimation is performed iteratively and the iteration does not stop until some pre-defined criterion is satisfied. Another possible classification distinguishes between parametric and non-parametric approaches. Parametric approaches compute the location based on the a priori knowledge of a model, while non-parametric approaches process straightforward the data with the usage, in some cases, of some statistic parameters (mean, variance). In [Seco, 2009] a classification of localization methods into four categories is proposed: geometry-based methods, minimization of a cost function, fingerprinting, and Bayesian techniques. In

this thesis, a classification of location and tracking algorithms is proposed with the following categories: geometric, linearization, cost-function minimization, Bayesian, multidimensional scaling and fingerprint methods. Several techniques have been also proposed to enhance the basic localization methods.

Although most of the proposals of location and tracking algorithms that can be found in the literature include the evaluation of these proposals against other existing algorithms, many times these studies are too simplistic and do not account realistically for the implications of the indoors environment and the distance estimation technology, UWB in our case. In this thesis, an evaluation of different algorithms for IR UWB indoor tracking systems is provided in Section 5.3.

3.2.2.1 Geometric methods

Geometric positioning techniques solve the position of the target node as the intersection of position lines obtained from a set of measurements at a number of reference nodes. For example, a range measurement (obtained from a TOA or an RSS measurement) determines a line of position (LOP) for the target's location as a circle around the reference node. Then, the intersection of three LOPs, obtained from three TOA or RSS measurements, can be used to solve for the position of the target. Determination of the target position from a set of range measurements is called spherical trilateration.

Let d_1, d_2 and d_3 represent the range measurements obtained from three TOA or RSS measurements. Then, the following three equations must be solved jointly in order to estimate the position of the target via trilateration [Sahinoglu, 2008]:

$$d_i = \sqrt{(x_i - x)^2 + (y_i - y)^2} \quad , i=1, 2, 3 \tag{3.1}$$

where (x_i, y_i) is the known position of the i-th reference node, and (x, y) is the position of the target node. The position (x, y) can be solved from (3.1) as

$$x = \frac{(y_2 - y_1)\gamma_1 + (y_2 - y_3)\gamma_2}{2\left[(x_2 - x_3)(y_2 - y_1) + (x_1 - x_2)(y_2 - y_3)\right]} \tag{3.2}$$

$$y = \frac{(x_2 - x_1)\gamma_1 + (x_2 - x_3)\gamma_2}{2\left[(x_2 - x_1)(y_2 - y_3) + (x_2 - x_3)(y_1 - y_2)\right]} \tag{3.3}$$

where

$$\gamma_1 = x_2^2 - x_3^2 + y_2^2 - y_3^2 + d_3^2 - d_2^2 \tag{3.4}$$

$$\gamma_2 = x_1^2 - x_2^2 + y_1^2 - y_2^2 + d_2^2 - d_1^2 \tag{3.5}$$

In the case of TDOA-based positioning, each TDOA measurement determines a hyperbola for the position of the target node, so it is referred as hyperbolic trilateration. For three reference nodes, two range differences (obtained from TDOA measurements) define two hyperbolas, which are sufficient to obtain the position of the target node. For AOA measurements, two reference nodes are sufficient to determine the position of the target node by intersecting two lines, which is called triangulation. The geometric techniques can also be applied to hybrid systems, in which multiple types of measurements, such as TDOA/AOA or TOA/AOA, are employed in position determination. Nevertheless, in this thesis we will focus on TOA-based systems.

Another approach to TOA location is based on linear LOPs [Caffery, 2000]. Each circular LOP intersects with another circular LOP at two points. These two points can be used to generate another LOP that is linear and passes through those two points. For three TOA measurements and corresponding circular LOPs, three linear LOPs can be generated. The new linear LOPs also intersect at the location of the transmitter.

The equations for the new linear LOPs can be found by squaring and differencing the ranges in (3.1) for each pair circular LOPs. However, while it is possible to obtain three linear LOPs, only two are independent, and as it turns out, the third will always intersect the other two LOPs at the same point that they intersect each other. Based on this fact, a location algorithm based on the intersecting linear LOPs only requires two of the possible three LOPs that could be generated. The location of the target node can be computed as the intersection of two linear LOPs, which produces a similar result to the one presented in (3.2) and (3.3).

Note that for the geometric solutions it is assumed that all the measurements are error free, so three reference nodes for TOA, RSS and TDOA-based positioning (two for AOA-based positioning) are used in the geometric solutions, as more measurements would not change the estimated position. Therefore, there always exists a single point at which all the LOPs, obtained from a number of measurements, intersect. However, in practice, we would like to use the method when there are more than the minimum number of reference nodes and when there are measurement errors in the TOAs. In such a case, the LOPs may intersect at multiple points without intersecting altogether at a single point [Caffery, 2000]. The geometric techniques do not provide a theoretical basis for such data fusion approaches. The simplest and common way for is to calculate a mean value of the intersection coordinates. More advanced mechanisms for the combination of the intersection points are proposed in [Chen, 2009].

3.2.2.2 Linearization methods

The localization problem can be seen as the solution to a system of non-linear equations given by:

$$z_i = f_i(x, y) + n_i,\ i = 1,\ldots, N \tag{3.6}$$

where N is the number of measurements, n_i is the noise at the i-th measurement, and $f_i(x, y)$ is the true value of the i-th signal parameter, which is a function of the position of the target, (x, y).

In case of TOA-based systems, $f_i(x, y)$ in (3.6) can be expressed as

$$f_i(x, y) = \sqrt{(x_i - x)^2 + (y_i - y)^2} \tag{3.7}$$

where (x_i, y_i) is the position of the i-th reference node.

In vector notations, the measurement model in (3.6) can be expressed as

$$\mathbf{z} = \mathbf{f}(x, y) + \mathbf{n} \tag{3.8}$$

where $\mathbf{z} = [z_1 \cdots z_N]^T$, $\mathbf{f}(x, y) = [f_1(x, y) \cdots f_N(x, y)]^T$ and $\mathbf{n} = [n_1 \cdots n_N]^T$.

For ease of analysis, we assume that each measurement error n_i is a zero-mean white Gaussian process with known variance σ_i^2. Even in this simple situation, the resulting set of equations is nonlinear and, in the general case, over-determined, and therefore, it cannot be solved in an exact closed way. However, both approximate closed-form and exact iterative solutions can be provided using linearization techniques.

One simple linearization scheme expands equation (3.6) and groups together the nonlinear terms in an additional variable [Cheung, 2004]. If no measurement errors are considered, through a straightforward manipulation we arrive to the following matricial form:

$$\mathbf{A}\boldsymbol{\theta} = \mathbf{b} \tag{3.9}$$

or

$$\begin{bmatrix} x_1 & y_1 & -0.5 \\ \vdots & \vdots & \vdots \\ x_N & y_N & -0.5 \end{bmatrix} \begin{bmatrix} x \\ y \\ R^2 \end{bmatrix} = \frac{1}{2} \begin{bmatrix} x_1^2 + y_1^2 - z_1^2 \\ \vdots \\ x_N^2 + y_N^2 - z_N^2 \end{bmatrix} \tag{3.10}$$

where $R^2 = x^2 + y^2$. In the presence of measurement errors, $\boldsymbol{\theta}$ can be estimated using the standard least-squares (LS) solution:

$$\hat{\boldsymbol{\theta}} = \arg\min_{\boldsymbol{\theta}} (\mathbf{A}\boldsymbol{\theta} - \mathbf{b})^T (\mathbf{A}\boldsymbol{\theta} - \mathbf{b}) = (\mathbf{A}^T\mathbf{A})^{-1}\mathbf{A}^T\mathbf{b} \tag{3.11}$$

Although this method provides a closed form solution, the results are not optimal, since the third element of vector $\boldsymbol{\theta}$ is not an independent variable. If the measurement error is assumed to follow a zero-mean Gaussian distribution $p_n(n)$=N(0,$\boldsymbol{\Sigma}$) where $\boldsymbol{\Sigma}$ is the covariance matrix of the measurement error, least-squares solution is found by the pseudoinverse:

$$\hat{\boldsymbol{\theta}} = (\mathbf{A}^T\boldsymbol{\Sigma}^{-1}\mathbf{A})^{-1}\mathbf{A}^T\boldsymbol{\Sigma}^{-1}\mathbf{b} \tag{3.12}$$

$\boldsymbol{\Sigma}^{-1}$ can be seen as a weighting matrix, where the weights are inversely proportional to the variance of the measurements since a larger variance means a less reliable measurement.

Another simple linearization technique based in linear LOPs [Caffery, 2000] consists in subtracting the first equation of (3.10) from the remaining others; obtaining a linear system of equations of the general form given by equation (3.9), with

$$\mathbf{A} = \begin{bmatrix} x_2 - x_1 & y_2 - y_1 \\ \vdots & \vdots \\ x_N - x_1 & y_N - y_1 \end{bmatrix}, \boldsymbol{\theta} = \begin{bmatrix} x \\ y \end{bmatrix}, \mathbf{b} = \frac{1}{2}\begin{bmatrix} (x_2^2 + y_2^2) - (x_1^2 + y_1^2) + z_1^2 - z_2^2 \\ \vdots \\ (x_N^2 + y_N^2) - (x_1^2 + y_1^2) + z_1^2 - z_N^2 \end{bmatrix} \tag{3.13}$$

and consequently the Least Squares solution in equation (3.11) applies. Although these equations are truly linear in the mobile station (MS) coordinates, we have discarded information during the linearization process, and therefore this method does not provide optimum estimations either.

Another linearization technique is based on the definition of Range Differences (RD) [Smith, 1987]. Let N denote the number of sensors, and let d_{ij} denote the RD between sensors i and j (i, j = 1,...,N). The vector of (x,y) spatial coordinates for the i-th sensor is denoted $\mathbf{x}_i$, and the position of the target is denoted $\mathbf{x}_s$. The distance between the target and sensor i is denoted by $D_i = ||\mathbf{x}_i - \mathbf{x}_s||$, and the distance from the origin to the point $\mathbf{x}_i$ is denoted R_i. Similarly, $R = ||\mathbf{x}_s||$. We have the following basic relation:

$$d_{ij} = D_i - D_j, \; i = 1,..., N, \; j = 1,..., N \tag{3.14}$$

The localization problem is to determine $\mathbf{x}_s$ given d_{ij} for i and j between 1 and N. Note that there are $N(N-1)/2$ distinct RDs d_{ij} (excluding $i=j$, and counting each $d_{ij} = -d_{ji}$ pair once).

It is desired to estimate the source location as the one which best fits the measured RDs. The L_2 norm of the vector difference between the measured range differences and those given by a hypothesized source location is a natural choice for a goodness-of-fit criterion. However, it is a non-convex function of the source location, and serious difficulties occur in computing its minimizer. The source localization problem can be solved in closed form by picking the source location as the minimizer of the norm of a so-called "equation error," i.e., the minimizer of the difference between values of functions of the measured range differences and functions of a hypothesized source location.

We first map the spatial origin to an arbitrary sensor, say the *j*-th. From the Pythagorean theorem and (3.14), we have N - 1 equations as:

$$0 = R_i^2 - d_{ij}^2 - 2R_s d_{ij} - 2\mathbf{x}_i^T \mathbf{x}_s \tag{3.15}$$

As the delays are typically not measured precisely, a so-called "equation error" is introduced into the left side of (3.15), and minimized in a least-squares sense to provide an estimate of the true solution. Without loss of generality, let j = 1. Then (3.15) becomes

$$e_i = R_i^2 - d_{i1}^2 - 2R_s d_{i1} - 2\mathbf{x}_i^T \mathbf{x}_s \quad i = 2, 3, ..., N \tag{3.16}$$

where e_i is the equation error to be minimized. The set of N - 1 equations (3.16) can be written in matrix notation as

$$\mathbf{e} = \boldsymbol{\delta} - 2R_s \mathbf{d} - 2\mathbf{S}\mathbf{x}_s \quad i = 2, 3, ..., \tag{3.17}$$

where

$$\boldsymbol{\delta} = \begin{bmatrix} R_2^2 - d_{21}^2 \\ R_3^2 - d_{31}^2 \\ \vdots \\ R_N^2 - d_{N1}^2 \end{bmatrix}, \mathbf{d} = \begin{bmatrix} d_{21} \\ d_{31} \\ \vdots \\ d_{N1} \end{bmatrix}, \mathbf{S} = \frac{1}{2} \begin{bmatrix} x_2 & y_2 \\ x_3 & y_3 \\ \vdots & \vdots \\ x_N & y_N \end{bmatrix}$$

It is worth noting that the equation error vector (3.17) is linear in $\mathbf{x}_s$, given R_s, and it is linear in R_s, given $\mathbf{x}_s$. The formal least-squares solution for $\mathbf{x}_s$ given R_s is

$$\mathbf{x}_s = \frac{1}{2}(\mathbf{S}^T\mathbf{S})^{-1}\mathbf{S}^T(\boldsymbol{\delta} - 2R_s\mathbf{d}) \tag{3.18}$$

If it is desired to weight the RDs according to a priori confidence in each RD, then the weighted equation error energy $\mathbf{e}^T\mathbf{W}\mathbf{e}$ is minimized for:

$$\mathbf{x}_s = \frac{1}{2}(\mathbf{S}^T\mathbf{W}\mathbf{S})^{-1}\mathbf{S}^T\mathbf{W}(\boldsymbol{\delta} - 2R_s\mathbf{d}) \tag{3.19}$$

where **W** is a symmetric positive definite (or simply diagonal and positive). The source range R_s, is not typically known a priori, and to obtain $\mathbf{x}_s$ minimizing $\mathbf{e}^T\mathbf{W}\mathbf{e}$ it is necessary to allow R_s to vary, maintaining the relation $R_s = ||\mathbf{x}_s||$. This is a difficult nonlinear minimization problem. However, in this case, the nonlinearity can be approximately eliminated. Two techniques are proposed:

- Spherical Interpolation (SI) [Smith, 1987]: The basic idea of the new closed-form solution is to substitute (3.18) into (3.17) and minimize the equation error again, this time with respect to R_s. This yields a linear least-squares problem for finding R_s. The technique is made possible by the fact that the formal least-squares estimate of $\mathbf{x}_s$, given R_s, in (3.17) is itself linear in R_s. When the minimizing R_s value is found in this new linear equation, the corresponding value of $\mathbf{x}_s$ via (3.18) is automatically a minimizer of the squared equation-error norm with respect to $\mathbf{x}_s$, given this R_s.
- Spherical intersection (SX) [Schau, 1987]: The SX solution is obtained by substituting the least-squares solution for $\mathbf{x}_s$ given R_s (3.18) into the quadratic equation $R_s^2 = \mathbf{x}_s^T\mathbf{x}_s$. This yields to a quadratic equation with two possible solutions. The positive root is taken as an estimate of the distance R_s. This value of R_s is then substituted into (3.18) to obtain the source location $\mathbf{x}_s$.

Closed-form solutions, while convenient, do not provide maximum likelihood position estimations, and will in general be biased, even for the case of unbiased Gaussian errors in the measurements. Least-squares estimations can be obtained from the nonlinear equations by non-linear least-squares (NL-LS) minimization methods.

3.2.2.3 Cost function minimization methods

Optimization-based methods are based on the minimization of a certain objective function to produce the optimal position estimate.

- Non-linear least-squares minimization

Since the aim of positioning is to obtain an accurate position estimate, it is natural to define the objective function as the sum of the squared range errors:

$$F(\mathbf{x}) = \sum_{i=1}^{N}(z_i - f_i(\mathbf{x}))^2 \tag{3.20}$$

where $f_i(\mathbf{x})$ is defined in equation (3.7). There exist many optimization methods to minimize the pre-defined objective function to achieve the optimal performance (i.e. the optimal position estimate in our case).

A simple approach for solving the nonlinear least squares problem in (3.20) is the steepest descent method [Caffery, 1998], where successive location estimates are updated according to the recursion:

$$\mathbf{x}_{k+1} = \mathbf{x}_k - \mu \nabla_{\mathbf{x}} F(\mathbf{x}_k) \tag{3.21}$$

where μ is a constant (scalar or diagonal matrix), $\mathbf{x}_k = (x_k, y_k)$ and $\nabla_{\mathbf{x}} F(\mathbf{x}_k)$ is the gradient vector of $F(\mathbf{x})$ with respect to x and y evaluated in $\mathbf{x}_k$. The recursion in equation (3.21) continues until $\|\nabla_{\mathbf{x}} F(\mathbf{x}_k)\|$ is smaller than some prescribed tolerance ε. One drawback of the steepest descent method is its slow convergence.

Another simple approach is linearizing $f(\mathbf{x})$ with a Taylor series expansion [Foy, 1976]. In Taylor series method, a set of nonlinear equations is linearized by expanding it in a Taylor series around a point (initially an estimate of the actual position) and keeping only terms below second order. The set of linearized equations is solved to produce a new approximate position and the process continues until a pre-specified criterion is satisfied.

The mathematical problem is to estimate target's position $\mathbf{x}$ in (3.8) given the N measurements z_i and the function $f_i(\mathbf{x})$. The errors n_i are assumed to have zero-mean and a covariance matrix $\mathbf{\Sigma}$. If $\mathbf{x}_0 = (x_0, y_0)$ is an initial guess of the solution, then $\mathbf{x}=\mathbf{x}_0+\boldsymbol{\delta}$ where $\boldsymbol{\delta}=(\delta_x, \delta_y)$. Expanding $\mathbf{f}$ in Taylor series and keeping only terms below second order:

$$\mathbf{n} = \mathbf{z} - \mathbf{f}(\mathbf{x}_0) + \mathbf{J}(\mathbf{x}_0)\boldsymbol{\delta} \tag{3.22}$$

where $\mathbf{J}$ is the Jacobian of $\mathbf{f}$ (matrix of partial derivatives of f_i with respect to x and y). Then the value of $\boldsymbol{\delta}$ that gives the least-sum-squared error in these relations with the terms in the sum weighted according to the covariances of the measurement errors is:

$$\boldsymbol{\delta} = (\mathbf{J}^T(\mathbf{x}_0)\mathbf{\Sigma}^{-1}\mathbf{J}(\mathbf{x}_0))^{-1}\mathbf{J}^T(\mathbf{x}_0)\mathbf{\Sigma}^{-1}(\mathbf{z} - \mathbf{f}(\mathbf{x}_0)) \tag{3.23}$$

Then, a new solution $\mathbf{x}_1$ is computed as $\mathbf{x}_1 = \mathbf{x}_0+\boldsymbol{\delta}$ and the process is repeated. The iterations will have converged when δ_x and δ_y are essentially zero. Taylor linearization might be prone to convergence errors and sensitivity to initial conditions. A good position seed for the Taylor expansion can be provided by the closed form solutions described in the previous subsection. Furthermore, there is a functional dependence with the geometric arrangement of the reference nodes placed at positions $\{\mathbf{x}_i\}$. When the target is either close to the reference

nodes or near the perimeter of the area defined by the polygon with the reference nodes as its vertices, then the linear approximation approach has convergence problems. This may lead to large errors of the position estimation relative to estimations of the measured quantities themselves. This phenomenon of amplification of the error is called the dilution of precision (DOP).

Another possible approach is the Newton-Gauss method [Yu, 2006]. Expanding the objective function in the Taylor series at the current point $\mathbf{x}_k$ and taking the first three terms, we have:

$$F(\mathbf{x}_k, \mathbf{s}_k) \approx F(\mathbf{x}_k) + \mathbf{g}_k^T \mathbf{s}_k + \frac{1}{2}\mathbf{s}_k^T \mathbf{G}(\mathbf{x}_k)\mathbf{s}_k \tag{3.24}$$

where $\mathbf{s}_k$ is the directional vector (or increment vector) to be determined, $\mathbf{g}_k$ is a vector of the first partial derivatives (also called gradient) of the objective function at $\mathbf{x}_k$, and $\mathbf{G}(\mathbf{x}_k)$ is the Hessian of the objective function. Minimization of the right hand side of (3.24) yields

$$\mathbf{G}(\mathbf{x}_k)\mathbf{s}_k = -\mathbf{g}_k \tag{3.25}$$

The minimization in which $\mathbf{s}_k$ is defined by equation (3.25) is termed Newton's method [Fletcher, 1987]. To avoid the calculation of the second order information in the Hessian, a simplified expression can be approached from (3.25), resulting in

$$\mathbf{J}_k^T \mathbf{J}_k \mathbf{s}_k = -\mathbf{J}_k^T \mathbf{f}(\mathbf{x}_k) \tag{3.26}$$

where $\mathbf{J}_k$ is the Jacobian matrix of $\mathbf{f}(\mathbf{x})$ at $\mathbf{x}_k$. This is termed the Gauss–Newton method. When $\mathbf{J}_k$ is full rank, which is the usual case of an over-determined system, we have the linear least-squares solution

$$\mathbf{s}_k = -(\mathbf{J}_k^T \mathbf{J}_k)^{-1} \mathbf{J}_k^T \mathbf{f}(\mathbf{x}_k) \tag{3.27}$$

The Gauss–Newton method may not perform well when the second order information in the Hessian is non-trivial. A method to overcome this is the Levenberg–Marquardt method. The Levenberg–Marquardt search direction is defined as the solution of the equations

$$(\mathbf{J}_k^T \mathbf{J}_k + \lambda_k \mathbf{I})\mathbf{s}_k = -\mathbf{J}_k^T \mathbf{f}(\mathbf{x}_k) \tag{3.28}$$

where λ_k is a non-negative scalar which controls both the magnitude and direction of $\mathbf{s}_k$.

Finally, quasi-Netwon methods are similar to Newton methods, but the Hessian matrix $\mathbf{G}(\mathbf{x}_k)$ in (3.25) is now approximated by a symmetric positive definite matrix $\mathbf{B}_k$, which is updated during each iteration. At the k th iteration, set

$$\mathbf{s}_k = -\mathbf{B}_k \mathbf{g}_k \tag{3.29}$$

Using line search along $\mathbf{s}_k$ produces

$$\mathbf{x}_{k+1} = \mathbf{x}_k + \alpha \mathbf{s}_k \tag{3.30}$$

where α is the step size. Then $\mathbf{B}_k$ is updated to yield $\mathbf{B}_{k+1}$. There exist different ways of updating $\mathbf{B}_k$. One well known updating formula is the DFP (Davidon–Fletcher–Powell) formula [Fletcher, 1963]. The initial matrix $\mathbf{B}_1$ can be any positive definite matrix. It is usually set to be the identity matrix in the absence of any better estimate. Another important formula is the BFGS (Broyden–Fletcher–Goldfarb–Shanno) formula [Fletcher, 1987] although it requires significantly greater computational effort.

The cost function can be enhanced with the use of weights. The weights α_i reflect the reliability of the measured distance for the reference node i.

$$F(\mathbf{x}) = \sum_{i=1}^{N} \alpha_i^2 (z_i - f_i(\mathbf{x}))^2 \tag{3.31}$$

Another possible improvement is a constrained NL-LS approach based on the fact that the range error is always positive. The range estimates are always greater than the true ranges due to multipath and NLOS propagation. Therefore, the true location of the target must lie inside the circles of radius z_i and centered in the reference node i for i=1,...,N, since the target cannot lie farther from a reference node than its corresponding range estimate. Mathematically, this implies

$$z_i - f_i(\mathbf{x}) \geq 0 \tag{3.32}$$

The area within the constraint boundaries is known as the feasible region. A constrained NL-LS approach can be used to force the estimate at each iteration to satisfy (3.32). There are many approaches to forming numerical solutions for NL-LS problems with nonlinear inequality constraints. One simple method uses penalty functions to modify the objective function and form a solution using an unconstrained approach [Beveridge, 1970]. The penalty function provides a large penalty to the objective function when one or more of the constraints are violated. The objective function in (3.31) is modified to include the penalty functions as follows:

$$F(\mathbf{x}) = \sum_{i=1}^{N} \alpha_i^2 (z_i - f_i(\mathbf{x}))^2 + P \sum_{i=1}^{N} \left[z_i - f_i(\mathbf{x}) \right]^{-1} \tag{3.33}$$

where P is positive for minimization. As any constraint is approached during the search, the penalty term forces toward infinity, thus forming a natural optimum within the feasible region. This approach requires that the initial guess is placed within the feasible region.

Initially, an unconstrained search method is used to provide an artificial optimum $\mathbf{x}_1$ with a large value of $P = P_1$. The next stage is initialized with the previous estimate $\mathbf{x}_1$ and uses a smaller $P = P_2$ to provide a better approximation to the true optimum. The penalty constraints become smaller at each stage. In this way, the solution approaches the constraints more closely, if the optimum happens to lie close to one of the constraints. The search continues until several iterations fail to produce a change in the objective function. This formulation essentially replaces a constrained optimization by a sequence of unconstrained optimizations.

Another constrained optimization algorithm denoted as Range-Scaling Algorithm (RSA) is proposed in [Venkatraman, 2004]. If the measured ranges are represented as z_i and the true ranges are denoted as $f_i(\mathbf{x})$, then the true ranges can be written in terms of the measured ranges as:

$$f_i(\mathbf{x}) = \alpha_i z_i \text{, i=1, 2, 3} \tag{3.34}$$

where, for NLOS propagation,$0<\alpha_i \leq 1$. The values are restricted in such a way since the NLOS error is a large positive bias that causes the measured ranges to be greater than the true ranges. It is assumed that the measurement noise is a zero-mean Gaussian random process with relatively small standard deviation and that its effect is negligible compared to the NLOS error. The vector of scale factors $\mathbf{v}$ is defined as:

$$\mathbf{v} = \left[\alpha_1^2 \;\; \alpha_2^2 \;\; \alpha_3^2 \right]^T \tag{3.35}$$

The goal of the algorithm is to compute values for α_1, α_2 and α_3 so that the LOS ranges to the reference nodes can be estimated. Once the adjusted ranges are determined, they can be used in any TOA-based geometrical algorithm. Using geometric and trigonometric relationships it is possible to obtain a non-linear relationship $g(\mathbf{v})$ between α_1, α_2 and α_3, such as $g(\mathbf{v}) = 0$ that can be used as a nonlinear constraint on their values. Furthermore, given the NLOS corrupted range measurements and reference nodes locations, the lower and upper bounds of the scale factors α_i can be derived. Since the NLOS error is always positive, the measured ranges are greater than the true ranges ($\alpha_i \leq 1$) and the target location lies in the

region of overlap of the range circles. On the other hand, if the NLOS error is too large, then the true range circles will not overlap or intersect. Since we know that the true range circles should intersect at the target location, this is not possible and, therefore, lower bounds on α_i can be obtained ($\mathbf{v}_{min}$).

The location-estimation problem is formulated as a nonlinear optimization problem with both nonlinear and linear constraints. The cost function to be minimized is taken to be the sum of the square of the distances from the target location to the points of intersection of the range circles closest to it (denoted as *U*, *V* and *W*). The objective function to be minimized for the nonlinear optimization problem is, therefore:

$$f(x,y)=(x-U_x)^2+(y-U_y)^2+(x-V_x)^2+(y-V_y)^2+(x-W_x)^2+(y-W_y)^2 \quad (3.36)$$

Target location can be computed in terms of the scale factors by substituting (3.34) in the true range equations given in (3.7) and solving for *x* and *y* using the linear lines-of-position (LLOP) algorithm [Caffery, 2000] that was previously explained in subsection 3.2.2.1. Then the objective function $F(\mathbf{v})$ in terms of v rather than the target coordinates can be obtained. Then the constrained minimization problem can be defined as $\mathbf{v}_{opt}=\arg\min F(\mathbf{v})$ subject to $g(\mathbf{v})=0$ and $\mathbf{v}_{min}\leq\mathbf{v}\leq\mathbf{v}_{max}$ where $\mathbf{v}_{max}=[1\ 1\ 1]^T$. Finally, target location is determined by substituting $\mathbf{v}_{opt}$ into the LLOP algorithm solution.

- Maximum likelihood estimation

If the probability density function of the noise **n** is known, parametric approaches can be employed. Depending on the availability of prior information about the position of the target node **x**, Bayesian or maximum likelihood (ML) estimation techniques can be applied [Sahinoglu, 2008]. In case there is no prior information about **x** the ML estimation is commonly used, which finds the value of **x** that maximizes the likelihood function:

$$\hat{\mathbf{x}}_{ML} = \arg\max_{\mathbf{x}} p(\mathbf{z}|\mathbf{x}) \quad (3.37)$$

Since **f** (x,y) is a deterministic function, by substituting equation (3.8) in equation (3.37), the likelihood function can be expressed as

$$p(\mathbf{z}|\mathbf{x}) = p_n(\mathbf{z}-\mathbf{f}(x,y)|\mathbf{x}) \quad (3.38)$$

where $p_n(\cdot|\mathbf{x})$ represents the conditional probability density function of the noise vector **n** for the target position **x**. Direct optimization of the cost function is applicable to arbitrary error probability density functions (PDF) $p_n(\cdot|\mathbf{x})$, and provides maximum likelihood position

estimations. If the noise components are independent, the likelihood function in (3.38) can be expressed as

$$p(\mathbf{z}|\mathbf{x}) = \prod_{i=1}^{N} p_{ni}(z_i - f_i(x,y)|\mathbf{x}) \tag{3.39}$$

where $p_{ni}(\cdot|\mathbf{x})$ represents the conditional probability density function for the i-th noise component given the target position $\mathbf{x}$. The independent noise assumption is usually valid for TOA, RSS and AOA measurements. However, for TDOA measurements the noise components are correlated since each TDOA is computed with respect to the same reference node. In LOS conditions, the parameters of the noise can be assumed to be known, since the measurement noise is mainly due to thermal noise. Also, it is possible to model each noise component by a zero mean Gaussian random variable in LOS scenarios

$$p_{ni}(n) = \frac{1}{\sqrt{2\pi}\sigma_i} \exp\left(-\frac{n^2}{2\sigma_i^2}\right) \tag{3.40}$$

Then, the likelihood function in (3.38) can be expressed as

$$p(\mathbf{z}|\mathbf{x}) = \frac{1}{(2\pi)^{N/2}\prod_{i=1}^{N}\sigma_i} \exp\left(-\sum_{i=1}^{N}\frac{(z_i - f_i(x,y))^2}{2\sigma_i^2}\right) \tag{3.41}$$

From (3.41), the ML estimator in (3.37) can be obtained as

$$\hat{\mathbf{x}}_{ML} = \arg\min_{\mathbf{x}} \sum_{i=1}^{N} \frac{(z_i - f_i(x,y))^2}{\sigma_i^2} \tag{3.42}$$

which is equivalent to the non-linear least-squares estimator in equation (3.31). Note that the weights are inversely proportional to the variance of the measurements since a larger variance means a less reliable measurement. Consequently, NL-LS minimization techniques previously explained are ML estimators for uncorrelated Gaussian noise.

In case of TDOA-based location, the noise vector is modeled as a multivariate Gaussian random variable. For a noise distribution with zero mean and a known covariance matrix $\mathbf{\Sigma}$, the ML position estimate can be calculated as:

$$\hat{\mathbf{x}}_{ML} = \arg\min_{\mathbf{x}} (\mathbf{z} - \mathbf{f}(x,y))^T \mathbf{\Sigma}^{-1} (\mathbf{z} - \mathbf{f}(x,y)) \tag{3.43}$$

which is called the Weighted Least Squares (WLS) solution.

In case of NLOS propagation, the noise distribution can be considerably different from the Gaussian model in (3.40). As an example, for TOA estimation, the range measurements in NLOS conditions contain an NLOS error, in addition to the error observed in LOS measurements which are mainly due to background noise. The NLOS error is always positive since the first arriving signal component travels an extra distance. Therefore, the measurement noise can be modeled as the sum of two noise terms, one related to the background noise, and the other related to the NLOS error. Common models for the NLOS error include Exponential distribution [Cong, 2005], Gamma distribution [Qi, 2004] and distributions based on certain scattering models [Al-Jazzar, 2002]. In [Denis, 2004], a weighted sum of Gaussian and Exponential components for different channel configurations {LOS, NLOS, NLOS2} is proposed.

Some protection against NLOS outliers is achieved by converting the unconstrained minimization problem in equation (3.37) into a constrained one, as suggested in [Morley, 1995]. Let the excess-range error that corrupts a measured ranging estimate be a random variable R, with probability density function $e^+(R)$. $e^+(R)$ is strictly one sided, i.e. $e^+(R < 0) = 0$, since multipath reflections always cause a propagation time larger than that corresponding to the actual range, and is also zero at values above the measured range; i.e. $e^+(R > z) = 0$. Using $e^+(R)$ at each range estimation z_i, the location estimate is defined as that $\mathbf{x}$ for which the product of all ranging estimate probabilities is maximized

$$\hat{\mathbf{x}} = \arg\max_{\mathbf{x}} \prod_{i=1}^{N} p_{e^+}(z_i - f_i(x, y)\big|\mathbf{x}) \tag{3.44}$$

The same optimization methods presented for NL-LS can be used to minimize the objective function to achieve the optimal position estimate, such as gradient descent, Taylor series, Gauss–Newton, quasi-Newton or Levenberg-Marquardt. As the objective function is non-convex, convergence problems may arise for bad initialization values and also when the target is close to the reference nodes or near the perimeter of the area defined by the polygon with the reference nodes as its vertices.

3.2.2.4 Bayesian methods

Bayesian methods for position estimation can be viewed as an extension of the ML estimators when prior information about the distribution of target's position $\mathbf{x}$ is available [Fox, 2003]. The information about the position of the target at time t is modeled as a probability distribution $p(\mathbf{x}_t|\mathbf{z}_1, \mathbf{z}_2, \ldots, \mathbf{z}_t)$, based in the set of all past sensor measurements $\mathbf{z}_1, \mathbf{z}_2, \ldots, \mathbf{z}_t$ obtained up till time t.

The estimation of the position of the target proceeds in two stages, called respectively the prediction and the correction steps. In the prediction step the a priori estimated position is extrapolated from previous data, without actually taking a measurement:

$$p^{-}(\mathbf{x}_t) = \int p(\mathbf{x}_t \,|\mathbf{x}_{t-1})\, p(\mathbf{x}_{t-1}) d\mathbf{x} \tag{3.45}$$

where $p(\mathbf{x}_t|\mathbf{x}_{t-1})$ is a motion model which represents the estimation of the target's position in the next time interval from the current estimated position.

After the prediction step, the correction step matches the computed estimation of position with the set $\mathbf{z}_t$ of sensor measurements collected in the time interval from t-1 to t. By Bayes rule, the posterior probability is found by multiplying the prior probability $p^{-}(\mathbf{x}_t)$, by the observation model $p(\mathbf{z}_t|\mathbf{x}_{t-1})$:

$$p(\mathbf{x}_t) = a_t\, p(\mathbf{z}_t \,|\mathbf{x}_{t-1})\, p^{-}(\mathbf{x}_{t-1}) \tag{3.46}$$

where a_t is a normalization constant such that the integral of the probability distribution over all possible positions in the displacement area is 1. The observation model $p(\mathbf{z}|\mathbf{x})$ describes the probability of receiving a measurement $\mathbf{z}$ when the user is standing at position $\mathbf{x}$ and is equivalent to the probability $p_n(\mathbf{z}_t\text{-}f(\mathbf{x}_t))$ according to the distribution of the measurement error n. Equations (3.45) and (3.46) are applied consecutively each time a new measurement is available to refine the current estimation of the target's position.

Bayesian estimation methods have a number of advantages for indoor positioning. They are robust to NLOS situations, which can be incorporated directly in the observation model. Depending on how much information we have about the probabilities of LOS and NLOS, and the PDFs of the error in both instances, effective mitigation of nonline-of-sight effects can be achieved.

$$p_n(n) = p_{LOS} N(0, \sigma_n^2) + (1 - p_{LOS})\, p_n^{NLOS}(n) \tag{3.47}$$

Bayesian location methods are iterative, which permits to improve upon previous location estimations by processing many imprecise measurements. Bayesian localization permits to accommodate naturally measurements of different nature (for example, TOA and RSS), by simply multiplying their respective observation models, which is known as Data Fusion.

Many different implementations exist in the generic frame of Bayesian localization. Kalman filters are the simplest case, in which the position error follows a normal distribution [Daum, 2005]. The Kalman filter addresses the general problem of trying to estimate the

state $\mathbf{x} \in R_n$ of a discrete-time controlled process that is governed by a linear stochastic difference equation. When the difference equation is not linear, the Extended Kalman Filter (EKF) linearizes about the current mean and covariance. Multihypothesis tracking is an extension of the Kalman filter, in which several different hypotheses for the target are simultaneously considered.

An efficient implementation of Bayesian localization which has received much attention lately is the particle filter [Gustafsson, 2002]. The advantage of the particle filter over the Kalman filter is that it allows using non-Gaussian noise. It can be visualized as an adaptive sampling of the position estimation PDF $p(\mathbf{x})$ which focuses in the areas with higher position probability for improved efficiency. In a particle filter, the probability distribution of the location is approximated by a discrete set of n points (the particles):

$$p(\mathbf{x}_t) = \left\{\left(\mathbf{x}_t^i, w_t^i\right)\right\}, \; i=1,...,n \tag{3.48}$$

where $\mathbf{x}^i_t$ is the location of the i-th particle at time t, and w^i_t is a positive weight given by the probability density of obtaining a measurement $\mathbf{z}_t$ at a position $\mathbf{x}^i_t$.

$$w_t^i = w_{t-1}^i p(\mathbf{z}_t \mid \mathbf{x}_t^i), \; i=1,...,n \tag{3.49}$$

The weights are normalized such that $\Sigma_i \; w^i_t = 1$ and the estimated position is approximated by:

$$\hat{\mathbf{x}}_t \approx \sum_{i=1}^{n} w_t^i \mathbf{x}_t^i \tag{3.50}$$

The two steps of Bayesian localization are computed over the particles of equation (3.48), which are resampled spatially at each stage to concentrate in regions where the probability density has been found to be higher.

3.2.2.5 Multidimensional-scaling methods

A novel approach was provided in [Cheung, 2005] where the use of Multidimensional Scaling (MDS) for positioning using TOA measurements was proposed. MDS is a multivariate data analysis technique used to map "proximities" into a low-dimensional space. These "proximities" can be either dissimilarities (distance-like quantities) or similarities (inversely related to distances). Classical MDS is a subset of MDS where the dissimilarities are Euclidean distances. Given n points and corresponding distances, MDS finds a set of points in a space such that a one-to-one mapping between the original configuration and the

reconstructed one exists. Then it is possible to map back the solution to the absolute reference system by Procrustes transformation.

Defining $\mathbf{x}_i$ (i = 1,...,n) as the vectors containing the coordinates for the n points in a η dimensional space, then the dissimilarities are expressed by $d_{ij}^2 = (\mathbf{x}_i\text{-}\mathbf{x}_j)(\mathbf{x}_i\text{-}\mathbf{x}_j)^T$. Therefore the inner product between two objects $\mathbf{x}_i$, $\mathbf{x}_j$, belonging to the original configuration of points can be written as $\mathbf{[B]}_{i,j} = b_{i,j} = \mathbf{x}_i \cdot \mathbf{x}_j^T$. Defining $\{\delta_{i,j}\}$ as the set of all inter-distances, then for the Classical scaling $\{\delta_{i,j}\}=\{d_{i,j}\}$ holds.

The Classical scaling solution, once that the set of all inter-distances $\{\delta_{i,j}\}$ is provided, constructs **B** before, and then recovers the unknown objects coordinates as the least square solution on the inner product matrix **B**. To overcome the indeterminacy of the solution due to translation, the centroid of the configuration is placed at the origin ($\Sigma_i \mathbf{x}_i = \mathbf{0}$, i = 1,...,n).

Grouping $\{\delta_{i,j}\}$ into a Euclidean Distance Matrix (EDM) $\mathbf{D}_{[n\times n]}$, $\mathbf{B} = \mathbf{X}\cdot\mathbf{X}^T$ can be written using the objects inter-distances as $\mathbf{B} = -1/2\ \mathbf{J}\cdot\mathbf{D}^2\cdot\mathbf{J}$, with $\mathbf{D}^2$ as the matrix of the squared distances, the "centering matrix" **J** defined as $\mathbf{J} = \mathbf{I} - n^{-1}\mathbf{e}\cdot\mathbf{e}^T$, **e** as the [n×1] unitary vector, and $\mathbf{I}_{[n\times n]}$ the identity matrix. It should be noticed that **J** defines a linear transformation and it is characterized by the orthogonal property $\mathbf{J}\cdot\mathbf{J}^T = \mathbf{I}$. Now, since **B** is a symmetric, positive semi-definite matrix of rank(**B**) = η , its eigen-decomposition, expressed by $\mathbf{B} = \mathbf{V}\cdot\mathbf{L}\cdot\mathbf{V}^T$, with **V** and **L** as the eigenvectors and the diagonal-eigenvalue matrix of **B**, allows to recover **X**. Indeed, due to rank(**B**) = rank($\mathbf{X}\cdot\mathbf{X}^T$) = rank(**X**) = η , and assuming both eigenvectors and eigenvalues ordered in descending order, **B** can be rewritten as $\mathbf{B} = \mathbf{V}_\eta\cdot\mathbf{L}_\eta\cdot\mathbf{V}_\eta^T$, with $\mathbf{L}_\eta$ = diag (l_1,...,l_η) and $\mathbf{V}_\eta$ ([$n\times\eta$]) containing the first η eigenvalues and eigenvectors respectively. Therefore, it follows that **X**, which includes the recovered coordinates for the n objects, is given by $\mathbf{X} = \mathbf{V}_\eta\cdot\mathbf{L}_\eta^{1/2}$.

X corresponds to the original configuration up rigid transformations (translation, rotation and reflections) on the axes. If η + 1 reference points, or more, are known, then it is possible to map back the solution to the absolute reference system used by Procrustes transformation. A survey on different Procrustes techniques can be found in [Sibso, 1978].

Classical scaling is based on the assumption that the dissimilarities are precisely Euclidean distances without any additional transformation. Nevertheless, in typical wireless network localization problems, ranging information is often imperfect and incomplete. Metric Least Squares MDS solves the aforementioned problem by minimizing an objective function (stress function) [Destino, 2006]. An example of stress function, corresponding to the least squares on the distance is

$$\sigma(\mathbf{X}) = \sum_{i=1}^{n}\sum_{j=1}^{n} w_{i,j}(\delta_{i,j} - d_{i,j}(\mathbf{X}))^2 \tag{3.51}$$

which is a weighted least squares minimization problem and consequently can be solved with the same methods presented in Section 3.2.2.3. Nevertheless, such a function is proven to be non-convex in the **X** variable; therefore, either a global optimization technique or a reliable starting point is required to avoid local minima. In [de Leuuw, 2009] a majorization technique is proposed to minimize stress and this MDS solving strategy is known as SMACOF (Scaling by MAjorizing a COmplicated Function). The principle of majorization is to construct a surrogate function which majorizes a particular objective function. SMACOF consists of an iterative procedure that attempts to find the minimum of a non-convex function by tracking the global minimum of the so-called majored convex function successively constructed from the original objective and basis on the previous solution. Furthermore several extensions of the basic SMACOF approach in terms of constraints on the configuration are provided.

3.2.2.6 Fingerprint methods

Due to the high variability of measured RSSI in indoor environments, fingerprint methods have been proposed for the implementation of WLAN-based location systems as they may provide an accurate estimation of position, although the concept is also applicable to TOA-based location systems. Fingerprint methods consist in two phases. In the calibration stage, a test mobile station moves through a grid of sufficiently dense set of positions $\{\mathbf{x}_j\}$ that cover the indoor environment and records the estimated distance to the different base stations BS_i, $\{d_i(\mathbf{x}_j)\}$, where $i = 1, \ldots, n$. In the localization stage, the system measures the set of distances $\{\delta_i\}$, which is compared to the previously recorded set and the position that matches it most closely is chosen as the estimation of location. One obvious choice for finding the optimal estimate of position consists in picking the grid point $\mathbf{x}_j$ which minimizes the Euclidean distance in the measurement variable space:

$$\mathbf{z}_j^2 = \sum_{i=1}^{n} (\delta_i - d_i(\mathbf{x}_j))^2 \tag{3.52}$$

A simplified analysis of this situation is given in [Kaemarungsi, 2004]. Other techniques that have been used for finding the optimal estimate of position include Bayesian inference methods [Roos, 2002], neural networks [Fang, 2008], decision trees [Yim, 2008] and statistical learning [Brunato, 2005].

Nevertheless, fingerprint methods have some drawbacks that impair their application in real situations. The calibration phase is time consuming, particularly in case of wide areas or high accuracy requirements, position estimations can only be produced in those areas where recorded data exists, and finally, in the event of modification of the indoor environment, their accuracy is greatly decreased. Consequently, fingerprint methods will not be further considered in this thesis.

3.2.2.7 Enhancements

In addition to the basic algorithms that have been presented, several enhancements to the basic algorithms have been proposed in order to overcome the problems and limitations location algorithms, and particularly to deal with NLOS propagation. Some of the most important enhancements are:

- Measurement smoothing: In order to reduce the noise of the measurements, measurements can be smoothed through averaging multiple consecutive ranging samples. In [Macagnano, 2008], pre-filtering with a wavelet-based technique is proposed.
- Weighted minimization: As it was previously commented, the use of weights in least-squares minimization methods can be used to improve the performance. Weights are inversely proportional to the variance of the measurements since a larger variance means a less reliable measurement [Cheung, 2004]. The weights proposed in [Destino, 2009] have a dispersion component, which captures the effect of noise under the assumption of bias-free samples, and a penalty component, which quantifies the risk of the latter assumption and penalizes it proportionally.
- Constrained minimization: As it was previously mentioned, the performance can also be improved by imposing constraints on the minimization based on the fact that the range error is always positive, as the range estimates are always greater than the true ranges due to multipath and NLOS propagation [Beveridge, 1970], [Venkatraman, 2004], [Morley, 1995].
- NLOS identification and mitigation: The ability to cope with NLOS conditions is the major challenge for accurate localization in indoor environments, as it introduces high positive biases to distance estimations. NLOS identification attempts to distinguish the nodes by LOS and NLOS channel conditions whereas NLOS mitigation attempts to counter the positive bias introduced in NLOS signals. Several NLOS identification and mitigation techniques for UWB have been proposed based on different signal parameters and statistics, such as SNR variation [Schroeder, 2007], RSS and delay

spread [Venkatesh, 2007], multipath channel statistics [Güvenç, 2008], mean square error [Shen, 2010], standard deviation, etc. Mitigation can be achieved by reducing the weight of NLOS measurements in weighted least squares minimization approaches [Güvenç, 2008], using the NLOS statistical model in maximum likelihood estimators [Cong, 2005], or even completely removing the NLOS measurements [Shen, 2010]. A comprehensive overview of NLOS identification and mitigation techniques can be found in [Schroeder, 2007] and [Khodjaev, 2009].

- Ranging contraction: Another NLOS mitigation technique is proposed in [Destino, 2010] based on the fact that the range error is always positive. The feasibility region is built as the area formed by the intersection of the circles with centre at the anchors and radio equal to the estimated distance. Then the contracted distances are computed as the shortest distance from each anchor to the aforementioned feasibility region and a minimization algorithm is applied using the contracted distances instead of the estimated ones.
- Data fusion: In order to improve positioning accuracy and reliability, a popular approach is to combine TOA estimations with data from different sources such as other signal parameters (AOA, RSSI), motion sensors (speedometers, accelerometers, gyroscopes) and geographic information (maps, floor plans), which is known as data fusion.
- Map matching: A particular case of data fusion with geographical information, map-matching techniques are widely extended in vehicle navigation applications in order to match the position provided by GPS and inertial sensors with the road map information [French, 1989]. The use of floor plans to enhance the movement model for pedestrian navigation was proposed in [Khider, 2009] and map filtering for indoor localization is also proposed in [Widyawan, 2008].

In this thesis, the enhancement of some location and tracking algorithms through the use of geographic information is proposed. In particular, floor plans will be used for NLOS identification and mitigation and to improve the motion model, whereas the algorithms are multidimensional scaling with weighted least squares minimization, Kalman filters and particle filters.

3.2.3 Location and tracking systems

Nowadays, a few UWB-based indoor Real-Time Location Systems can be found in the market, namely PLUS by Time Domain, Shappire Dart by Multispectral Solutions (now part

of Zebra Enterprise Solutions), and Series 7000 by Ubisense. Although there are some differences, the basic architecture of these systems is similar and is composed by the following elements:

- UWB tags: These are the elements to be located. Usually they are transmit-only devices that generate the UWB signal in order to be located by the UWB sensors. For Time Domain and Ubisense a control channel (different than the UWB channel) in the 2.4 GHz band is used for tag configuration.
- UWB sensors/receivers: These are the elements that receive the UWB signal from the tags and estimate the TOA relative to the synchronization signal (the Ubisense sensors also estimate the AOA). Interconnection between the sensors is wired (Ethernet).
- Connection hardware: Network equipment, generally a hub or switch, is used to interconnect the sensors with the location engine in order to transmit the location information and to provide synchronization and power (if Power over Ethernet is supported).
- Software location engine: The location engine processes tag location information to compute the position. It runs on a host computer connected to the network hardware, except for the Shappire Dart where the location engine is integrated in the connection hardware. A Graphical User Interface (GUI) is provided for system configuration and location display.

These systems have the following limitations:

- They are proprietary solutions, closed and not compliant with any standard.
- In spite of UWB simultaneous location and communication capability, UWB is only used for location. Other technologies are used for sensor connection and synchronization (Ethernet) and for tag control and configuration (proprietary radio at 2.4 GHz). This increases the cost and complexity of the devices.
- As sensors are connected via Ethernet, cabling is required and as a result the cost and complexity of the system deployment increases, and flexibility is reduced.
- Tags do not have any data transmission capability, so they cannot provide any functionality other than location.
- The location information can only be accessed through the software platform, and is not provided to the tags. Moreover, the tags do not provide any interface for the integration into a user device.

In contrast, UWB systems combining location and data transmission (for example in the framework of IEEE 802.15.4a standard) would increase flexibility reducing the cost and complexity of the system deployment. Furthermore, an existing UWB-based wireless sensor network (e.g. fire detection sensor network) could be reused to provide mobile users tracking. Finally, solutions based on a standard, would allow interoperability between different existing solutions and facilitate integration into user's devices.

UWB-based combined communication and location systems have been proposed in the framework of European projects EUROPCOM and PULSERS/EUWB. In [Lo, 2008] the EUROPCOM design of a UWB-based ad hoc network for search and rescue operations in disaster zones is presented. The network architecture defines physical entities and includes a complete protocol stack, from the physical layer up to the application layer. In [Pezzin, 2009] an overview of the LDR-LT open prototyping platform designed in the framework of the PULSERS II and EUWB projects is provided. This platform illustrates a fully integrated solution from physical layer up to application layer. In [Chu, 2005] a UWB-based system for indoor 3-D location services is introduced. The system relies on a three-tier hierarchical sensor architecture to cover a large indoor space while conserving battery power. The communication between the different tiers and the location procedure are also defined. Finally, in [Wu, 2009] a group of communication protocols and localization algorithms for wireless sensor networks in coal mine environments is proposed, namely a new UWB coding method, called U-BOTH (UWB based on Orthogonal Variable Spreading Factor and Time Hopping), an ALOHA-type channel access method and a message exchange protocol to collect location information.

Nevertheless, combined location and communication systems have a major drawback. TOA estimation requires the exchange of ranging frames between the element to be located and some fixed reference nodes, and additional frames are required to transmit the estimated distances to the location engine. This means that a non-negligible latency is associated to the position update process and that some temporal resources must be dedicated to location with the consequent reduction of the available data rate for non-location data communication. Consequently, multiple access and resource allocation protocols must be carefully designed in order to minimize the time delay and the throughput associated to the location functionality.

The design of MAC and network layers optimized for simultaneous location and communication has been addressed in the course of the three phases of PULSERS/EUWB project. In [Giancola, 2005] an early approach to UWB MAC and network layer issues for LDR-LT applications is provided. Various intended UWB system architectures and their key requirements and parameters are introduced. For such systems, potential MAC schemes and

network solutions are illustrated and discussed. New ideas about wireless UWB access, synchronization, resource allocation, and topology management are also presented. The MAC layer designed in the PULSERS project LDR-LT systems, is described in [Bucaille, 2007]. The MAC developed in PULSERS is based on the IEEE 802.15.4 standard, although it deviates from the standard in a few areas such as the support to peer-to-peer communications, the systematic usage of guaranteed time slots for data transmissions, dedicated time slots for ranging or allocation requests, specification of a new ranging procedure, and finally, the definition of a relaying functionality in layer 2. Furthermore, mesh algorithms are also specified. Finally, the paper focuses on the localization procedures implemented in the MAC layer. In [Macagnano, 2007] the performance of the designed MAC is studied under the point of view of tracking. Specifically, the time delay necessary to collect the ranging information in both, star and meshed topology networks, is studied as function of the number of mobiles in the network. Furthermore, a few enhancements are proposed in order to minimize the exchange of packets necessary to update the ranging information between two successive estimates of the node positions.

Besides PULSERS/EUWB project, few works can be found dealing with practical aspects such as the design of the functional architecture or the procedure for the transmission of the associated information between the different elements of the system. In [Venkatesh, 2006], MAC layer design for IR-UWB location networks is analyzed. A network in which stationary reference nodes are deployed in an ad hoc manner and determine their locations based on a small number of fixed anchors with known locations is considered. Location and range information is propagated through the network of reference nodes in order to periodically estimate the locations of mobile nodes. The principal objective of the design is to minimize the localization error and convergence time of location estimates in the presence of node mobility. A link between the throughput of the applied MAC protocol and the resulting localization accuracy is established. A spread-spectrum based MAC protocol is developed that is shown to outperform the CSMA protocol in terms of accuracy and the convergence time of location-estimates.

Chapter 4

UMTS/UWB Coexistence and Interoperability

4.1 Introduction

Low emitted power limits UWB coverage to short range, focusing the applications of UWB on Personal Area Networks. However, interconnecting in the same device UWB and Wide Area Network (WAN) access provided by wired or wireless technologies, would allow a wider scope of UWB applications. For example, using a UMTS or WiMAX gateway would allow remote monitoring of a UWB sensor network in isolated buildings such as farms or warehouses. The interconnection of UWB multimedia & data home networks with a WAN access could provide with Internet access to all the home electronic devices in the network. Further interoperability applications could be considered in a similar way.

Interoperability applications require harmless coexistence between UWB and the other technologies. In order to guarantee that actual and future radio services are not interfered by UWB, regulatory bodies have proposed restrictive spectrum masks that limit the power spectral density of UWB. Nevertheless, coexistence when UWB is collocated with other radio interface in the same device (i.e. distance shorter than 1 m), has not been subject of such interest by the regulatory framework, as avoiding the interference is under the scope of the device manufacturer. In this case coexistence is particularly critical, as UWB and the victim service are in close proximity and degradation may occur even for services working in different frequency bands due to out-of-band emission.

In this scenario, the cooperation of both interfaces could be really helpful in order to ensure harmless coexistence between them. In case any degradation is detected on the victim service, protection mechanisms are applied on the UWB interface in order to mitigate it.

In this chapter a UMTS/UWB interoperability platform is presented. This platform is used to evaluate the coexistence of UWB and UMTS/HSPA when collocated in the same device. Furthermore, cooperative mitigation techniques are proposed and assessed as a solution to guarantee harmless coexistence in interoperability applications. UMTS has been selected due to the interest of integrating UWB interfaces into mobile phones for high capacity data transmission, for example to provide connectivity with a PC (Personal Computer) or display. Furthermore, as UMTS and UWB operate in different frequency bands, coexistence studies have mainly focused in other technologies rather than UMTS, but when both transceivers are collocated in the same device, interference may occur due to out-of-band emission. Concerning UWB, WiMedia-based HDR UWB systems have been considered, as LDR systems are not so problematic regarding coexistence due to their low activity factor.

4.2 UMTS/UWB Interoperability Platform

In order to exploit the benefits of cooperation between UWB and WAN radio services, a UMTS/UWB interworking platform has been deployed focusing in a mobile health (m-health) scenario. This platform aims to provide medical assistance from a specialist doctor to patients living in isolated areas, thanks to the use of a mobile medical center. With this multimedia application, the specialist has all data required to perform a correct diagnosis remotely, since the application includes biomedical data transmission (electrocardiogram, blood pressure and pulsioximetry), videoconference, video transmission and chat [Viruete, 2005].

UWB is used to connect all the medical sensors and multimedia devices within the nomadic medical centre, taking advance of low cost, low power consumption and high data rate capacities of UWB. UMTS provides access to WAN and is used to forward this information, collected and processed by the application, to the remote specialist.

Following, the software and hardware components of the UMTS/UWB platform are described.

4.2.1 Platform architecture

The platform architecture is detailed in Figure 4.1. The application client on the nomadic medical centre collects the data from the different medical devices. It is connected through an UWB link to the bridge, which provides Internet access to the nomadic medical centre

through UMTS. Finally, the remote specialist is connected to the Internet through a fixed access.

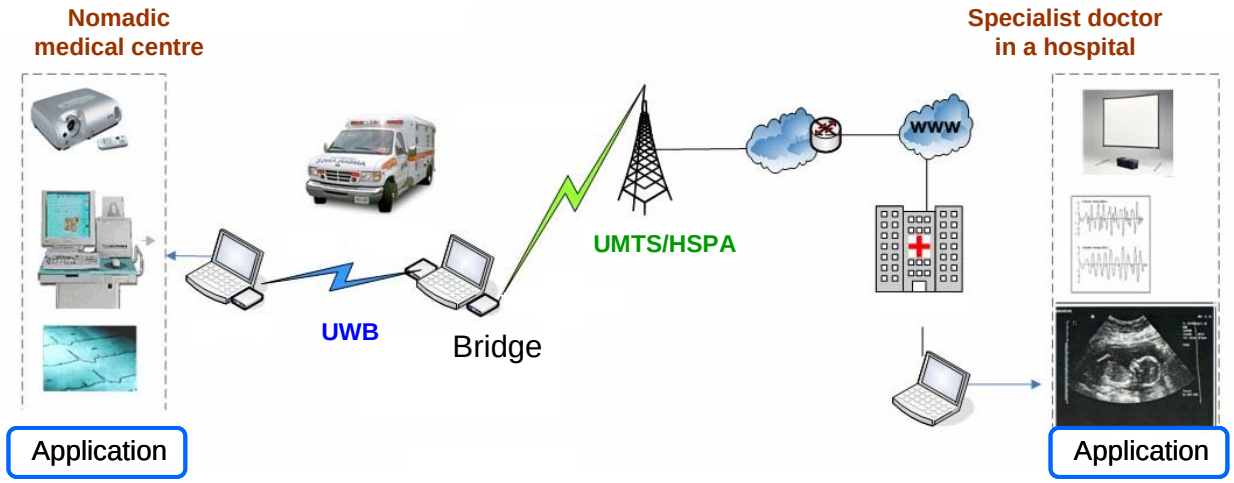

Figure 4.1. Interworking UWB/UMTS platform scenario

An objective of this initial architecture is to be independent of the WAN access technology, so the transition is performed at IP level (independent of WAN access technology PHY and MAC layers). Furthermore, the interoperability software is independent of the demonstration application. Regarding the server and the client, the application is also independent of the access technology (Ethernet, WiFi, UMTS, UWB…).

4.2.2 UWB and UMTS equipment

The UWB equipment used in the platform is a WiMedia compliant MB-OFDM UWB device (Wisair's UWB Development Kit DV9110M). This UWB kit operates in Band Group #1, which comprises Band #1 (3168-3696 MHz), Band #2 (3696-4224 MHz), and Band #3 (4224-4752 MHz). It supports all the TFC codes and PHY data rates considered on ECMA-368. Concerning power, a maximum PSD of -42 dBm/MHz is supported, which can be decreased in 1 dB steps down to -57 dBm/MHz.

Figure 4.2. Wisair Development Kit DV9110M

The equipment used in the UMTS interface of the dual device is a PCMCIA card, Aircard 850 by Sierra Wireless. It operates in the 2.1GHz band and supports HSDPA, with data rates up to 1.8 Mbps (downlink) and 384 Kbps (uplink) when HSDPA is available.

4.2.3 Interoperability software

The interoperability software is a bridge connecting UWB and UMTS interfaces, so that UWB devices get WAN access. Starting from a device in which both network interfaces implement TCP/UDP protocol stack, the bridge provides the following functionalities:

- NAT (Network Address Translation): Since the UWB network IP addresses are private, the bridge has to map the outer connections to inner connections.
- Forwarding: The bridge has to route the packets from the inner network to the UMTS terminal and vice versa.
- Monitoring & configuration: The bridge has to monitor transmission parameters on the UMTS interface and to monitor and configure transmission parameters on the UWB interface.

The NAT procedure addresses the modification of IP addresses and ports with the aim of mapping the private and public connections. These translations are saved in a gateway table in order to adequately forward the packets between the internal and external network. The NAT procedure implemented on bridge's software is performed at Transport Layer and the use of sockets to interconnect both networks becomes necessary.

Through a GUI, the user is able to select the interfaces to perform the bridging (UMTS or UWB). Moreover the possibility of visualizing all the connections created through the bridge is also offered to the user, showing the IP addresses and the ports taking part in the communication, offering also the possibility to display statistics corresponding to the amount

of data received/sent on each interface and the throughput, instantaneous or average, of the data traffic on each direction.

4.2.4 Application software

Within the mobile healthcare system that has been presented, the teleechocardiography module, which implements ultrasound video transmission in real-time, has been selected for testing purpose. This module allows acquiring, processing, storing and transmitting ultrasound and medical videos in real time.

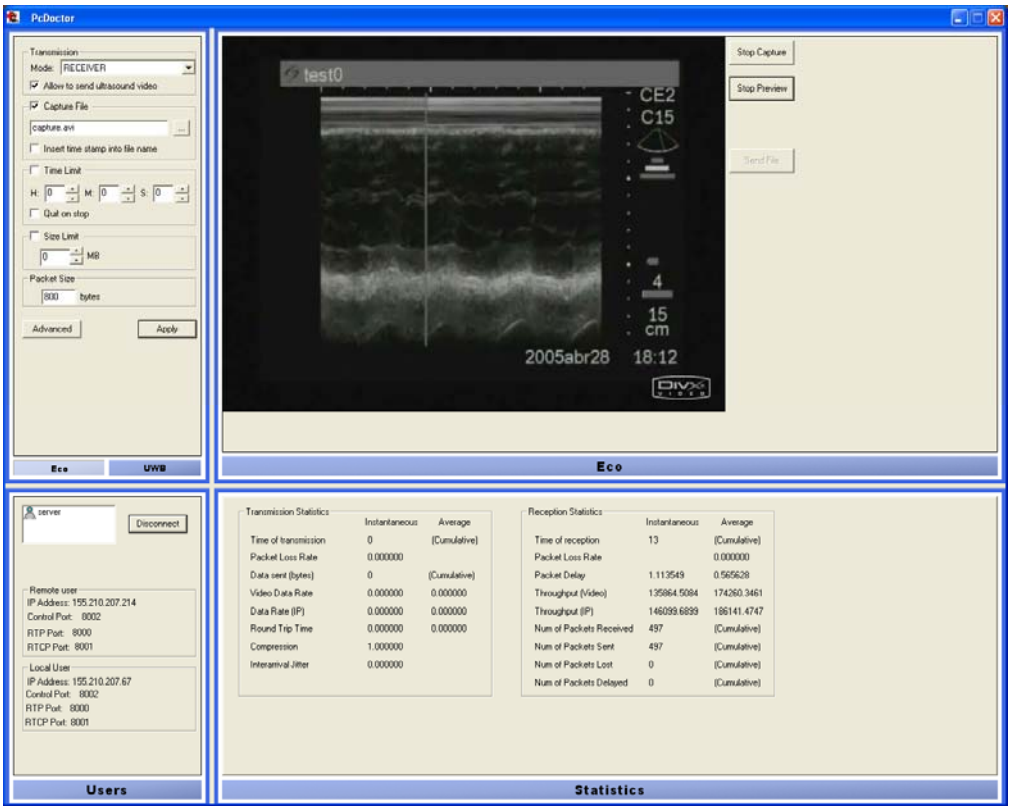

Figure 4.3. GUI of the echocardiography streaming module

Real-time video transmission is done by means of RTP (Real-time Transport Protocol) and RTCP (Real-Time Control Protocol) protocols. On the transmitter side, compressed video frames are fragmented according to a maximum packet size. With each one of these fragments an RTP packet is built and transmitted over the network.

In order to measure the performance of the interworking UMTS-UWB platform, a real-time Quality of Service (QoS) monitoring module has been developed. Instantaneous and average values for some parameters are shown on the statistics displaying area. Final

average values are also stored in a report file, as well as traces of all values obtained during the transmission. Different parameters have been considered in order to evaluate the performance:

- RTP packet loss rate is defined as the ratio of the number of RTP data packets lost and the number of RTP data packets sent.
- Average throughput is defined as the amount of data received per second. Throughput was measured at application level (video data) and does not take account of headers for lower layer protocols.
- Round-trip delay is a measure of propagation delay using RTCP Sender Report and Receiver Report timestamps. It can be used as an approximation to packet delay.
- Interarrival jitter is an estimate of the statistical variance of the RTP data packet interarrival time. It is defined to be the mean deviation (smoothed absolute value) of the difference in packet spacing at the receiver compared to the sender for a pair of packets.
- PSNR (Peak Signal to Noise Ratio) is commonly used as a measure of quality of reconstruction in image compression, etc. It is a function of the Mean Square Error of the received sequence compared to the original sequence.

For testing purpose, the user is able to set the main attributes for video acquisition (resolution, color format and frame rate) and choose between the different compression algorithms available in the device. For some of them, such as DivX and XVid, the user can choose the target data rate and other compression parameters. The user can also control physical parameters of the UWB devices, such as transmission power, PHY data rate and TFC code.

4.3 Evaluation of Coexistence between UMTS and UWB

4.3.1 Measurement methodology and scenario

To have a more accurate idea about the interference effects of the UWB technology on UMTS, coexistence and interworking of both technologies are compared with other ideal assumptions, that can be represented by a single UMTS link (for coexistence scenarios) and

the interworking between UMTS and Ethernet (for interworking scenarios). For that purpose, some previous tests considering a single UMTS link scenario and a UMTS and Ethernet interworking scenario were performed. Eventually, the following scenarios were set-up:

- UMTS coexisting with UWB

The video client device presents two interfaces, UWB with a private network and UMTS with the Internet. The video streaming is transmitted from a video server placed in the public network to the video client over an UMTS link. At the same time, the video client is on an independent and continuous UWB transmission with an UWB device placed in the private network. See Figure 4.4.

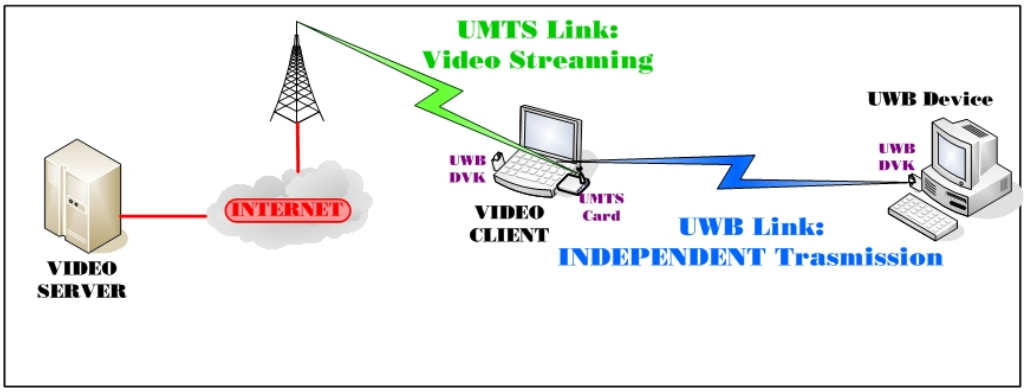

Figure 4.4. UMTS coexisting with UWB scenario

- UMTS interworking with UWB

The video server is located in the public network and the video client is placed in the UWB network, and because of that it has no direct link with the video server. So that, it requires the intervention of an UMTS/UWB dual bridge in order to allow the video-streaming transmission. Provided that both UWB transceivers are close enough to consider the UWB lossless, packet losses are mostly due to the UMTS link and we may study the influence on the QoS performance of possible interference provoked by UWB compared to a UMTS/Ethernet scenario. See Figure 4.5

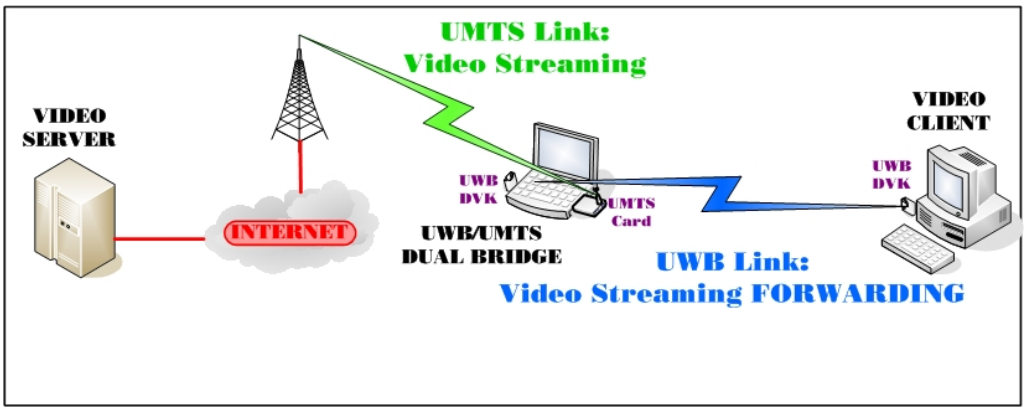

Figure 4.5. UMTS interworking with UWB scenario

The distance between the UWB devices was set to 1.5 meters. In order to evaluate collocation of UWB and UMTS in the same device, the distance between the UWB antenna and the UMTS antenna was set to 20 cm, which is the FCC definition of collocation as it is implicit in a note that appears in the corner of the FCC grant certificates [Rahim, 2009]. On the other hand, this distance is large enough to avoid being affected by other considerations such as near field. A medical video sequence of duration equal to 100 seconds was selected. Different video resolutions and compression levels were chosen in order to generate a set of video data rates (128, 192, 256, 320 and 384 kbps). UWB physical parameters were set to -42 dBm/MHz and -55 dBm/MHz for transmission PSD, TFC1 (hopping between the three bands), and 53.3 Mbps for PHY data rate.

4.3.2 Coexistence between UMTS and UWB

In order to evaluate the coexistence of UMTS and UWB, a measurement campaigns was carried out considering the coexistence scenario. As reference, the scenario with the single UMTS video client without the UWB devices was also considered. Average RSSI measured on the UMTS card was -77 dBm.

For all the scenarios, RTP packet loss rate increases as video data rate increases , as shown in Figure 4.6. There are no significant differences between the performance of the UMTS receiver coexisting with UWB whether at -42 dBm/MHz or at -55 dBm/MHz, which is the expected result as UMTS and UWB operate in different frequency bands.

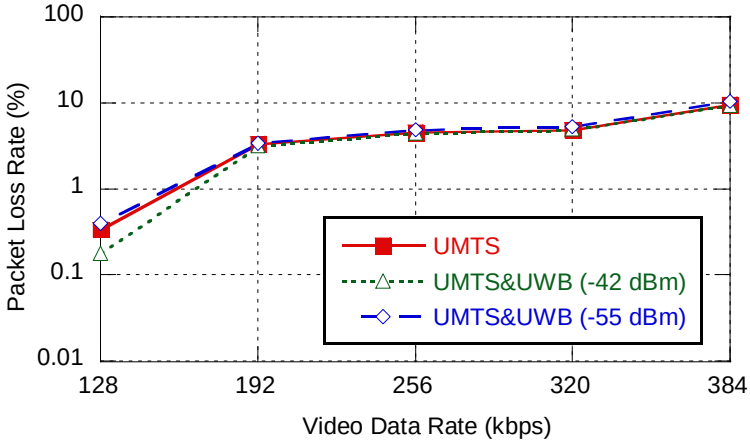

Figure 4.6. RTP packet loss rate for UMTS coexisting with UWB

Obviously, as it can be observed in Figure 4.7, throughput depends on the data rate generated by the transmitter, as long as it does not exceed available throughput. Maximum data rate in the downlink is limited to 384 kbps for UMTS. Values obtained for throughput are similar whether the UMTS coexists with a UWB device or not, which was expected as there were not significant differences on packet losses.

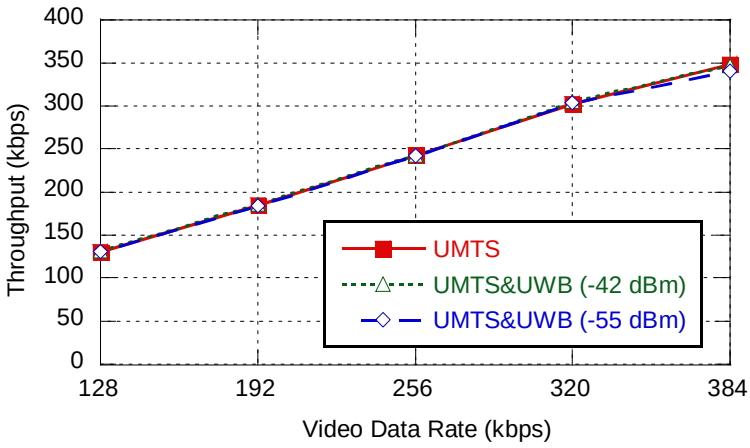

Figure 4.7. Average throughput for UMTS coexisting with UWB

Results for round-trip delay are shown in Figure 4.8. Values around 800 milliseconds were obtained for data rates less than 300 kbps. For 320 kbps it increases to 900-1000 milliseconds and for 384 kbps to 1.7-1.8 seconds. The reason is that data rate is close to maximum available throughput, so some packets must wait before being sent. Concerning the different scenarios evaluated, the presence of a UWB device transmitting does not seem to have any effect and the results obtained are similar for all the configurations.

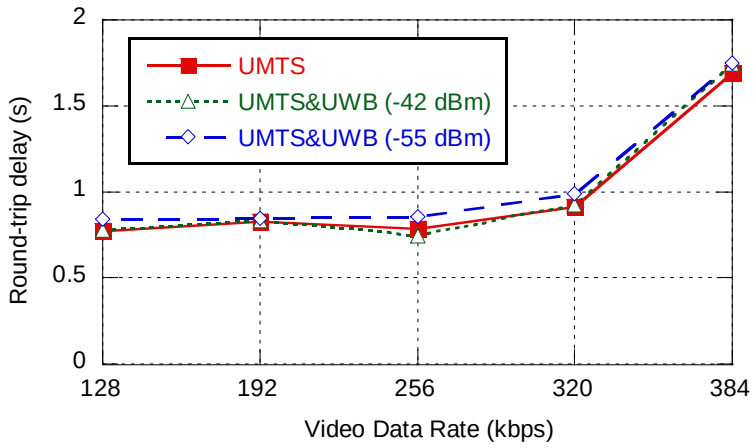

Figure 4.8. Round-trip delay for UMTS coexisting with UWB

Figure 4.9 shows results obtained for jitter. Low data rates show higher values than high data rate, where use of available throughput is close to its maximum. Concerning the different scenarios, values obtained for jitter are similar for all the configurations tested.

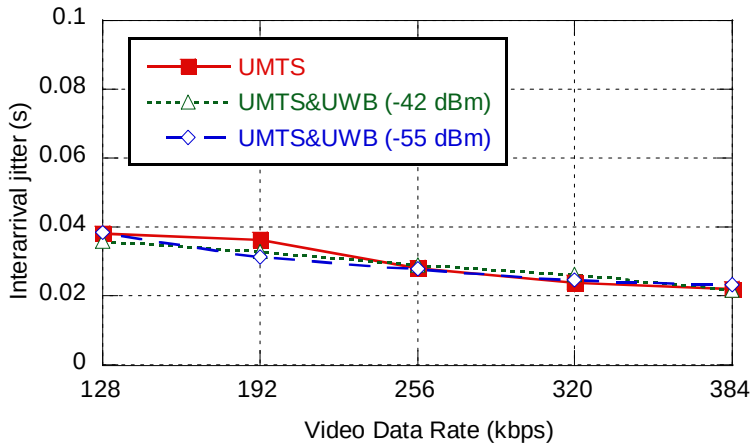

Figure 4.9. Interarrival jitter for UMTS coexisting with UWB

In general, tests performed with data rates less than 200 kbps obtained higher PSNR, particularly the tests performed at 128 kbps, which is expected as packet losses are lower (see Figure 4.10). For data rates over 200 kbps, the observed PSNR stays around 23-24 dB although packet losses increases. It must be taken into account that PSNR degradation is not only due to transmission losses, but to video compression and lack of synchronization also. As a consequence, PSNR in lossless conditions (cable) was also measured as a reference. Concerning the different scenarios, no significant degradation is shown when the UMTS device is collocated with a UWB device.

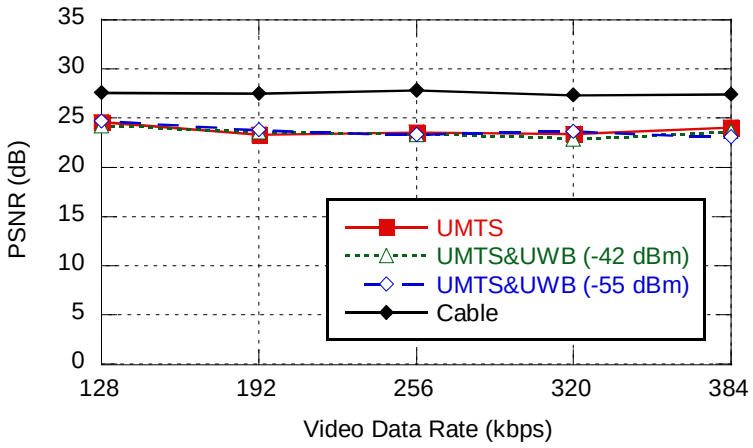

Figure 4.10. PSNR for UMTS coexisting with UWB

4.3.3 UMTS-UWB interworking tests

In order to evaluate the performance of the UMTS-UWB platform, tests were performed for the interworking scenario, the UMTS+Ethernet scenario and the single UMTS video client as a reference.

Results obtained for RTP packet loss rate for UMTS interworking with UWB show no significant difference compared to results obtained for UMTS interworking with Ethernet (see Figure 4.11). Compared to results obtained for a single UMTS receiver, they are similar for low data rates and slightly higher for data rates over 300 kbps, which means that packet losses are mainly due to UMTS. Losses due to interworking with Ethernet or UWB are not significant compared to losses on UMTS.

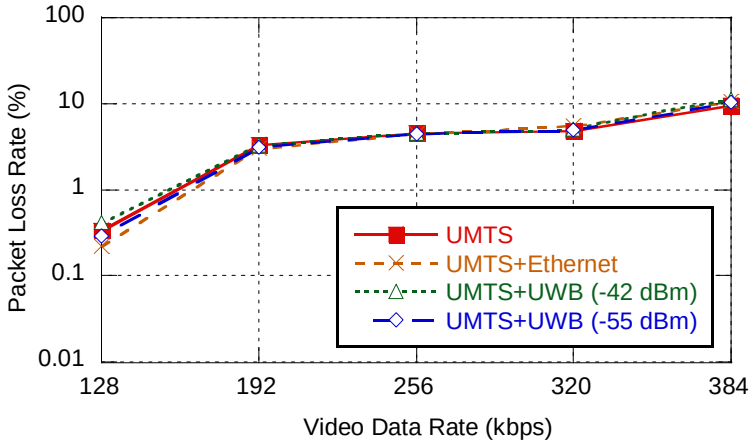

Figure 4.11. RTP packet loss rate for UMTS-Ethernet and UMTS-UWB platforms

Values obtained for throughput (Figure 4.12) are also similar for all the scenarios tested, which was expected as there was not significant differences on packet losses.

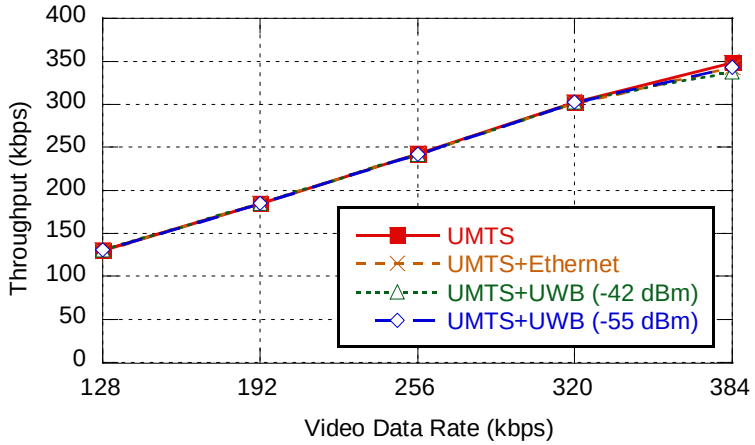

Figure 4.12. Average throughput for UMTS-Ethernet and UMTS-UWB platforms

Concerning round-trip delay, values obtained for UMTS interworking with Ethernet and UMTS interworking with UWB are slightly higher than values for the scenario with a single UMTS receiver for data rates over 300 kbps, as shown in Figure 4.13. Anyway the influence of the bridge and UWB link on the delay is small compared to the delay introduced by the network and the UMTS link.

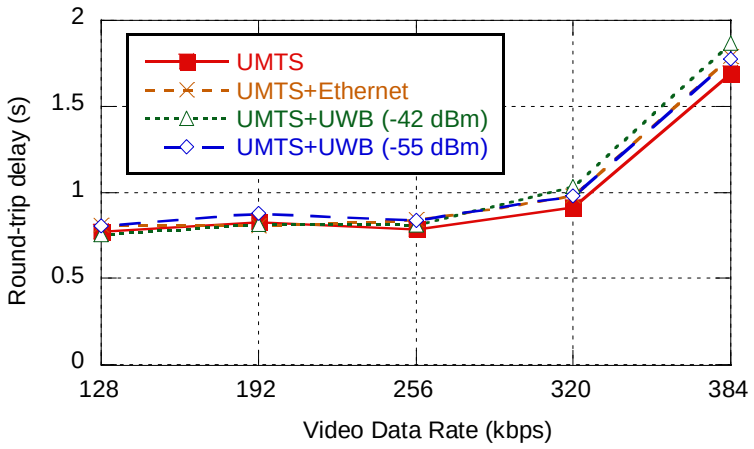

Figure 4.13. Round-trip delay for UMTS-Ethernet and UMTS-UWB platforms

Values obtained for interarrival jitter are similar for all the configurations tested (single UMTS, UMTS interworking with Ethernet, UMTS interworking with UWB), as it can be observed in Figure 4.14.

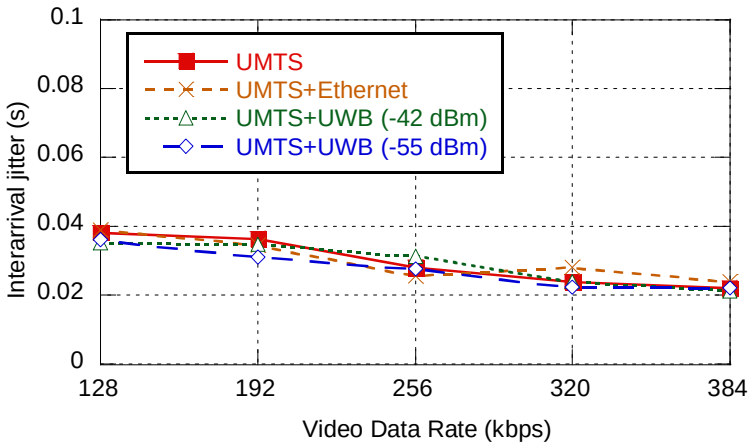

Figure 4.14. Interarrival jitter for UMTS-Ethernet and UMTS-UWB platforms

Concerning video quality and PSNR, there are not significant differences in results obtained for each scenario, as shown in Figure 4.15. PSNR obtained for UMTS interworking with Ethernet for 130 kbps shows a high value, but this could be due to better conditions (RSSI, interferences...) on the UMTS link when the tests were performed.

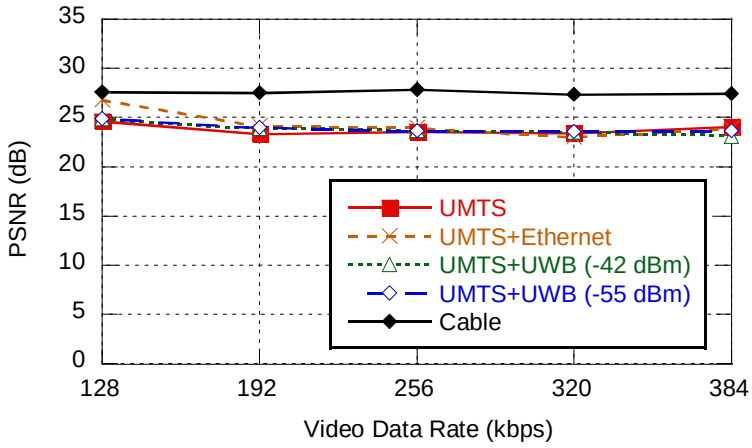

Figure 4.15. PSNR for UMTS-Ethernet and UMTS-UWB platforms

To sum up, there are no significant differences between the performance of the interworking UMTS-UWB platform compared to a UMTS-Ethernet platform for the considered parameters (packet loss rate, throughput, round-trip delay, interarrival jitter and PSNR) and for the Power Spectral Densities considered (-42 dBm/MHz and -55 dBm/MHz). Results obtained for the UMTS-UWB platform are also close to results obtained for a single UMTS receiver.

4.3.4 Coexistence for an HSDPA service

Another measurement campaign was carried out in a laboratory with HSDPA coverage, with an average RSSI on the UMTS card of -80 dBm. As in the first measurement campaign no degradation was detected for a distance of 20 cm between the UMTS card antenna and the UWB board antenna, this time the devices were placed as close as it was possible, with a distance of 3.5 cm between the antennas. The same scenarios of the first campaign were considered, with a Power Spectral Density of -42 dBm/MHz on the UWB device.

Concerning RTP packet loss rate (Figure 4.16), it is relatively low for video data rates less than 1000 kbps, but severely degrades for higher rates. The behavior is similar whether the UMTS-HSDPA receiver is coexisting with a UWB device. There are some differences in the obtained values due to the high variability of the Packet Loss Rate measured on the UMTS-HSDPA receiver, but there is no evidence of any degradation on the UMTS-HSDPA receiver due to the presence of UWB.

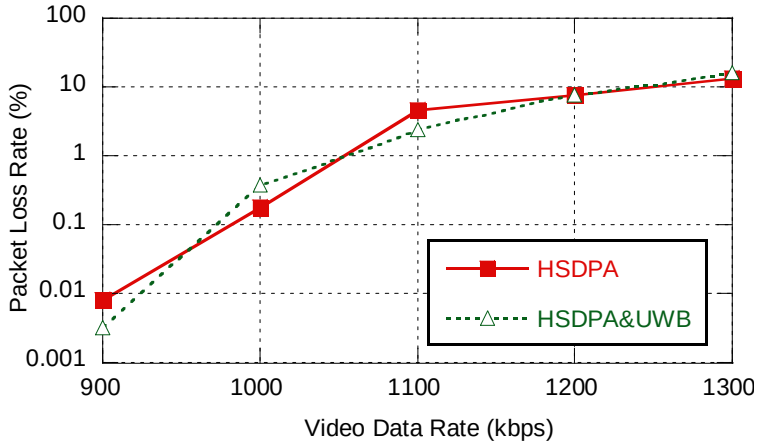

Figure 4.16. RTP packet loss rate for UMTS-HSDPA coexisting with UWB

Figure 4.17 shows results obtained for throughput. There are also slight differences between the values obtained for the UMTS-HSDPA receiver on its own and coexisting with UWB, but no degradation is detected due to the presence of UWB. Maximum data rate on the UMTS HSDPA downlink is theoretically limited to 1.8 Mbps, but in practice the throughput at application layer was limited to 1100 kbps. As a reference, another scenario with the transmitter and the receiver connected by an Ethernet crossover cable has been considered. In that case, throughput is similar to video data rate as there are no losses.

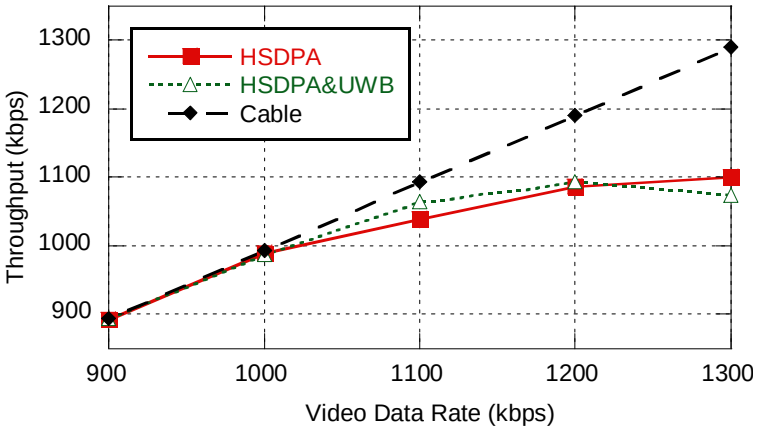

Figure 4.17. Average throughput for UMTS-HSDPA coexisting with UWB

Results for round-trip time are shown in Figure 4.18. The values obtained are almost identical whether the UMTS-HSDPA receiver is coexisting with a UWB device or not. Round-trip time increases as video data rate increases. As a reference, round-trip time obtained for an Ethernet cable connection between the transmitter and the receiver has been included, which is obviously much lower than in the UMTS scenario and lies between 3-8 milliseconds.

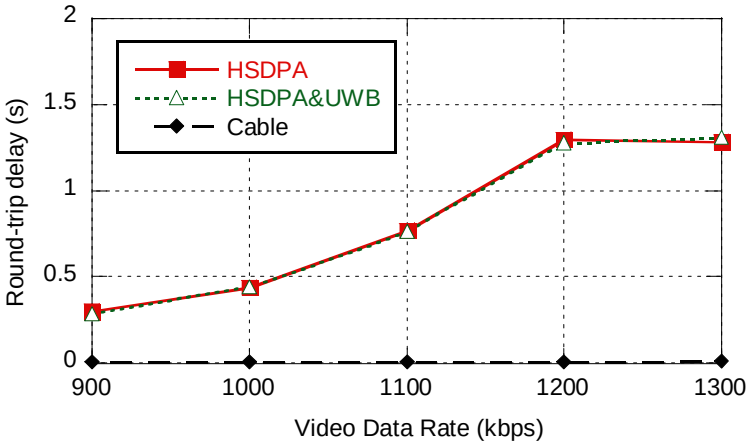

Figure 4.18. Round-trip delay for UMTS-HSDPA coexisting with UWB

Values obtained for interarrival jitter (Figure 4.19) are around 8 ms, whether for the UMTS-HSDPA receiver on its own or coexisting with a UWB device. Values obtained for an Ethernet cable connection between transmitter and receiver are much lower, as it was expected.

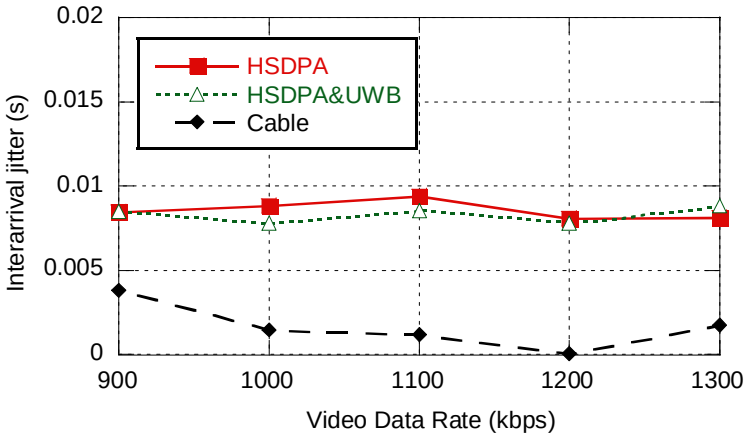

Figure 4.19. Interarrival jitter for UMTS-HSDPA coexisting with UWB

Finally, concerning video degradation, PSNR measured on the received video is also similar whether the UMTS-HSDPA receiver coexists with a UWB device or not (Figure 4.20). That was an expected result as there was no difference in terms of packet losses or delay. PSNR degrades as video data rate increases due to the increase of packet loss rate and delay. As a reference, PSNR measured for a lossless transmission over an Ethernet cable is included.

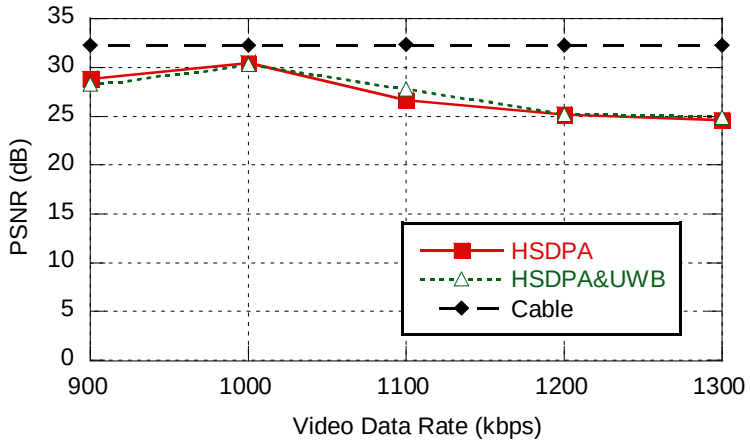

Figure 4.20. PSNR for UMTS-HSDPA coexisting with UWB

The same tests were performed on a different location in order to evaluate the coexistence under bad UMTS coverage conditions. For this purpose a location with very weak UMTS received signal was chosen. The average RSSI measured for the UMTS link was -101 dBm, compared to -80 dBm that was measured on the previous tests.

As shown in Figure 4.21, even in that weak signal conditions, there was no evidence of degradation due to the presence of UWB and similar results were obtained whether the UWB

transmitter was present or not, even though the distance between the UWB and UMTS devices was just 3.5 cm.

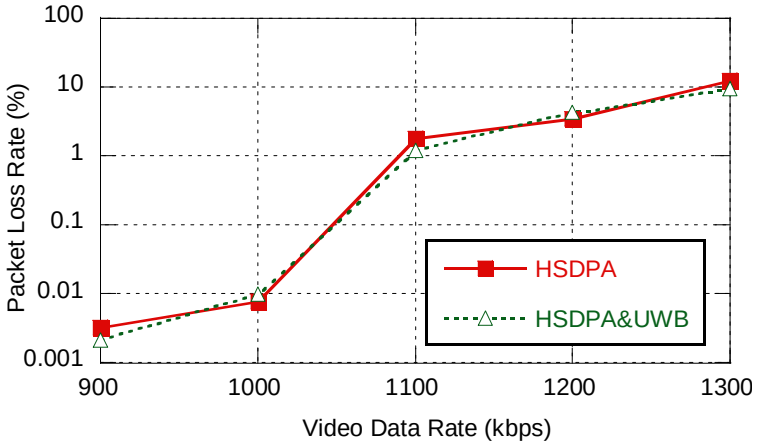

Figure 4.21. RTP packet loss rate for HSDPA coexisting with UWB (RSSI < -100 dBm)

To sum up, according to the results of the measurement campaigns carried out, there is no evidence of any degradation on UMTS link due to the presence of a UWB device, even if the distance between them is just a few centimeters. No degradation is detected if HSDPA is used either, even in very weak coverage conditions (UMTS RSSI < -100 dBm).

4.4 Cooperative Mitigation Techniques

4.4.1 Proposal of cooperative mitigation techniques

The interoperation of UWB and other radio technologies is a very flexible solution to extend the scope of UWB applications, although harmless coexistence between them must be assured. Mitigation techniques arise as a promising solution to minimize the effect of UWB systems on the existing radio services. Two approaches are widely spread:

- LDC (Low Duty Cycle): Based on the establishment of temporal restrictions to UWB transmissions. It is especially suitable for UWB applications with a low activity factor, for instance LDR-LT UWB systems.
- DAA (Detect and Avoid): Based on the detection of the presence of a victim service and the consequent application of a protection procedure on the UWB transmission in order to reduce the interference.

DAA technique presents a higher complexity, as a mechanism to detect the presence of the victim service is required, such as spectrum sensing, energy detection or BER measurement. Also a protection mechanism must be applied on the UWB device, such as power reduction, change of emission frequency band, suppression of interference band or application of notch or FIR filters.

DAA techniques can be classified into cooperative and non-cooperative depending on the participation of the victim service in the detection phase. Cooperative techniques are based in the interaction and information exchange between the different radio services, so the victim service itself can inform the UWB transceiver of its activity state. DAA implementations have mainly focused in non-cooperative strategies but cooperative techniques are a very interesting solution to ensure harmless coexistence of different radio services collocated on the same device.

As non-cooperative DAA, cooperative DAA techniques comprise two phases: detect phase and avoid phase [Giuliano, 2005]. Detect phase aims to detect if there is any possible interference between the different radio services. The difference with non-cooperative DAA mechanisms is that the degradation is directly measured on the victim service, which reduces drastically the non detection or false alarm probabilities. Possible monitored parameters are:

- Link quality parameters, such as BER, SNR and LQI (Link Quality Indicator). The presence of interference degrades link quality and these parameters are directly affected.
- Power based parameters, such as received power or RSSI. These parameters do not measure the level of interference, but they can be used to detect when the victim service is operating in critical conditions (for instance, received signal is weak) so it is more likely to be degraded by the presence of interference.
- Operation: If the victim service is considered critical, it can be detected when it is transmitting or receiving in order to apply the protection mechanisms whenever the victim service is in operation.

If any degradation on the victim service is detected, a protection mechanism will be applied on the interferer service in order to avoid any interference (avoid phase). Possible mechanisms available for UWB are:

- Frequency band switch: Two approaches can be taken. If the UWB is able to operate in different band groups, a different band-group would be selected if a victim service is detected. If the UWB device operates in a single band-group, which is the most usual case, it can be forced to operate in a single band taking advance of the TFC

codes. Therefore, in normal operation the UWB device would hop between the three frequency bands and if a victim service is detected in any of the bands, protection would be applied forcing the device to operate in a single band, thus avoiding interfering with the victim service. In particular, TFC codes #1, #2, #3 and #4 hop between the three sub-bands f1, f2 and f3, while TFC #5 only operates in sub-band f1, TFC #6 only operates in sub-band f2 and TFC #7 only operates in sub-band f3. Frequency band switch is the preferred method as it entails little degradation on the UWB link, but it is only effective if the victim service shares the same frequency band with UWB.

- Power decrease: In case the victim service does not operate in the same frequency band as UWB, it will be affected only by UWB out-of-band emission. To mitigate the interference, transmission power of the UWB device may be decreased. Taking advance of the TPC capabilities of UWB devices, in particular transmission power dynamic range and step size granularity, several solutions can be designed that may be more or less optimal. Nevertheless, we chose a simple approach that gives priority to protection on the victim service over UWB link performance. We define a protection level, i.e. the minimum transmission power supported by the UWB device, so that the UWB device commonly operates at its regular power level and switches to the protection level when degradation on the victim service is detected.
- Stop transmission: In case the degradation on the victim service is critical, the UWB transmission could be put on hold while the victim service is in operation.

4.4.2 Assessment of cooperative techniques

Protection mechanisms applied on the UWB interface mitigate interference on the victim device, but they may lead to degradation in the UWB link performance. Consequently, in order to assess cooperative mitigation techniques we must evaluate the effect on both the victim service and the UWB link.

The effect of the different protection procedures on the victim service, have been studied with the UMTS-HSDPA and UWB coexisting scenario. Packet Loss Rate was measured on a video-streaming transmission between a transmitter connected to Internet and a UMTS-HSDPA receiver. Video data rate was set to 1100 kbps as it is the maximum throughput that was achieved in previous test (Section 4.3.4). A UWB device was placed close to the UMTS receiver (3.5 cm between the antennas) transmitting a random sequence. Transmission power was set to -42 dBm/MHz, TFC code was set to TFC1 and PHY data rate was set to 53.3 Mbps, although these parameters are modified depending on the protection methods. Two

protection methods have been considered: frequency band switch and power decrease. Nevertheless, as no degradation has been detected on UMTS-HSDPA performance coexisting with UWB devices in the previous tests, the effect of mitigation techniques is expected to be negligible.

Concerning UWB link performance, as losses in the UWB link of the UWB/UMTS platform are not significant, the effect has been studied on a single UWB link. For this purpose, the control software tool of the UWB Development Kit has been used. This tool allows setting the main physical parameters (TFC code, transmission power and PHY data rate). It also features a packet generator and statistics monitoring. Packet loss was measured for different values for distance between the devices, transmission power, TFC code and PHY data rate. Bursts of 200,000 packets of 1512 bytes length were generated and the results obtained for five different repetitions of each experiment were averaged.

Frequency band switch is the preferred method as it entails little degradation on the UWB link. Nevertheless, this mechanism is appropriate when UWB and the victim service share the same frequency band (e.g. WiMAX at 3.5 GHz), but has is not effective for services operating in a different frequency band, such as UMTS. As it can be observed in the Figure 4.22, there is no degradation in terms of Packet Loss rate in the UMTS-HSDPA receiver independently of the TFC code used in the UWB receiver.

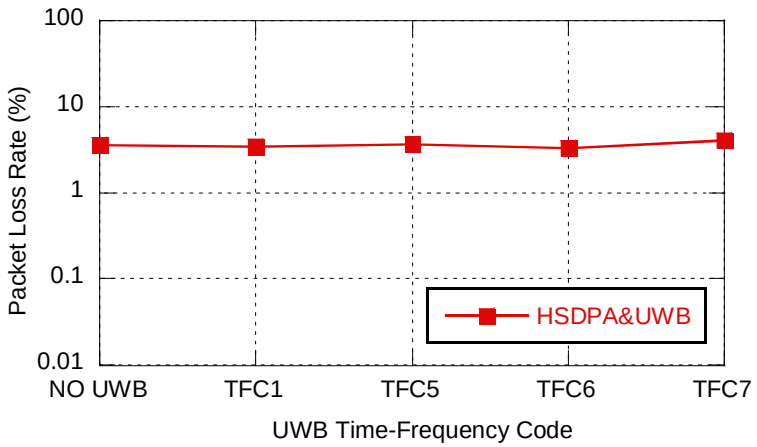

Figure 4.22. RTP packet loss rate for UMTS-HSDPA coexisting with UWB depending on UWB time-frequency code

The UWB link performance in terms of Packet Loss Rate was evaluated for the different TFC codes. In general, for PHY data rates less than 400 Mbps, packet losses are typically below 1% and the performance is very similar for every TFC code. Only for the highest data rates, which present higher losses, it is possible to appreciate some difference. Figure 4.23

shows performance for options TFC1, TFC5, TFC6 and TFC7 with a PHY data rate of 480 Mbps. TFC codes using hopping between the 3 bands, as TFC1, show an intermediate performance compared to TFC codes restricted to a single band, which can have either better (TFC6 in this case) or worse (TFC5 and TFC7) performance depending on the hardware and the channel frequency response and the presence of interferers. The better performance of the intermediate band (TFC6) is probably due to a better response of the hardware elements (antenna, amplifier...) as a flat response over a 1.5 GHz band is almost impossible to achieve.

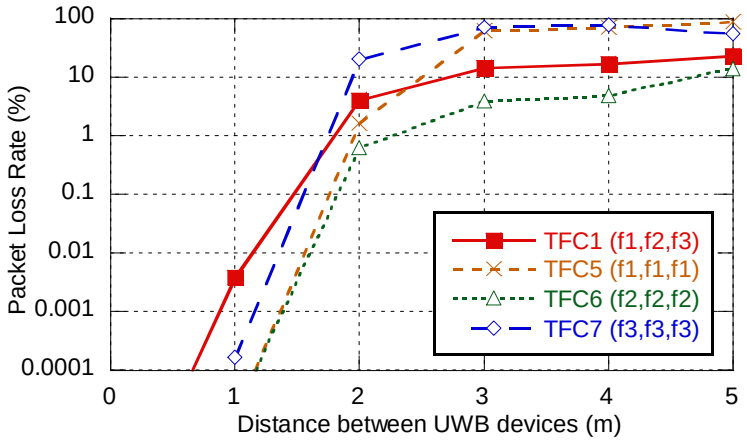

Figure 4.23. UWB link performance depending on TFC code

Concerning the power reduction method, in Figure 4.24 the Packet Loss Rate on the UMTS-HSDPA receiver for the different values of transmission power on the UWB device can be observed, with the Packet Loss Rate measured for the UMTS-HSDPA receiver on its own as a reference. As no degradation was detected on the UMTS-HSDPA receiver on Section 4.3.4, Packet Loss Rate measured should be independent of the UWB transmission power and similar to the scenario with the UMTS-HSDPA receiver on its own. Results obtained confirm this statement, with slight differences due to the variability of observations.

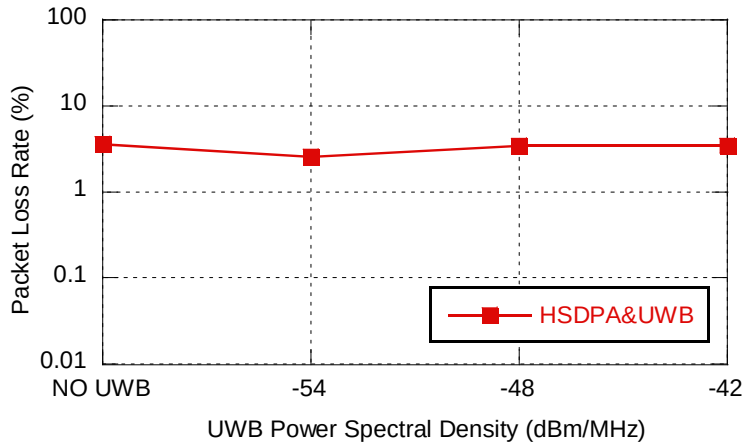

Figure 4.24. RTP packet loss rate for UMTS-HSDPA coexisting with UWB depending on UWB transmission power

Power-reduction method entails degradation on the UWB link, as it can be observed in Figure 4.25. As it could be expected, power reduction leads to a decrease in RSSI and consequently packet losses increase and range is reduced. If we consider 1% as an acceptable value for packet loss rate, with -42dBm/MHz we can reach up to 5 meters, while with -54dBm/MHz range is reduced to 3 meters.

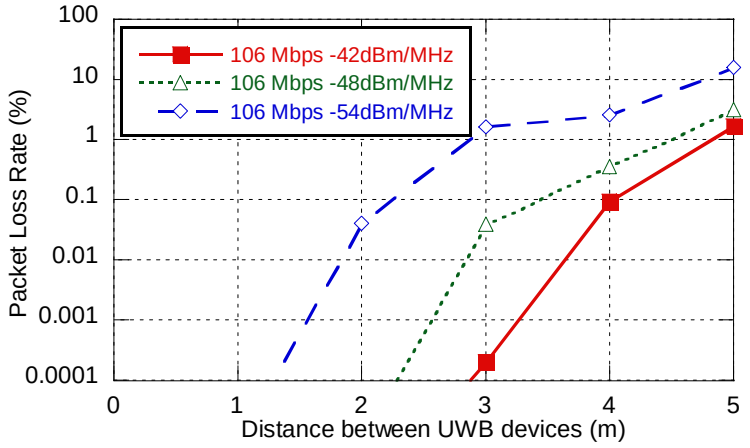

Figure 4.25. Packet loss rate for a UWB link depending on transmission power and distance

Degradation produced by power-reduction method is highly dependent on PHY data rate. As it can be observed in Figure 4.26, degradation is critical for data rates over 400 Mbps, leading to link unavailability for distances over 2 meters. But if PHY data rate is reduced, 106 Mbps for instance, we can obtain a comparable performance with -54 dBm/MHz compared to 400 Mbps and -42 dBm/MHz.

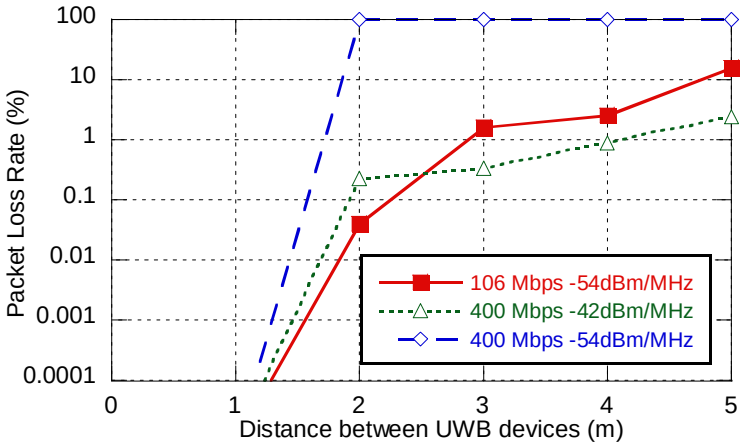

Figure 4.26. Packet loss rate for a UWB link when power and PHY data rate are reduced

Therefore, as transmission power is reduced, PHY data rate should be reduced too in order to compensate the degradation produced by power reduction method and keep a suitable packet loss rate. As it can be observed in Figure 4.27, UWB PHY rate does not have any influence on the performance of the UMTS-HSDPA link, and there is no degradation on the UMTS-HDSPA receiver regardless of the PHY rate selected.

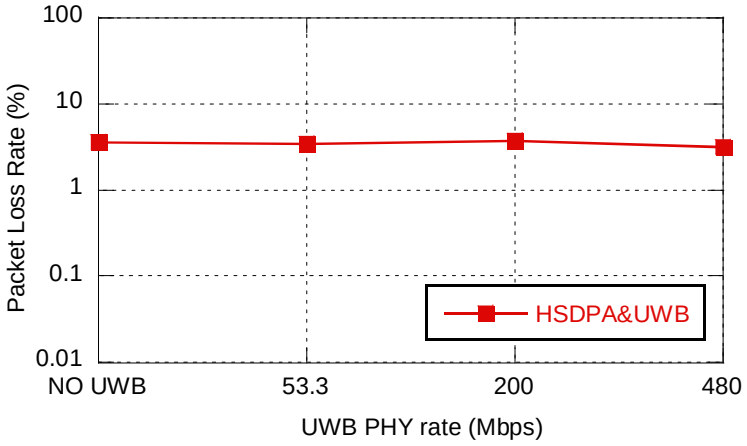

Figure 4.27. RTP packet loss rate for UMTS-HSDPA coexisting with UWB depending on UWB PHY data rate

Finally, the stop-transmission method entails eventual transmission denials on the UWB link when the victim service is active, leading to a decrease on average UWB link throughput and delay. Nevertheless, this mechanism is not a valid solution for interoperability applications as they require that both interfaces operate at the same time.

4.4.3 Cooperative interoperability platform

The UMTS/UWB interoperability platform presented in Section 4.2 has been enhanced in order to demonstrate the feasibility of cooperative mitigation techniques. Specifically, the interoperability software has been modified. Taking advance of the API (Application Programming Interface) interfacing the UMTS card different thresholds have been defined for the UMTS link parameters. The PCMCIA card reports the status of the RSSI and BER. A threshold is set that indicates a situation of a potential degradation (e.g. -100 dB for RSSI). If the threshold is crossed, protection mechanisms are applied to mitigate the potential interference. Protection mechanisms range from stopping UWB transmission to setting a certain protection value for UWB transmitted power, TFC channel and PHY data rate. This is achieved through the API of Wisair's DV9110. Figure 4.28 shows the tab of the interoperability software GUI where the normal operation and protection values for the UWB interface are set.

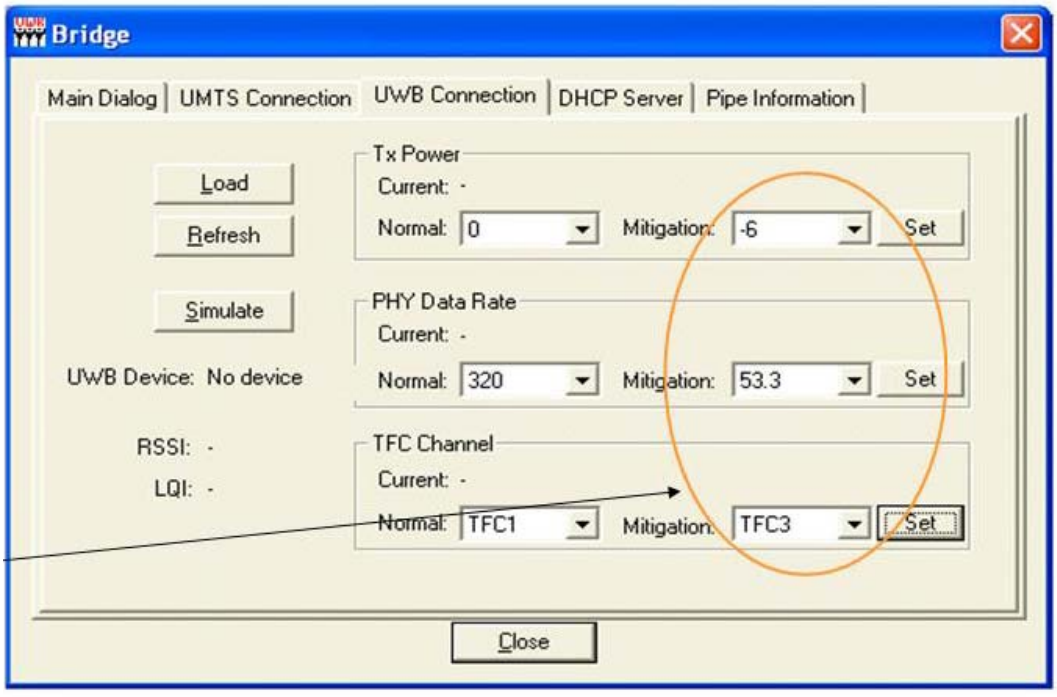

Figure 4.28. Interoperability software GUI. UWB connection tab

Different tests were carried out in order to validate the implementation of cooperative mitigation techniques on the UWB/UMTS platform. When cooperative techniques are not active, the UWB devices operate at the normal values for Tx power, PHY data rate and TFC channel. Then a low threshold was set for UMTS RSSI in order to force the activation of the

cooperative mitigation techniques and the operation of the UWB devices at the protection values. This way we will appreciate better the effect of protection, keeping conditions on UMTS link constant. Otherwise, results would be mainly influenced by the UMTS link conditions.

As it was shown in previous sections, there is not degradation in UMTS performance due to the presence of a UWB transmitter collocated in the same device, so no improvement on UMTS performance is expected of the application of the mitigation techniques. As expected, results were similar to those shown in Section 4.3.3. There is no appreciable degradation on the UWB link and the whole platform performance due to the application of the cooperative mitigation techniques, which confirms the feasibility of implementing cooperative techniques in the dual device.

In fact there would be some degradation for PHY data rates over 400 Mbps, which are addressed to very specific applications (e.g. uncompressed high definition video-streaming) or when the distance between the UWB devices is close to the maximum range, which entails an effective range reduction. But in most of the cases, with PHY data rates fewer than 200 Mbps and distances less than 3 meters, degradation is negligible.

These results do not show the need of implementing cooperative mitigation techniques in the case of UMTS, as current PSD limits fixed by the regulation already guarantee harmless coexistence. The full potential of cooperative mitigation techniques further studies would be exploited when UWB coexists with radio technologies which work in the same frequencies as UWB, such as 3.5GHz WiMAX. Nevertheless, the implementation of cooperative mitigation techniques may be used to apply a higher level of protection on UMTS when it is collocated with UWB on the same device. This would relax physical design requirements, thus encouraging mobile operators and manufactures to develop dual UMTS-UWB devices, for instance UWB enabled mobile phones. The main advantage cooperative mitigation techniques over non-cooperative DAA is that degradation is directly measured on the victim service, drastically reducing the non-detection and false-alarm probabilities.

Chapter 5

Location and Tracking Techniques

5.1 Introduction

As it has been already stated, UWB is one of the most promising technologies addressed to indoor location and tracking systems. Several studies can be found in the literature concerning both distance estimation techniques and location & tracking algorithms that have been summarized in Section 3.2.

The potential benefit of UWB lies on the possibility to obtain a high precision TOA estimation. Nevertheless, in certain conditions the accuracy of TOA estimation can be severely degraded, especially in multipath environments. This context encourages the research on more robust and accurate distance estimation algorithms as they have a great influence on the whole location system performance. Section 5.2 provides a qualitative and quantitative evaluation and comparison of different TOA based distance estimation mechanisms joint to receiver architectures proposed for UWB systems. First, different TOA estimation alternatives are presented and evaluated based on two basic types of reception schemes: the Energy Detection receiver based on energy integration, and the Stored Reference receiver based in signal correlation. Then, more complex designs aiming to mitigate some of the limitations of the basic receivers are presented. That is the case of the Dirty Template and the ED&SR. Different TOA estimation algorithms have been considered, studying their performance, evaluating their accuracy and analyzing the effect of characteristic parameters of the transmitted signal, signal-to-noise ratio and propagation conditions.

Although most of the proposals of location and tracking algorithms that can be found in the literature include the evaluation of the proposal, in general these studies focus on the algorithm optimization in a simple scenario with a single terminal and a few previously defined reference nodes. Performance evaluations comparing different algorithms can also be

found, but most of them are too simplistic and do not account realistically for the implications of the indoors environment and the distance estimation technology. The rigorous evaluation of location and tracking algorithms should take into account the specific error distribution of UWB-based distance estimation and the implications of indoor tracking scenarios, such as user's mobility, the number of reference nodes and the distance between them. In Section 5.3 a realistic evaluation of the performance of different location & tracking algorithms for UWB-based indoor tracking systems is provided. With this purpose, a specific UWB ranging model is used to characterize the distribution of distance estimation error. On the other hand, positioning systems are closely related to Geographic Information Systems (GIS) in applications such as vehicle navigation systems. Indoor scenarios are likely to have geographic information available, such as wall and floor plans, which could be used to improve localization, for example through the identification of NLOS situations. The use of geographic information in indoor environments for the design of enhanced location and tracking algorithms is proposed and evaluated in Section 5.3.3.

5.2 Distance Estimation

In Section 3.2.1, the main approaches and algorithms for TOA-based distance estimation have been presented, as well as some state-of-the-art proposals. In this section, a qualitative and quantitative evaluation of different TOA based distance estimation mechanisms joint to receiver architectures proposed for UWB systems is provided. First, basic TOA estimation alternatives are evaluated based on the two basic types of reception schemes: the Energy Detection (ED) receiver based on energy integration, and the Stored Reference (SR) receiver based in signal correlation. Then, more complex designs aiming to mitigate some of the limitations of the basic receivers, such as the Dirty Template and the ED&SR, are evaluated.

5.2.1 Evaluation of TOA estimation algorithms

5.2.1.1 Simulation models and assumptions

In order to perform a comparative evaluation of the different receiver types and TOA estimation algorithms described on Section 3.2.1, a system simulator has been developed in C++, which implements in detail the behavior and characteristics of the physical layer on realistic scenarios. The simulator allows a flexible set of the main parameters values of the UWB transmitter, channel and receiver, which includes TOA estimation. These parameters

can be set by the user in order to adjust the operation point of the proposed algorithms and to compare them in different scenarios.

Channel modeling has been performed following the recommendations of the IEEE 802.15 Task Group 4a for a frequency range between 2 and 10 GHz [Molisch, 2004]. For each different environment, LOS (Line Of Sight), OLOS (Obstructed Line Of Sight) and NLOS (Non Line Of Sight) situations are considered. In particular, residential environments have been considered in this paper. Table I summarizes the main parameters of the residential LOS channel (CM1) and residential NLOS channel (CM2).

Table 5.1. Channel model. Residential environment

		LOS (CM1)	**NLOS (CM2)**
Distance	d	5 m	5 m
Sampling rate	F_s	10 GHz	10 GHz
Channel energy (normalized)	E	$1.92865 \cdot 10^{-15}$ dB	$2.89298 \cdot 10^{-15}$ dB
Delay spread (average)	DS_{avg}	17.1252 ns	13.4295 ns
Delay spread (RMS)	DS_{RMS}	18.3386 ns	16.037 ns
Number of multipath components		70	69
Number of significant multipath components			
-10dB of the maximum		8	6
85% of the maximum energy		11	7
First path delay	τ_{TOA}	16.6 ns	23.2 ns

In order to compare the performance of each solution, the simulator provides a measurement of the error committed on the distance estimation, Mean Absolute Error (MAE), which is defined as

$$MAE = \frac{1}{N}\sum_{n=1}^{N}\left|d_{prop} - \hat{d}_{prop}{}^{n}\right| = \frac{1}{N}\sum_{n=1}^{N}\left|d_{prop} - c \cdot \hat{\tau}_{TOA}{}^{n}\right| \tag{5.1}$$

where:

d_{prop}: distance between the transmitter and the receiver.

c: speed of light in a vacuum.

N: number of estimations.

$\hat{d}_{prop}{}^{n}$: n-th estimation of distance.

$\hat{\tau}_{TOA}{}^{n}$: n-th estimation of Time of Arrival.

For each TOA estimation algorithm, prior simulations have been performed to set optimal values for its parameters. Then, the accuracy has been evaluated for different SNR values. 5000 random channel realizations have been generated for each scenario, with a distance between the transmitter and the receiver characterized by a propagation time, $\tau_{prop} \equiv \tau_{TOA}$, defined as a uniform random variable within the interval $(0,T_f]$. Then, the impulse response for each channel is sampled with 10 GHz as sampling rate.

For simulation purposes, it was considered that the transmitter sends a training sequence defined as $d_{TS}[k]=0 \ \forall k$. The signal was generated for a random user with f_s=10 GHz as sampling rate and T_f=100 nanoseconds as frame duration, which implies a range of 30 metres, d_{prop}~U [0,30) m, as propagation time should not exceed frame duration, $\tau_{TOA} \leq T_f$. In order to avoid interframe interference, a guard frame is added between pulses, thus halving the value of PRF and data rate. Pulse shape is Gaussian doublet with T_p=1 ns duration. And, finally, a Time Hopping code based on quadratic congruences is used, with the maximum period, $L_c=N_c$=100, in order to randomize the signal spectrum. Therefore, chip duration, T_c, is equivalent to pulse duration.

5.2.1.2 Basic receivers and TOA estimation algorithms

In this section the simulation results obtained for each receiver type and TOA estimation algorithm are presented. The accuracy of each solution is measured in terms of MAE.

As a first step, an ideal channel has been considered. It can be demonstrated that with a single component channel and low noise level, the estimation error depends on the sampling rate of the receiver. Considering a block duration of T_b=1 ns on the ED receiver and a sampling interval of T_b=0.1 ns on the SR receiver, MAE tends (with high SNR) to 15 cm and 0.75 cm respectively. In an ideal scenario, this resolution is the maximum accuracy that could be achieved with those sampling rates according to the theoretically predicted. Higher sampling rates would lead to lower minimum MAE, but complexity and cost of the receivers would increase and it would not ensure a better performance on non-ideal channels.

$$E_{\min}(d,T_b) = \left| d - c \cdot \left(\left[\frac{d/c}{T_b} \right] + 0.5 \right) \cdot T_b \right| = \begin{cases} 15 \text{ cm for ED} \\ 0.75 \text{ cm for SR} \end{cases} \tag{5.2}$$

A LOS channel was applied to take into account multipath effect. Figure 5.1 shows the results of the SR receiver combined with MES algorithm in a LOS channel and the influence of the sampling interval (T_b) and the number of pulses used in the TOA estimation (K). As it can be observed, at least K=32 is required in reasonable SNR scenarios. For this reason, this value will be used in the following analysis. The link budget, according to the transmission

power limits specified by the regulators, determines the maximum achievable SNR for a given distance.

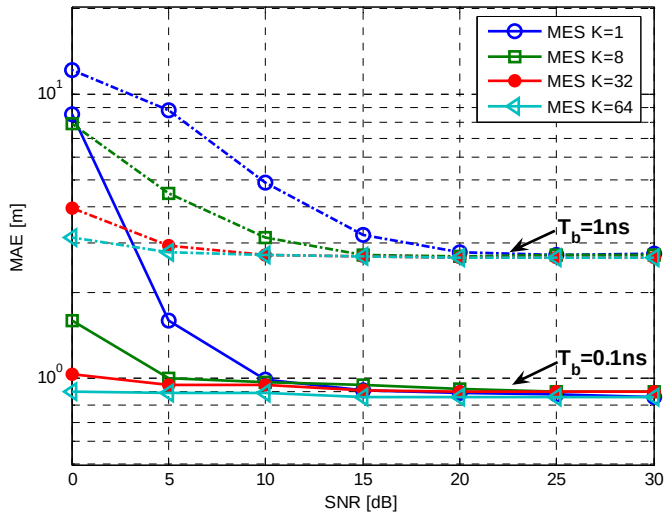

Figure 5.1. MAE vs SNR for the SR receiver and MES algorithm with different number of pulses (K) and sampling intervals (T_b). Channel CM1 (LOS)

Other parameters as ξ_{norm} (in TC and MES-SB), N_w (in MESS and WMES) and W_{sb} (in MES-SB) could be adjusted prior to a comparative evaluation of TOA estimation algorithms in LOS and NLOS scenarios. Concerning TC, the ξ_{norm} value is a trade-off between the maximum accuracy that can be achieved with high SNR and the estimation error with low SNR, as it can be observed in Figure 5.2. ξ_{norm} =0.4 has been chosen as it combines a good accuracy with high SNR (up to 40 cm) and reasonable degradation for SNR less than 10 dB (1 m for SNR=5 dB). Lower values can achieve a better accuracy with high SNR values, but are severely degraded even for SNR=10 dB. And higher values of ξ_{norm} would present less degradation for low SNR, but accuracy on high SNR conditions would be worse. Therefore, the optimal value for ξ_{norm} is highly dependent on the channel characteristics.

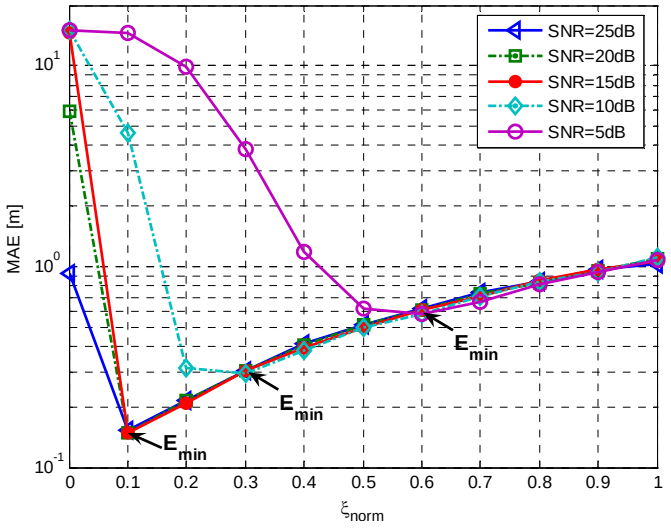

Figure 5.2. MAE vs ξ_{norm} for the ED receiver, TC algorithm and K=32 with different SNR levels. Channel CM1 (LOS)

Concerning MESS, the optimal N_w value is around 30 ns, which is approximately equal to the channel delay spread, as the window must contain all the components of the received signal. On the other hand, on W-MESS the energy of the received signal is correlated with the estimated PDP of the channel and the window size is not critical as long as it is greater than the delay spread. Finally, on MES-SB the optimal value for W_{sb} is again related to the channel delay spread and values of 20 and 30 ns have been selected for the ED and SR receivers respectively, whereas ξ_{norm} has been set to 0.4 to solve the trade-off between maximum achievable accuracy with high SNR and degradation with low SNR.

Figure 5.3 and Figure 5.4 show the results obtained, in terms of MAE as a function of SNR, for each TOA estimation algorithm on the ED and the SR receiver respectively in a LOS scenario. On both receivers the MES-SB algorithm gets the best performance and a good accuracy is obtained even in the low SNR region. The TC algorithm gets slightly better results, but only with high SNR. If SNR decreases, accuracy degrades and it becomes the less suitable on the low SNR region. The MES algorithm does not show a good accuracy independently of the SNR due to the characteristics of the multipath channel, as the leading edge is not necessarily the component with the maximum energy. The MESS algorithm is not suitable for exponential PDP channels and only for the ED receiver shows a better performance than MES in the high SNR region, being consequently discarded. Finally, W-MESS improves the performance of MES, but just for the ED receiver gets results close to MES-SB and TC, although it requires a priori knowledge of the channel.

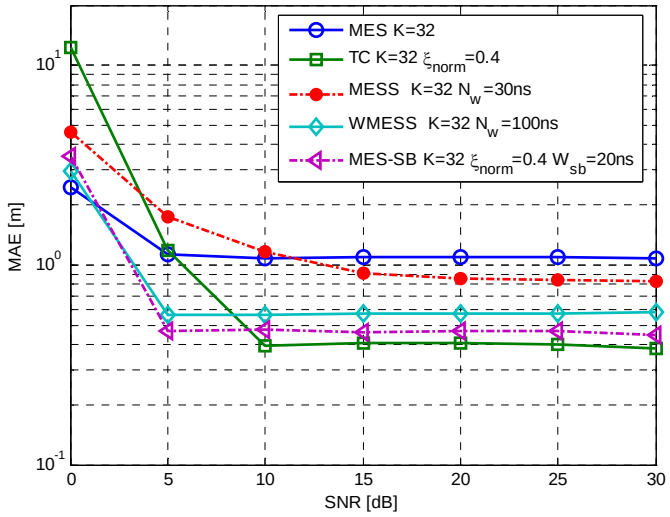

Figure 5.3. MAE vs SNR for the ED receiver with different TOA estimation algorithms. Channel CM1 (LOS)

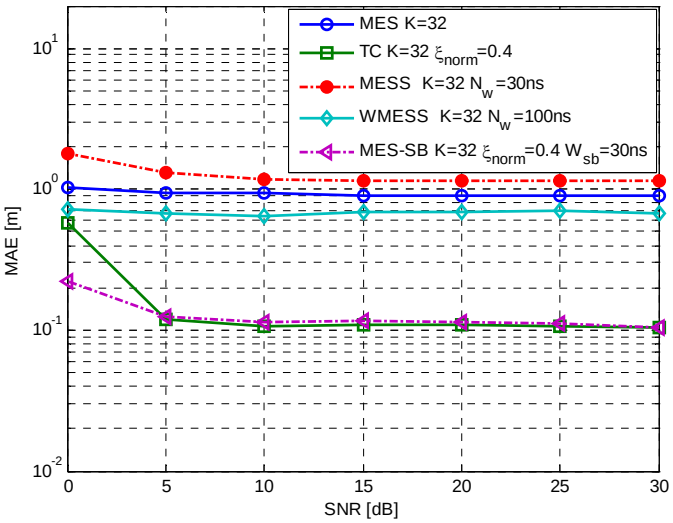

Figure 5.4. MAE vs SNR for the SR receiver with different TOA estimation algorithms. Channel CM1 (LOS)

A non-line of sight scenario was also considered. In this case, there is an intrinsic error as the first path is missing, so the leading edge of the received signal does not correspond to the distance between the transmitter and the receiver. Errors lower than 2 m on distance estimation cannot be obtained with the proposed algorithms, so the advantages of some algorithms over the others are not very significant.

Figure 5.5 and Figure 5.6 show the performance of each TOA estimation algorithm for the ED receiver and the SR receiver respectively. The SR receiver was the optimal detection technique in LOS scenarios, as it has been shown on the simulation results. However, when a NLOS scenario is considered the difference is not significant. The performance of MES-SB and TC is quite similar except for the low SNR region where TC is significantly degraded. The MES algorithm should be discarded as the error is high even in the high SNR region. Finally, performance of W-MESS is comparable to MES-SB and TC for the ED receiver, but not for the SR receiver, although it is still better than MES.

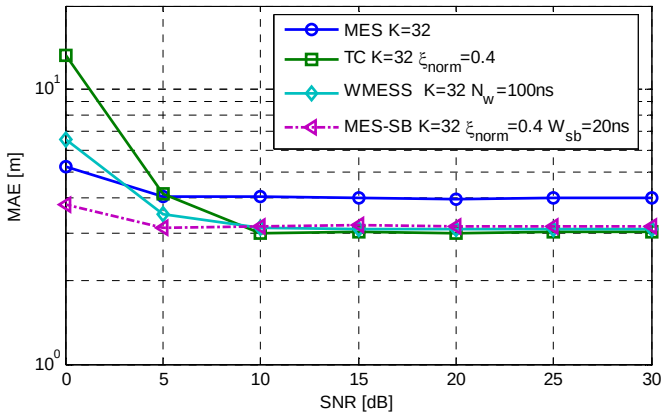

Figure 5.5. MAE vs SNR for the ED receiver with different TOA estimation algorithms. Channel CM2 (NLOS)

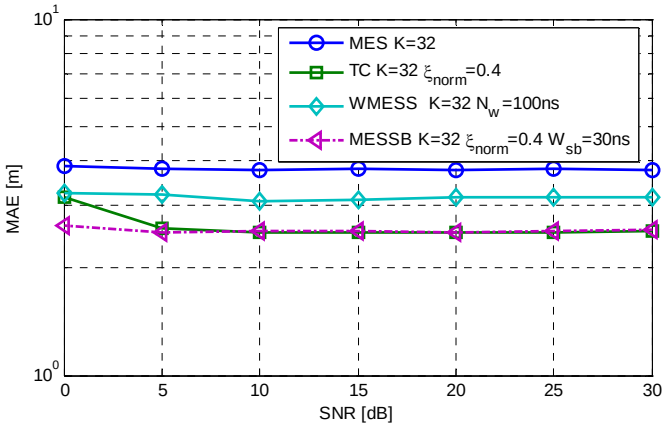

Figure 5.6. MAE vs SNR for the SR receiver with different TOA estimation algorithms. Channel CM2 (NLOS)

5.2.1.3 Dirty Template and ED&SR receivers

Figure 5.7 shows a comparative evaluation and results of Dirty Template and ED&SR receivers, in a LOS scenario. Concerning the DT receiver, some transmitted parameters have been modified in relation to previous simulations. A BPSK modulation has been used. The number of pulses per symbol has been increased to 10 in order to use longer templates and, therefore, the data rate has been reduced. Finally, no guard frame is used as interframe interference is allowed, as long as there is no interference between different symbols. Simulations for ED&SR receivers have been performed using 50 pulses for the first step (N_1), 25 for the second step (N_2), 5 ns as block duration and the same transmitted signal parameters previously defined.

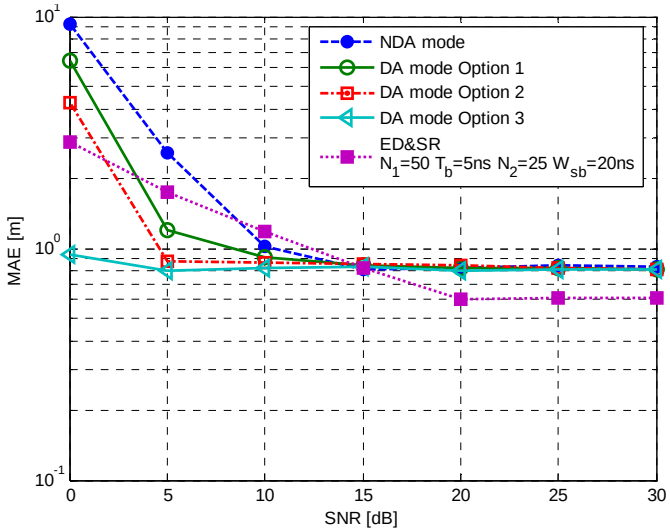

Figure 5.7. MAE vs SNR for DT and ED&SR receivers. Channel CM1 (LOS).

Within the DT modes and options, the best performance is obtained with the DA option 3, which is less sensitive to noise. DA option 2 gets worse results in the low SNR region, as well as DA option 1, which shows a similar performance to option 2. On the other hand, NDA mode gets the worst results in the low SNR region, but it has the advantage that estimation is obtained from a modulated data sequence, so distance estimation and data transmission can be done simultaneously.

As it can be observed, accuracy measured for a LOS scenario and medium-high SNR levels tends to 80 cm, which is comparable to the results for the MES algorithm on the SR receiver (Figure 5.4) despite the lack of knowledge of the transmitted signal and the channel. Better performance could be achieved using threshold based algorithms (TC, MES-SB) instead of choosing the maximum correlation sample as the leading edge.

The ED&SR receiver presents a MAE that tends to 60 cm on high SNR levels, which is better than results for MES algorithm, but not as good as results for the SR receiver with TC and MES-SB algorithms. The main advantage of this receiver is that it does not require high sampling rates.

5.2.1.4 Multiscale Product based TOA estimation

Multiscale product (MP) based algorithms aim to improve the performance of the basic TOA estimation algorithms as MES, TC and MES-SB, in order to reach high accuracy even for low SNR without using the more complex SR receiver. Performance of W-MP MZ-DWT, MEP and MEP-SB has been evaluated and compared to basic TOA estimation algorithms. Figure 5.8 shows the performance of the different TOA estimation algorithms with the ED receiver in a LOS scenario. The W-MP MZ-DWT algorithm performs better than MES, although not as well as the other algorithms. On the other hand, MEP and MEP-SB show a better performance than MES and W-MP MZ-DWT. MEP-SB shows a remarkable performance for medium-high SNR values, comparable to MES-SB, whereas MEP shows the best performance for SNR= 0 dB.

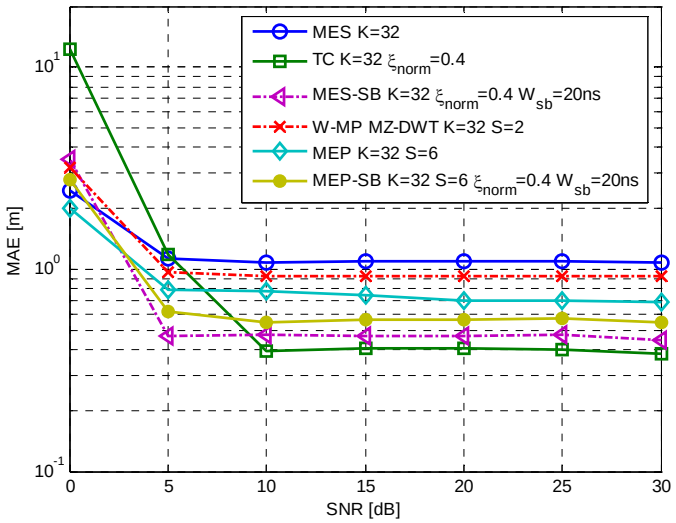

Figure 5.8. MAE vs SNR for ED receiver with MP-based algorithms. Channel CM1 (LOS)

5.2.1.5 Conclusions

The maximum achievable accuracy on an ideal (no multipath) channel depends on the sampling rate of the receiver. Therefore there is a trade-off between accuracy and complexity of the receiver. For a reasonable level of complexity, simulations results show that the minimum MAE tends to 40 cm for the ED receiver and 10 cm for the SR receiver.

Nevertheless, accurate positioning is only possible in LOS conditions. On the NLOS channel, minimum MAE increases to 1.5 m due to the fact that the first path is not present.

SR receiver is the optimal detection technique, but it requires high sampling rates and knowledge of the shape of the transmitted signal. The first requirement can be relaxed through combined ED&SR receivers, and the second one through Dirty templates based receivers. These receivers present intermediate results between the ED and the SR receivers with a lower level of complexity than the SR receiver. Concerning TOA estimation algorithms, threshold based algorithms (TC and MES-SB) show the best performance, but it must be taken into account that their optimal parameters (threshold and window size) depend on the SNR and channel characteristics (Delay Spread).

5.2.2 Distance estimation with real UWB devices

In order to confirm the results obtained in the simulations, some measurements have been performed with real UWB devices. With this purpose, open IR-UWB platforms developed within the framework of PULSERS PHASE II and EUWB projects have been used. The description of this platform can be found in [Pezzin, 2009], and a more detailed description of the physical layer can be found in [Pezzin, 2007]. Following, a summary of the TOA estimation procedure is provided.

The modulation scheme of the platform is based on DBPSK. Demodulation of incoming signal is performed using differential correlation between the incoming signal corresponding to the current data symbol and the previous one. In order to improve the signal to noise ratio, redundancy is added to the current symbol by repeating it several times using a PN (Pseudo Noise) code of length n_{PN} (typ. n_{PN}=12). As Pulse Repetition Period (PRP) is 240 ns, symbol duration is 2.88 μs and raw bit rate 347 kbps. Sampling rate is 1 GHz and therefore block duration T_b=1 ns.

TOA estimation is carried out in two phases. The first phase is common with the demodulation process. It includes the coherent integration of n_{IC} PRPs (typ. n_{IC}=3) and the correlation of current symbol with the previous one, with a window size of 8 ns. This way a coarse estimation (with a precision of about 8 ns) of the time of flight is provided to the fine ranging module. In the second phase (fine ranging), the results of the correlation for n_{ACC} PRPs (typ. n_{ACC}=4, $n_{PN} = n_{IC} \cdot n_{ACC}$) is accumulated using chunks of 1 ns (one sample) instead of 8 ns. To do this, the 8 partial correlation results corresponding to the related 1 ns incoming signal chunks are provided by the correlator used in the demodulation module and are then processed by 8 parallel PN decoding and accumulation modules. A second stage of accumulators performs additional accumulations on the absolute values of the resulting

metrics for K consecutive symbols in order to reach the required processing gain. Once these accumulations are performed, the first significant path is detected and its index gives the fine grain resolution required for precise ranging.

A measurement campaign was carried out using the IR-UWB prototypes. Line-of-sight and distances up to 5 m in steps of 0.25 m were considered. Under these conditions, the error is mostly due to the TOA estimation procedure, as channel effects will be negligible. For each distance, 150 ranging samples were obtained and the mean and standard deviation of the signed error was computed, as well as the mean absolute error. As it can be observed in Figure 5.9, the mean is always close to zero, as it could be expected for short distances. Nevertheless, for distances greater than 3 m, the mean error is mostly positive, as channel effects, for instance multipath propagation, become more important. On the other hand, standard deviation varied from 10 cm to 40 cm, with an average value of 25 cm. Figure 5.10 shows the mean absolute error, which lies between 10 cm and 15 cm, being very close to the theoretical minimum MAE of 7.5 cm that can be achieved with T_b=1 ns.

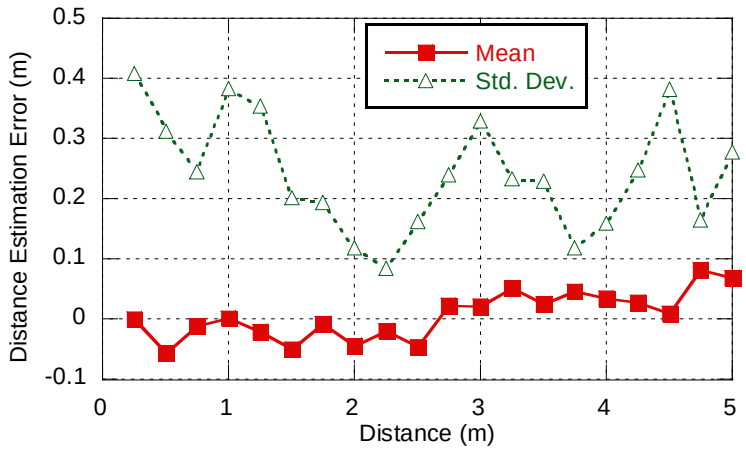

Figure 5.9. Distance estimation error vs distance for real UWB prototypes

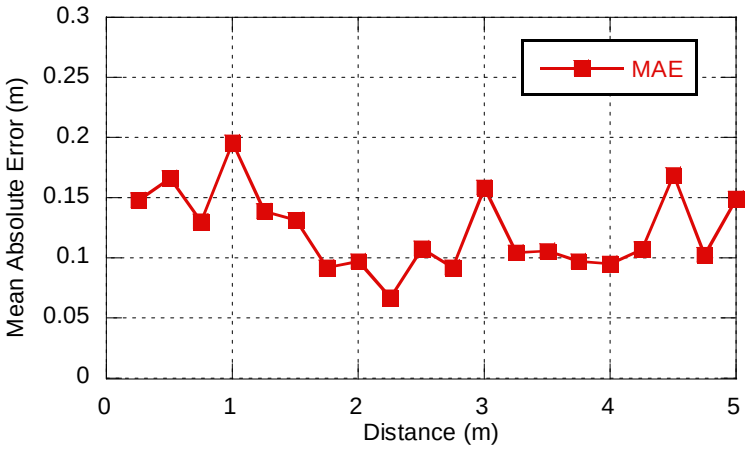

Figure 5.10. MAE vs distance for real UWB prototypes

5.3 Location and Tracking Algorithms

As it has been shown in the state-of-the-art, several location & tracking algorithms have been proposed in the literature to compute user's position according to the estimated distances to some reference nodes, each one providing the best performance in certain conditions. Nevertheless, most of these proposals are evaluated under too specific or simplistic conditions that do not account realistically for the specific implications of the UWB-based distance estimation and the indoors scenario. In this section, an objective evaluation of different location and tracking algorithms with a realistic UWB indoor ranging model is provided. Two scenarios, based on the statistical ranging model and on a wall plan, are considered. Finally, enhanced versions of the algorithms taking advance of available location information are proposed and evaluated.

5.3.1 Simulation models and assumptions

In order to evaluate different tracking algorithms and to assess the impact of different system design parameters, a custom simulation tool has been developed, using C++ as programming language and Visual Studio .NET as development platform.

The simulation scenario is the representation of a relatively wide indoors area of dimensions *length* x *width*. On this scenario a UWB network is deployed. The network is composed of N_a anchors, fixed and regularly distributed at known positions, and N_m targets, mobile nodes to be located. The location controller (LC) is the functional unit that executes

the tracking algorithm to obtain the estimated position of the targets. For simplicity, the scenario is covered by a single UWB piconet, so data transmission between different piconets and handover are not further considered.

In order to track the position of the target nodes, the distances between the target and a certain number of anchor nodes are estimated (ranging). Estimated distances are generated according to an IR-UWB ranging model. Ideally, instantaneous and lossless acquisition and transmission of the distances has been assumed. Tracking may be performed with all the anchors in coverage of a given target or with a subset of them. Ideal anchor selection is assumed, so the closest anchors are always selected.

5.3.1.1 IR-UWB ranging model

The ranging model characterizes the ranging error distribution and is used to generate the distance estimation samples. Range measurements based on round-trip TOA estimation through n-Way Ranging transactions can be modeled as:

$$\tilde{d}_{ij} = d_{ij} + \varepsilon_{ij} + n_{ij} = d'_{ij} + n_{ij} \tag{5.3}$$

where d_{ij} is the actual distance between nodes i and j, d'_{ij} is the biased distance (with bias ε_{ij}) and n_{ij} is a residual error term.

The biased distance is modeled as a weighted sum of Gaussian and Exponential components conditioned upon the actual distance and channel configuration. The pdf of d', conditioned upon d and a particular channel configuration C, is described as follows:

$$p_C\left[d'/(d,C)\right] = G_C \frac{1}{d}\frac{1}{\sqrt{2\pi}\sigma_C} e^{-\frac{\left(\frac{d'}{d}-1\right)^2}{2\sigma_C^2}} + E_C \frac{1_{\{d'>d\}}}{d}\lambda_C e^{-\lambda_C\left(\frac{d'}{d}-1\right)} \tag{5.4}$$

where $d \neq 0$, $\{ G_C , \sigma_C \}$ and $\{ E_C , \lambda_C \}$ are the weights and parameters of Gaussian and Exponential mixture components, $1_{\{x>y\}}$= 1 whenever x>y and 0 otherwise, and C takes its value among {LOS, NLOS, NLOS2}. The model is enhanced by taking into account the probability $W_C(d)$ to have a particular channel configuration at a distance d. These weights are described as Gaussian-like functions:

$$W_C(d) = \frac{\xi}{\sqrt{2\pi}\varsigma_C} e^{-\frac{(d-d_C)^2}{2\varsigma_C^2}} \tag{5.5}$$

This model for the ranging bias was proposed and validated through a measurement campaign with real UWB equipment in an office environment in [Denis, 2004], where the values for the different parameters of the model were also identified.

The residual error is modeled as additive and centered, with a variance σ_n^2 that depends on detection error terms affecting unitary TOA estimates, i.e. receiver sampling rate, and involved protocol durations, and is independent of the distance between the nodes. As a result of the measurements presented in Section 5.2.2, we have considered two values for the simulations: a pessimistic value of $\sigma_n = 0.7$ m and a realistic value of $\sigma_n = 0.3$ m.

5.3.1.2 Evaluation scenario

Two different evaluation scenarios have been considered:

- Statistical scenario

In this scenario, the mobile nodes can move around the whole area as it is shown in Figure 5.11. A Random Walk Model is used to model target's motion, with random directions and speeds that are constant during a certain interval of time, after which new random directions and speeds are set [Bai, 2006]. A bounce-back technique is used in case the target reaches the limits of the area. When a target reaches the cell border, it is bounced back by changing its direction. Consequently, the dynamic model is characterized by the maximum and minimum speeds and the direction change rate. The indoor environment is taken into account through the ranging model that was previously presented.

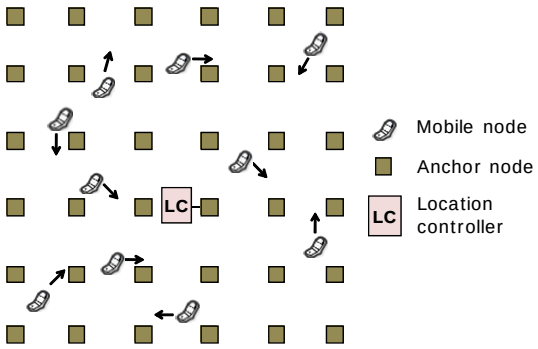

Figure 5.11. UWB location simulator statistical scenario

- Scenario based on wall & route plan

In this scenario, the dynamic model of the targets and the channel configuration is determined by a wall & route plan that is previously defined.

Target's motion model is geographically restricted through a Pathway Mobility Model [Bai, 2006]. The mobile nodes move along predefined routes. Routes are determined by segments, which represent corridors, and nodes, that are the intersection of different segments. At the first iteration, the target is placed in the proximity of a random origin node (with a random deviation from the origin node of 1 meter on each coordinate). Then a random destination node neighbor to the origin node, i.e. there is a segment between origin and destination nodes, is selected according to the given probabilities for going straight, turning left, turning right or going back. A destination point in the proximity of the destination node is selected (with a random deviation from the destination node of 1 meter on each coordinate), and a random speed between maximum and minimum speed is set. When the target reaches the destination point, new destination point and speed are set.

Concerning distance estimation, the same ranging model is used with the difference that the weight of each channel configuration component is determined by the number of walls between the target and the anchor, so one of the channel configuration components (LOS for 0 walls, NLOS for 1 wall and NLOS2 for 2 or more walls) is given a weight of 1 and the other configurations are given null weight.

Figure 5.12 shows the scenarios designed for an area of 50 m x 50 m and a distance between anchors of 12.5 m, 10 m and 8.33 m respectively.

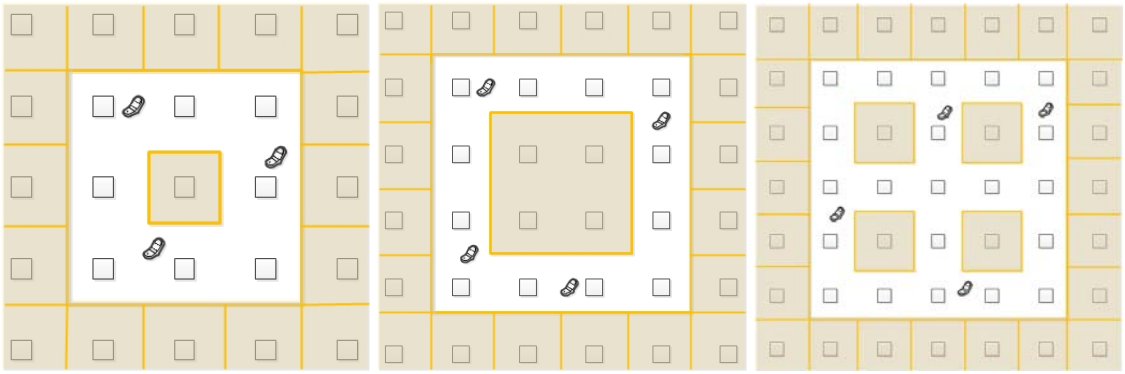

Figure 5.12. Wall & anchor layout for scenarios with 12.5 m, 10 m, and 8.33 m between anchors

5.3.1.3 Location & tracking algorithms implementation

With respect to the tracking technique itself, parametric and non-parametric approaches can be distinguished. Parametric approaches compute the location based on the a priori knowledge of a model, while non-parametric approaches process straightforward the data with the usage, in some cases, of some statistic parameters (mean, variance). The advantage

of non-parametric approaches is the ability to exploit the data remaining completely model independent. Specifically, the following location & tracking algorithms have been implemented:

- Trilateration

Trilateration is a non-parametric algorithm that computes the position based on the distance estimated between the target and three anchor nodes using a geometrical method for determining the intersection of three sphere surfaces. Consequently, only three anchors are used for position computation. If a higher number of anchors are selected, then the three with smallest estimated distance to the target are used. A more detailed explanation of this method is provided in Annex I.1.

- Weighted Least Squares – Multidimensional Scaling (WLS-MDS)

The algorithm WLS-MDS is a completely non-parametric approach combining Multidimensional Scaling (MDS) with Weighted Least Squares minimization (WLS). MDS is used to obtain a previous estimation of the solution. Then, target node location is computed as a solution of a weighted least squares minimization. Specifically, an iterative optimization algorithm known as SMACOF is used. Mathematical background of MDS is detailed in Annex I.2 and SMACOF is explained in Annex I.3.

In short, the WLS-MDS localization algorithm consists of four major steps.

- First, for each measured link, the distance estimate is computed.
- Second, for each measured link a weight is computed in order to capture the reliability of the ranging samples. Specifically, such a weight consists of a dispersion component, which captures the effect of noise under the assumption of bias-free samples, and a penalty component, which quantizes the risk of the latter assumption and penalizes it proportionally.
- MDS is used to obtain a previous estimation of the solution.
- Finally, the last step is the minimization of the objective function.

Concerning the algorithm implementation, DotNetMatrix library has been translated from C# to C++ to provide support for creating and manipulating matrixes, including different matrix decomposition methods, whereas Altaxo library has been used to perform a pseudo-inverse computation required in SMACOF.

- Least Squares – Distance Contraction (LS-DC)

This solution combines the distance contraction (DC) algorithm with least square minimization (LS). A detailed description of DC algorithms is presented in Annex I.4. Once the distances have been estimated, the existence of a feasibility region is checked. The feasibility region is defined as the area formed by the intersection of the circles with centre at the anchors and radio equal to the estimated distance. If the feasibility region does not exist, distance contraction cannot be applied and LS-MDS approach is used instead. If the feasibility region exists, an initial point is computed inside the feasibility region and the contracted distances are computed as the shortest distance from each anchor to the aforementioned feasibility region. Finally, a minimization algorithm is applied using the contracted distances instead of the estimated ones. Since the function becomes convex, any minimization algorithm (i.e. global distance continuation, steepest descent) can be used thus reducing complexity, although here SMACOF has been used in order to be comparable with WLS-MDS.

As for the WLS-MDS implementation, DotNetMatrix library has been translated from C# to C++ to provide support for creating and manipulating matrixes, including different matrix decomposition methods, whereas Altaxo library has been used to perform a pseudo-inverse computation required in SMACOF. Additionally, DotNumerics library has been used to perform the different majorization and minimization functions required in the distance contraction algorithm.

The main advantage of this solution over WLS-MDS is its low complexity, as there is no need of sophisticated optimization algorithms since the function becomes convex. Furthermore, distance contraction already mitigates the error due to NLOS so there is no need of implementing additional NLOS identification and link weighting mechanisms.

- Extended Kalman Filter (EKF)

The Extended Kalman Filter is a Bayesian technique known for its low-complexity, performance and stability as a tracking algorithm. Fundamentals of the Extended Kalman Filter were already discussed in the state-of-the art and a detailed mathematical description can be found in Annex I.5.

Focusing on the specific implementation of the EKF for our tracking application, we have defined the state vector $\mathbf{x}$ to contain target's position $\mathbf{p}_t$ and speed $\mathbf{v}_t$ as variables of our process. The measure vector $\mathbf{z}$ is defined containing the n process observations, namely the estimated distances between the target and the anchors, where n is the number of anchors used for location. The functions that describe the evolution of the state vector through time and the relation between the state vector and the measure vector are:

$$\begin{pmatrix} \mathbf{p}_{t+1} \\ \mathbf{v}_{t+1} \end{pmatrix} = \begin{pmatrix} \mathbf{I} & T_s \cdot \mathbf{I} \\ 0 & \mathbf{I} \end{pmatrix} \begin{pmatrix} \mathbf{p}_t \\ \mathbf{v}_t \end{pmatrix} + \begin{pmatrix} T_s^2 / 2 \cdot \mathbf{I} \\ T_s \cdot \mathbf{I} \end{pmatrix} \mathbf{a}_t \tag{5.6}$$

$$\tilde{\mathbf{z}}_t(i) = \mid \mathbf{p}_i - \tilde{\mathbf{p}}_t \mid + \mathbf{e}_t \tag{5.7}$$

where $\mathbf{a}_t$ is the process noise, $\mathbf{e}_t$ is the measurement noise, T_S is the time between two consecutive updates and $\mathbf{p}_i$ is the position of anchor *i*.

Then, the different covariance and Jacobian (partial derivatives) matrixes were built. The covariance matrixes **Q** and **R** are defined by different parameters, namely the variance of process noise (acceleration) σ_a^2 and the variance of measurement noise (ranging error) σ_e^2. Covariance matrixes **Q** and **R** might change with every time step or measurement, although in a first approach these matrixes are considered to be constant during the simulation. Several simulations were run in order to find the optimum values that minimized the error, and the following values were set: σ_a^2=3 and σ_e^2=0.7.

For the implementation of the filter, we have taken advance of kfilter, which is a C++ variable-dimension extended Kalman filter free software library under a GNU license. In order to ensure a fast convergence from the beginning, the first position is computed using trilateration and this position is used to initialize the filter. On each step, the vectors and matrixes are resized according to the number of measurements available.

- Particle Filter (PF)

Particle Filters (PF) are recursive implementations of Monte Carlo based statistical signal processing. The particle filter is based on a high number of samples of the state vector or particles, which are weighted according to their importance (likelihood) in order to provide an estimation of the state vector. Fundamentals of Particle Filters were already discussed in the state-of-the art, and mathematical background can be found in Annex I.6. The advantage of particle filters over other parametric solutions is that non-linear models and non-Gaussian noise can be defined. As a drawback, their computational complexity is higher, so they are suitable in applications where computational power is rather cheap and the sampling rate slow.

As for EKF, a state vector **x**, a measure vector **z**, and the functions that describe the evolution of the state vector through time (5.6) and the relation between the state vector and the measure vector (5.7) are defined. But here the measurement noise $\mathbf{e}_t$ is not necessarily considered Gaussian. Instead, two measurement error models have been defined:

- Two component error model (PF2): defined as a weighted sum of two Gaussian components for the different channel configurations (LOS/NLOS). The weights of each component are also Gaussian-like functions as defined in eq. (5.5).
- Three component error model (PF3): defined as a weighted sum of three Gaussian components for the different channel configurations (LOS/NLOS/NLOS2). The weights of each component are also Gaussian-like functions as defined in eq. (5.5).

Consequently the filter is defined by the variance of process noise σ_a^2 (acceleration) and the parameters of the measurement error model (mean and variance of the weights and mean and variance of each Gaussian component). Several simulations were run with different values for these parameters in order to find the optimum values that minimized the error.

For the implementation of the particle filter, we have taken advance of SMCTC, a C++ template class library for the implementation of general Sequential Monte Carlo algorithms, which is provided under a GNU license. In order to ensure a fast convergence from the beginning, the first position is computed using trilateration and this position is used to initialize the particles.

5.3.2 Performance evaluation

The performance of each algorithm has been evaluated in terms of absolute positioning error (mean, variance, root mean square error, error distribution...) for the two evaluation scenarios considered (statistical and based in wall & route plan). Different parameters such as the number of anchors used for location, the distance between anchors and the residual ranging error have been considered. Finally, the impact of target mobility and position update rate has also been analyzed.

For these simulations, a common set of parameters has been defined. Simulation duration has been set to 10000 seconds and the number of targets to be tracked to 10. The area size has been set to 50 m x 50 m. Concerning the dynamics of the mobile nodes, minimum and maximum speeds have been set to 0.1 and 3 m/s respectively, and direction changes every 20 seconds. Position update rate has been set to 1 update per second and UWB nodes range to 15 m.

5.3.2.1 Evaluation with the statistical scenario

The performance of each algorithm has been evaluated depending on the number of anchors used for position computation and for different configurations, i.e. distance between anchors.

Figure 5.13 shows the mean absolute error for the different tracking algorithms for a distance between anchors of 10 m., which means that the area will be covered by 36 anchors, and the pessimistic value of ranging residual error σ_n=0.7 m. As it can be observed, the best performance is achieved with the particle filter with 3 components (PF3). Nevertheless, it must be noted that the performance of the particle filter is not very realistic. The reason is that, in the simulator, distance estimation samples are generated using a statistical ranging model. As the particle filter also uses a statistical measurement error model to weight the particles, after parameter optimization, the model behaves almost exactly as the ranging model. This way, the measurement error model can deal even with highly biased measurements and the error of the particle filter decreases as the number of anchors used to compute the position increases. In a real system, this would require a costly characterization of the particular ranging model of the scenario, and alternatively the use of a generic measurement model would not provide so good results. As it can be observed, performance already degrades using a 2-component particle filter (PF2) even if it is also optimized through simulations. Therefore, the results for the particle filter must be considered only as a reference rather than a realistic performance.

LS-DC, WLS-MDS and EKF have a similar evolution with an optimum number of anchors for location of 5, although LS-DC shows the best performance. If more anchors are used, the added anchors will be more distant and will have a higher ranging bias, thus increasing the positioning error. Finally, trilateration shows the worst performance, which is independent on the number of anchors used to compute the position, as it always uses the three closest anchors. For every algorithm, there is an increase of the error when only 3 anchors are used, and the error remains constant for more than 7 anchors, as the target is not likely to be in coverage of more than 7 anchors.

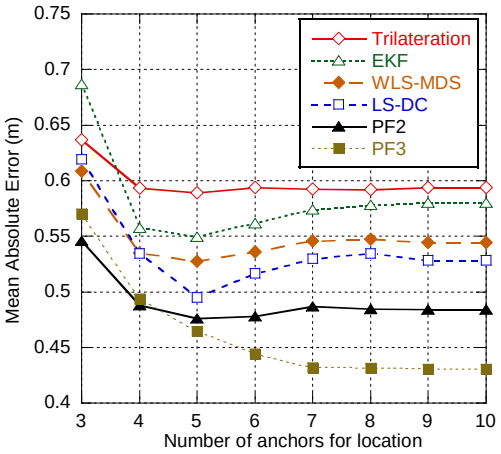

Figure 5.13. Positioning error. Distance between anchors = 10 m. σ_n=0.7 m.

Statistical distribution of the error is analyzed in Figure 5.14 for the trilateration algorithm and 4 anchors used for location. As it can be observed, the error on a coordinate (coordinate x is shown) shows a Gaussian distribution with zero mean. If Gaussian distribution is assumed for the error on each coordinate, then the positioning error, which is the square root of the sum of the square error on coordinate x and the square error on coordinate y, has a Chi distribution with two degrees of freedom. The other algorithms show similar error distributions.

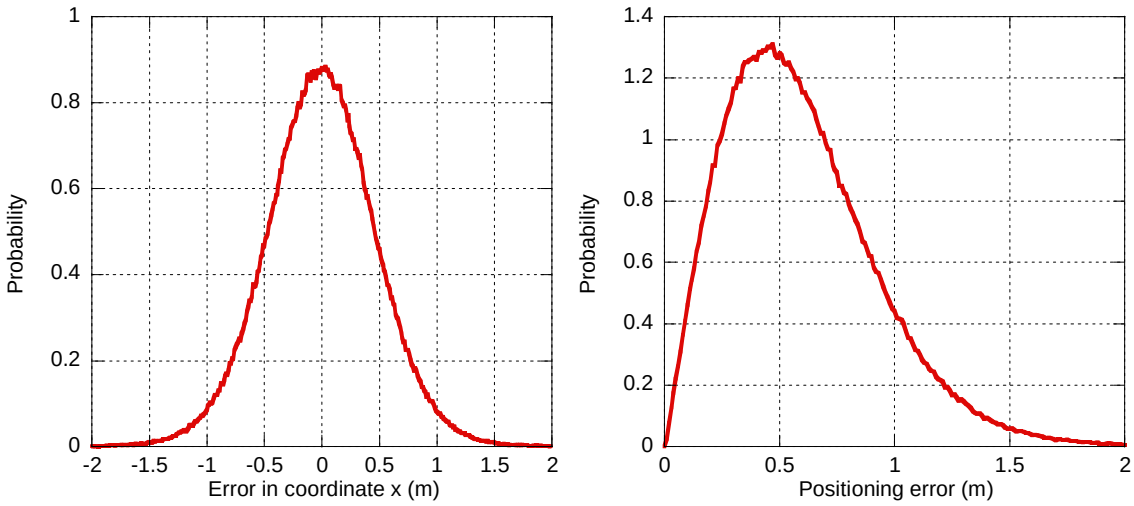

Figure 5.14. Probability Distribution Function of error in coordinate x and positioning error for trilateration

Figure 5.15 shows the performance when the distance between anchors is increased to 12.5 m. (scenario covered by 25 anchors) and reduced to 7.15 m (scenario covered by 64 anchors). As the distance between anchors is increased, some of the anchors used for positioning will be relatively far from the target. In this situation, the 3-components particle filter outperforms the other algorithms, as it takes advance of its precise measurement error model, which can deal with highly erroneous estimations from distant anchors. The 2-components particle filter is not as good, as it more simple LOS/NLOS model cannot deal with the estimations from distant anchors, which have an important NLOS2 component. Concerning the rest of algorithms, LS-DC is the one that deals better with this configuration, as distance contraction compensates the positive bias of the distant anchors, showing a performance that is close to the 2-components particle filter. Trilateration and WLS-MDS, have a similar performance, whereas the Kalman filter shows the worst performance, as its simple Gaussian error model cannot deal with the high bias of the error for very distant anchors. In any case, error is constant for more than 6 anchors, as the target will never be in coverage of more than 6 anchors. On the other hand, when the distance between anchors is

reduced, the selected anchors are closer to the target, so the optimum number of anchors for LS-DC, WLS-MDS and EKF increases to 7. In this situation, LS-DC is able to reach a mean error similar to the particle filter when 7 or fewer anchors are used. As more anchors are used, the added anchors will be more distant to the target, so the error for LS-DC increases whereas the error for the particle filter decreases, as it can deal with highly biased measurements. EKF and WLS-MDS show a very similar performance. Finally, trilateration only shows a slight improvement compared to the previous situation.

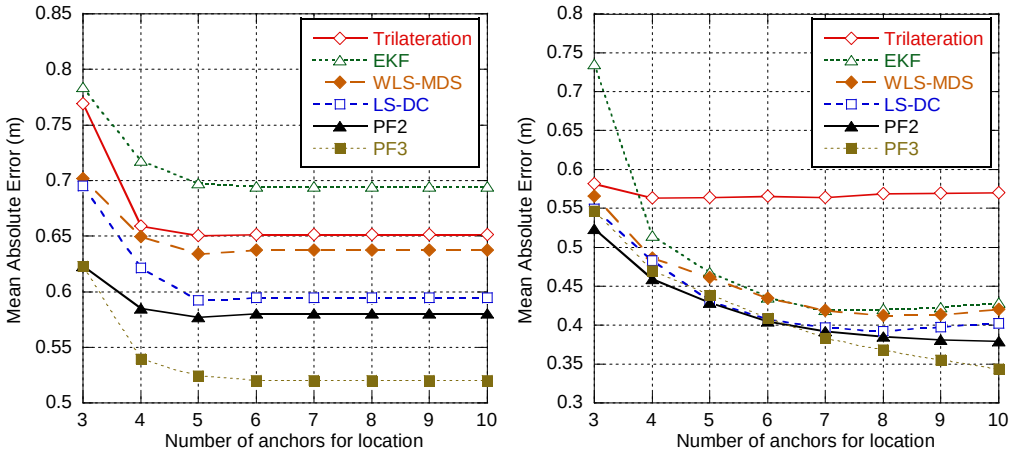

Figure 5.15. Positioning error. Distance between anchors = 12.5 m and 7.15 m. σ_n=0.7 m.

Following the performance of the tracking algorithms for the realistic value of residual ranging error σ_n = 0.3 m. Figure 5.16 shows the mean absolute error for a distance between anchors of 10 m (36 anchors) and 7.15 m (64 anchors). As ranging residual error is reduced, close anchors will provide more accurate estimations, and the impact of ranging bias for distant anchors will be more important. For a distance between anchors of 10 m and compared to the same configuration with ranging residual error σ_n = 0.7 m, MAE is reduced for all the algorithms. Nevertheless, it is noticeable that trilateration shows a much better performance, comparable to LS-DC when 3, 4 or 5 anchors are used. The optimum number of anchors is also reduced to 4 for the LS-DC and EKF and 3 for WLS-MDS, and performance severely degrades as the number of anchors increases. The reason is that now distance estimation for close anchors will be much more accurate than distance estimation for distant anchors, as ranging bias has a higher impact than residual ranging error. When distance between anchors is reduced to 7.15 m, the performance of all the algorithms improves, as the anchors selected will be closer and will provide very accurate estimations as ranging residual noise is low. Both LS-DC and WLS-MDS are very close to the performance of the particle filter when 4 anchors are used, with a minimum average error of 14 cm. On the other hand, EKF shows the worst performance.

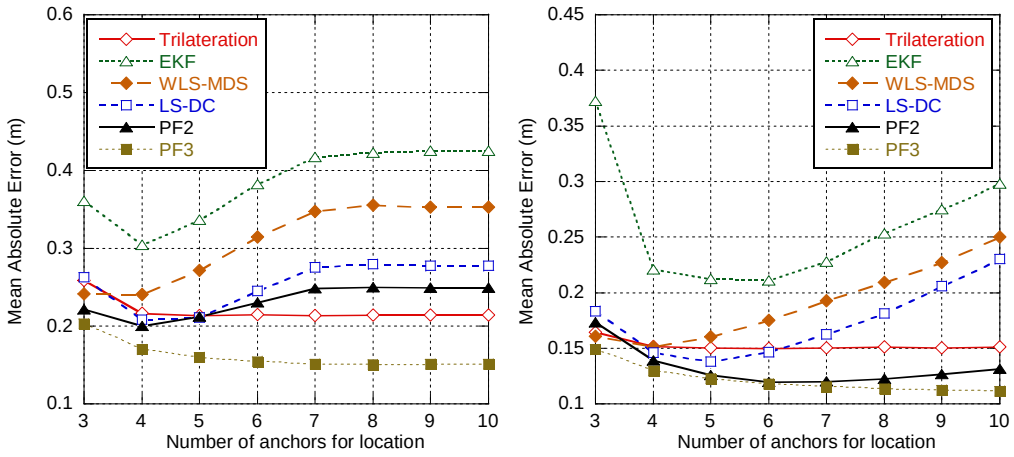

Figure 5.16. Positioning error. Distance between anchors = 10 m and 7.15 m. σ_n=0.3 m.

To sum up, concerning distance between anchors, positioning error decreases as distance between anchors is reduced. When distance between anchors is below 10 m, LS-DC provides similar results to particle filter, whereas trilateration only shows a slight improvement. Nevertheless, in order to minimize the number of anchors that are needed to cover a certain area, a high distance between anchors is desirable. When distance between anchors is over 10 m, the 3-components particle filter outperforms the other algorithms, as its measurement error model can compensate high ranging bias, whereas LS-DC shows a better performance than EKF and WLS-MDS, which are the most sensitive to the increase of distance between anchors, as they are more sensitive to ranging bias.

On the other hand, the performance of all the algorithms improves as ranging residual error decreases, which can be achieved increasing the resolution in TOA estimation, and a mean error around 15-30 cm for 10 m between anchors can be obtained for σ_n=0.3 m. Trilateration is the most sensitive to TOA estimation, getting the worst results for high ranging residual error. This means that trilateration requires accurate distance estimation in order to provide good results.

5.3.2.2 Evaluation with the scenario based on wall & route plan

A similar analysis has been done for the scenarios based on wall & route plan that were shown in Figure 5.12. Figure 5.17 shows the mean absolute error for the different algorithms for a distance between anchors of 10 m, and values of ranging residual error σ_n = 0.7 m and 0.3 m. Again the best performance is achieved with the 3-components particle filter, as it can deal even with severe NLOS situations. Nevertheless, the particle filter with 2 components does not provide so good results as for the statistical scenario (Figure 5.13), as it does not take into account severe NLOS situations. This emphasizes the need of an accurate ranging

model characterization in order to obtain good results with the particle filter, and shows the degradation when a generic model is used.

LS-DC, WLS-MDS and EKF have a similar evolution with an optimum number of anchors for location of 5 for σ_n = 0.7 m and 4 for σ_n = 0.3 m. As more anchors are used, the added anchors are likely to be in NLOS or severe NLOS, so the positioning error increases for EKF and LS-DC. Nevertheless, the error does not increase for WLS-MDS due to link weighting, as anchors in NLOS/NLOS2 situations will have a lower weight and will not be detrimental to position optimization. This was not noticeable in the statistical scenario as ranging error samples were generated as a weighted sum of the different channel components (LOS/NLOS/NLOS2) and were uncorrelated, so dispersion-based weighting did not have an appreciable effect, whereas in this scenario the ranging error is generated using only the channel component determined by the wall layout, which is generally the same for consecutive samples. Finally, trilateration shows the worst performance for σ_n = 0.7 m, which is independent on the number of anchors used to compute the position, as the three closest anchors are always used. Nevertheless, it is noticeable that trilateration shows now a much better performance for σ_n = 0.3 m, better than the rest of algorithms apart from the 3-component particle filter.

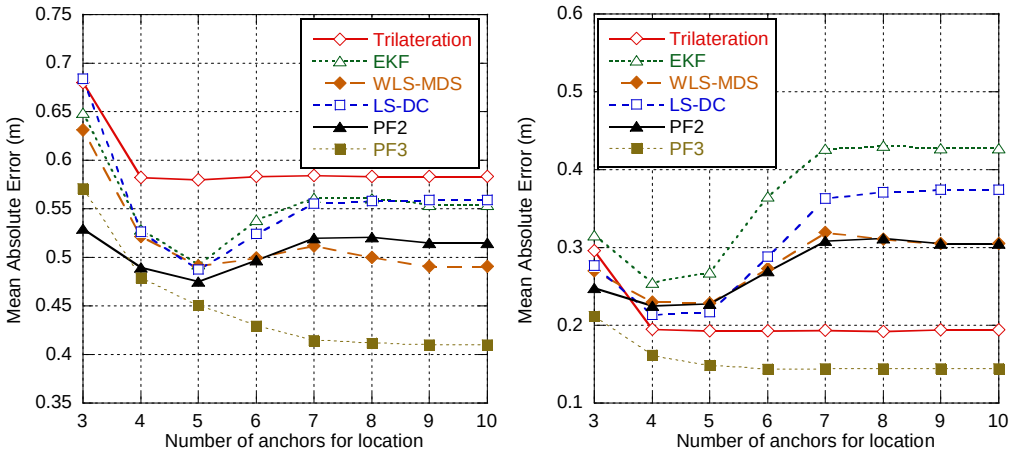

Figure 5.17. Positioning error. Distance between anchors = 10 m. σ_n=0.7 m and σ_n=0.3 m.

The performance for the scenario with a distance between anchors of 12.5 m is shown in Figure 5.18. As expected, accuracy is degraded for all the algorithms. Similarly to the statistical scenario, the 3-components particle filter outperforms the other algorithms, as it takes advance of its precise measurement error model, which can deal with highly erroneous estimations from distant anchors. Again, the 2-components particle filter does not provide so good results as in the statistical scenario, as it more simple LOS/NLOS model cannot deal with the NLOS2 situations. Concerning the rest of algorithms, LS-DC and WLS-MDS show

a performance comparable to the 2-components particle filter, as distance contraction and dispersion-based weighting respectively are able to deal with the high bias of the distant anchors. Finally, trilateration show the worst performance for σ_n = 0.7 m and EKF provides the worst performance for σ_n = 0.3 m. In any case, error is constant for more than 6 anchors, as the target will never be in coverage of more than 6 anchors.

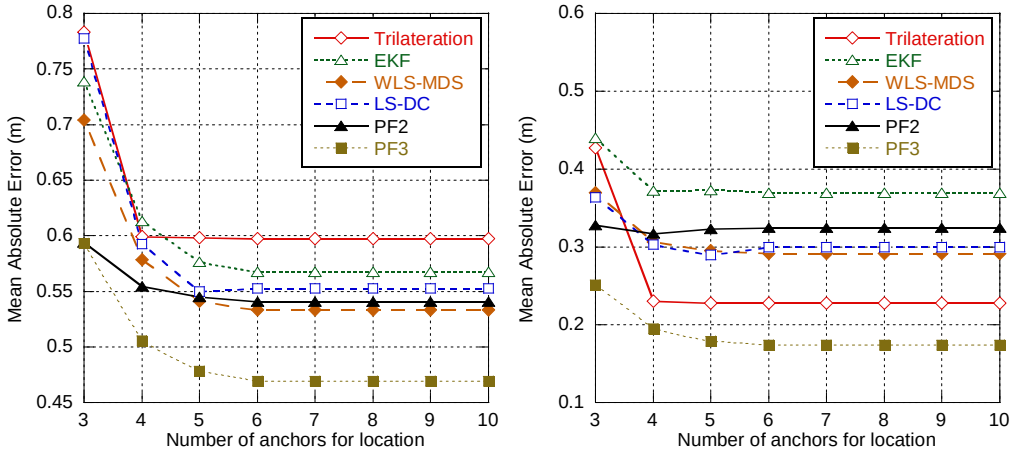

Figure 5.18. Positioning error. Distance between anchors = 12.5 m. σ_n=0.7 and σ_n=0.3.

Figure 5.19 shows the results for the scenario with a distance between anchors of 8.33 m, so 49 anchors cover the scenario. The 3-component particle filter shows again the best performance, whereas trilateration shows the worst for σ_n = 0.7 m and EKF shows the worst for σ_n = 0.3 m. LS-DC, WLS-MDS and EKF have a similar performance with an optimum number of anchors of 5 for σ_n = 0.7 m, reaching an error level close to the particle filter in that case. LS-DC and EKF are degraded for a higher number of anchors, whereas WLS-MDS is able to maintain its performance. For σ_n = 0.7 m, LS-DC and WLS-MDS are close to the performance of the particle filter when 4 anchors are used, with a minimum MAE of 19 cm for LS-DC.

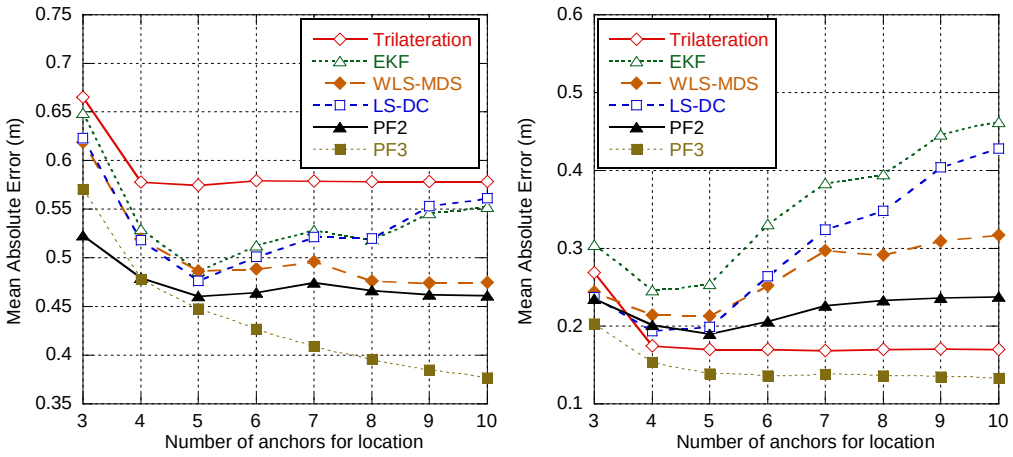

Figure 5.19. Positioning error. Distance between anchors = 8.33 m. σ_n=0.7 and σ_n=0.3.

To sum up, with the scenario based on wall & route plan some conclusions arise. The 2-component particle filter does not get so good results as its LOS/NLOS model is not well suited for eventual severe NLOS (NLOS2) situations, which emphasizes the need of an accurate ranging model characterization for the particle filter. EKF and LS-DC are also degraded when more than 5 anchors are used as the added anchors are likely to be in NLOS or NLOS2 situation. WLS-MDS is not degraded as link weighting mitigates this effect through the use of low weights in NLOS/NLOS2 situations. Nevertheless, it must be noted that the comparison should be established considering the minimum error for the optimal number of anchors, and our goal should be minimizing the number of anchors used. Concerning the minimum error, LS-DC generally provides equal or better results than WLS-MDS and EKF. Finally, trilateration only shows good results for low ranging error, which again means that it requires high resolution in TOA estimations.

5.3.2.3 Effect of target mobility and position update rate

Finally, a very important parameter that impacts on the accuracy of the tracking algorithms is the position update rate, which defines how often the positions of the mobile nodes are updated, or inversely the position update interval. Position update rate is closely related to target mobility, as higher target speed requires more frequent position updates in order to accurately track the target. In the simulator, target mobility is characterized by target speed and direction change rate.

In order to assess the effect of target mobility and position update rate, the statistical scenario has been considered in order to allow full mobility along the area. 10 meters between anchors and 4 anchors used for location have been considered. Two parameters are going to be used to measure the error. Positioning Error measures the error in the position

estimated by the algorithm on each update. Tracking Error measures the error in the position available at the target at every simulation step, not only when it is updated. This error is not only due to the error in the position estimation, but also to the movement of the target since the last position update.

Figure 5.20 shows the positioning error and the tracking error for the different algorithms depending on the target speed. Concerning the positioning error, non-parametric methods such as trilateration and LS-DC show no dependence on target speed, as position computation is independent on previous position estimations. Nevertheless, WLS-MDS shows a slight dependency on target speed due to link weighting, as weights are based on the dispersion of distance estimations using the last 5 samples, so it degrades as target speed increases. On the other hand, the Kalman filter depends on target speed, as position computation is based on previous position and target's dynamic model. Kalman filter shows a slightly better performance than LS-DC if target speed is below 1.5 m/s, but severely degrades for higher speeds. Finally, although the particle filter uses the target's dynamic model to move the particles, it is almost independent on target speed, as particles are weighted on each step according to the likelihood of their position in relation to the measurements, so the new position is almost independent of the previous one.

Concerning the tracking error, it grows as target speed increases, as the target will have travelled a larger distance since the last position update. This means that if we look up the target's position at a random time and not only when it is updated, the mean error will be similar for all the algorithms, as the effect of not having the position updated is more important than the positioning accuracy of the different algorithms. Nevertheless, for speeds below 0.6 m/s the effect of not having the position updated is not so important and the error is mostly due to positioning error, and for speeds higher than 2 m/s EKF gets worse due to the degradation in positioning accuracy as the filter cannot track the target.

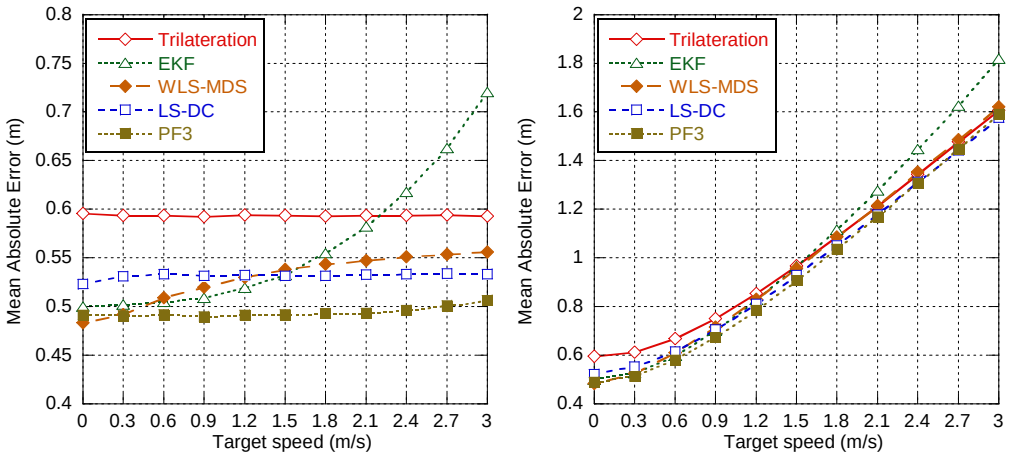

Figure 5.20. Positioning error and tracking error depending on target speed

Figure 5.21 shows the positioning error and the tracking error for the different algorithms depending on position update interval. Concerning the positioning error, trilateration and LS-DC are independent of position update interval as position computation is independent on previous position estimations, whereas WLS-MDS shows a slight dependency due to dispersion-based weighting. EKF shows again a strong dependency on position update interval. As the new position is computed based on previous position, interval between two successive updates must be as short as possible in order to accurately track the target. EKF shows a better performance than LS-DC for update intervals shorter than 800 ms and severely degrades as the position update interval. Positioning accuracy for the particle filter shows a slight dependence on position update rate, increasing from 45 cm for a position update interval of 400 ms to 55 cm for a position update interval of 2 s.

Concerning the tracking error, as it was previously noted for target speed, when the position update interval is over 800 ms, the effect of not having the position updated is more important than the difference in positioning accuracy, so all the algorithms show similar results except EKF, which shows a worse performance due to the degradation in positioning accuracy. When the position update interval is below 800 ms, the effect of not having the position updated is not so important and the error is mostly due to the positioning error.

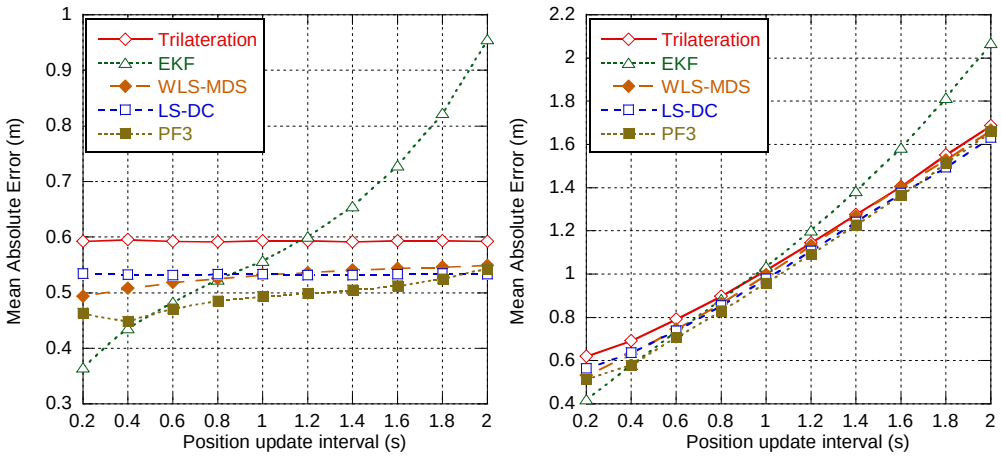

Figure 5.21. Positioning error and tracking error depending on time between updates

To sum up, non-parametric algorithms, i.e. trilateration, WLS-MDS and LS-DC, are independent of target mobility and position update rate as each position computation is independent of the previous estimated position, although WLS-MDS shows a slight dependency due to the dispersion-based weighting. On the other hand, EKF is highly dependent on target speed and position update rate, as estimated position is computed based on previous position. With a position update interval of 1 s, targets up to 1.5 m/s can be tracked with same accuracy as LS-DC, and in order to track faster targets position update interval should be reduced to 600-800 ms, which would entail a higher need of resources. Finally, despite using target's dynamic model, particle filter is only slightly dependent on position update rate, and is able to accurately track targets up to 3 m/s.

5.3.2.4 Conclusions

According to the analysis presented here, the highest accuracy is obtained for the particle filter. Nevertheless, as it was previously commented, results for the particle filter are not very realistic, as the error in distance estimations is generated using a statistical ranging model and the measurement error model of the filter can be optimized to behave similarly. Consequently, it can cope with the highly biased measurements from the distant anchors and get almost the best possible accuracy. This algorithm assumes that the error model is known, which would entail that an exhaustive calibration campaign should be performed in order to identify the specific model of the particular location where the tracking system is going to be deployed, or alternatively a generic ranging model should be used that will not be specific for that location, thus introducing some error. As it was shown, the use of a 2-component model does not provide so good results, especially in the scenario based on walls & routes plan, which emphasizes the need of an accurate error model characterization for the particle

filter. Finally, it must be noted that computational complexity of this algorithm is higher than the other algorithms.

Concerning the rest of algorithms, both WLS-MDS and LS-DC approaches provide the highest accuracy in most of the configurations simulated. Dispersion-based weighting and distance contraction are able to deal with biased estimations for distant and NLOS anchors better than other schemes such as 2-component particle filter or Kalman filter. Furthermore, they are completely non-parametric algorithms, so no characterization of the target dynamics or the measurement model is required, and are independent of the target speed and position update rate. Another advantage of WLS-MDS is that it allows computing the position of multiple targets simultaneously.

Extended Kalman filter is a relatively easy and fast parametric algorithm that only needs a simple characterization of the dynamic and measurement models. It has a good performance on static and slow moving targets with speeds less than 1 m/s, but severely degrades as speed increases. This is an important limitation for our scenario, as the goal is to track moving users at pedestrian speeds up to 3 m/s. Furthermore, its simple Gaussian measurement model cannot deal with highly biased estimations for distant or NLOS anchors.

Finally, trilateration is a very simple method that may be suitable if a very high accuracy is not required. It provides a good performance when distance estimations are very accurate, i.e. ranging residual error is low, but fails for higher ranging error levels, as it cannot take advance of diversity of measurements as it always uses three measurements for position computation. Nevertheless, low ranging residual error requires high TOA resolution and consequently high sampling rate, which would increase complexity and cost of the UWB devices.

5.3.3 Geographically enhanced algorithms

This section focuses on the use of geographical information, such as the knowledge of walls location and potential user's routes, in order to improve existing location and tracking algorithms. Actually, most of the LT applications require the integration of positioning systems with Geographic Information Systems that are used to analyze and display the location information. Geographic information available in the GIS, such as a floor plan, can be used not only for visualization purposes, but also to improve positioning. For example, the wall layout information could be used for optimal NLOS identification. In fact, the use of geographic information in order to improve localization is not a new topic. Map-matching techniques are widely extended in vehicle navigation applications in order to match the position provided by GPS and inertial sensors with the road map information.

The wide indoor scenarios considered (airports, shopping malls, etc.) are likely to have geographical information available, such as a plan with the wall layout. Furthermore, user's movement in this kind of scenarios is usually confined to an area of interest where the users are likely to move along, i.e. main corridors, thus defining the potential paths. This geographical information can be exploited by the location and tracking algorithms in order to improve accuracy or alternatively reduce the amount of resources needed to reach a certain accuracy level, for example reducing the number of anchors used for location, reducing the position update rate or increasing the distance between anchors, thus reducing the total number of anchors.

Parametric algorithms have a higher potential to be enhanced through the modification of the target dynamic model and the measurement model according to the geographic information available. Specifically, two are the main enhancements envisioned. NLOS identification aims to identify which links are in NLOS conditions according to the wall layout and the estimated target position, and to use this information in the measurement model. The other enhancement consists on the modification of target's dynamic model taking advance of the available path information. Concerning non-parametric algorithms, the use of geographic information is also possible, although potential enhancements are more limited. Approaches featuring weighted least square based optimization (e.g. SMACOF), such as WLS-MDS or WLS-DC, can be modified so weights are set according to NLOS identification.

Specifically, enhancements for the following algorithms are proposed: Extended Kalman filter, Particle filter, WLS-MDS and WLS-DC. The performance of each enhancement has been evaluated in terms of the mean absolute error. Similar simulation parameters as in the previous sections have been used. The scenario based in walls & routes plan with 36 anchors (10 m between anchors) has been considered.

5.3.3.1 WLS-MDS

As WLS-MDS is non-parametric algorithm, the potential use of geographical information is limited. Nevertheless, knowledge of wall layout can be used for NLOS identification in order to reduce the weight of NLOS measurements in the optimization phase.

Specifically, we have implemented NLOS identification based on the wall layout and the previous estimated position of the target. For each target-anchor pair, channel configuration is identified and the following weights are applied W_{LOS}=1; W_{NLOS}=0.6, W_{NLOS2}=0.1. These weights can be applied independently or in addition to dispersion-based

link weights (W_d). Therefore, we have four possible schemes: LS-MDS (no weighting), WLS-MDS Disp (with dispersion-based link weighting), WLS-MDS NLOS (with wall-layout based NLOS identification) and WLS-MDS Disp+NLOS (with dispersion-based link weighting and wall-layout based NLOS identification).

Figure 5.22 shows the mean absolute error for the different schemes depending on the number of anchors used to compute target's position for σ_n=0.7 m and σ_n=0.3 m. LS-MDS using no weighting shows the worst performance, with an optimum number of anchors of 5 for σ_n=0.7 m and degradation in accuracy for a higher number of anchors, as the added anchors will likely be in NLOS situation and will have a negative effect on estimated position. The use of dispersion-based weights in WLS-MDS Disp shows better accuracy, also with an optimum number of anchors of 5 for σ_n=0.7 m, but in this case accuracy is not degraded for a higher number of anchors, as NLOS anchors have higher dispersion and consequently will get lower weights. The scheme with NLOS identification based in wall layout, WLS-MDS NLOS, shows even better results, as it allows an optimum identification and weighting of links in NLOS conditions, and accuracy improves as the number of anchors increases. Combining both weighting techniques in WLS-MDS Disp+NLOS provides only slightly better results than using only NLOS identification. For 5 anchors and σ_n=0.7 m, LS-MDS shows a MAE of 52 cm, compared to 49 cm for WLS-MDS Disp, 46 cm for WLS-MDS NLOS and 45.5 cm for WLS-MDS Disp+NLOS. When σ_n=0.3 m, the influence of channel conditions is higher, and so is the importance of NLOS identification. The optimal number of anchors is reduced to 4 for LS-MDS and 5 for the rest of schemes. The minimum MAE for LS-MDS is 24.5 cm compared to 23 cm for WLS-MDS Disp, 18.5 cm for WLS-MDS NLOS and 17.5 cm for WLS-MDS Disp+NLOS.

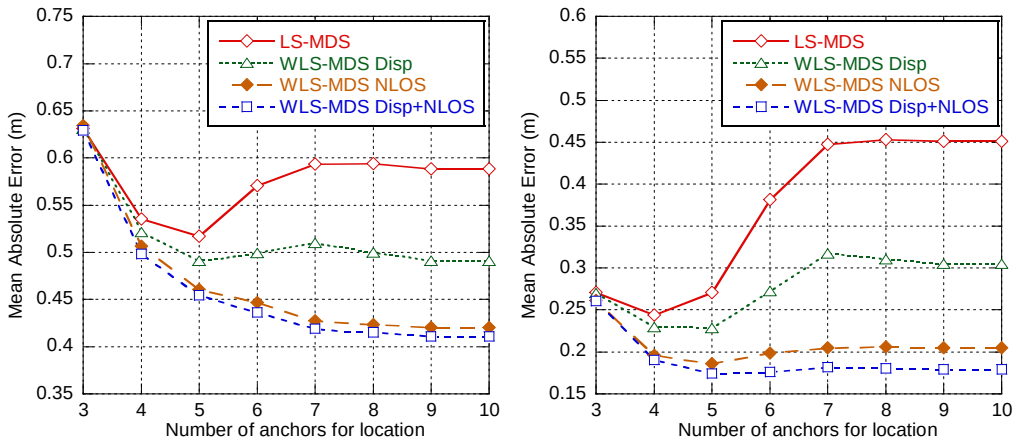

Figure 5.22. Positioning error for enhanced MDS. σ_n=0.7 m and σ_n=0.3 m.

5.3.3.2 LS-DC

Again we have evaluated four possible schemes: LS-DC (no weighting), WLS-DC Disp (with dispersion-based link weighting), WLS-DC NLOS (with wall-layout based NLOS identification) and WLS-DC Disp+NLOS (with dispersion-based link weighting and wall-layout based NLOS identification).

Figure 5.23 shows the positioning error for the different schemes depending on the number of anchors used to compute target's position for σ_n=0.7 m and σ_n=0.3 m. As it can be observed, when Distance Contraction is used, the use of dispersion-based weights provides little benefit. WLS-DC Disp shows a similar performance to LS-DC when 5 or fewer anchors are used for location, and only shows a little gain when 6 or more anchors are used. Nevertheless, this is not interesting as the goal is to minimize the number of anchors used and the minimum error is reached when 5 anchors are used. On the other hand, methods using NLOS identification based on wall layout knowledge show a better performance, and accuracy improves as the number of anchors increases, as it allows an optimum identification and weighting of links in NLOS conditions. The method using both dispersion-based weighting and NLOS identification, WLS-DC Disp+NLOS, shows a similar performance to the method using NLOS identification, WLS-DC NLOS. For σ_n=0.7 m and 5 anchors, LS-DC shows a MAE of 49 cm, compared to 48.5 cm for WLS-DC Disp and 45 cm for WLS-DC NLOS and WLS-DC Disp+NLOS. For σ_n=0.3 m, the relative gain of NLOS identification is higher. The optimal number of anchors is reduced to 4 for LS-DC and WLS-DC Disp and 5 for WLS-DC NLOS and WLS-DC Disp+NLOS. The minimum MAE for LS-DC and WLS-DC Disp is 21 cm compared to 17 cm for WLS-DC NLOS and WLS-DC Disp+NLOS.

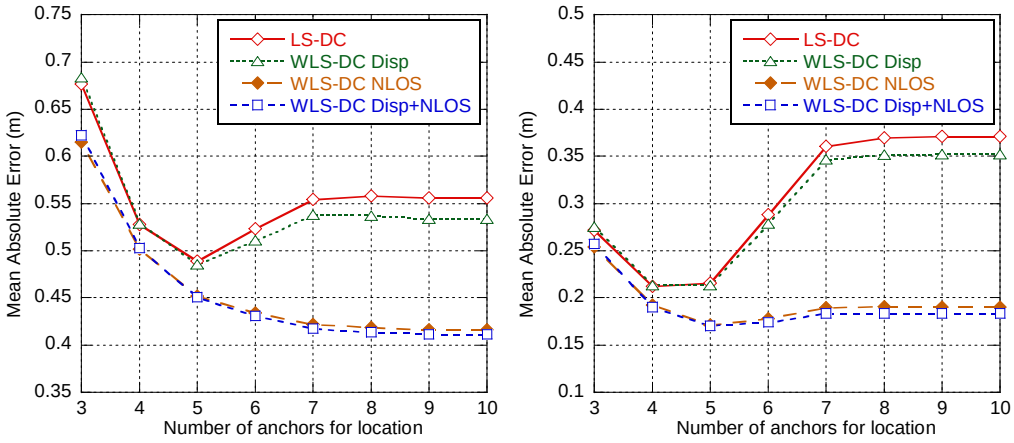

Figure 5.23. Positioning error for enhanced LS-DC. σ_n=0.7 m and σ_n=0.3 m.

5.3.3.3 Extended Kalman Filter

As it was commented in the Extended Kalman Filter description, the process noise covariance matrix **Q** and the measurement noise covariance matrix **R** might change with every time step or measurement. This way, we can enhance our EKF implementation taking advance of the availability of geographical information. Specifically, the following enhancements have been implemented:

- NLOS identification: Using the wall layout information and the previous estimated position of the target, we can identify the channel configuration (LOS/NLOS/NLOS2) between each target-anchor pair. Different variances can be used in the measurement noise covariance matrix **R** depending on the channel configuration for a certain target-anchor pair. Specifically, the following values are used: $\sigma_{LOS}^2=0.9\cdot\sigma_e^2$, $\sigma_{NLOS}^2=1.3\cdot\sigma_e^2$, $\sigma_{NLOS2}^2=7\cdot\sigma_e^2$
- Path information: Using the information concerning the different nodes and segments defined in the scenario, we can identify if a target is in a node (intersection) or a segment (corridor) according to its previous estimated position. If the target is in a node, the variance of the process noise, which represents acceleration, is increased as the target is likely to have a direction change. On the other hand, if the target is in a segment, the process noise can be reduced. Specifically, the following values are used: $\sigma_{node}^2=5\cdot\sigma_a^2$, $\sigma_{segment}^2=0.1\cdot\sigma_a^2$

Therefore, we have four possible schemes: EKF, EKF-NLOS (with wall-layout based NLOS identification), EKF-path (with use of path information) and EKF-NLOS+path (wall-layout based NLOS identification and use of path information).

Figure 5.24 shows the mean absolute error for the different schemes depending on the number of anchors used to compute target's position for σ_n=0.7 and σ_n=0.3 m. EKF with no enhancements shows the worst performance in both cases. For σ_n=0.7 m, the optimum number of anchors of EKF is 5 and accuracy is degraded for a higher number of anchors, as the added anchors will likely be in NLOS situation and will have a negative effect on estimated position. The use of route information in EKF-path provides a gain in accuracy between 3 cm and 6 cm, also with an optimum number of anchors of 5. The scheme with NLOS identification based in wall layout, EKF-NLOS shows a similar gain when 5 anchors are used but accuracy improves as the number of anchors increases, as NLOS identification allows a better characterization of the measurement noise of links in NLOS/NLOS2 conditions. Combining both techniques in EKF-NLOS+path provides the best results, with a similar evolution to EKF-NLOS but a gain in accuracy between 3 and 6 cm. For σ_n=0.7 m

and 5 anchors, EKF shows a MAE of 49 cm, compared to 45 cm for EKF-path and EKF-NLOS and 41 cm for EKF-NLOS+path.

On the other hand, for a ranging residual error σ_n=0.3 m, the accuracy and variability of the estimated distances is improved and the gain of using routes information is reduced. On the other hand, the influence of channel conditions is higher, and so is the importance of NLOS identification. The optimal number of anchors is reduced to 4 for EKF and EKF-path and 5 when NLOS identification is used. The minimum MAE for EKF is 25.5 cm compared to 24 cm for EKF-path, 18 cm for EKF-NLOS and 16.5 cm for EKF-NLOS+path.

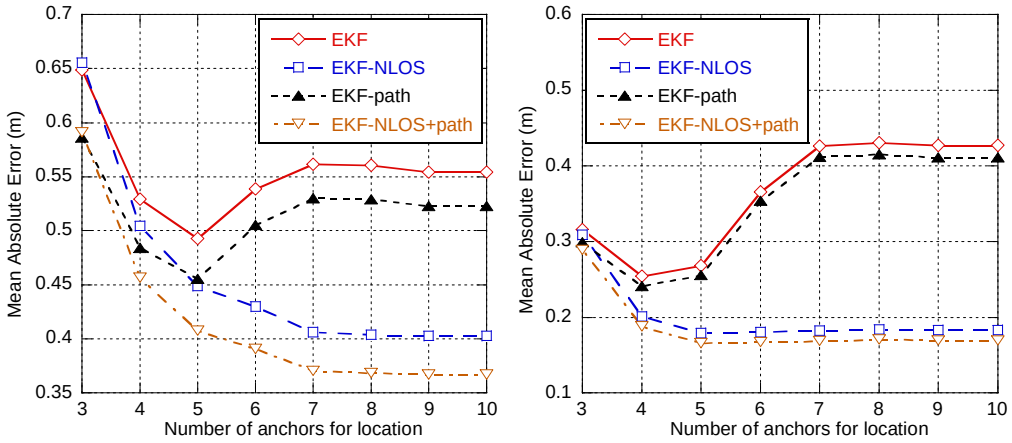

Figure 5.24. Positioning error for enhanced EKF. σ_n=0.7 m and σ_n=0.3 m.

5.3.3.4 Particle filter

As the motion and observation models for the particle filter are not necessarily linear, this algorithm has a higher potential to be enhanced taking advance of the availability of geographical information. Specifically, the following enhancements have been implemented:

- NLOS identification: Using the wall layout information and the position of each particle, we can identify the channel configuration (LOS/NLOS/NLOS2) between each particle-anchor pair. Thus we modify the 3-components error model so only the component corresponding to the channel configuration of the particle-anchor pair is used, instead of a weighted sum of the three components. This enhancement is not only expected to improve accuracy, but also facilitates characterization of the measurement model as it is not longer necessary to characterize the distribution of the weights of each channel configuration depending on the distance.

- Path information: The first approach is taking into account the area where the target may be located (colored white in Figure 5.12). For every particle, we identify if the

particle is inside or outside that area. Weight (likelihood) of particles outside the location area is decreased by a certain factor W_{out}. On the other hand, using the information concerning the different nodes defined in the scenario, we can identify when a target is approaching a node according to its previous estimated position. If the target is approaching a node, then it is likely to have a direction change. Then we can change the direction and speed of a certain percentage of the particles p_{change} according to the probabilities defined for going straight, turning left, turning right or going back. The values of W_{out} and p_{change} were optimized through simulations to W_{out} = 1/6 and p_{change} = 0.9.

Therefore, we have four possible schemes: PF3, PF3-NLOS (with wall-layout based NLOS identification), PF3-path (with use of path information) and PF3-NLOS+path (wall-layout based NLOS identification and use of path information).

Figure 5.25 shows the positioning error for the different schemes depending on the number of anchors used to compute target's position for σ_n=0.7 m and σ_n=0.3 m. For σ_n=0.7 m, the mode with no enhancements shows the worst performance, with an optimum number of anchors of 6. The use of route information in PF3-path provides a gain of 5 cm when 3 anchors are used, and the gain is reduced to 1cm as the number of anchors increases. The scheme with NLOS identification based in wall layout, PF3-NLOS shows a similar gain when 4 anchors are used but accuracy improves as the number of anchors increases, as NLOS identification allows a better characterization of the measurement noise of links in NLOS/NLOS2 conditions. Combining both techniques in PF3-NLOS+path provides the best performance, similar to PF3-path when 3 anchors are used and to PF3-NLOS when 4 or more anchors are used. If we set the number of anchors used to 5, PF3 shows a MAE of 42 cm, compared to 41 cm for PF3-path and 39 cm for PF3-NLOS and PF3-NLOS+path. On the other hand, for σ_n=0.3 m, the gain of the different enhancements is reduced as the accuracy and variability of the estimated distances is improved. In fact the use of routes information does not provide any appreciable improvement. PF3-NLOS provides a gain in accuracy of 2 cm when 3 anchors are used that is reduced to 0.5 cm if more anchors are used. MAE when 5 anchors are used is 14.8 cm for PF3 and PF3-path, compared to 14.4 cm for PF3-NLOS and PF3-NLOS+path.

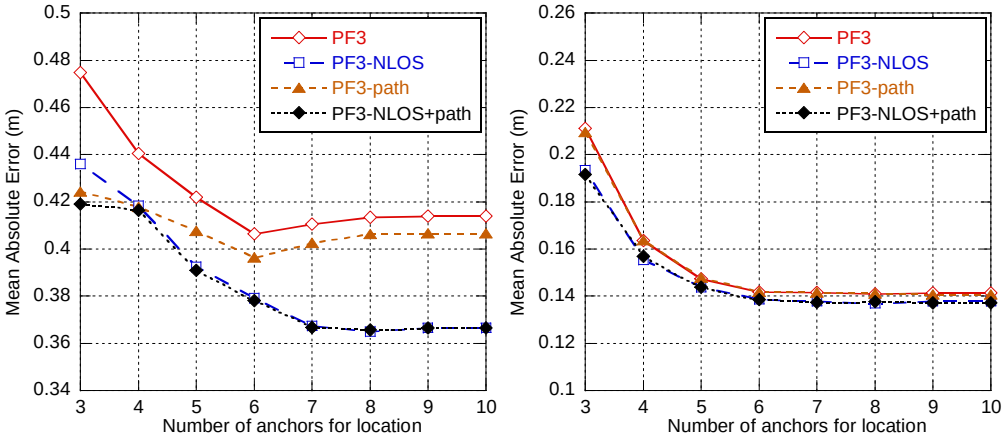

Figure 5.25. Positioning error for enhanced Particle Filter. σ_n=0.7 m and σ_n=0.3 m.

5.3.3.5 Enhanced algorithms comparison

Figure 5.26 shows the comparative performance of the different geographically enhanced algorithms for a ranging residual error σ_n=0.7 m. The enhanced EKF shows the greatest improvement compared to the non-enhanced version with a performance similar to PF for a high number of anchors. The reason is that the simple Gaussian measurement noise model was unable to deal with NLOS situations, which is solved with NLOS identification and the use of different measurement noise variances depending on the channel configuration. Nevertheless, the enhanced PF also shows a very good performance when 3 or 4 anchors are used, which is interesting in order to minimize the amount of temporal and physical resources that are needed to compute user's position. Finally, as it was previously stated, non-parametric approaches have less potential to be improved and enhanced WLS-MDS shows the worst results. Nevertheless, as a completely non parametric approach WLS-MDS is model independent so no model characterization is required.

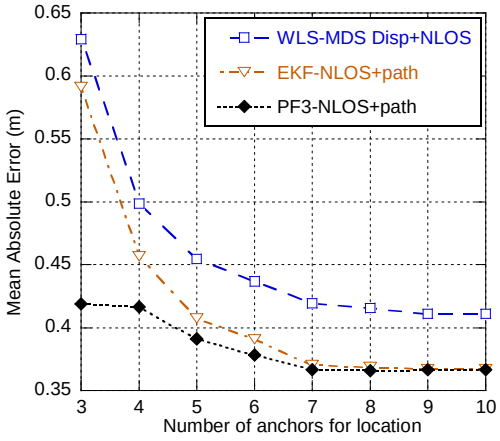

Figure 5.26. Positioning error for the different enhanced algorithms

5.3.3.6 Conclusions

As it has been shown, geographical information such as the location of walls and the potential location area and routes of the target can be used to enhance the existing location & tracking algorithms, thus improving their performance. In general parametric algorithms have a higher potential for improvement, as dynamic and measurement models can be modified to take advance of the geographical information. Nevertheless, non-parametric algorithms can also be enhanced using techniques such as weighted least squares optimization.

If we set the number of anchors used to locate a target to 5, the geographically-enhanced EKF provides an accuracy gain of 8 cm compared to simple EKF. Concerning the Particle Filter, this algorithm already provided very good results although a further gain of 3 cm can be obtained using the geographical information. For WLS-MDS and WLS-DC, weighting based on NLOS identification shows a 5 cm gain compared to dispersion-based weighting. In general, NLOS identification based on wall layout knowledge provides high accuracy gain due to the specific characteristics of indoor environments, as NLOS situations are frequent and cause important degradation on positioning accuracy. On the other hand, the use of path information only provides a slight gain, as the location area is large in relation to the scenario and the movement of people highly variable and unpredictable (they can suddenly stop or change direction), specially compared to vehicle tracking applications where the location area is constrained to roads, as is vehicle direction, and speed varies progressively.

In case a high level of accuracy is not required, geographical information could be also used to reduce the amount of resources needed to reach a certain accuracy level. For example, distance between anchors can be increased, so fewer anchors are needed to cover

the location area. Or alternatively, the number of anchors used to locate a target can be reduced, thus reducing the amount of ranging exchanges and therefore the amount of temporal resources needed. As it will be shown in the following chapter, when a real MAC is taken into account, the amount of resources used for location is important as it impacts on both positioning accuracy and system capacity.

Chapter 6

Combined Communication and Location Tracking UWB System

6.1 Introduction

As it was mentioned in Section 3.2.3, a few UWB-based indoor location systems can already be found in the market. Nevertheless, these systems only use UWB for distance estimation, while communication between the different elements involved in the positioning system is done using other technologies, generally wired. In contrast, UWB systems combining location and data transmission (for example in the framework of IEEE 802.15.4a standard) would increase flexibility reducing the cost and complexity of the system deployment. In this scenario, accuracy is not the only evaluation criteria, but also the amount of resources associated to the location service, as it impacts not only on the location capacity of the system, but also on the available data rate for non-location data communication.

Although several studies can be found in the literature addressing UWB-based localization, as it was shown in Section 3.2, these studies mainly focus on distance estimation and position calculation algorithms. Practical aspects such as the design of the functional architecture, the procedure for the transmission of the associated information between the different elements of the system, and the need of tracking multiple terminals simultaneously in various application scenarios, are generally omitted. These aspects would lead to consider the amount of resources associated to the global location service as a quality parameter, and a dynamic scenario of mobile terminals and reference nodes for positioning.

Nevertheless, the application of the UWB technology for the development of combined data transmission and location networks in relatively wide indoor scenarios has to face important challenges. A non-negligible latency is associated to the position update process,

and some temporal resources must be dedicated to localization with the consequent reduction of the available data rate for non-localization data communication. The implications of a real system such as transmission delay and resource constraints are not usually considered on the existing studies. Specifically, latency due to distance estimation and transmission has a negative impact on positioning accuracy. On the other hand, the amount of resources allocated to location limits the capacity of the tracking system in terms of the amount of users that can be tracked simultaneously. Position update latency and resource limitation should be taken into account in the system design in order to guarantee that the system can cope with the required accuracy and number of users and on the other hand to provide a suitable data rate for communication with a reasonable complexity level.

This chapter deals with the design of a combined communication and indoor location system based on UWB technology, and provides a complete system-level evaluation. Furthermore, the impact of MAC layer constraints in 802.15.4a-based UWB systems is analyzed. In order to optimize the latency of position updates and the amount of resources needed, different functional architectures and strategies for the acquisition and dissemination of location information are proposed and evaluated.

6.2 System Description

The objective of the combined data communication and location tracking UWB system is to track the position of mobile users in relatively wide indoor environments. The proposed system is composed of multiple IEEE 802.15.4a-based UWB piconets, although for simplicity a single piconet is considered. The UWB piconet is composed of mobile nodes to be tracked (targets) and fixed nodes with known positions (anchors). Distances between the target and the anchor nodes are estimated through a ranging frame exchange. The distance between neighbor anchors is a key design parameter, as a short distance between anchors entails more accurate estimations, but a high number of anchors would be needed to cover the scenario, so increasing the cost and complexity of the tracking system. Location controllers (LC) are the functional units which execute the tracking algorithm to obtain the estimated position of the targets. Depending on the location of the LC, several architectures (centralized and distributed) can be defined.

The main characteristics of the location system and the different options considered are detailed below.

6.2.1 EUWB PHY/MAC structure and network topology

In order to provide a realistic basis for the design of the combined communication and location tracking UWB system, the PHY and MAC layers developed within PULSERS and EUWB projects have been assumed. The description of the EUWB open IR-UWB platform can be found in [Pezzin, 2009], and a more detailed description of the physical and MAC layers can be found in [Pezzin, 2007] and [Bucaille, 2007] respectively.

6.2.1.1 PHY layer

The PHY layer of EUWB platforms was already described on Section 5.2.2. The chosen modulation scheme is based on Differential BPSK (DBPSK). This modulation scheme is interesting since it provides good immunity to clock drift and does not require any channel estimation. Demodulation of incoming signal is performed using differential correlation between the incoming signal corresponding to the current data symbol and the previous one. In order to improve the signal to noise ratio before taking a decision on the current symbol, redundancy is added to the current symbol by repeating it several times. In order to avoid spectral spikes, the repeated pulses energy is spread using a pseudo-noise (PN) code of length n_{PN} (typ. n_{PN}=12). The specifications of the EUWB transceiver are given in Table 6.1.

TOA estimation is carried out in two phases. The first phase is common with the demodulation process. It includes the coherent integration of n_{IC} PRPs (typ. n_{IC}=3) and the correlation of current symbol with the previous one, with a window size of 8 ns. This way a coarse estimation (with a precision of about 8 ns) of the time of flight is provided to the fine ranging module. In the second phase (fine ranging), the results of the correlation for n_{ACC} PRPs (typ. n_{ACC}=4, $n_{PN} = n_{IC} \cdot n_{ACC}$) are accumulated using chunks of 1 ns (one sample) instead of 8 ns. To do this, the 8 partial correlation results corresponding to the related 1 ns incoming signal chunks are provided by the correlator used in the demodulation module and are then processed by 8 parallel PN decoding and accumulation modules. A second stage of accumulators performs additional accumulations on the absolute values of the resulting metrics for K consecutive symbols in order to reach the required processing gain. Once these accumulations are performed, the first significant path is detected and its index gives the fine grain resolution required for precise ranging.

Table 6.1. PHY parameters

Parameter	Value
Frequency range	3.5-4.5 GHz
Sampling period	1 ns
Pulse Repetition Period	240 ns
PN code length	12
Symbol duration	2.88 µs
Raw bit rate	347 kbps

6.2.1.2 MAC layer

EUWB MAC layer has been designed for LDR-LT applications. It is based on IEEE 802.15.4 standard [IEEE, 2006], with enhancements to meet quality of service requirements and to provide efficient support for ranging and localization with a UWB physical layer.

A MAC superframe structure is defined, which is divided into timeslots where the different frames (beacon frames, hello frames, data frames, ranging frames, timeslot requests…) are sent. Superframe structure is shown in Figure 6.1. Two main periods are defined in the superframe, namely Control Period and Data Period. In the Control Period two parts are identified:

- Beacon Period (BP): used for the beacon alignment. The first beacon slot is reserved for the coordinator. Maximum length is 12 slots.
- Topology management Period (TP): Used for the periodic broadcast of hello frames from each node. This way the neighborhood is known locally for each node of the network. Maximum length is 3 slots (12 sub-slots as each slot is divided in 4 sub-slots).

Data Period is used for data frames, ranging frames, GTS request frames and other command frames. Data Period is composed of:

- Contention Free Period (CFP): It is composed of Guaranteed Time Slots (GTS) for data, ACK and ranging frames transmission, and a GTS request period. CFP has a maximum length of 26 slots, 20 slots for the GTS Period and 6 slots for the GTS Request Period. Ranging slots are considered as data slots, and ranging frames are sent in the CFP period as other data frames. The number of GTS used for ranging can be freely defined. It depends of the number of devices which are requested to perform ranging as well as the number of ranging measurements needed for a localization update. A classical case will be to have 8 slots for data communication and 12 slots for ranging enabling 4 devices using 3-way ranging.

- Contention Access Period (CAP): Used for the transmission of command frames through a slotted ALOHA multiple access scheme. Each CAP slot is divided into subslots in order to relay commands. Maximum length is 12 slots (48 subslots)

Consequently, the maximum number of slots in the superframe is 53. If the maximum number of slots is not achieved in the superframe, an inactive period (IP) is defined before the beginning of the next superframe. Table 6.2 summarizes the main MAC parameters.

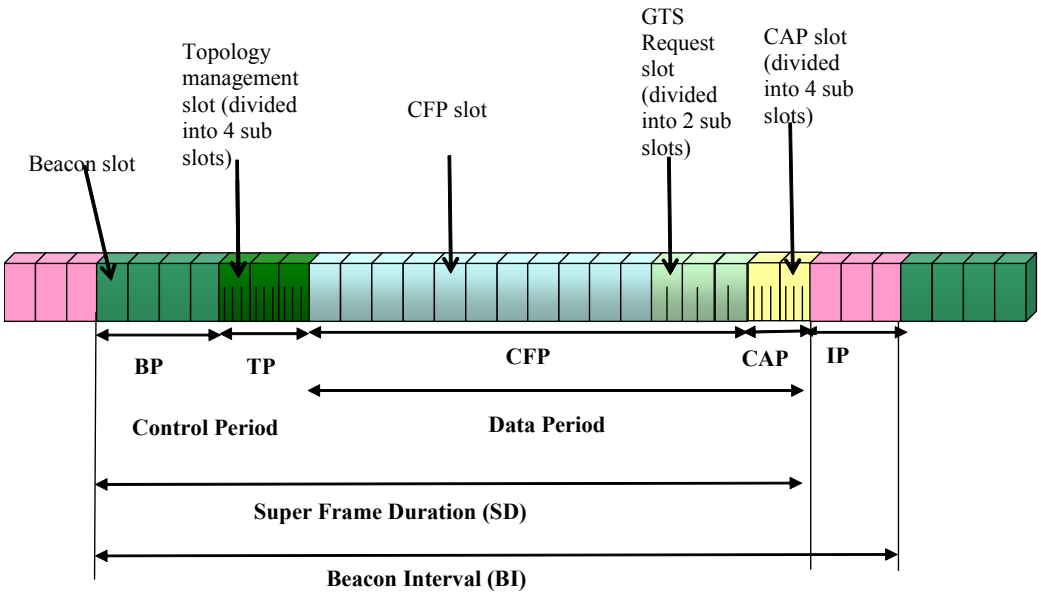

Figure 6.1. EUWB MAC superframe structure

Table 6.2. MAC parameters

Parameter	Value
Slot length	160 bytes
Slot duration	3.686 ms
Maximum superframe length	53 slots
Beacon Interval	195.379 ms
Maximum Beacon Period length	12 slots
Maximum Topology Management Period length	3 slots (12 subslots)
Maximum CFP length	26 slots
Number of slots for data communication	8 slots
Number of slots for ranging	12 slots
GTS request period length	6 slots (12 subslots)
Maximum CAP length	12 slots (48 subslots)

6.2.1.3 Network topology

Concerning network topology, the piconet is the basic unit. Piconets are based in a mesh centralized topology, which is defined by centralized allocation management and centralized common timing reference synchronization. Indeed a coordinator is elected in the network so as to transmit beacon frames and to handle the scheduling procedures.

Figure 6.2 illustrates the construction of a mesh centralized network. First a scheduling tree is built, which is used to transport beacon, association/disassociation request frames and GTS request command frames. In the scheduling tree, the Piconet Coordinator is on top of the tree. Then the different devices are defined by their scheduling tree level. The typical maximum tree level that must be taken into account for the application scenario is 4.

Then the tree is extended to a meshed scheduling tree by enabling the transmission out of the tree for the data. Data frames, hello frames, ACK frames and ranging frames can be sent on non-tree links. Concerning data frames, if source and destination nodes are not physically connected, frames are relayed at MAC level using consecutive timeslots. Ranging frames are not relayed and can be sent only between neighbors. The neighborhood is known locally for each node of the network thanks to the hello frames that are periodically broadcasted.

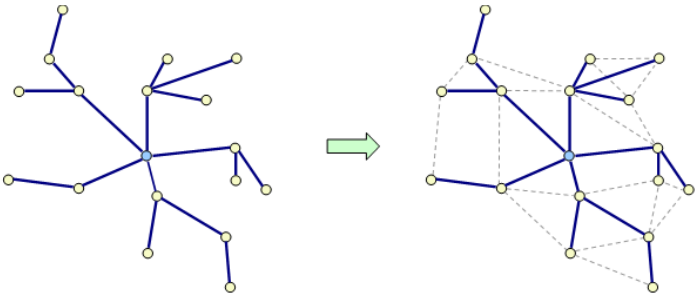

Figure 6.2. Mesh centralized topology

It is to be noticed that the relaying procedure is performed at the MAC layer level. The source node requests an allocation to the coordinator for the entire route. Indeed, when a node has data to transmit, it will send a GTS request on the tree to the coordinator with its address as the source address and the destination address of the transmission. The request will correspond to the number of GTS slots needed for the data transmission on a link. The coordinator, which has the knowledge of the whole network, will look on its routing table if there are relays between the source and the destination. If there are relays, the coordinator will allocate the GTS for each link based on the request made by the source node.

6.2.2 Acquisition & distribution of location information

In order to track the position of the target nodes, location information, basically the distances estimated between the target and anchor nodes, must be acquired and transmitted to the location controllers, which are the functional units that execute the tracking algorithm to obtain the estimated position of the targets.

The acquisition of the location information is done through the ranging procedure. Three procedures are defined [Bucaille, 2007]:

- One way ranging: The target node transmits a ranging packet and every anchor measures the time of arrival of the ranging packet. The position of the target can be obtained from the differences between the times of arrival on each anchor. Only one time slot is needed but it requires synchronization between all the anchors.
- Two way ranging: The procedure initiator (target or anchor) transmits a ranging request to another node, which estimates the time of arrival and sends a ranging response after a predefined time. The initiator measures the time of arrival of the response and can estimate the transmission delay and the distance between the nodes. Two time slots are needed, but there is no need of synchronization between the nodes.
- Three way ranging: Similar to the two way ranging scheme, but in this case two ranging responses are sent in order to compensate the clock drift. The ranging procedure can be initiated by the target nodes or by the anchor nodes and the distance is estimated by the initiator. It requires three time slots, but estimated distances are much more accurate.

In order to achieve the highest accuracy and to eliminate the need of synchronization, the use of Three Way Ranging is preferred. On the other hand, either the target or the anchor nodes may initiate the ranging exchange and estimate the distance, being the acquisition function allocation a design alternative that may impact on the need of resources

Once the distances between the target and the anchor nodes are estimated, they must be transmitted to the location controller in a data frame (measurement report data frame). Finally, the location controller executes the tracking algorithm to calculate the position and transmits the updated position to the target node (position update data frame).

Position update rate, or inversely the interval between updates, defines how often the positions of the mobile nodes are updated. Frequent updates allow more precise tracking of mobile targets, but require a higher amount of resources. Position update rate is closely

related to target mobility, as a higher target speed requires more frequent position updates in order to accurately track the target.

6.2.2.1 Anchor selection

Tracking may be performed with all the anchors in coverage of a given target or with a subset of them. The number of anchors used for position calculation is an important design parameter, as a higher number of anchors allows higher reliability, but also increases the amount of resources needed for location. Furthermore, distant anchors are expected to provide less accurate distance estimations. If ranging is performed with a subset of the neighbor anchors, then a selection procedure must be defined in order to select the closest anchors. This procedure must be based in the available information such as previously estimated distances, estimated position of the target, position of the anchors, power measurements, etc.

Four anchor selection methods are proposed:

- Ideal selection: On each update, the closest anchors are selected according to the real distance between the target and the anchors. This method is only considered as a reference.
- Periodic broadcast (PB): Periodically, as given by the interval between periodic updates, ranging is performed with all the neighbor anchors. Then the closest anchors according to the measured distances are selected to be used in the subsequent updates until the next periodic broadcast update. If coverage with one of the select anchors is lost, a broadcast update is done regardless of the time since the last periodic broadcast update.
- Estimated position (EP): On each update, the closest anchors are selected according to the estimated distance between the target and the anchors computed using target's estimated position.
- Estimated position with periodic broadcast (EP-PB): Similar to the estimated position method, but with an additional broadcast update with all the neighbors that is performed periodically as given by the interval between periodic update. This aims to prevent the possible feedback if the error in estimated position causes an incorrect anchor selection.

6.2.2.2 Enhanced acquisition and distribution strategies

In order to reduce the amount of resources needed to acquire and distribute the location information, different enhanced modes are proposed [Macagnano, 2007]. These enhancements include:

- Data aggregation: All the distances estimated can be aggregated and sent by the ranging initiator (target or anchor) in a single measurement report data packet to the LC.
- Broadcast/multicast request: In order to reduce the number of slots, in case ranging is initiated by targets, a target can aggregate multiple ranging requests into a single ranging request sent to all its neighbor anchors (target broadcast request) or to a set of anchors (target multicast request). In case ranging is initiated by anchors, an anchor can aggregate multiple ranging requests into a single ranging request sent to all its neighbor targets (anchor broadcast request) or to a set of targets (anchor multicast request).
- Multicast response: In case ranging is initiated by targets, and after receiving the ranging requests from different targets, an anchor can aggregate the responses to the involved targets into a single ranging response (anchor multicast response). In case ranging is initiated by anchors and after receiving the ranging requests from different anchors, a target can aggregate the responses to the involved anchors into a single ranging response (target multicast response).

If the initiator is the target node, anchor multicast response would require the simultaneous update of the position of all the targets in order to be able to aggregate the responses to multiple targets into a multicast response packet. The same applies for anchor broadcast/multicast request when the initiator is the anchor node, as the anchor must aggregate the requests to multiple targets into a multicast request packet. Finally, it also applies to data aggregation when the initiator is the anchor node, as the anchor must aggregate distances estimated to multiple targets into a single measurement report data packet sent to the LC. This would increase complexity, as a coordination mechanism should be defined in order to synchronize the updates.

6.2.3 Tracking function distribution in the network

The tracking functionality is executed by the LCs, which can be physically located in one or more anchor nodes or in the target nodes. Depending on the location of the LC, several functional architectures (centralized and distributed) can be defined.

If a centralized in the network architecture is assumed, the tracking functionality is implemented in one or more previously defined anchor nodes that become LCs. Using one LC entails a higher need of resources, as multiple hops will be needed to forward the location information to the LC. Defining multiple LCs reduces the need of resources, but increases complexity, as the tracking functionality must be implemented in several nodes and a procedure should be implemented to assign each target to the closest LC.

In the distributed architecture, each target picks dynamically one of its neighbor anchors to execute the tracking functionality. Therefore, there may be as many simultaneous LCs as targets. As the LC is always executed by an anchor neighbor to the target, only one timeslot will be needed to exchange data frames between the target and the LC, and resources will be consequently reduced. As a drawback, the tracking functionality must be implemented in every anchor.

Finally, in the architecture centralized in the mobile nodes the LC function is implemented in the target nodes. The target nodes perform ranging with their neighbor anchors and obtain their own position applying the tracking algorithm. Therefore, there is no need of transmitting the estimated distances and the updated position. Nevertheless, the feasibility of this architecture depends on the computational capacity of the devices to be tracked.

With respect to the tracking technique itself, the following algorithms have been considered: Trilateration, Extended Kalman Filter, Weighted Least Squares with Multidimensional Scaling, Least Squares with Distance Contraction and Particle Filter. A complete analysis of location and tracking algorithms was already provided in Section 5.3.

6.3 Evaluation of Architectures and Strategies

In this section, a prior evaluation of the different architectures and strategies for the acquisition and distribution of location information in terms of the amount of resources used for location (number of time slots needed for acquisition and distribution of location information) is presented. With this purpose, the simulation tool presented in Section 5.3.1 has been used. Ideally, transmission has been considered instantaneous and lossless, and the availability of timeslots unlimited. The impact of delay and resource constraints will be assessed in Section 6.4. The influence of the number of anchors used for location and the different anchor selection methods have also been evaluated.

For these simulations, a common set of parameters has been defined. Simulation duration has been set to 10000 seconds and the number of targets to be tracked to 10. The area size has been set to 50 m. x 50 m. and the distance between anchors to 10 m., resulting in 36 anchors. Concerning the dynamics of the mobile nodes, minimum and maximum speeds have been set to 0.1 and 3 m/s respectively, and direction changes every 20 seconds. Position update rate has been set to 1 update per second and UWB nodes range to 15 m. Three way ranging has been considered.

For the tracking functional architectures that have been described in Section 6.2.3, the following notation has been used:

- 1LC: Architecture centralized in the network with 1 location controller
- 4LC: Architecture centralized in the network with 4 location controllers
- Distr.: Architecture distributed in the network
- Mobile: Architecture centralized in the mobile nodes

For the data acquisition & distribution enhancements, which were described in detail in Section 6.2.2.2, the following notation has been used:

- SRq: Single request
- MRq: Multicast request
- SRp: Single response
- MRp: Multicast response
- NDA: No data aggregation
- DA: Data aggregation

6.3.1 Impact of the tracking system architecture

First, the impact of each one of the proposed functional architectures (centralized in the network, distributed and centralized in the mobile nodes) on the amount of resources needed for location is evaluated.

Figure 6.3 shows the results obtained for the different architectures in terms of total number of time slots needed for location. Concerning the architecture centralized in the network, the existence of 1 LC and 4 LCs have been considered. The architecture centralized in the mobile nodes is the optimum in terms of resources, with a reduction of 40% in the amount of slots needed compared to the architecture centralized in the network with 1 LC.

This architecture requires that the location function is implemented in the mobile nodes, so the feasibility of this architecture depends on the specific devices to be tracked. The distributed architecture presents a reduction of almost 20% in the amount of time slots needed compared to the architecture centralized in the network with one location controller. Very similar results are obtained for the architecture centralized in the network with 4 location controllers, which only requires implementing the location functionality in 4 of the 36 anchor nodes, so this architecture is preferred over the distributed one.

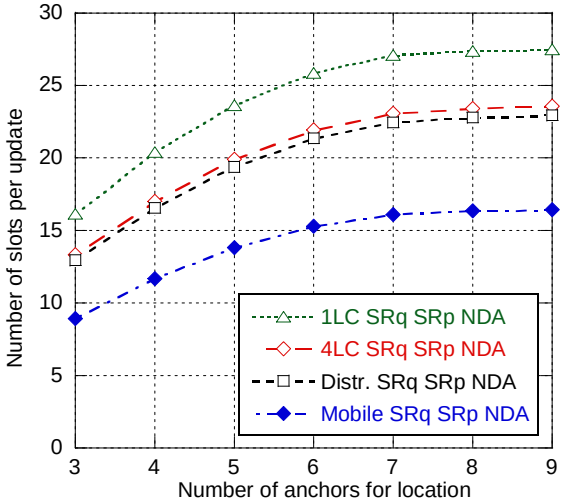

Figure 6.3. Resources needed for location for the different functional architectures

6.3.2 Location acquisition & distribution enhancements

The amount of resources needed for location have been simulated for each enhancement based on an architecture centralized in the network with one LC.

Figure 6.4 summarizes the results obtained for each one of the acquisition and distribution enhancements when the ranging exchange is initiated by the target (TI) or by the anchors (AI). When the ranging is initiated by the target, DA and MRp reduce in approximately 25% the amount of slots needed for location. Concerning MRq and BRq, the first one is preferred as it reduces the total amount of slots needed in approximately 15% in any case, while BRq shows a similar reduction when 7 or more anchors are used but a higher need of resources when 6 or less anchors are used. Therefore BRq will not be considered so far. When the ranging procedure is initiated by the anchors, using MRq a reduction of approximately 12% is obtained, which is smaller compared to the 15% reduction when the target initiated the ranging procedure. The reason is that, for the selected number of targets and anchors, the average number of targets requesting ranging with an anchor is less than the

number of anchors used for location. For the same reason, DA gain is reduced to 17%. In contrast, reduction due to MRp increases to approximately 34%.

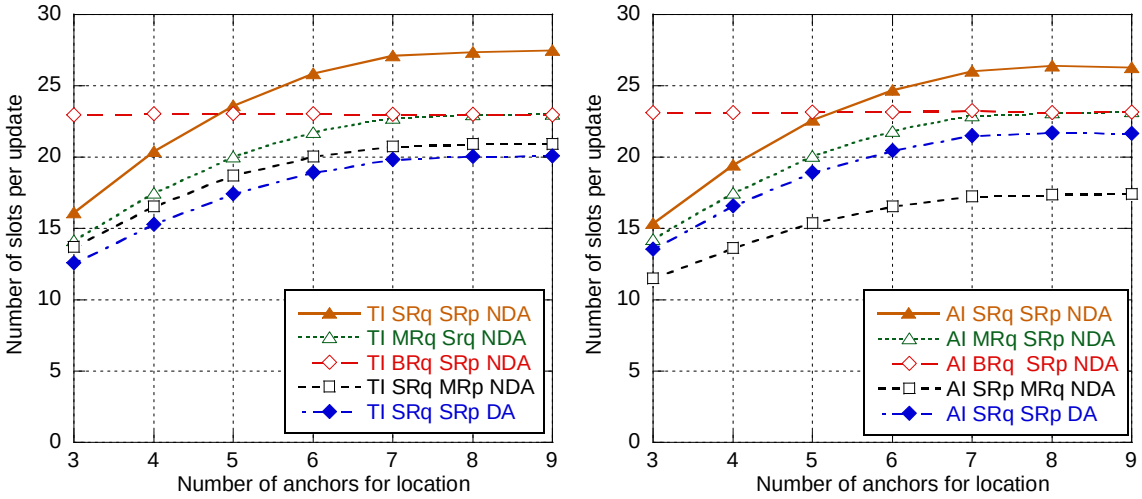

Figure 6.4. Resources needed for location for the different enhanced modes

As it was previously discussed, some enhanced modes require the coordination of the updates of different targets. In Figure 6.5, a comparison is established between the basic modes (TI/AI SRq SRp NDA), the best enhanced modes that do not require position update coordination (TI MRq SRp DA and AI SRq MRp NDA) and the best enhanced modes considering position update coordination (TI/AI MRq MRp DA). When no enhancements are applied, the number of slots needed when the anchors start the ranging procedure is slightly lower than the number of slots needed when the target starts the ranging procedure. Concerning the best enhanced modes without coordination, when the target is the initiator MRq and DA can be applied and a reduction of 40% in the number of slots needed is obtained, getting better results than when the anchor is the initiator, as only MRp can be applied without coordination. When position updates are synchronized and all the possible enhancements are applied, very similar results are obtained whether ranging is initiated by the targets or by the anchors, and the number of slots needed is almost independent of the number of anchors for location, varying from 8 to 9 slots per update, which means a reduction between 50%-65% compared to the basic modes.

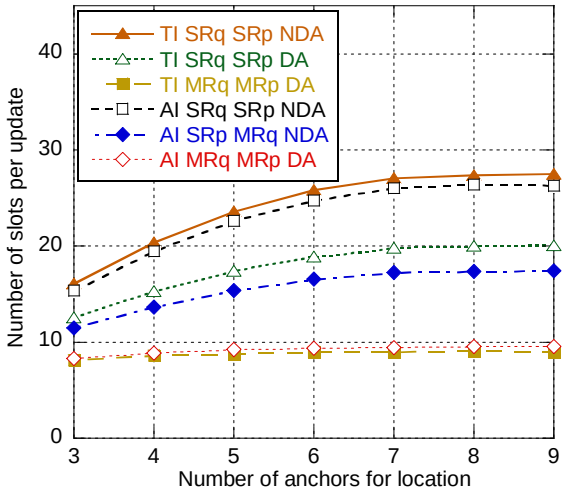

Figure 6.5. Resources needed for location for different initiators and enhanced modes

6.3.3 Impact of number of anchors used for location

Besides choosing an appropriate functional architecture and implementing acquisition & distribution enhancements, a possible strategy in order to keep the amount of resources needed under a reasonable value is limiting the number of anchors to be used for location. Therefore, the ranging procedure would not be performed with all the neighbor anchors, but only with a certain number of them. This would reduce the amount of slots needed for ranging requests, ranging responses and measurement reports.

As it was already shown in Figure 6.3, the amount of timeslots needed increase as a higher number of anchors are used and remains constant for more than 7 anchors, as for a distance between anchors of 10 meters it is not very likely that the target is in coverage of more than 7 anchors. If the number of anchors used for location is limited to 4, and considering an architecture centralized in the network with 1 LC, the amount of resources needed for location would be reduced from 27 to 20 slots per update.

Of course, this also impacts on the positioning error, as a higher number of anchors entails higher accuracy and reliability. Nevertheless, as it was explained in Section 5.3.1.1, the ranging bias is dependent on the distance and as a result the ranging error for the closest anchors is lower than for the more distant anchors, so position estimation might degrade if distant anchors are used. As it can be observed in Figure 5.13, this results in an optimum number of anchors that minimizes the positioning error, which depends on several factors (ranging residual error, distance between anchors, location algorithm…).

6.3.4 Impact of the distance between anchors

The distance between anchors is another important parameter that impacts both on positioning accuracy and need of resources. As the distance between anchors is reduced, the target is in coverage of more anchors and the need of limiting the number of anchors used for location becomes more important in order to avoid an excessive use of resources.

Figure 6.6 shows the amount of resources needed depending on the number of anchors used for location for different values of the distance between anchors. As it can be observed, for 6.25 m between anchors, the number of timeslots needed increases linearly according to the number of anchors used for location, as the target is always in coverage of more than 10 anchors. For 8.33 m between anchors, the number of timeslots increases linearly for less than 8 anchors, with a smaller increase for more than 8 anchors. For 10 m between anchors, the increase is not linear as the target may not be in coverage of the selected number of anchors, eventually remaining constant for more than 7 anchors.

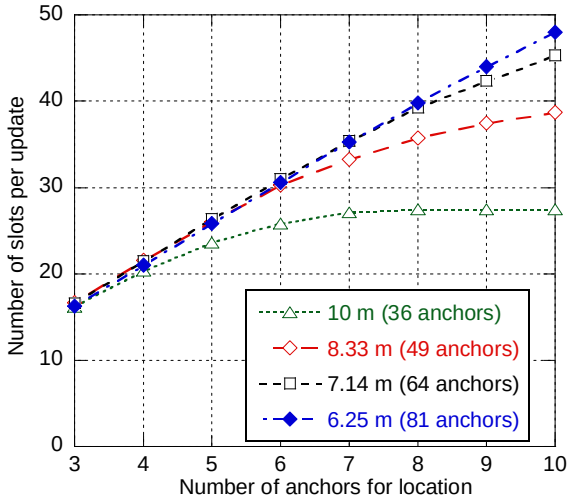

Figure 6.6. Resources needed for location for different total number of anchors

As it was shown in Section 5.3.2.1, as the distance between anchors is reduced, the positioning error decreases, as long as that the closest anchors are selected. So far we have considered an ideal approach and the closest anchors were always picked. Anchor selection methods are discussed in the following section.

6.3.5 Impact of position update rate

Position update rate, or inversely the interval between updates, defines how often the positions of the mobile nodes are updated. As it was already shown in Figure 5.21, the

interval between updates may impact on the positioning accuracy of some algorithms, for instance EKF, and is critical in case the tracking error is considered. On the other hand, position update rate also impacts on the need of resources. As it can be observed in Figure 6.7, the amount of resources needed is inversely proportional to the interval between updates. Consequently, there is a trade-off between accuracy and the amount of slots required. The value of the interval between updates must be set according to expected target speed, being 1 second a suitable value for pedestrian targets with speeds up to 3 m/s.

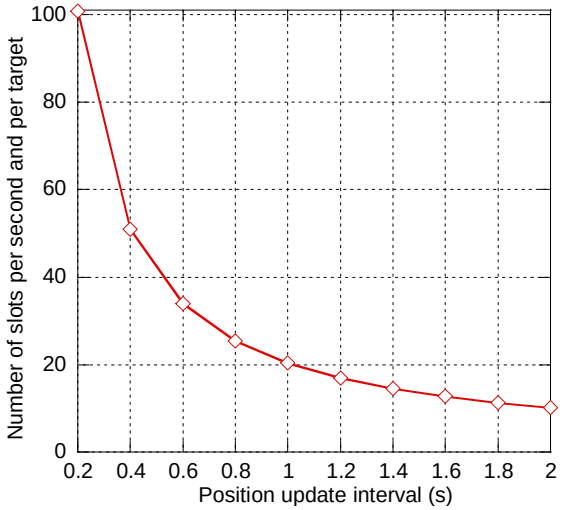

Figure 6.7. Resources needed for location vs. interval between updates

6.3.6 Anchor selection

Limiting the number of anchors used for location can reduce both the positioning error and the need of resources. But in order to reduce the positioning error, it is necessary that the closest anchors are selected. In this section four anchor selection methods are analyzed, which were presented in Section 6.2.2.1: Ideal selection, Periodic Broadcast (PB), Estimated Position (EP) and Estimated Position with Periodic Broadcast (EP-PB).

Figure 6.8 shows the positioning error and the need of resources for the different selection methods. Distance between anchors has been set to 10 meters and, for PB and EP-PB, the interval between periodic updates has been set to 10 seconds. An architecture centralized in the network with no enhancements has been used. When 4 or 5 anchors are used, the EP-PB method presents the best results in terms of MAE, very close to the ideal selection, while PB method presents the highest error. For 6 or more anchors results are similar regardless of the method, as most of times the target will not be in coverage of more than 5 or 6 anchors. Concerning the need of resources, as periodic broadcast updates are

performed with all the anchors in coverage, methods featuring periodic broadcast updates, namely PB and EP-PB, require more slots. Number of slots used by PB is higher than EP-PB as PB also performs broadcast updates when coverage is lost with one of the selected anchors. For 7 or more anchors all the methods use the same amount of slots, as it is not likely that the target will be in coverage of more than 7 anchors.

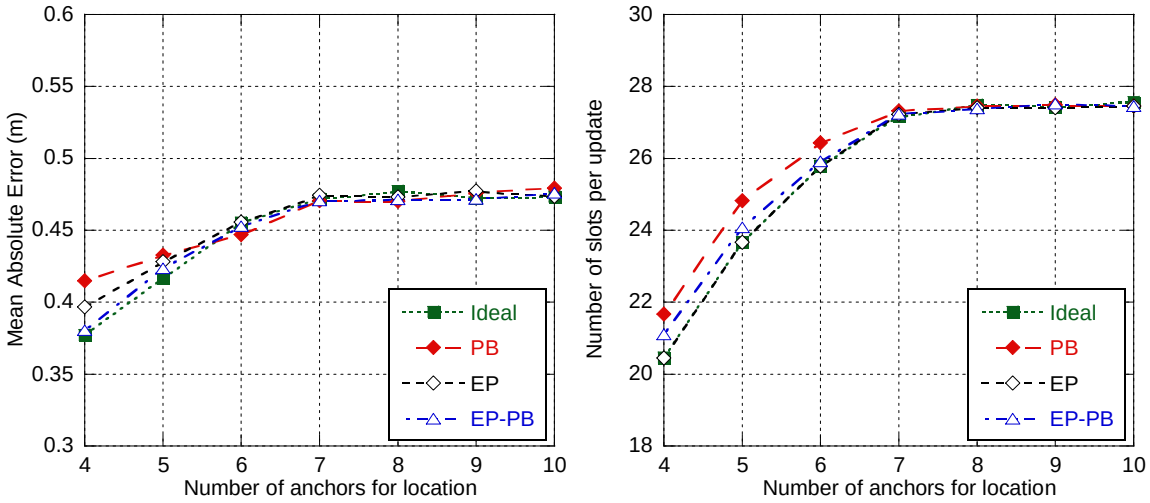

Figure 6.8. Comparison of anchor selection methods (distance between anchors = 10 m.)

The same analysis has been done with distance between anchors of 7.15 meters and results are shown in Figure 6.9. With this configuration, the error of non-ideal methods is not so close to the ideal selection, as the target has more anchors in coverage and the probability of not picking the optimal ones increases. Results for EP and EP-PB are slightly higher than for the ideal selection. On the other hand, PB presents a higher MAE than the other methods, as the anchors selected in the periodic broadcast update will no longer be the closest ones after a few seconds. Concerning the need of resources, the methods with periodic broadcast updates require a higher number of slots, especially PB as it also performs broadcast updates when coverage with a selected anchor is lost. As the target has more anchors in coverage, the broadcast updates require more slots and the difference between methods with and without periodic broadcast updates increases.

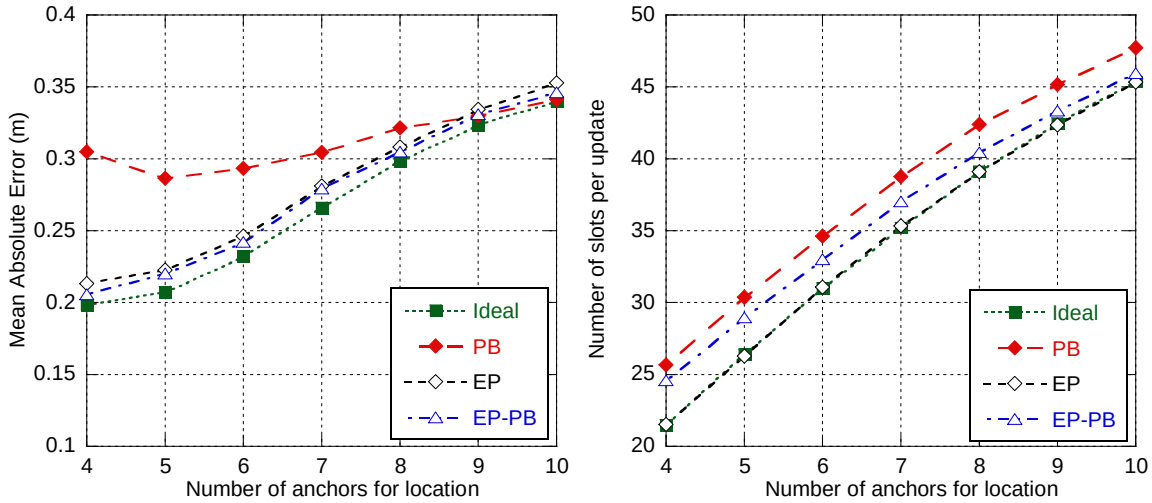

Figure 6.9. Comparison of anchor selection methods (distance between anchors = 7.15 m.)

In Figure 6.10 the impact of the interval between periodic updates for PB and EP-PB methods on the positioning error and on the need of resources is analyzed. Number of anchors used for location has been set to 4 and distance between anchors has been set to 10 meters. Ideal selection method has also been included as a reference. The PB method gets even better results than the ideal selection when the interval between periodic updates is equal or less than 2 seconds, as it performs ranging with all the neighbor anchors and the ones with shortest estimated distance are used. This way, if the distance estimated for one of the closest anchors is strongly biased (i.e. due to an obstacle) another anchor with a better estimation may provide a shorter estimated distance and be used instead, providing a better result than if only the four closest anchors were selected as in the ideal case. The EP-PB method obtains a similar result to PB for equal or less than 2 seconds between updates and to the ideal selection for higher values. Obviously, as the interval between periodic updates is reduced, the number of slots required for PB and EP-PB methods increases. For values of the interval between periodic updates higher than 6 seconds, the number of slots for PB method remains constant as broadcast updates will occur due to loss of coverage with one selected anchor before the periodic broadcast update takes place.

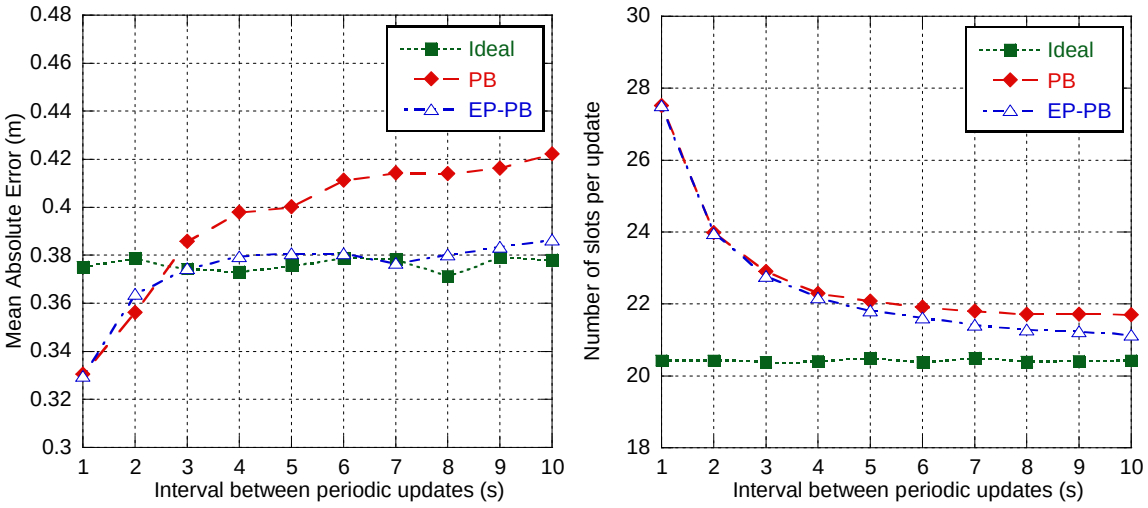

Figure 6.10. Impact of the interval between periodic updates

To sum up, the importance of the anchor selection method increases as distance between anchors decreases as there are more anchors in coverage of the target. PB requires a time between periodic updates of 3-4 seconds to provide good position estimation, but this entails a higher need of resources. EP provides good results, although it may eventually produce high errors if the error in the estimated position causes an incorrect selection. Several solutions can be proposed to avoid this problem, one of them being the combination of EP with periodic broadcast updates, (EP-PB), which provides a performance close to the ideal with a non excessive need of resources.

6.4 Impact of MAC Layer Design

In this section, the impact of the proposed MAC layer is evaluated. Specifically, latency due to distance estimation and transmission has a negative impact on positioning accuracy, and limited availability of resources limits the amount of mobile nodes that can be tracked and the frequency of position updates.

Several simulations have been performed for the different proposed architectures and acquisition and dissemination of location information strategies. For these simulations, a common set of parameters has been defined. Simulation duration has been set to 10000 seconds. The area size has been set to 50 m. x 50 m. By default, the area is covered by 36 anchors uniformly distributed with a distance between anchors to 10 m., 1 target is tracked and 4 anchors are used to position each target, although these parameters are varied through the simulations. Concerning the dynamics of the mobile nodes, minimum and maximum

speeds have been set to 0.1 and 3 m/s respectively, and direction changes every 20 seconds. Position update rate has been set to 976 ms (5 superframes) and UWB nodes range to 15 m. Three way ranging has been considered and trilateration has been used as tracking algorithm.

6.4.1 Effect of position update latency

According to the position update process described in Section 6.2.2 and to the MAC superframe structure shown in Section 6.2.1.2, there are many sources of delay in the position update process: delay associated to the request and allocation of free ranging slots, duration of the ranging exchanges, transmission of the estimated distances to the location controller, latency of position computation and transmission of the updated position to the target. Delay prior to the start of the ranging exchanges has no appreciable effect on positioning accuracy. Nevertheless, delay between the ranging exchanges and the final position availability has a negative effect on positioning accuracy due to the movement of the target. We define position update latency as the time between the start of the ranging exchanges and the availability of the position at the target.

Figure 6.11 shows the effect of position update latency on the average positioning error for the different tracking algorithms and σ_n=0.7. As it can be observed, all the algorithms show a similar evolution and the error grows as position update latency increases. For 200 ms, which is approximately the duration of a MAC superframe, MAE increases around 18 cm compared to the case when no latency is considered. For 400 ms (2 superframes) the error increase can be as high as 45 cm. Therefore, position updates should be carried out preferably within a single superframe.

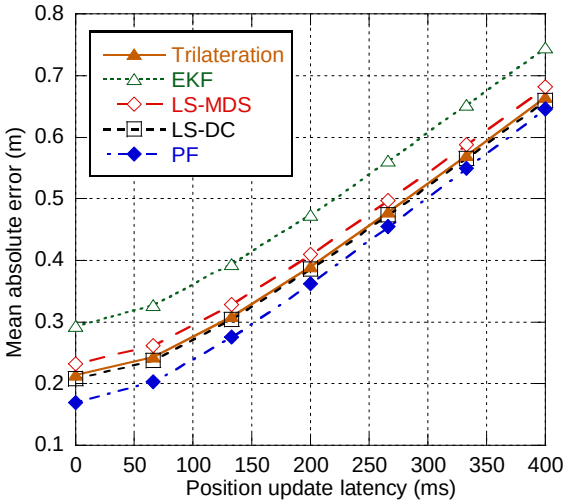

Figure 6.11. Positioning error depending on position update latency

6.4.2 Effect of target mobility

Following, the effect of target mobility on the positioning error is analyzed, considering the specific MAC superframe structure presented in Section 6.2.1.2. Figure 6.12 shows the positioning error for the architecture centralized in the network with a single LC and 4 anchors used for location. As it can be observed, when delays are taken into account, all the algorithms are degraded due to the movement of the target between distance estimation and position computation. Non-parametric algorithms, namely trilateration, LS-MDS and LS-DC, which are ideally independent on target speed, have a similar evolution. EKF severely degrades for speeds greater than 1.5 m/s as the estimation is based on target's previous position. Finally, although PF uses the target's dynamic model to move the particles, particles are weighted on each step according to their likelihood, so the new position is almost independent of the previous one and degradation is slightly higher than for non-parametric methods.

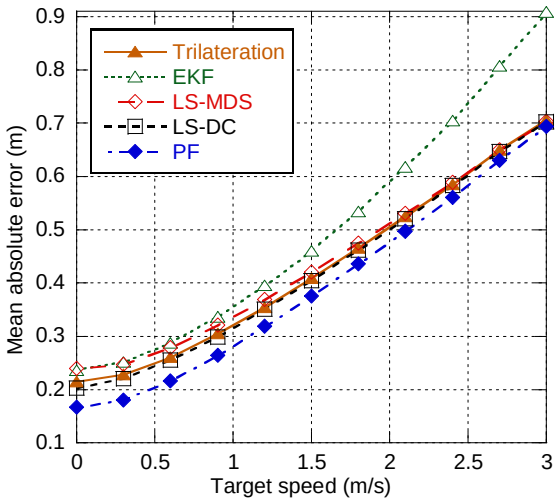

Figure 6.12. Positioning error depending on target speed

6.4.3 Data acquisition & distribution enhancements

The amount of resources needed for location have been simulated for each enhancement based on an architecture centralized in the network with one location controller, one mobile target and a distance between anchors of 10 meters, which results into 36 anchors. The number of anchors used for positioning the target is variable.

In order to analyze the results, it is necessary to understand how the position update process is carried out for each one of the enhancements. With this purpose, Figure 6.13

shows a scheme of the update process for the architecture centralized in the network with 1 LC, single request, single response and no data aggregation, depending on the number of anchors used for positioning. Each row represents the GTS period of a superframe, which is used for ranging exchanges and data transmission. GTS period duration is 20 slots, with 12 slots allocated to ranging and 8 slots to data transmission. Concerning the frames sent on each slot, the following notation has been used:

- Rq_{ij}: Ranging request from target *i* to anchor *j*
- Rq_i: Multicast ranging request from target *i*
- Rp_{ij}: Ranging response from anchor *j* to target *i*
- Rp_j: Multicast ranging response from anchor *j*
- MR_{ij}: Measurement report data frame with distance between target *i* and anchor *j*
- MR_i: Aggregated measurement report data frame with distances estimated by target *i*
- PU_i: Position update data frame for target *i*

As Three-Way ranging is used, two ranging responses are generated for each ranging request. As the architecture is centralized in the network with 1 LC, in general multiple hops will be needed to relay the data frames from the target to the LC and vice versa. Consequently, in the scheme MR and PU frames use 2 slots, as it has been identified that for this configuration (36 anchors and 1 LC) the average number of hops between the target and the LC is approximately 1.9, although it varies between 1 and 3 slots depending on the distance between the target and the LC.

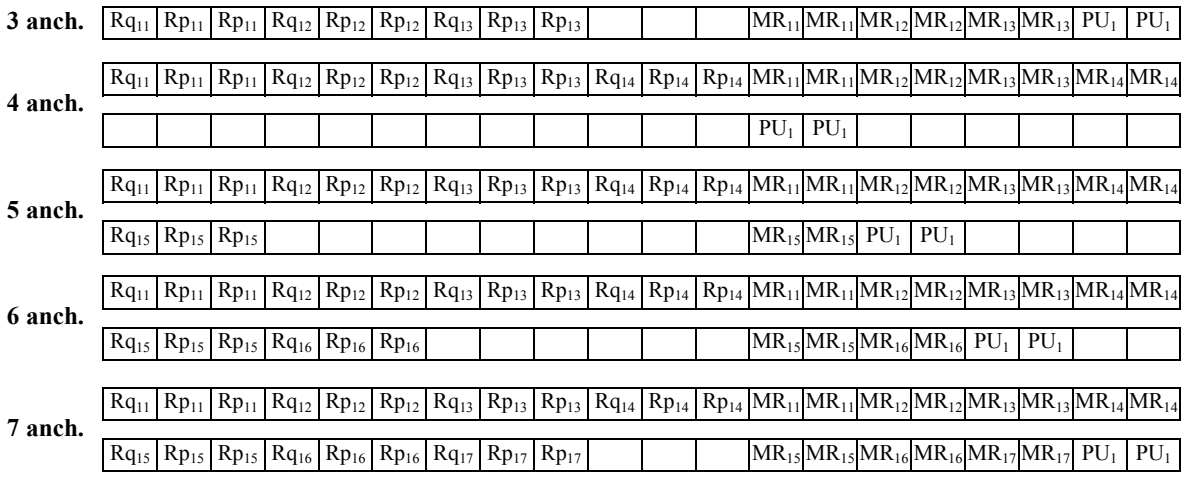

Figure 6.13. Update process scheme for 1LC SRq SRp NDA depending on the number of anchors

Figure 6.14 shows a similar scheme when multicast request is used. Note that now only one ranging request is used on each update process.

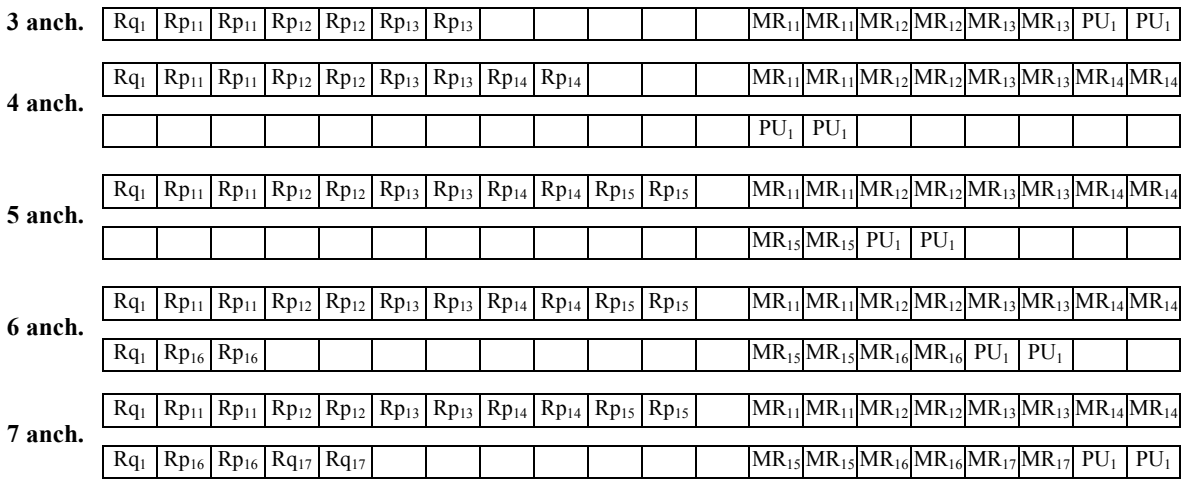

Figure 6.14. Update process scheme for 1LC MRq SRp NDA depending on the number of anchors

Figure 6.15 shows the update process scheme when data aggregation is applied. It must be noted that now only one measurement report is sent to the LC, although it may need multiple slots. Finally, Figure 6.16 shows the update process scheme when both multicast request and data aggregation are applied. Multicast request has not been considered as only one target is tracked.

Figure 6.15. Update process scheme for 1LC SRq SRp DA depending on the number of anchors

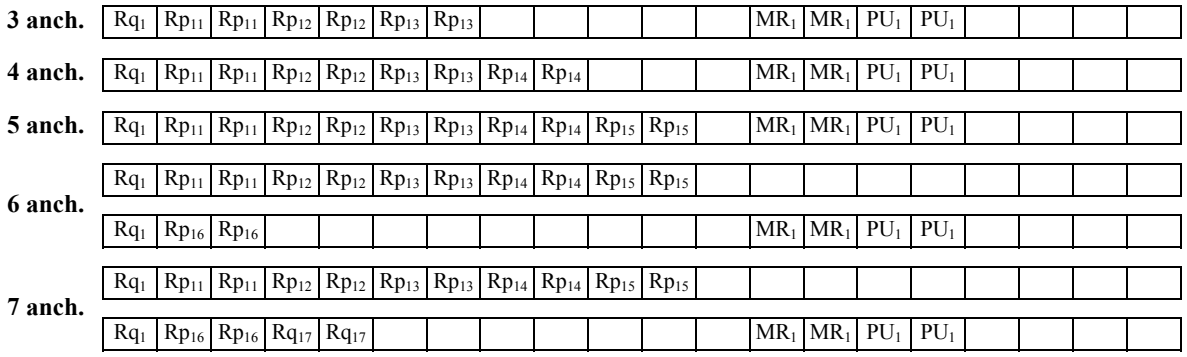

Figure 6.16. Update process scheme for 1LC MRq SRp DA depending on the number of anchors

Figure 6.17 shows the Mean Absolute Error for each one of the acquisition & distribution schemes depending on the number of anchors. The ideal case when MAC timing and constraints are not considered is included as a reference. In general, the error for the MAC simulations is always higher than the ideal case due to the latency of the position update process, in particular the number of superframes that are needed. Note that results are constant for 7 or more anchors as with this configuration (10 m between anchors) the target is not likely to be in coverage of more than 7 anchors.

Concerning the Srq SRp NDA mode, the error when 3 anchors are used is slightly higher than the ideal case, as when the target is 1 or 2 hops away from the LC the process will be carried out within a single superframe, and only when the target is 3 hops away from the LC a second superframe would be needed, thus increasing the latency and the error. When 4 anchors are used, 2 superframes would be needed also when the target is 2 hops away from the LC, so the error increases. For 5 anchors, 2 superframes are always needed in order to

perform all the ranging exchanges, so the error increases. For 6 anchors there is a further increase of the error as 3 superframes would be needed when the anchor is 3 hops away from the LC. When 7 anchors are used, the need of superframes is similar to the case with 6 anchors, but in this case there are 3 recently estimated distances (in the same superframe) and 4 delayed estimated distances (in the previous superframe), whereas with 6 anchors there was 2 recently estimated distances and 4 delayed, so there is a slight decrease of the error. Results are very similar for MRq SRp NDA except when 5 anchors are used. In this case, with single request always 2 superframes were needed to perform all the ranging procedures, whereas if multicast request is used all the ranging exchanges can be carried out within a superframe, and only 1 superframe will be neeeded if the target is 1 hop away from the LC, so the error is similar to the case with 4 anchors.

When data aggregation is used, the limitation will be always due to the ranging exchanges, as location data exchanges will be carried out always in a single superframe. With single request (SRq SRp DA) one superframe will be needed when 3 or 4 anchors are used, and two superframes for 5, 6 or 7 anchors, so there is an important increase of the error when 5 anchors are used. Then the error slightly decreases as the ratio of recent and delayed estimated distances increases (1 recent and 4 delayed for 5 anchors, 3 recent and 4 delayed for 7 anchors). Results for multicast request (MRq SRp DA) are similar, although the error increase occurs when 6 anchors are used, as for 5 anchors the update process can be carried out within one superframe.

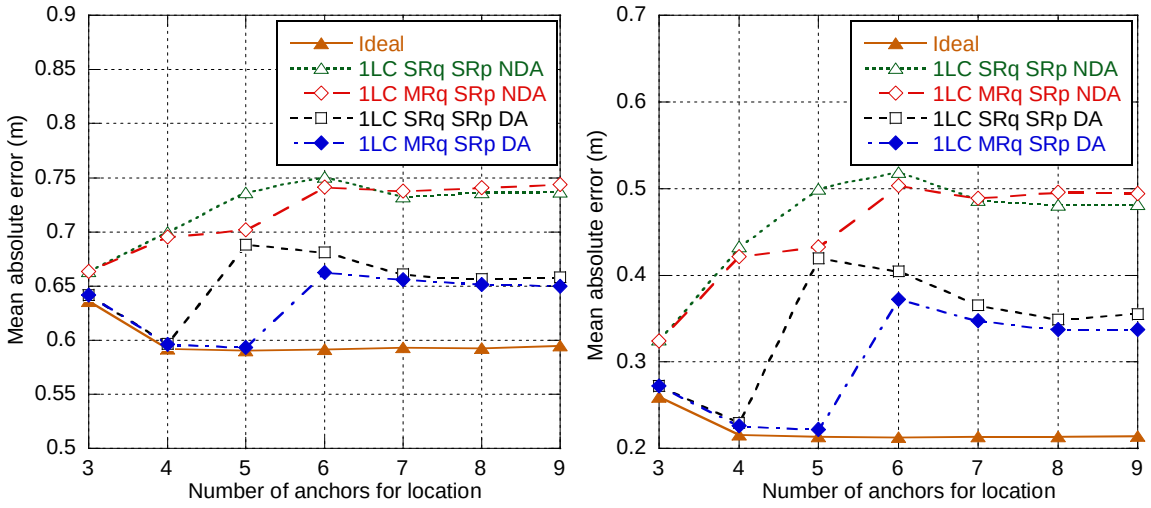

Figure 6.17. MAE for different acquisition & distribution modes depending on the number of anchors for location (σ_n=0.7 and σ_n=0.3)

The main conclusion is that when the update process is carried out within a single superframe, e.g. with MRq SRp DA and 3, 4 or 5 anchors, the latency is relatively small, e.g. 16 slots (59 ms), and the error increase is negligible. When the update process requires more than one superframe, latency will take values over 200 ms and the error increase is significant.

Following the effect of simultaneously tracking multiple targets is analyzed. Now the number of anchors used for location is set to 4 and the number of targets is variable. Figure 6.18 shows a scheme of the update process for the architecture centralized in the network with 1 LC, single request, single response and no data aggregation, depending on the number of targets. As it can be observed, the availability of data slots is the limiting factor, and the data slots get saturated when 4 or more targets are tracked.

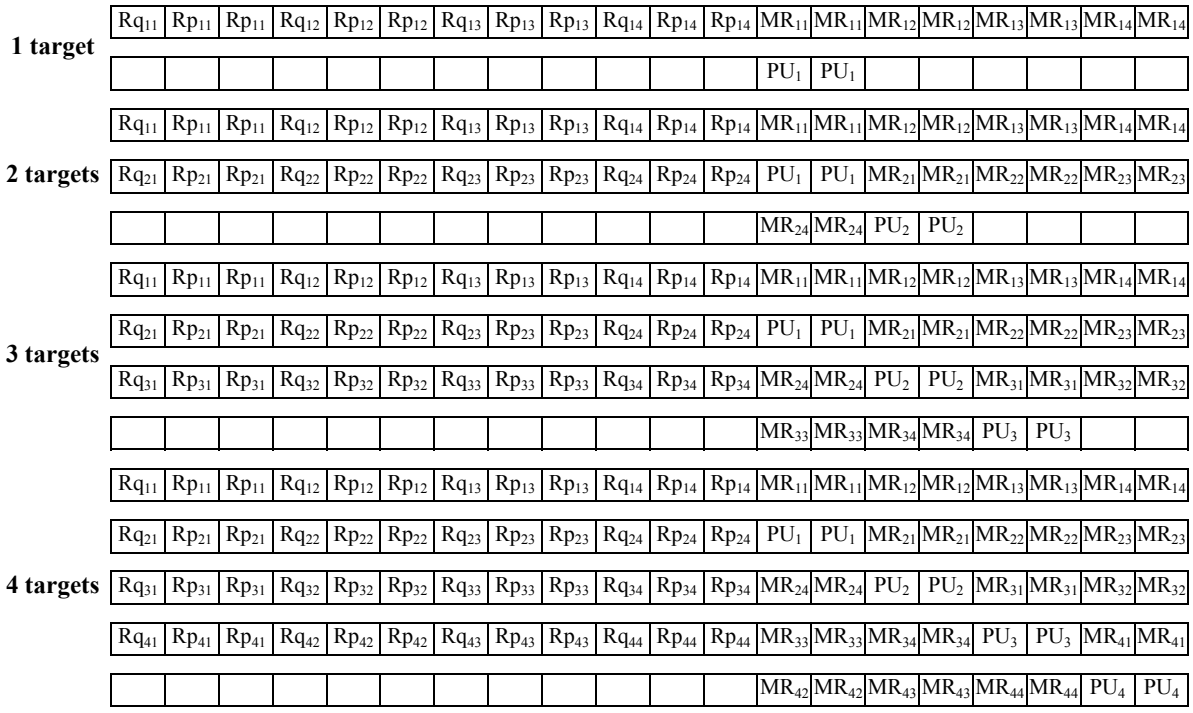

Figure 6.18. Update process scheme for 1LC SRq SRp NDA depending on the number of targets

Figure 6.19 shows the update process scheme when data aggregation is applied (SRq SRp DA). With data aggregation the availability of data slots is not further a limitation. Every target is updated in a single superframe, and up to 5 targets could be tracked considering an update rate of 5 superframes.

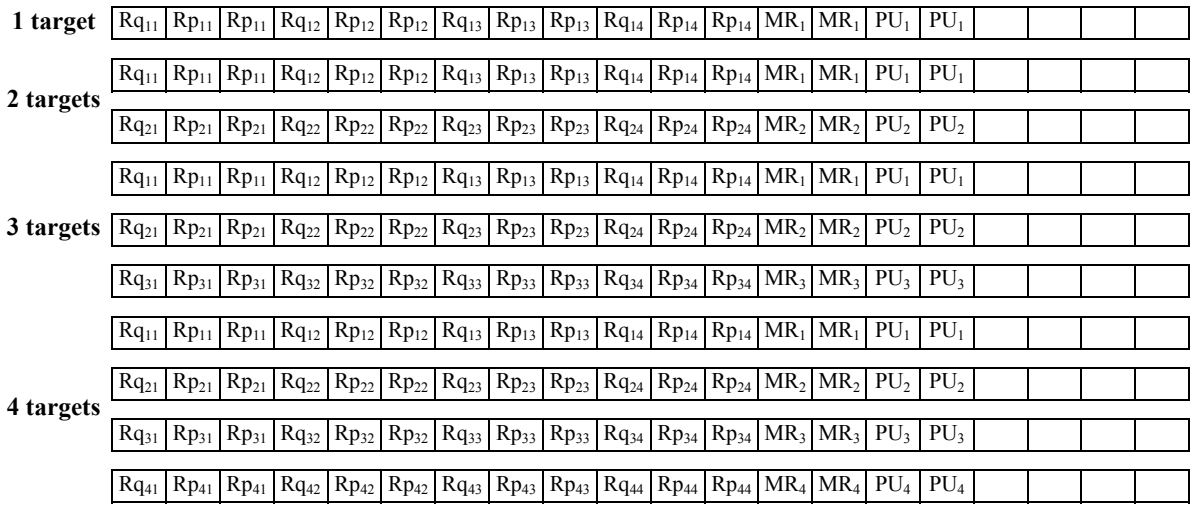

Figure 6.19. Update process scheme for 1LC SRq SRp DA depending on the number of targets

Figure 6.20 shows the update process scheme when both multicast request and data aggregation are applied (MRq SRp DA). Note that updates are not carried out in different superframes, but update of target #2 already starts in superframe #1 in order to make the most of the available ranging slots and increase the capacity.

Figure 6.20. Update process scheme for 1LC MRq SRp DA depending on the number of targets

Finally, Figure 6.21 shows the update process scheme when all the enhancements are applied (MRq MRp DA). Note that now ranging responses are not sent per each target-anchor pair, but per each anchor. Some anchors may be used by multiple targets, so in

general the amount of responses and consequently the number of ranging slots will decrease, thus increasing the capacity.

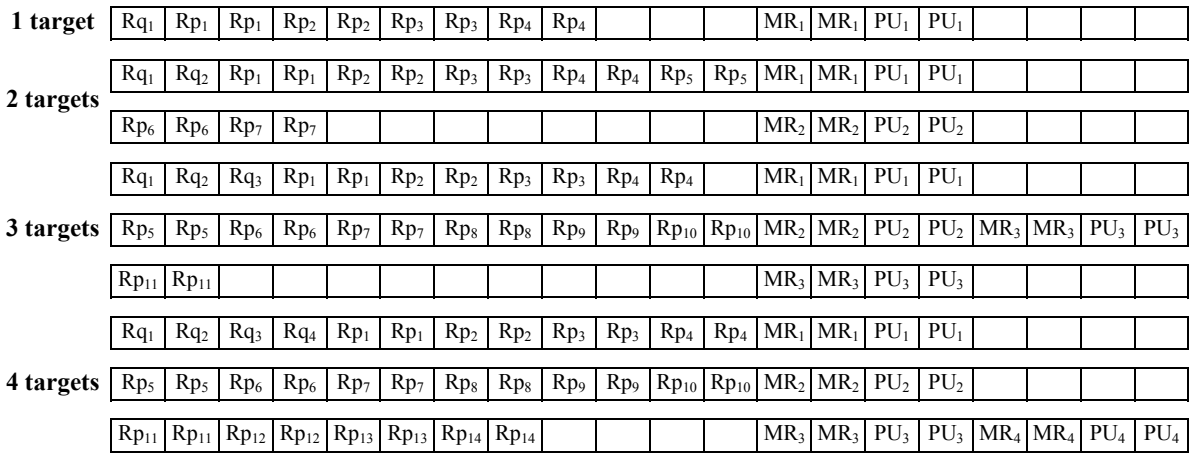

Figure 6.21. Update process scheme for 1LC MRq MRp DA depending on the number of targets

The average error for the different modes depending on the number of targets is shown in Figure 6.22. For the mode with no enhancements (SRq SRp NDA) the error grows exponentially, as there are not enough data slots and latency increases as the number of targets grows. For more than 4 targets, the data slots are completely saturated, which entails that the latency increases on every update until it stabilizes between 800-1000 ms (4-5 superframes) and the error can be as high as 2 m. When data aggregation is used (SRq SRp DA) every update is carried out in a single superframe, so the error is just slightly higher than the ideal simulator. For 6 or more targets, there will be not enough superframes and the actual time between updates will increase. This entails a delay between the selection of the anchors and the update process, and consequently a slight increase of the error.

When both multicast request and data aggregation are applied (MRq SRp DA), the error increases as the number of targets grow, as the update of target #2 starts in superframe #1 and finishes in superframe #2, update of target #3 starts in superframe #2 and finishes in superframe #3, and update of target #4 starts in superframe #3 and finishes in superframe #4, as it can be observed in Figure 6.20. For 5 and 6 anchors there is no increase, as update of target #5 would take place in superframe #4 and update of target #6 would take place in superframe #5. For 7 and more targets we would have a further increase.

Finally, when all the enhancements are applied (MRq MRp DA), the behavior is difficult to predict, as it depends on how many anchors are shared between the targets and how the ranging exchanges are coordinated, but in general the average latency of the updates

will be a little bit higher and so will be the error. For more than 6 targets there is an important increase of the error, as ranging exchanges may typically finish in the fifth superframe and there may be not enough data slots to transmit the location information for the remaining targets, which may be delayed one or more superframes.

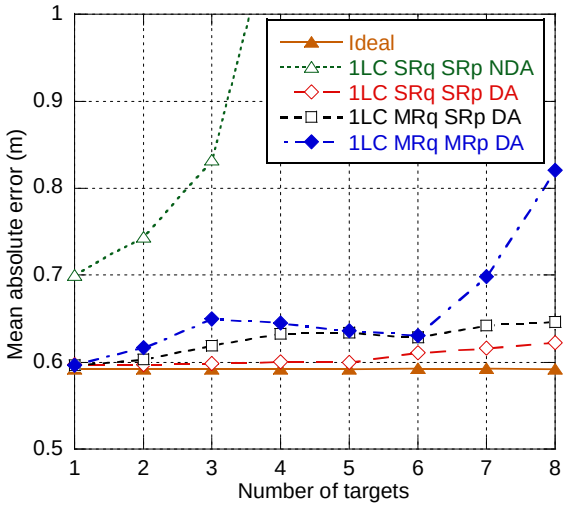

Figure 6.22. MAE for different acquisition & distribution modes depending on the number of targets (σ_n=0.7)

Figure 6.23 shows the actual time between updates and the % of GTS slots used in order to evaluate system capacity. When no enhancements are applied (SRq SRp NDA), the amount of slots used increases quickly and the system is eventually saturated for more than 4 targets, with a residual 18% left for communication. The amount of GTS slots used is reduced for the enhanced modes. As with DA a single measurement report packet is sent, capacity of these modes is limited by the availability of ranging slots to 5 targets (SRq SRp DA), 6 targets (MRq SRp DA) and 8 targets (MRq MRp DA) per picocell.

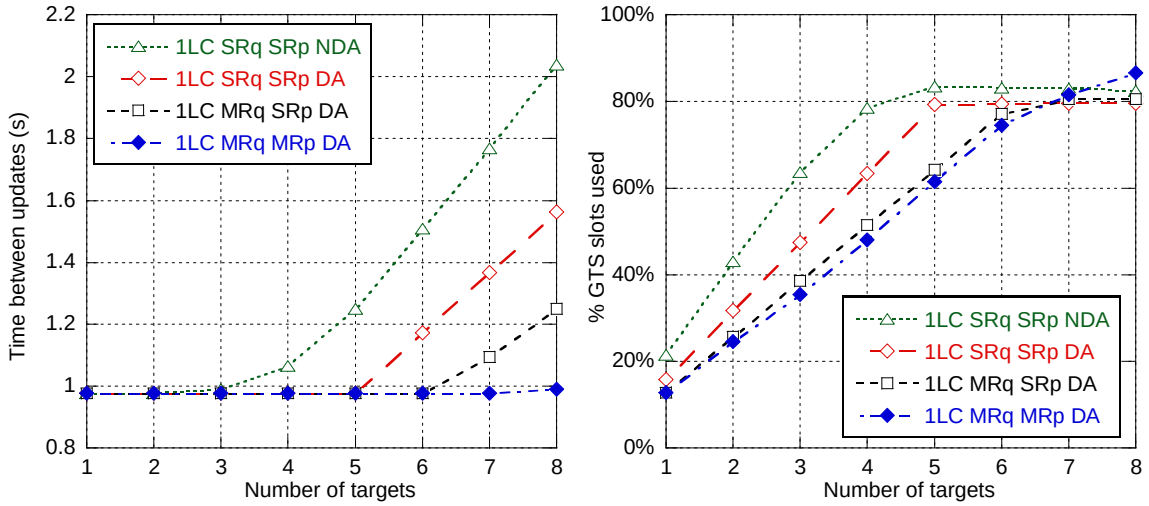

Figure 6.23. Time between updates and % GTS slots used for different acquisition & distribution modes

6.4.4 Impact of the tracking system architecture

As it was previously explained, the tracking functionality is executed by the location controllers, which can be physically implemented in one or more anchor nodes or in the mobile nodes, depending on the architecture that is defined.

As in the previous section, the update process schemes for the different architectures depending on the number of anchors used for location are presented. A SRq SRp NDA mode has been considered. The scheme for the architecture centralized in the network was already presented in Figure 6.13. Figure 6.24 shows the scheme for a distributed architecture. Note that now only one slot is allocated to each data frame (MR and PU), as the LC functionality will be always executed by an anchor neighbor to the target. Figure 6.25 shows the scheme for an architecture centralized in the mobile nodes. In this case, the target computes its own position, so there is no need of using data frames for transmitting the distances and the position, and position can be computed right after the last distance is estimated.

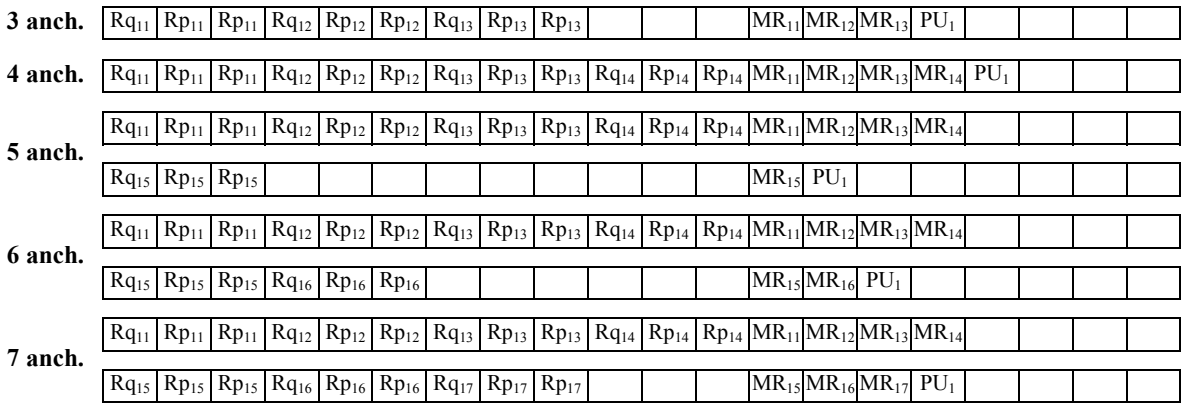

Figure 6.24. Update process scheme for Distributed SRq SRp NDA depending on the number of anchors

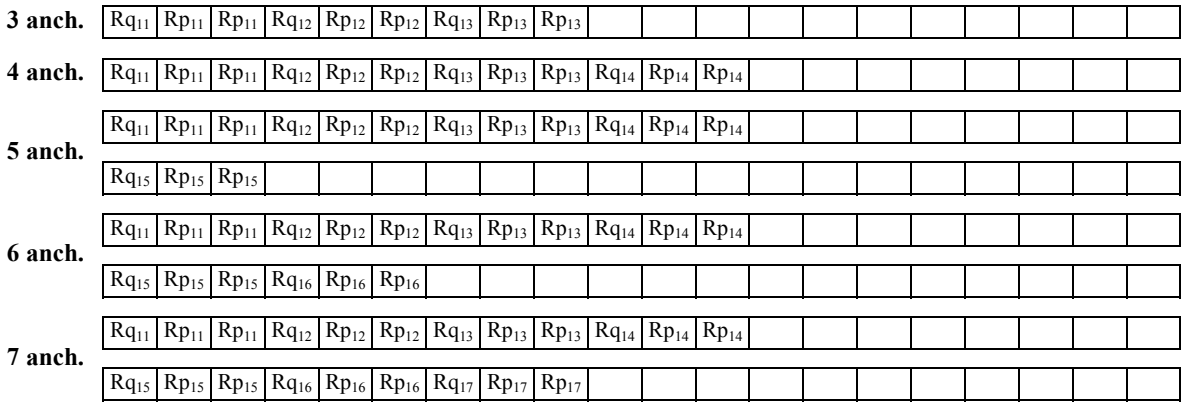

Figure 6.25. Update process scheme for Mobile SRq SRp NDA depending on the number of anchors

Figure 6.26 shows the average error obtained for the different architectures depending on the number of anchors used for location. Results for the architecture centralized in the network with 1 location controller (1LC) where already discussed in previous section. For the distributed architecture, the limitation is due to the ranging exchanges, as data frames transmission can always be done within a superframe. Consequently there is an important increase of the error when 5 anchors are used, as a second superframe will be needed, and a slight decrease for more anchors. A slightly higher error level is obtained for an architecture centralized in the network with 4 LC, as most of time the target will be neighbor to one of the location controllers. Finally, the architecture centralized in the mobile nodes shows a similar evolution but with a slightly lower error, as the position can be computed as soon as the last distance is estimated, so the latency of the update process is always a little bit shorter.

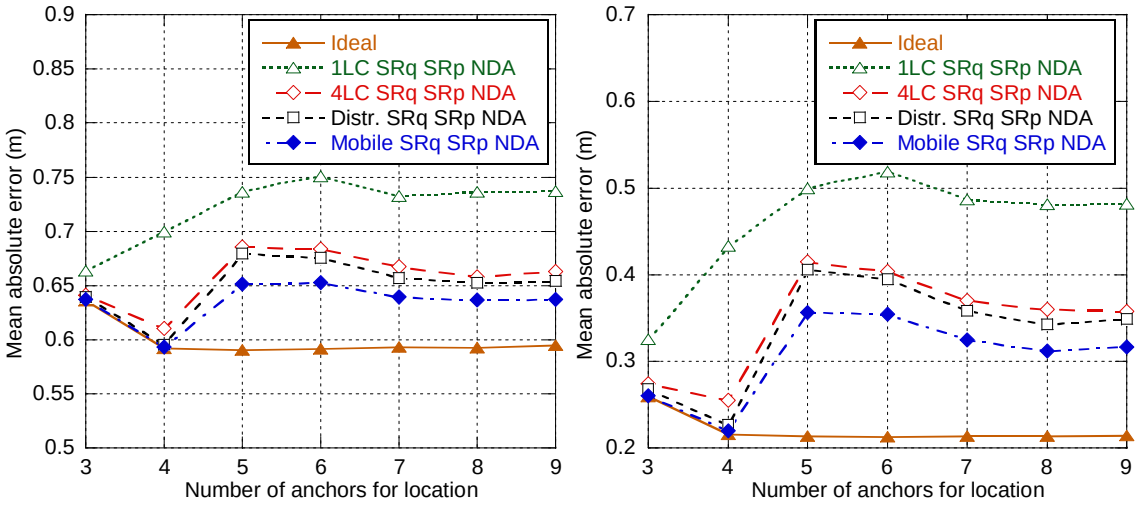

Figure 6.26. MAE for different tracking architectures depending on the number of anchors for location (σ_n=0.7 and σ_n=0.3)

Following, the impact of the tracking architecture is analyzed depending on the number of targets that are simultaneously tracked. A SRq SRp NDA mode was considered. The update process scheme for the architecture centralized in the network was already presented in Figure 6.18. Figure 6.27 shows the update process scheme for the distributed architecture. Note that only one slot is needed to transmit the location data frames (MR and PU), as the LC functionality is always executed by an anchor neighbor to the target. Figure 6.28 shows the update process scheme for the architecture centralized in the mobile. Note that no location data transmission is needed, as the mobile computes its own position.

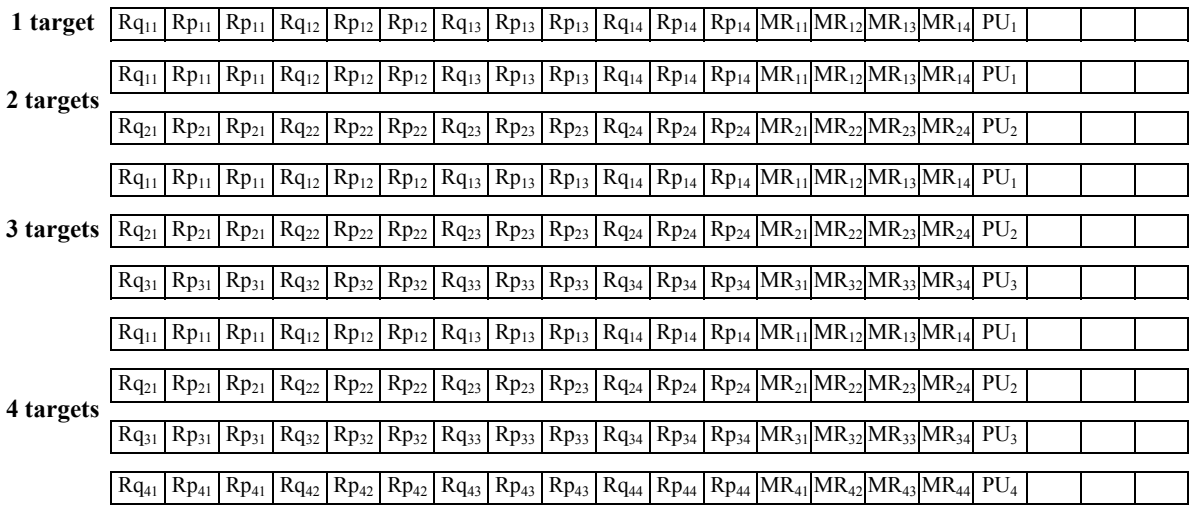

Figure 6.27. Update process scheme for Distributed SRq SRp NDA depending on the number of targets

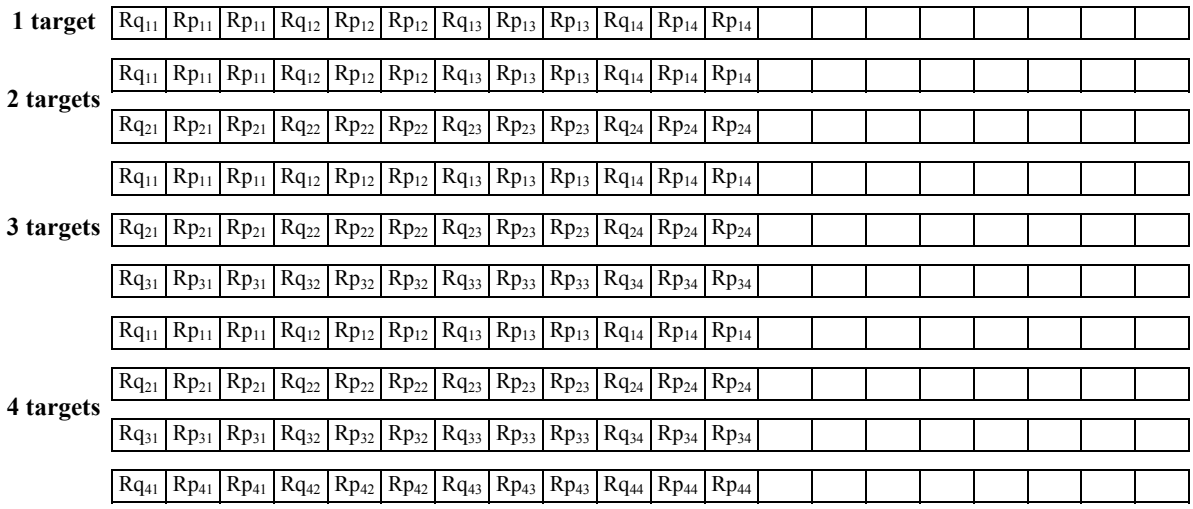

Figure 6.28. Update process scheme for Mobile SRq SRp NDA depending on the number of targets

The positioning error for the different tracking architectures depending on the number of targets is shown in Figure 6.29. As it was already explained in the previous section, the error for the architecture centralized in the network with 1 LC grows exponentially as the number of targets increases, as there are not enough data slots available. Concerning the architectures distributed and centralized in the mobile, every update process is carried out within a single superframe, so the error is very similar to the ideal. Only for 6 or more targets the error increases, as the ranging slots get saturated, thus increasing the actual time between updates and causing a delay between the anchor selection and the actual start of the ranging exchanges. A similar evolution is shown with an architecture centralized in the network with 4 LCs but with a slightly higher error level, as most of the time the target will be neighbor to a LC, but sometimes it will need 2 hops to reach the LC and the update process will then need 2 superframes, thus increasing the latency and the error.

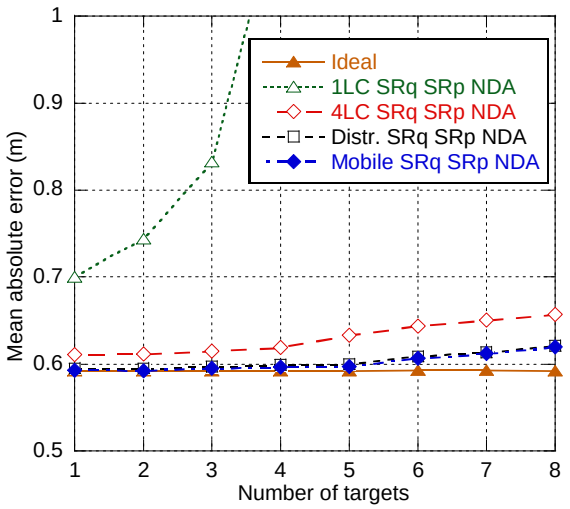

Figure 6.29. Average error for different tracking architectures depending on the number of targets (σ_n=0.7)

The actual time between updates and the % of GTS slots used can be observed in Figure 6.30. As it was previously mentioned, the architecture centralized in the network with 1 LC can track up to 4 targets until slots allocated to location data transmission get saturated. The architectures distributed and centralized in the network with 4 LCs can track up to 5 targets until ranging slots get saturated, with a residual 10-15% of slots available for data transmission. Finally the architecture centralized in the mobile nodes can also track up to 5 targets but, as location data transmission is not needed, with a lower use of resources, and consequently higher capacity available for data transmission. Therefore, the architecture centralized in the mobile nodes is the optimal in terms of use of resources.

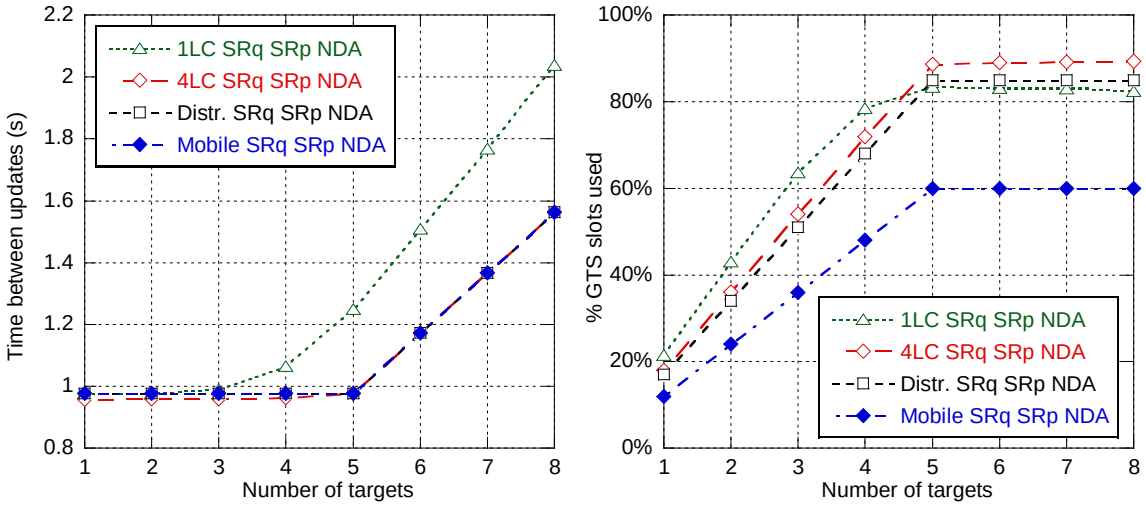

Figure 6.30. Time between updates and % GTS slots used for different tracking architectures depending on the number of targets

6.4.5 Complete system evaluation

Following, the different tracking architectures are combined with the acquisition & distribution enhancements by considering the enhanced mode with multicast request and data aggregation (MRq SRp DA). Multicast response has not been considered as it requires the coordination of the updates that is only feasible with the architecture centralized in the network.

Figure 6.31 shows the MAE obtained for the different architectures with a MRq SRp DA mode. With this mode, all the architectures are limited by the ranging exchanges, so they all show a similar evolution with an error increase when 6 anchors are used as a second superframe will be needed. On the other hand, the architecture centralized in the mobile nodes shows a slightly lower average error as the position is computed right after the last distance is estimated and consequently latency is always a little shorter.

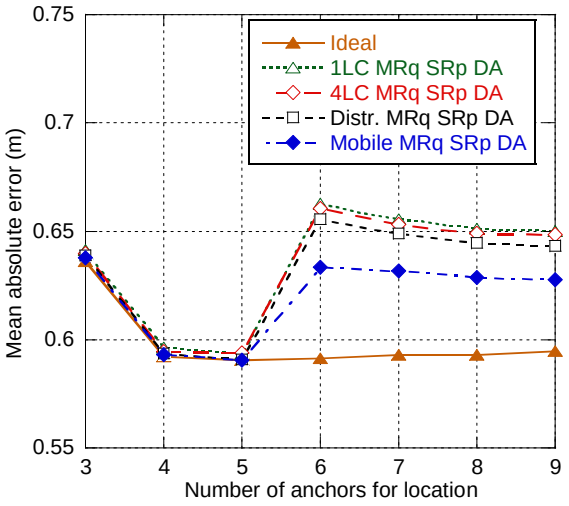

Figure 6.31. MAE for different tracking architectures depending on the number of anchors for location (σ_n=0.7, mode MRq SRp DA)

Figure 6.32 shows the average error for the different architectures considered for a MRq SRp DA mode depending on the number of targets. As it can be observed, the architectures centralized in the network with 1 LC, distributed and centralized in the mobile nodes all have a similar evolution. As it can be observed in Figure 6.20, the update of target #1 takes place in superframe #1 so the error for 1 target will be just slightly higher than the ideal. The update of target #2 starts in superframe #1 and finishes in superframe #2, update of target #3 starts in superframe #2 and finishes in superframe #3, and update of target #4 starts in superframe #3 and finishes in superframe #4, so updates of targets #2, #3 and #4 have a higher latency and the error increases as 2, 3 and 4 targets are tracked. For 5 and 6 anchors there is no increase, as update of target #5 would take place in superframe #4 and update of target #6 would take place in superframe #5. For 7 and more targets there would be a further increase. The architecture centralized in mobile nodes presents a smaller error as position can be computed as soon as the last distance is estimated, so its latency is the smallest, whereas the architecture centralized in the network with 1 LC shows a higher error as multiple slots may be needed to relay the location data frames, so its latency is the highest. On the other hand, the architecture centralized in the network with 4 location controllers does not show a similar behavior, but a more regular increase. This is due to the fact that when multiple location controllers are used position updates are not completely periodic, as there are also asynchronous updates when a target changes from one LC to another, thus randomizing the timing of the updates.

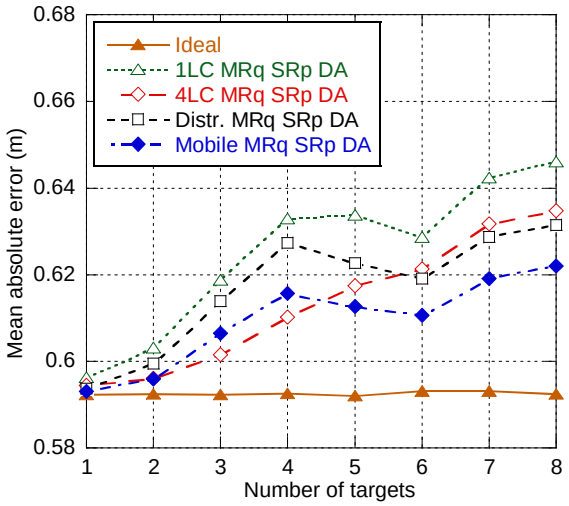

Figure 6.32. MAE for different tracking architectures depending on the number of targets (σ_n=0.7, mode MRq SRp DA)

Concerning the actual time between updates, with all the architectures up to 6 targets can be tracked, as it can be observed in Figure 6.33. Note that actual time between updates for the architecture centralized in the network with 4 location controllers is slightly smaller due to the asynchronous updates happening when a target moves from one LC to another. Concerning the % of GTS slots used, the architecture centralized in the mobile nodes is the optimal in terms of use of resources, whereas the architecture centralized in the network with 1 LC requires the highest amount of resources.

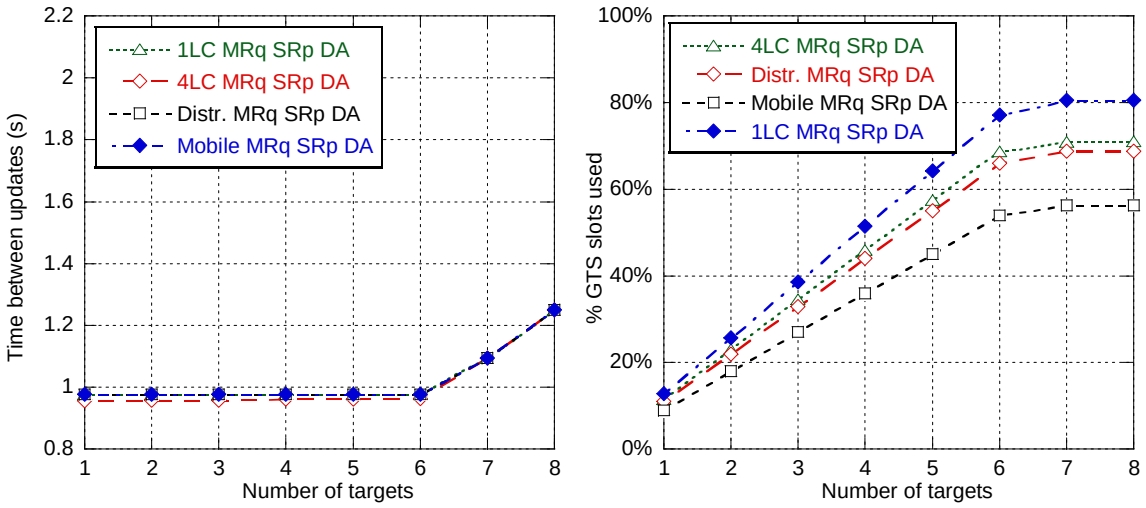

Figure 6.33. Data slots available for communication for different tracking architectures depending on the number of targets (mode MRq SRp DA)

Finally, accuracy and capacity of the system is evaluated for the different algorithms considering the real MAC implementation and σ_n=0.3. In order to minimize latency, the architecture centralized in the mobile nodes has been considered, together with MRq, SRp and DA enhancements. MRq has not been considered as it requires the coordination of the updates, which is complex to implement for the architecture centralized in the mobile nodes. Figure 6.34 shows the average positioning error for the different algorithms. Results for 5 or less anchors are similar than those of Figure 5.16 as latency is relatively small. When 6 anchors are used, there is an important increase of the error for all the algorithms, as each update will require two superframes, thus increasing latency.

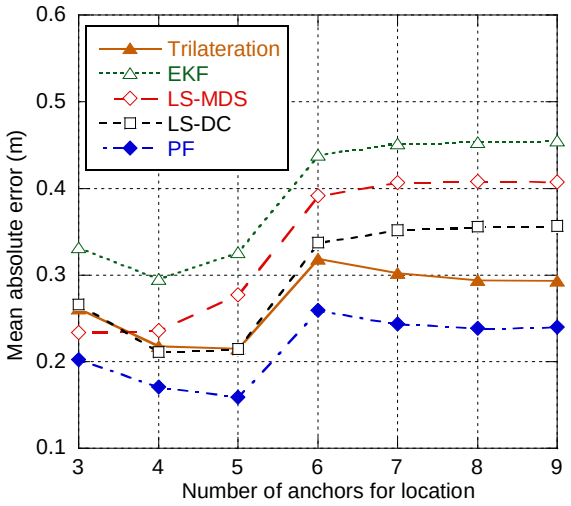

Figure 6.34. MAE for the architecture centralized in the mobile nodes (σ_n=0.3, MRq SRp DA).

In order to evaluate capacity, we have selected two options, LS-MDS with 3 anchors and LS-DC with 4 anchors, which provide an average positioning error of 23 and 21 cm respectively. Again, the architecture centralized in the mobile nodes and MRq, SRp and DA enhancements have been considered. As it can be observed in Figure 6.35, the system can track up to 6 anchors in case of LS-DC with 4 anchors, and up to 8 anchors in case of LS-MDS with 3 anchors, leaving a residual 40% of GTS slots available for data transmission.

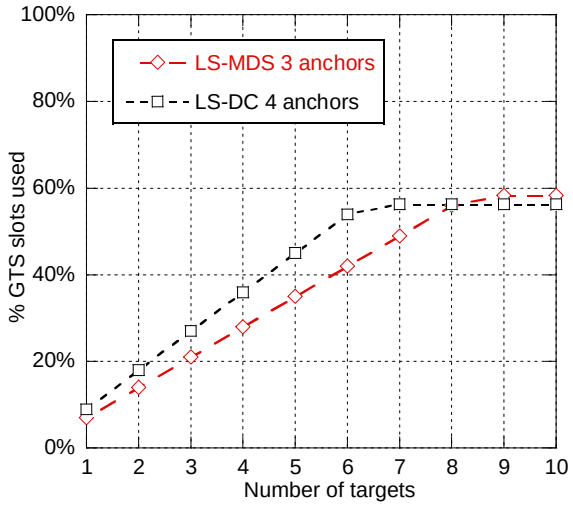

Figure 6.35. % of GTS slots used for LS-MDS (3 anchors) and LS-DC (4 anchors)

6.5 Conclusions on the System Design

In the design of a UWB combined communication and tracking system in the framework of IEEE 802.15.4a, the timing and structure of the MAC layer must be taken into account, as the delay and the limitation of resources impact not only on the capacity of the communication systems, but also on the accuracy and the capacity of the tracking system.

As it was demonstrated through several simulations, the positioning error is sensitive to the latency of the position update process, and specifically the delay between the distance estimation and the position computation. If the position update process is carried out within a single superframe, this latency is relatively small and the error increase is negligible. But if the position update process covers multiple superframes, the latency will be over 200 ms and the error increase is significant.

Also the limitation in resources, specifically the number of slots allocated for ranging and data transmission on each superframe, entails a limitation of the number of targets that can be tracked simultaneously. Furthermore, the allocation of resources to the tracking functionality results in a reduction of the resources available for communications.

Consequently, the design of the tracking functionality must take into account these effects and implement suitable architectures and location information acquisition and distribution strategies that reduce the position update latency and the amount of resources used. The architecture centralized in the mobile nodes is optimal in terms of latency and

resources needed, as there is no need of transmitting the estimated distances to the network. Nevertheless it requires some computational capacity on the mobile targets in order to calculate their own position. If an architecture centralized in the network is used, the use of data aggregation for the transmission of the distances to the location controller is mandatory in order to reduce the amount of data slots needed.

The need of limiting the number of anchors used to locate a target is clear in order to optimize the positioning error, minimize latency and maximize capacity. In our system, the limitation to 4 anchors is proposed, as it is a value that provides a low error for most of the algorithms with a suitable resource consumption. The limitation of the number of anchors used entails that a selection procedure must be used. As the position of the target is not known, other available information must be used. The EP-PB method based on the estimated position with periodic broadcast updates provides a very good performance close to the ideal with a non excessive need of resources.

Concerning, the MAC layer design, the number of slots allocated to ranging should be set in accordance with the procedure defined for distance acquisition in order to guarantee that the distance acquisition can be done in a single superframe and at the same time optimize the amount of resources used. For instance, if the number of anchors used for location is set to 4 and singles request and single response is used, 12 slots should be allocated to ranging, but if multicast request is used or the number of anchors used for location is reduced to 3, only 9 slots should be allocated to ranging. In this context, a flexible allocation of ranging slots within the GTS period is preferred over a fixed one, in order to assure that there are enough slots to complete the update on a single superframe and, on the other hand, guarantee that there are not idle ranging slots, thus optimizing the amount of resources available for data communication.

Another important design parameter is the position update rate. Position update rate must be set according to the motion model of the targets and in particular to target speed. For pedestrian speeds up to 3 m/s, 1 update per second is a suitable value.

Finally, concerning the location and tracking algorithms to be implemented in the location controllers, WLS-MDS and LS-DC provide very good results on most of the configurations considered, with the advantage that, as completely non-parametric methods, knowledge of the motion and measurement models is not required. Furthermore, they provide some kind of mitigation of NLOS bias through weighting and distance contraction respectively.

Chapter 7

Applications of Location Information in Radio Access Networks

7.1 Introduction

Indoor location and tracking systems have a wide variety of application scenarios, including industrial, medical, home automation or entertainment sectors. Some examples of possible applications of location-awareness in indoor environments include:

- Monitoring the assembly line in a factory, in order to track the state of a certain product, get valuable information about the manufacturing times, identify bottlenecks, automatically set the right machine or tool configuration for a certain product, etc.
- Tracking the stocks in a warehouse, allowing automatic inventory and fast location of a certain stock.
- Tracking the workers in dangerous environments, such as an electrical substation, controlling that they stay in the secure area and warning if they enter a forbidden area.
- Locating medical equipment and personnel in a hospital.
- Developing intelligent audio guides that select narration according to the position of the visitor in a museum.
- Tracking sportsmen or sport teams, in order to provide valuable information about their performance or to enhance the experience of spectators and remote viewers.

Besides the straight applications of UWB indoor location and tracking systems, further applications would be allowed by integrating UWB location into mobile network access devices (e.g., mobile phones) in order to complement in indoor environments the location

information provided by GPS in outdoor environments. 3G/4G networks and particularly systems such as LTE-Advanced or UMTS have the support of positioning services as an advanced objective aiming to improve the services offered to the user and even to improve the resource management of their networks. Location awareness offers a compelling new business opportunity for application developers, operators and content producers.

Focusing on users, the integration of positioning systems such as GPS in the new generation of smartphones and mobile devices is enabling the development of innovative Location Based Services (LBS). Using mobile devices, LBS leverage a user's physical location to provide enhanced services and experiences. LBS enable a range of applications, such as navigation and mobile map services, local search, workforce tracking, friend finders and safety applications.

On the other hand, network operators can also benefit of location-awareness in order to enhance their networks, for example, aiding network planning. The operator may be able to locate calls in certain areas to estimate the distribution of calls and user mobility for network planning purposes. These applications may be utilized for hot spot detection, user behavior modeling or to track dropped calls to identify problematic and poor quality areas.

This chapter deals with the applications of location-awareness in order to enhance user services and radio resource management. It must be noted that the analysis done in this section focuses on the applications of location-awareness regardless of the positioning technology used and is not specifically related to UWB location. In fact, most of the work carried out up to now has focused on outdoor environments supported by GPS or mobile network-based (GSM, UMTS) positioning.

Cellular and wireless technologies such as UMTS, WiMAX and 802.11 are commonly used to provide network access in different conditions. On the other hand, in order to retrieve the position of the device, satellite systems as GPS or Galileo may be used. But these systems are limited to outdoor environments, which is an important restriction as in many cases the devices will be indoors. Another possibility is using the information available in the cellular network, for instance the RSSI or the TDOA of signals received from different base stations, to provide location. Nevertheless, accuracy of these systems, especially in indoor environments, is limited to hundreds of meters due to multipath and NLOS conditions in addition to the large distance between the mobile and the base stations.

In this context, UWB arises as a good candidate to provide location information to mobile users in indoor environments. Due to the short range of UWB, usually limited to body and personal area networks, in contrast to high range of cellular networks such as WiMAX or UMTS, focused on metropolitan and wide area networks, it may seem at first

sight that the use of UWB might not be suitable to provide location information to cellular networks. Nevertheless, due to the new generation of high-capacity devices (smartphones, tablets...), the increasing number of users and the growing bandwidth requirements of novel services as mobile Internet access, video streaming or IPTV, cell sizes for new broadband cellular networks, such as LTE, must be reduced, and some scenarios with potential high user density and high bandwidth requirements such as airports, business districts, shopping centers, industrial areas, amusement parks, trade fairs, exhibition centers, sports complex, etc. must be covered by micro and picocells. Furthermore, in this kind of scenarios, the efficient radio resource management becomes critical in order to provide the required QoS to the highest number of users with the limited available resources. In this context, the use of UWB to support enhanced location-aware RRM algorithms and strategies that make more efficient use of the available resources becomes interesting.

As an example, Figure 7.1 shows a scenario where a UWB network deployed in a shopping centre could provide location information to a cellular network in order to enable location based services and to enhance resource management.

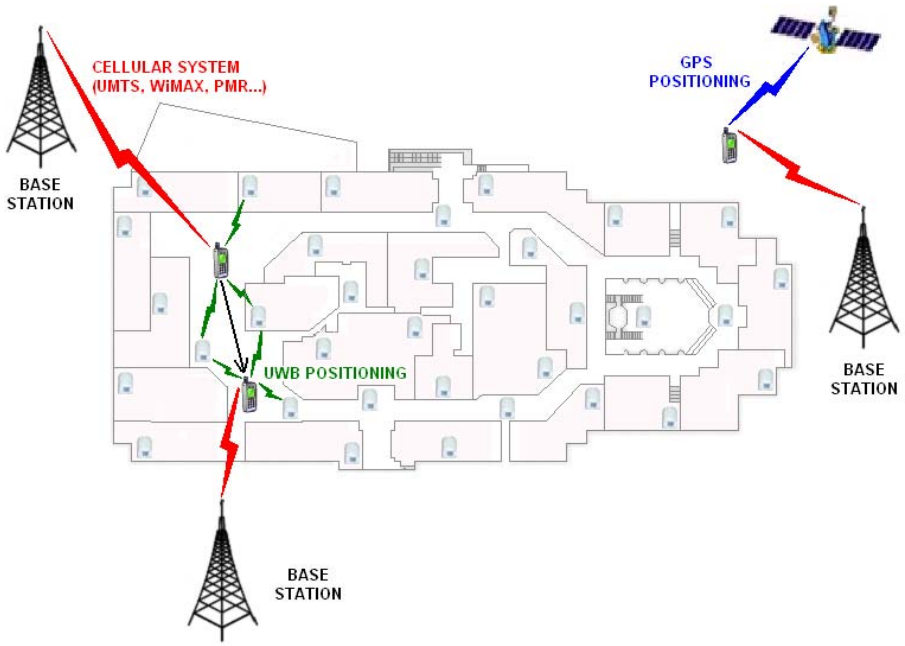

Figure 7.1. Location-aware services in heterogeneous networks

7.2 Location Based Services

7.2.1 Introduction

Although location-based services have been an issue in the field of mobile communications for many years, recent years have seen rapid growth in the area of LBS thanks to the advances in wireless communication and mobile Internet. Factors driving this increase include the appearance of smartphones and tablets with higher computational capacity and user-friendly interfaces including high-quality touchscreens and smartphone-oriented operating systems, the integration of inertial sensors, GPS receivers and improved cellular-based location within the smartphones and portable devices, the reduction of mobile Internet prices and the success of application stores (App Stores) providing thousands of applications. LBS, by delivering personalized information to mobile users based on their locations, are regarded as one of the killer applications in mobile Internet [Zimmerman, 2009]. For instance, LBS are ranked No.2 in Gartner's report on the "Top 10 Consumer mobile applications for 2012" [Shen, 2009]. Nevertheless, there exists neither a common definition nor a common terminology for them. For example, the terms location-based service, location-aware service, location-related service, and location service are often interchangeably used [Küpper, 2005].

In [Schiller, 2004], LBS are defined as services that integrate a mobile device's location or position with other information so as to provide added value to a user. The GSM Association simply defines LBS as services that use the location of the target for adding value to the service. Another similarly abstract definition of LBS is given by the 3GPP [3GPP, 2008]: LBS are services provided by a service provider that utilizes the available location information of the terminal. A similar definition for LBS is given by the international Open Geospatial Consortium [OGC, 2005]: wireless-IP services that use geographic information to serve a mobile user, any application service that exploits the position of a mobile terminal. These definitions describe LBS as the intersection of three technologies: New Information and Communication Technologies (NICTS) such as the mobile telecommunication system and handheld devices, Internet and Geographic Information Systems (GIS) with spatial databases [Shiode, 2004].

In research, LBS are often considered to be a special subset of the so-called context-aware services (from where the term location-aware service has its origin). Generally, context-aware services are defined to be services that automatically adapt their behavior, for

example, filtering or presenting information, to one or several parameters reflecting the context of a target. These parameters are termed context information. The set of potential context information is broadly categorized and may be subdivided into personal, technical, spatial, social, and physical contexts.

There exist a broad range of LBS applications, mostly aimed to outdoor environments and supported by GPS and mobile network-based (GSM, UMTS) positioning. LBS applications can be grouped in the following categories [Steineger, 2006]:

- Emergency services: emergency calls localization, roadside assistance for drivers…
- Navigation services: maps, directions, state of traffic, car park guidance…
- Information services: travel and tourist guides, mobile yellow pages, shopping guides…
- Tracking and management services: delivery tracking, vehicle tracking and fleet management, personnel tracking, assembly line monitoring, warehouse logistics…
- Billing services: road tolling, proximity payments…
- Advertising: proximity marketing, special offer alerts…
- Leisure and games: buddy finder, instant messaging, mobile games, social networks (foursquare)…

7.2.1.1 Components of location based services

Figure 7.2 shows the five basic components of LBS and their connections [Steineger, 2006]:

- Mobile user device: it enables the user to request the needed information and presents the results. In general are smartphones, PDAs, mobile phones, tablets, laptops... but can also be a navigation unit of a car or a toll box for road pricing in a truck.
- Communication Network: the mobile network transfers the user data and service request from the mobile terminal to the service provider and then the requested information back to the user.
- Positioning system: the user position can be obtained either by using the mobile communication network or by using specific positioning systems such as satellite systems (GPS, Galileo) and indoor location systems, generally based on medium and short range radio technologies (UWB, WiFi, ZigBee…).

- Service and Application Provider: the service provider offers a number of different services to the user and is responsible for the service request processing. Services may include providing a map relative to user's location, finding a route to an object of interest, searching yellow pages with respect to user's position or searching information on objects near the user.
- Data and Content Provider: service providers may not store and maintain all the information which can be requested by users, but request it from geographic data and location information databases from different public or private partners (e.g. mapping and traffic agencies, yellow pages, business directories, etc.).

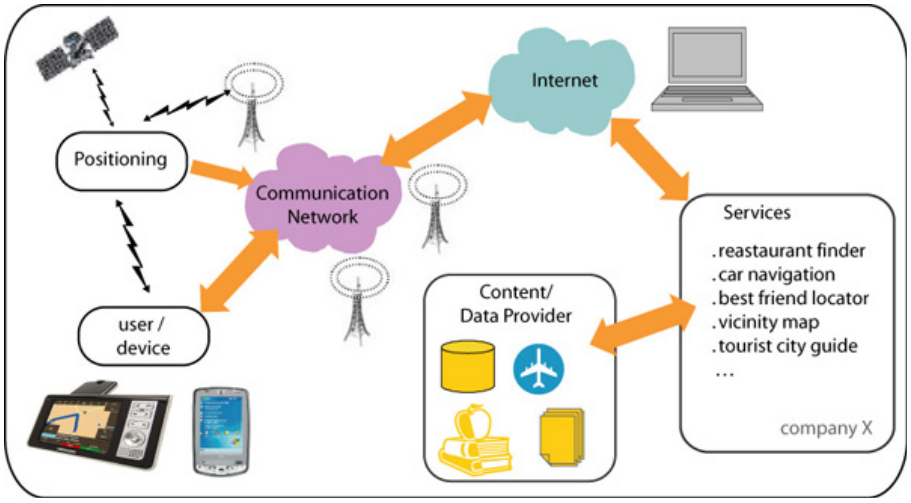

Figure 7.2. Components of LBS and their connections

7.2.2 Use cases of UWB-enabled location based services

Many location-enhanced services are affected by the unavailability of indoor location, which is not covered by satellite-based systems like GPS, and by the high time required to compute the initial position after activation. This fact opens the door to UWB as a key technology to be taken into account in the development of novel and promising location-aware services due to its intrinsic features for providing accurate indoor localization, extending the scope of LBS to a higher number of potential scenarios, applications and users. Among the potential LBS applications enabled by the integration of UWB and Radio Access Network, the following use cases have been identified:

a) Indoor Positioning Systems

The objective of this service is to provide users with a navigation tool similar to car navigation systems but aimed to indoor environments. Some interesting scenarios for this application are shopping malls, train stations, airports, exhibition centers, sports stadiums, hospitals, museums etc. In this kind of scenario, a set of fixed UWB anchors would be distributed in known positions in order to provide user's dual WAN/UWB devices with location information. On the other hand, the user would be connected through the WAN access to the navigation service provider, which would provide periodically updated maps according to user's position. Users could also request the navigation service to guide them to a certain place (a shop, check-in desk, his seat...) or get information of interest (special offers, arrival times, match statistics, etc.).

b) Location-based search

The objective of this service is to provide users with customized search results ordered according to proximity to the user. This can be useful for requesting the nearest business or service, such as a cash machine or restaurant in wide indoor environments such as shopping malls, airports, etc. With this purpose, user's search request should include user's position, and information in search databases should also include location information.

c) Proximity marketing

The objective of this service is to provide users with information such as latest bargains, special offers, discounts coupons, etc. of the shops and business nearby. With this purpose, the user's mobile phone should have integrated UWB interface. When another UWB device in the shop/business detects the presence of a user nearby, it will send an advertisement to the user's mobile phone, for instance an SMS. The advertisements could be targeted only to certain users according to characteristics such as age, user profile, etc. Advertisements are pushed to the user without any previous request from the user, therefore it is necessary a previous acceptance of the service by the user in order to protect non-users from receiving unsolicited messages.

d) Children surveillance

The goal of this application is to detect if a person is going out of a security zone. As an example a teacher could use this service in order to detect if a student is going out of the authorized zone (in the schoolyard, in a zone defined outside the school when they are going out...). All students would be equipped with UWB devices (on watches or wristbands). The teacher would get an alarm (SMS) when a student is going out of the security zone, and could retrieve the relative position of each student on its mobile terminal (UMTS). This solution can also be deployed in other environments for example for elderly people in an old

people's home. Another possible application is to support parents when visiting amusement parks, shopping centers, multiscreen movie complexes, museums, family entertainment centers, etc. so they would get a notification when children move apart from them and could locate him/her through a map tracking children's position.

e) Buddy-finder

The objective of this service is to notify users about the proximity of other service users that are linked to him/her (buddies). This way, a user entering a shopping mall, leisure centre, disco, etc. would receive a notification if any of the contacts on his mobile phone directory or instant messaging application contact list are in the same location. This application does not require very high accuracy, so less UWB transceivers could be used compared to other use cases. Users would only be able to locate users on their contact list that have this service and therefore have explicitly agreed to be found by their buddies. Users would start the buddy-finder service (most likely integrated in an instant messaging application) on their mobiles and a connection would be established with the service provider that would notify the users about the status of their buddies.

f) Proximity payments

The objective of this service is to allow users to make small monetary transactions with their mobile phones or other handheld devices just by placing it near a kiosk or payment station. Proximity payments are already being applied in multiple scenarios such as vending machines, ticketing, parking meters, public transportation (bus, subway, train…), road tolling, etc. With this purpose, the kiosk or payment station would have a UWB transceiver that would detect the proximity of user's UWB-enabled mobile phone or a smartcard with a UWB transceiver. There are many possibilities for the payment platform architecture, which can be based on the mobile operator, on credit card or financial companies, on Internet payment third parties or on prepaid smartcards. The payment platform can be contacted either by the kiosk (in that case the kiosk should have connection to Internet) or by the user's mobile phone.

g) Customized multimedia guide

The objective of this service is to provide museum visitors with an interactive location-aware multimedia guide. The guide would provide the visitor with the multimedia content (audio, pictures, text, video) according to user's location, so the users would automatically get the corresponding explanations as they are approaching a work of art. Furthermore, the application could have a navigation tool to guide the user through the museum. The user could choose between different available tours or even take a customized tour. The user

would be connected through the WAN access to the service provider, which would provide the multimedia content corresponding to user's location.

h) Parking space finder

The parking space finder service helps drivers to find available spaces when entering an indoor parking garage. Firstly, the user sends a service request via an SMS, through a call or by means of an application on his/her dual WAN/UWB mobile phone. The user position, which is obtained from a UWB-based location system, is also included in the service request. Then, the operator/service provider sends a query to a database of available parking bays, which is continuously updated thanks to the information from a UWB sensor network deployed in the indoor garage. The sensors will be interconnected and connected to the operator's network too. Finally, the network sends the user the geo-referred information about available parking spaces via an SMS or through a data connection and the application stored in the user device calculates the best route to the nearest parking spot. The information is displayed on a browser-type cartographic system.

7.2.3 Demonstrators

In order to show the potential of UWB-based localization to enable access to location based services in a heterogeneous scenario, the Shopping Centre demonstrator was developed within EUWB project. A UWB location and tracking system has been also integrated in e-Museum, a demonstrator of ambient intelligence in a smart museum environment.

7.2.3.1 Shopping Centre

The main objective of the shopping centre demonstrator is to build a platform for the development and test of location-aware services in heterogeneous networks. The demonstrator has been deployed in a reduced area of few meters length, as a scaled representation of a real indoor environment, for instance a shopping centre. As the dual device moves across the area, the position provided by the LT system is converted into a position in the real shopping centre. Following, a description of the most important elements of the demonstrator, which are depicted in Figure 7.3, and the developed services is given.

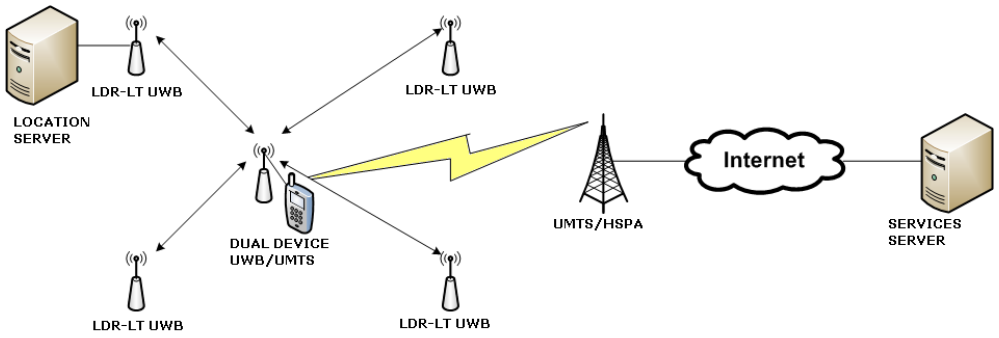

Figure 7.3. Location-aware services demonstrator

a) LDR-LT UWB piconet

The LDR-LT UWB piconet is composed of at least 4 fixed UWB nodes, in addition to the mobile node integrated in the user UWB/UMTS device. One of the fixed nodes acts as the piconet coordinator. The mobile node is continuously performing ranging with the coordinator and the fixed nodes are sending the estimated distances to the coordinator. On the other hand, the coordinator periodically sends the vector of estimated distances over the serial port to the location server application

For the implementation of the LDR-LT UWB piconet, the LDR-LT prototypes developed within the EUWB project have been used. The EUWB prototypes are 802.15.4a-based IR UWB devices implementing the PHY and MAC layers designed within the EUWB project. These prototypes were already introduced in Section 6.2.1 and a detailed description of the PHY and MAC layers can be found in [Pezzin, 2007] and [Bucaille, 2007] respectively. Figure 7.4 shows the physical view of the EUWB prototypes.

b) Location server

The function of the location server is to collect the distances estimated between the mobile and the fixed LDR-LT UWB nodes and to compute the position of the mobile user. Physically, it is implemented in a laptop/PC connected to the LDR-LT UWB piconet coordinator. In order to compute user's position, the EUWB Graphical User Interface is used. A snapshot of the EUWB GUI is shown in Figure 7.4. Through this GUI, the positions of the fixed anchor nodes are set. The application retrieves the estimated distances vector from the serial port and computes the mobile target position using the LS-DC algorithm that was explained in Section 5.3.1.3. Finally it displays the results both graphically and numerically. In order to implement the location server functionality, this application has been modified and specifically a TCP server port has been enabled, so any TCP client can connect and retrieve the position of the mobile target.

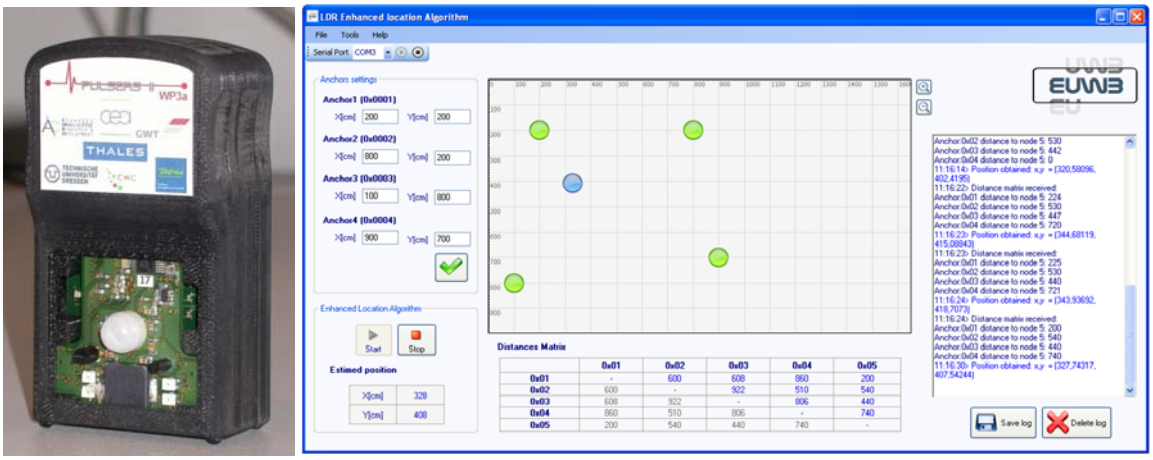

Figure 7.4. EUWB LDR-LT prototype and location server GUI

c) User UWB/UMTS device

The mobile user device is a dual LDR-LT UWB/UMTS device, in general a mobile phone, smartphone or PDA, although for demonstration purposes a laptop has been used. A UMTS PCMCIA card is used to provide UMTS access. On the other hand, the EUWB LDR-LT prototype with the role of mobile target is used for location purposes.

The services client application runs in the user device and provides the user with all the information concerning the shopping centre: map, shop list, shop information, bargains, etc. Through the client application, the user is able to access location based services. The communication with the services server application is done through TCP sockets. A snapshot of the client application GUI is shown in Figure 7.5.

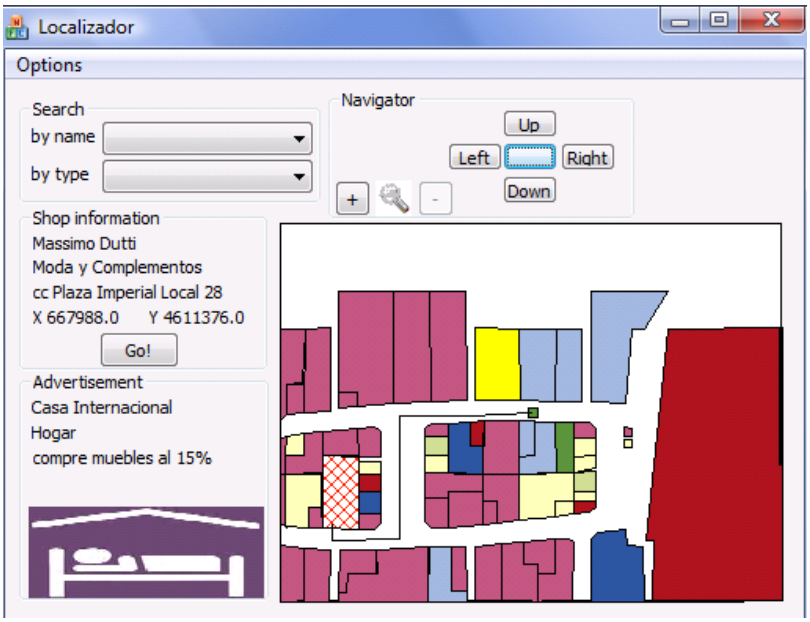

Figure 7.5. Client application main window

d) Services server

The function of the services server is to provide the requested information to the mobile user according to user's position, which can be provided by the client application or retrieved from the location server. It is physically located in a computer that must be connected to Internet with a public IP. It must have stored the geographical information about the shopping centre (shops, walls, corridors, intersections etc.). The services server runs the server application that communicates with the client application on the mobile node.

e) Location-based services description

The following location-based services have been implemented in the demonstrator:

- Navigation

The navigation service allows the user to display his position in the shopping centre map, explore the map and shops and ask for the shortest route to any shop. The service follows a pull scheme, as exchanges are always initiated by the client with a map or route request, which is processed by the server that sends the consequent response. Shopping centre information including a list of shops with shops information is initially sent to the client. Then the client sends a map request to the server. The map requests must include different parameters such as the window size, zoom level, scroll state and, depending on the scroll state, the user's position or the origin coordinates. Therefore, there are two possible operation modes. When scroll is not active, a request is sent periodically and the generated

map is centered on user's position and sized according to window size and zoom level. When scroll is active, a request is sent each time the user clicks on a scroll button and the map is generated according to the origin coordinates, window size and zoom level. Then the map is drawn in the client window and the user is able to select any shop just by clicking on it. Concerning the route functionality, when the user clicks on the button to ask the way to a certain shop, a route request is sent to the server including user's position and shop index. Then the server computes the shortest way to the shop and sends a response with the route. Finally the client draws the route in the map and periodically requests route updates.

- Location-based search

Location-based search allows the user to look for shops of a certain type, getting the search results ordered according to the distance from the user. The service is started when the user queries the application for shops of a certain type (restaurants, fashion, etc.). The client application then sends a search request to the server with the selected type. The service may follow either a pull or poll scheme, depending on whether user's position is provided by the client in the search request or retrieved from the location server by the services server, respectively. Then the server collects the shops belonging to that type, computes the distance to the user for each shop and sends the shop list to the client application. The client application displays the shop list and distances so the user is able to select a shop, which will be shown in the shop information area and highlighted in the map.

- Proximity marketing

The objective of proximity marketing is providing the user with relevant information of the nearby shops, such as bargains, special offers, etc. without any previous request of the user. The proximity marketing service is started in the application setup as the navigation service is started. Previously, there would be an implicit or explicit agreement of the user when installing the application. The service follows a push scheme, as the server sends the advertisements without a previous request from the user. Periodically, the server requests user's position from the user or from the location server. Then the server computes the distance from the user to the different shops featuring this service, selects the closest shop and, if it is under a certain threshold and it is different from the previously selected shop, sends the advertisement to the user. Finally, the advertisement is displayed in the advertisement area of the client application and the shop is highlighted in the map.

7.2.3.2 e-Museum.

Ambient Intelligence (AmI) refers to electronic environments that help to improve user experience. This experience is linked to many different devices. Thanks to a network of

devices, these environments are capable of sensing the presence of people and responding to it accordingly. In an AmI context, availability of location information is highly relevant, and UWB is very-well suited to provide this location information due to its high accuracy and good performance in indoor environments.

e-Museum is an Ambient Intelligence multidisciplinary demonstrator developed by different research groups within I3A (Instituto de Investigación en Ingeniería de Aragón). The demonstrator is permanently set-up in the laboratory of the I3A in Walqa Technology Park. e-Museum aims to be an intelligent museum that adapts to each visitor's characteristics, with virtual humans that act as museum guides and with works of art capable of answering questions about themselves. When a visitor enters this next-generation museum, he is identified by a location tag and, from that point on, guided by a human-faced robot capable of interacting with the person through the use of voice recognition and synthesis. Once a work of art is reached, e. g. a picture, the visitor can then interact with a screen next to it with a human-like avatar that answers artistic questions. User experience can also be improved by using personal voice-operated audioguides and Augmented Reality devices.

IR UWB has been selected in order to implement the indoor location and position tracking subsystem, which helps the system to locate people inside the museum and plan robots' goals. Specifically, the commercial Ubisense system has been used. The Ubisense UWB system works at a frequency band between 6 and 8 GHz and consists of four sensors and several tags to be located. The sensors are positioned in the four corners of the room, so as to allow the Ubisense location system to find the tags' position with an accuracy of 15 cm (depending on the environment and system configuration). A combination of AOA and TDOA information is used to compute position using a proprietary algorithm. The algorithm is Bayesian-based and can be optimized through several parameters concerning the motion model and the measurement noise.

7.3 Location-aware Radio Resource Management

7.3.1 Introduction

Radio Resource Management (RRM) comprises different system-level strategies and algorithms aiming to use the limited radio spectrum resources and radio network infrastructure as efficiently as possible. RRM algorithms at the radio interface such as power control, interference management, admission control, resource reservation for mobility

management, load control, channel allocation…, determine how the available radio resources of the system must be used and shared among the different users in an efficient way. In all the cases, the objective is to maximize the system spectral efficiency, while quality of service (QoS) and grade of service (GoS) requirements should be above a certain level.

The availability of positioning information in user stations can be exploited to design more advanced implementations of these Radio Resource Management strategies, thus increasing the efficiency of the cellular access networks (IEEE 802.16, UMTS, LTE…). In order to design even more efficient algorithms, location information can be combined with information of the environment topology (e.g. road network for tracking vehicles, presence of buildings or obstacles, etc.) and with statistic information (e.g. probability of different paths according to the aggregate history of mobility observed).

The increasing popularity of GPS (Global Positioning System) and the E-911 ruling issued by the FCC, requiring the accurate localization of mobile callers requesting emergency services via 911 by the operators of mobile communication networks, motivated the integration of localization systems within mobile cellular networks. This encouraged the research on the possible use of the location information on Radio Resource Management. Some proposals can be found in the literature since one decade, although research on the development of location-aware RRM algorithms for more efficient operation of wireless networks has gained an increasing interest with new and most sophisticated applications [Priggouris, 2006].

7.3.2 Applications of location-awareness in RRM

7.3.2.1 Handover management

As an essential functionality of the mobile networks, handover mechanism guarantees the user mobility in a mobile network wherein the subscriber can move around, keeping alive its connection to the network. When the mobile moves from the coverage area of one cell (source cell) to another (target cell), a new connection to the target cell has to be set up, and the connection with the old cell has to be released. Regardless of being necessary, all types of handovers have a common drawback; they decrease the overall system performance due to the signaling load caused by rerouting the ongoing connection to the new cells to where the mobile is entering. As a central component of Radio Resource Management (RRM), Handover Control (HC) is responsible for managing the ongoing calls even when mobile stations cross the border from one cell into another.

For the practical realization of handovers in a cellular network, each cell is assigned a list of potential target cells, which can be used for handing-off calls from this source cell to them. These potential target cells are called neighbors and the list is called neighbor list. During a call, one or more parameters of the signal in the downlink and/or uplink are monitored and assessed in order to decide when a handover may be necessary. Once the need of a handover is determined, the mobile and/or the base stations of the neighboring cells monitor each other others' signals and the best target candidates are selected among the neighboring cells. When the monitored parameters cross a certain threshold, the handover takes place.

The parameters used as criteria for requesting a handover are usually the received signal power, the received signal-to-noise ratio (SNR), the signal-to-interference ratio (Ec/Io), the bit error rate (BER), the block error rate (BLER), or the Received Signal Code Power (RSCP) in case of CDMA systems. The use of positioning information in the handover decision procedure, whether on exclusively location-based schemes or in hybrid schemes combining location information with received signal strength or link quality information, would provide the following advantages [Teerapabkajorndet, 2001]:

- Reduced power consumption in the mobile terminals, as there is no need of monitoring the signal strength of several base stations
- Reduced signaling load, as the mobile terminal just has to report its own position (or nothing if the position is retrieved by the network itself) instead of several measurements performed with different base stations
- Possibility of using information concerning the mobile's estimated trajectory to select the target cell instead of choosing the cell with higher signal strength, thus reducing the number of handovers needed and the associated signaling load.
- Higher stability of the parameters used for handover decision, as the positioning information is less sensitive to fading or presence of obstacles (in case of GPS or TOA based localization), which entails a better selection of the target cell and the crossover point, thus reducing the ping-pong effect and the number of handovers.

7.3.2.2 Admission control

Admission control is the radio resource management procedure by which the network decides if a connection establishment request is accepted or not, according to the available resources and the characteristics of the traffic and QoS required by the requested connection. The objective of admission control is to make sure that the number of users admitted to the system allows guaranteeing the quality of service at call level and packet level. Furthermore,

it must provide maximum efficiency avoiding the forced termination of calls in progress and blocking of new calls.

Location information of mobile terminals, and particularly their position and trajectory, can be very useful in order to determine which one is the optimum base station to establish a connection. For example, in case a terminal moving out of a cell requests a connection, knowledge of the trajectory of the mobile allows detecting this situation and allocating the resources for this connection in the cell the mobile is moving towards instead of the current cell, thus avoiding the handover.

Another example would be in case of having a macrocell overlapped to multiple microcells in order to serve the connections of high mobility users, thus minimizing the need of handovers. Knowledge of user mobility characteristics prior to the connection establishment allows that a connection requested by a high mobility terminal is established directly in the macrocell, thus avoiding the handovers that would take place within the microcells before the decision of transferring the connection to the macrocell is taken.

7.3.2.3 Load control and balance

The objective of Load Control (LC) function is to monitor and control the traffic load in the cells under a common base station controller in order to assure that the system is not overloaded and to guarantee the appropriate Quality of Service (QoS) levels. This information is reported to the admission control and the scheduler for radio resource management. In case an overload or congestion situation is detected, Load Control must take the necessary actions in order to regain a suitable load level. With this purpose, Load Control coordinates with other RRM functions such as admission control, handover control, power control and scheduler in order to take actions such as reallocating some user terminals in other cells, reducing the data rate or quality level of some connections or even forcing the termination of connections of non-priority users.

In order to maximize the capacity of a cellular network without suffering congestion, load balancing strategy attempts to distribute the traffic load among the cells as uniformly as it is possible. Nevertheless, this is not always possible as in general user and traffic distribution is not uniform and therefore some cells will present a high density of users while others will have a low utilization level. In this sense, the use of Fixed Channel Allocation (FCA) schemes is not very efficient. Dynamic Channel Allocation (DCA) maximizes global network capacity, but has higher complexity and is not suitable for systems with limited reuse of resources. Hybrid Channel Allocation (HCA) schemes combine both schemes in

order to solve their limitations, as Borrowing Channel Assignment (BCA) scheme, which allows borrowing unused channels from neighbor cells.

In order to balance traffic load or to solve specific congestion situations different strategies can be implemented. The performance of these strategies could be enhanced through the use of location information.

- Adaptation of resource allocation to the geographic distribution of traffic load, so the cells supporting a higher traffic load are allocated a higher amount of resources. User's position information would provide exact knowledge of the geographical distribution of traffic.
- Reallocation (as far as possible) of terminals near the cell-edge of cells with high traffic load in neighbor cells with higher availability of resources and able to provide similar quality of service. User's position and trajectory information would be helpful in order to identify which users are more suitable to be reallocated and to which cell should be transferred.
- As it is proposed in [Du, 2003], using smart antennas it is possible to dynamically change cell size and shape, reducing the coverage area of cells supporting a high traffic load and expanding the coverage area of neighbor cells, so some users of the congested cell would be transferred to neighbor cells. With this purpose, knowledge of the geographical distribution of traffic is necessary.

Furthermore, positioning information is not only useful for load balancing, but it can also be used for prediction of future traffic load on each cell. Knowledge of user's position and trajectory allows predicting not only incoming handover calls, but also outgoing handovers and the time that the calls will stay in the cell (dwell time). This way, and together with other statistical parameters related to new calls generation and call duration, it is possible to estimate the traffic load that a cell is going to support in a certain time interval and to detect future congestion situations, taking appropriate actions in advance (e.g. adaptation of resource allocation to cells, reallocation of cell-edge terminals, blocking admission of new calls…) in order to prevent congestion to occur.

7.3.2.4 Resource allocation and interference coordination in OFDMA networks

Orthogonal Frequency-Division Multiple Access (OFDMA) is a multiple access scheme based on OFDM digital modulation where subsets of carriers are allocated to the different individual users. OFDMA is used in mobile broadband cellular systems such as Mobile

WiMAX (IEEE 802.16e), and 3GPP LTE. In order to reach a spectral efficiency similar to WCDMA, frequency reuse factor should approximate to 1. Nevertheless, due to the reuse factor of 1, inter-cell interference (ICI) or inter-sector interference is a significant problem and its effect must be minimized, especially on the users at the cell border.

Users on the cell or sector border receive a high interference level in the same frequency band/channel from neighbor cells. Consequently, if no interference management mechanism is applied, the system will operate with low signal to interference plus noise ratio (SINR), and the performance experienced by users at the cell border will be significantly degraded. The higher the interference is, the higher the redundancy and the number of retransmissions needed to keep the QoS are, and consequently the throughput or effective data rate will be reduced. Obviously, this is not desirable in a real system, and therefore interference control techniques must be developed in order to reduce the ICI level.

Interference management mechanisms can be grouped into three main categories:

- Interference averaging or randomization schemes try to statistically average the interference so that the interference level remains as constant as possible, both in frequency domain and in time domain. This way, the concentration of interference on specific users or time intervals, which would cause important degradation on those users, is avoided. With this purpose, interleaving, scrambling, sub-channel permutation and frequency hopping techniques are used.
- Interference cancellation schemes try to eliminate or reduce the interference (at least the most significant component). An example of interference cancellation schemes is interference suppression through the use of multiple antennas and MIMO techniques.
- Interference coordination schemes are based in the implementation of restrictions in the resource allocation (power, frequency or temporal resources) both on the uplink (UL) and downlink (DL) in a coordinated way throughout the network, so the interference experienced by the users is reduced, and consequently the SINR experienced by the users, and specially by the cell-border users, increases.

Within this category, bandwidth partition and fractional reuse strategies can be considered. The bandwidth partitions established by these coordination schemes determine the limits within the scheduling strategies allocate the resources among the different users. In Fractional Frequency Reuse (FFR) schemes, the total bandwidth is divided into two sub-bands, one part allocated to the users within the inner area of the cell, and the other allocated to the outer users. The transmission power in the outer sub-band is higher than the power of the inner sub-band in order to reach the users in the cell-edge. If neighbor cells use different

sub-bands in their outer area, the interference in the outer area is reduced. Different frequency coordination proposals are considered [Xiang, 2007]:

- Hard fractional reuse (Figure 7.6) proposes the partition of the spectrum in 4 orthogonal bands. The first band is composed of the resources that can be allocated to the inner users and is common for all the cells, and the other three bands are allocated to the outer users in such a way that the same band is not used in adjacent cells [Lei, 2007].
- In soft fractional reuse (Figure 7.7), users in the outer area can only be allocated resources in the sub-band allocated to that area, whereas users in the inner area can be allocated any resource but with a maximum power level lower than that considered for the cell-edge users, as it is considered that the interference caused in other cells is attenuated. This scheme reduces the blocking probability associated to the static resource reservation for the cell-edge users [Liu, 2007b].

As it can be inferred from the previous description, users within a cell can be divided into two groups: inner users, which are likely to experience better conditions as they are closer to the base station (BS), and cell-edge users, which are more distant to the BS. In the downlink, users are considered outer or cell-edge according to channel conditions and not to geographic position, as it is possible that a user close to the BS has a bad channel condition due to possible fading, whereas an outer user has better channel conditions. Nevertheless, positioning information can be useful in order to know the relative distance from the user to the different base stations or, which is equivalent, the average path loss to the base station (which would provide diversity to the own average channel estimation), the average interference level estimation from the neighbor base stations or the dynamic level of the scenario (mobility of the users within the cell coverage area).

On the other hand, in the uplink the effect on the adjacent cells depends on the channel conditions between the user and the neighbor base stations, which vary depending on the user's position within the cell. The users are grouped according to the estimated interference level that they may cause in neighbor cells, or according to the power level they need to transmit. Outer users are the ones that need a higher transmission power in order to achieve the required SINR and also the ones closer to the neighbor base stations and consequently causing higher interference level on neighbor cells. In this case, the use of location information is much more relevant as a complement to the monitoring of the channel conditions and the interference level for classifying users depending on the potential effect their transmissions have on the adjacent cells.

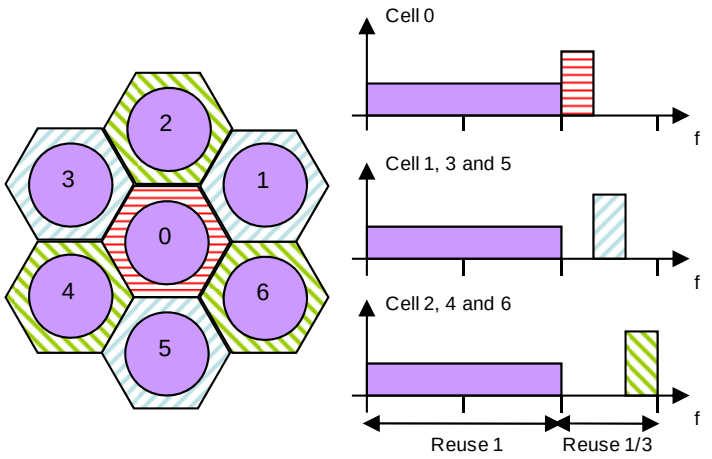

Figure 7.6. Hard fractional reuse

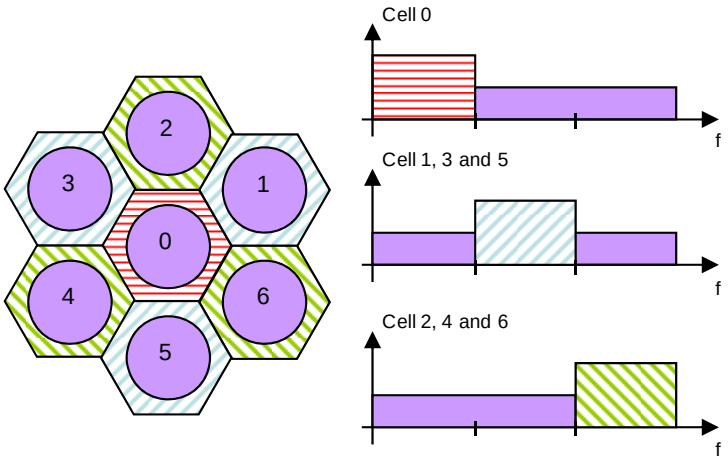

Figure 7.7. Soft fractional reuse

It should be noted that the application of any coordination method reduces the freedom of the scheduling, which may lead to a reduction of global throughput as the allocation of resources to users in some partitions may be blocked. Consequently, it is important to dynamically adjust the size of the sub-bands of each partition depending on the interference caused in other cells and also on the traffic load distribution within the cell [Nortel, 2006]. In this context, positioning information (as an addition to the channel and interference estimation) allows not only knowing the specific distribution of the users within the cell, but also the level and pattern of variability of that distribution (as a function of the speed and mobility pattern of the users), and consequently a better adjustment of the update interval is possible, as well as the own partition dimensioning.

When a reuse of 1 scheme at sector level is assumed, the inter-sector interference is high in the edge between sectors, and therefore reuse areas should be defined in order to reduce the interference, with a similar approach to the one described to avoid the inter-cell interference (Figure 7.8) [Alcatel, 2006]. Users can be classified into interfered users, which receive high interference level from an adjacent sector, and secure users, which are not affected by interference from adjacent sectors, so the orthogonal resources can be used for transmissions to the interfered users. This approach implies that every user must send differentiated information concerning the interference level experienced from each one of the adjacent sectors, both within the same cell and within adjacent cells, resulting in an increase of the signaling overhead.

In this case, the use of positioning information is especially relevant as channel quality is not a valid indicator of whether the user in the edge between two sectors or not. This information can be applied both for dimensioning the size of the resource partitions on the sector-edges and for the scheduling of transmission to each user, the later as a complement to the channel conditions monitoring. As low and high interference geographical regions are defined, user terminals only need to update their position in the BS when they enter or leave these regions, thus reducing signaling overhead.

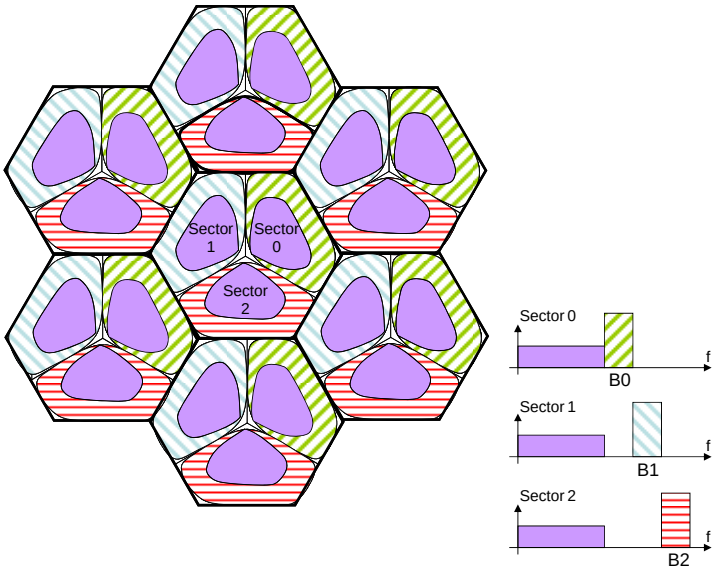

Figure 7.8. Reuse of 1 at sector level

7.3.2.5 Predictive Resource Reservation

The objective of resource reservation for mobility management is to guarantee the quality of service of calls in progress when a handover takes place, minimizing the handover

dropping probability and at the same time optimizing resource availability, avoiding as far as possible the disconnection of existing calls and the blocking of new calls in the target cell.

Several schemes have been proposed to prioritize handover calls in cellular systems. Handover prioritization schemes can be classified into two main strategies: static resource reservation strategies and dynamic resource reservation strategies. Static resource reservation strategies, such as the Guarded Channel (GC) scheme, reduce the handover dropping probability through the reservation of a fixed set of resources for handover calls in each cell, so new calls will be blocked if available resources are less or equal to the reserved resources, while handover calls will be accepted provided that there are available resources. On the other hand, in dynamic resource reservation strategies the amount of reserved resources is dynamically adapted to traffic load in the adjacent cells. Furthermore, both strategies can be combined in hybrid schemes. Given that the behavior of the different mobile users in terms of mobility may vary and that in general traffic distribution is not uniform in space and time, static resource reservation schemes are not very efficient.

Dynamic resource reservation strategies can be further classified into non-shared reservation schemes and shared reservation schemes. In non-shared reservation schemes, each reserved channel can be exclusively used by the user that made the corresponding reservation, while in the shared reservation schemes reserved channels constitute a reservation pool and can be allocated to any user requesting a handover, regardless of whether the user made a successful reservation or not.

The Shadow Cluster technique introduced the estimation of future need of resources and dynamic reservation aiming to limit handover dropping probability due to handover. This scheme is based in the analysis of the potential influence of a mobile station, characterized by the set of cells (cluster) the MS is expected to visit during the lifetime of the MS's connection, based on previous knowledge of the mobility pattern of the active MS. The main drawback of this scheme is that resources are reserved on each one of the cells in the cluster, which is often quite excessive and inefficient compared to other techniques, although it is effective in small cellular architectures.

More advanced solutions use the aggregate history of mobility observed at the cell level to predict (probabilistically) the direction of the MS and the time of the expected handoff. One problem with all history-based schemes is the overhead to develop, store and update traffic histories for the different cells. These histories can never be fully reliable as they continually go through short-term changes (e.g., diversion of traffic due to accidents), medium-term changes (e.g., traffic re-routing during road constructions and repair) and long-term changes (e.g., after opening a new shopping centre).

Aiming to solve these problems, Predictive Channel Reservation (PCR) based schemes use real-time position measurements to predict the future path of an MS and consequently make the necessary resource reservations [Chiu, 2000]. A first approach for position estimation is based on the measurement of received signal strength and the application of probabilistic propagation models to estimate the distance to different base stations. Received signal strength measurements suffer from different errors and biases (e.g. multipath, fading...) and, on the other hand, probabilistic propagation models also have a certain level of inaccuracy. Therefore, the efficient implementation of PCR schemes requires the accurate estimation of the MS's position. With this purpose, each MS periodically measures its position using GPS or any other technology, and reports it to the BS that uses the position information to make extrapolation for the projected future path of the mobile. Based on the projected path, the next cell that the mobile is heading to is determined. When the MS is within a certain distance from the next cell (threshold distance), the current BS sends a reservation request to the new BS in order to pre-allocate a channel for the expected handoff event. Shared (reservation pooling) and non-shared schemes can be considered. In case of no resources are available for the reservation, reservation requests can be either ignored or queued up until resources become available.

The value of threshold distance (TD) needs to be carefully selected as small values of TD may cause undesirable delay in the submission of reservations and large values of TD may cause frequent false reservations. However, TD does not take into account each individual MS's mobility behavior separately. This is not optimum, as the time for which a channel is reserved for a MS moving with low speed will be too long, and thus the overall channel utilization will deteriorate. On the other hand, a MS moving with high speed will make the reservation just before moving into the cell, and can eventually be dropped if there are not available resources. Consequently, the use of a threshold time is preferred over of a threshold distance [Xu, 2002]. In that case, the time within which the MS will reach the target is predicted according to the position, orientation and speed of the MS.

On the other hand, aggregate PCR schemes aim to estimate the global amount of resources to be reserved in each cell instead of per-user reservation, thus avoiding the consequent signaling overhead [Lu, 2006]. Moreover, the amount of resources reserved for each cell is dynamically adapted. The total amount of resources to be reserved in each cell is calculated as the sum of the resources required by each MS that is going to be transferred to that cell within the threshold time. In order to avoid the loss of efficiency associated with the mobile terminals that change their trajectory or calls that end before they arrive at the new cell, the amount of resources reserved is only a fraction of the actual resource requirement. Different factors have been proposed, such as the estimated time for handover, handover

probability, mobility ratio, dropping probability, etc. Furthermore, resources may not only be reserved in the predicted target cell, but also in other potential target cells (sub-target cells). Efficiency can be further improved using both incoming and outgoing handover prediction [Soh, 2004].

Finally, positioning information can be combined with topological information (e.g. roads, etc.) for more accurate path prediction [Soh, 2004]. Statistical data such as the transition probabilities in road junctions, time taken to transit each road segment, possible handovers along each segment and their probability, time in a road segment before handover, handover points, etc. can also be used for a more efficient implementation of PCR strategies.

Chapter 8

Conclusions

8.1 Conclusions

Due to its high bandwidth, Ultra-Wideband radio technology presents special characteristics that enable a variety of specific applications. On the one hand, taking advance of the high bandwidth, Very High Data Rate applications (up to 1 Gb/s) may be developed for wireless short-range data transmission. On the other hand, pulse-based modulations can be used in Low Data Rate solutions providing low complexity, low power consumption and, due to the short duration of the pulses, a very high resolution in Time of Arrival estimation and consequently distance estimation (in the order of a few centimeters) for Location and Tracking applications in indoor environments.

One of the key features of UWB is that it allows spectrum reutilization, as the transmission power is distributed over the wide frequency band, causing little interference on existing narrowband systems. Thus, UWB can operate as an unlicensed service sharing the spectrum with other licensed services. However, in order to guarantee that the existing and future licensed services are not disturbed by the presence of UWB, several coexistence studies were carried out in the framework of the regulatory process. These studies resulted in the definition of very strict spectral masks that limit the emitted power spectral density of UWB systems on different frequency bands. Mitigation techniques were also developed in order to increase the protection over the rest of radio technologies. Although these limits assure peaceful coexistence, they also limit the scope of UWB to indoor environments and its range to a few meters.

In order to extend the scope of UWB applications, the interoperation of UWB with WAN access technologies, such as UMTS or LTE, arises as a promising solution. Nevertheless, the integration of UWB and other radio technology in a single device entails that the distance between both radios may be reduced to a few centimeters. In these conditions coexistence issues becomes critical, as even in the case that both radio

technologies operate in different frequency bands, out-of-band emissions could cause degradation. In this thesis an interoperability platform between UWB and UMTS/HSPA has been proposed, and it has been shown that no degradation occurs even if the antennas are at a distance of 3 centimeters. The advantage of interoperability platforms is that cooperation between the different radio interfaces is possible. This way, mitigation techniques based on the cooperation of both radio interfaces have been proposed in order to guarantee harmless coexistence, applying protection mechanisms if any degradation is detected.

Focusing on Location and Tracking applications, UWB provides very high resolution in Time of Arrival and distance estimation. Distance estimation is usually a trade-off between accuracy and complexity, with very simple Energy Detection receivers providing coarse estimation in contrast to correlation-based receivers providing higher precision but requiring higher sampling rate and complexity. On the output of the receiver, TOA estimation algorithms are applied to estimate the first path of the signal. While robust TOA estimation algorithms are able to deal with noise and multipath effect, they are not able to cope with non-line-of-sight conditions, as the first path will be missing and the estimated distance will correspond to a secondary path.

On the other hand, there is a wide variety of location and tracking algorithms to obtain the position of a target node based on the estimated distance to some reference nodes, with different levels of accuracy, complexity and required knowledge of the process statistics. Geometric algorithms, such as trilateration, are simple and provide a closed-form solution, but their accuracy cannot be improved using a higher amount of measurements, so they only provide good results for very accurate estimations. Optimization-based methods are based on the minimization of a certain cost function. The squared error of the estimated distances and the distances provided by the computed position can be minimized using non-linear least squares minimization methods, which provide good results without any additional knowledge. On the other hand maximum-likelihood estimators minimize the probability of the measured distances according to the computed position, which requires the knowledge of the statistical model of the measurements. Within maximum likelihood estimators, Bayesian techniques, such as Kalman and particle filters, infer the position from past and previous measurements, and the knowledge of the target's motion model is also required. Their accuracy is highly dependent on the knowledge of the models, and for instance a Kalman filter with a simple Gaussian error model shows a bad performance, whereas a particle filter with a 3-component error model optimized through simulations shows the best performance. Nevertheless, an accurate model characterization would require a costly prior calibration of the scenario, so non-parametric methods such as least squares optimization are more suitable.

However, non-line-of-sight biased measurements are still a major challenge for any location and tracking algorithm. Different enhancements to the basic algorithms have been proposed in order to mitigate the effect of NLOS measurements, including measurement weighting, distance contraction and NLOS identification based on different signal parameters. In this thesis, the use of geographic information to develop enhanced location and tracking algorithms has been proposed. Geographic Information Systems are becoming increasingly extended and are generally combined with Location and Tracking systems for visualization purposes. Focusing on indoor environments, a wall plan is likely to be available, and areas of interest where the user is likely located may be defined. This information can be integrated in the models of parametric algorithms in order to enhance their performance. Non-parametric algorithms can also be enhanced taking advance of the wall plan to identify and consequently mitigate NLOS measurements.

One of the main limitations of existing commercial UWB location systems is that UWB is only used for location purposes, while communication between the different elements is generally wired. The use of UWB for simultaneous location and communication, for instance in the framework of the IEEE 802.15.4a standard, is a key aspect to reduce the cost and complexity of UWB location systems and increase their flexibility. Furthermore, this would allow the reutilization of an existing Wireless Sensor Network (e.g. fire detection sensors, temperature sensors, etc.) to provide location and tracking. In this context, accuracy is not the only requirement of the location systems, but also the amount of resources needed, as they impact both on the capacity of the location system and on the available data rate for data transmission. This way, implementation issues such as the functional architecture, the acquisition and distribution of the location information or the number of measurements used to compute the position have been analyzed in this thesis. Specifically, the architecture centralized in the mobile nodes is the optimal in terms of resources and, in case of architectures centralized in the network, the aggregation of all the measurements in a single packet is advisable in order to reduce the need of resources.

On the other hand, the implications of a real system, specifically an 802.15.4a-based MAC layer, have been also considered. In particular, the latency associated to the position update process due to the acquisition and distribution of the distances has a negative effect on the positioning accuracy. In order avoid this degradation, acquisition and distribution procedures should be designed in order to be carried out within a single MAC superframe. Also the limited availability of resources of 802.15.4 Low Rate networks, specifically the number of slots allocated for ranging and data transmission on each superframe, entails a limitation of the number of targets that can be tracked simultaneously (between 5 and 10 targets per picocell). If higher capacity is required, a system design specifically optimized for

location purposes would be preferred over an 802.15.4-based design, which is aimed to low-rate self-configuring wireless sensor networks.

Besides the straight application of UWB location and tracking systems in the industrial, medical or home automation sectors, the integration of UWB with cellular radio access technologies such as UMTS, LTE or WiMAX would leverage location to enable a wide range of services and applications. In fact, Location Based Services are becoming increasingly popular and are foreseen as one of the killer applications of mobile Internet. With GPS widely extended but unable to operate indoors and cellular networks providing coarse location information, UWB could extend the scope of Location Based Services to indoor scenarios such as shopping centers, business districts, congress and exhibition centers, airports, etc. Furthermore, with the increasing demand of capacity due to the growing popularity of mobile Internet, location-awareness could be also used by the operators to support the resource management of their networks. In fact, the design of efficient radio resource management strategies enhanced through the use of location-awareness is a topic of interest nowadays.

However, the commercial success of UWB depends of many factors other than the benefits of the technology. While the WiMedia MB-OFDM standard for Very High Data Rate applications has been selected by the USB Implementers Forum as the basis of Wireless USB and some other products for high definition video transmission are already available, the present and future of Impulse Radio UWB is unclear. The potential market of currently available location and tracking systems is very limited due to their high complexity and price. Wireless Sensor Network (WSN) applications have a greater potential market, although first chips have just appeared and no final products are available, while ZigBee is positioning itself as the dominant technology in this area. As these applications do not have high capacity requirements, low cost and power consumption will probably be the key requirements, and cost not only depends on complexity but also on the penetration of the technology and the amount of devices manufactured. But the market of WSN is not mature yet and for instance home automation, which was considered a very promising industry a few years ago, is not fulfilling the expectations and shows a very limited level of penetration.

8.2 Future Work

As it has been shown in Chapter 3, many of the topics addressed in this thesis have been widely studied in the last few years. On the other hand, the application of location-awareness in resource management is a relatively new topic with increasing interest, as the growing

capacity demand in cellular access networks requires more efficient resource management strategies. In this thesis, we have identified some potential applications of location awareness for radio resource management. However, in mobile and indoor environments, link quality is mainly determined by channel conditions rather than location, and strategies based only on location are not expected to provide improved performance. For example, a far BS with direct line-of-sight may provide a better link quality than a close BS in non-line-of-sight conditions. The effective application of location-awareness requires that the location information is combined with power or link quality information in order to improve the performance, reduce the complexity or reduce the power consumption. Consequently, research will focus on the design of novel algorithms combining both location and power/quality information. For instance, location information can be used in combination with a coverage map representing the expected received signal from the different BSs.

Concerning coexistence issues, UWB is expected to play a key role in Cognitive Radio, which is a research area of special interest nowadays. Due to its high bandwidth, the different frequency bands and power levels allowed by the regulatory bodies in different countries, and the requirement of not disturbing the operation of licensed services, flexible UWB systems should sense the spectrum in order to detect potential victim services and should adapt their emission mask in order to maximize the performance while being compliant with the specific regulation and not interfering with any operating system.

Finally, the current trend in location and tracking is to integrate the information available from different sources, such as satellite systems (GPS, Galileo), radio networks (UMTS, LTE, WLAN, WPAN...), inertial and motion sensors (speedometers, accelerometers, gyroscopes), and geographic information (maps, floor plans), which is known as data fusion. Data fusion provides higher accuracy and reliability, as potential erroneous measurements from one source can be mitigated with the information from the other sources. For example, car navigation systems combine GPS positioning with inertial sensors in order to keep tracking the car when GPS signal is unavailable (a tunnel, a narrow street...) and with geographic information in order to fit the estimated position into the road map. Focusing on UWB indoor location and tracking systems, the combination with both inertial sensors and geographic information would be very interesting, as it would allow correcting the high biases introduced on NLOS measurements and reducing the amount of UWB reference nodes required, which is an important limitation of UWB due to its short range.

8.3 Publications

The work carried out within this thesis has been presented in different international congresses and published in different scientific journals, which are collected here.

Scientific Journals:

- A. Hernández, R. Badorrey, J. Chóliz, I. Alastruey, A. Valdovinos, "Indoor wireless location with IR UWB systems. A performance evaluation of joint receiver structures and TOA based mechanism", *IEEE Transactions on Consumer Electronics* Vol.54, No.2, pp. 381-389, May 2008.
- J. Chóliz, A. Hernández, I. Alastruey, A. Valdovinos, "Coexistence and Interworking between UMTS and UWB. A Performance Evaluation of a UMTS/UWB Interoperability Platform", *Springer Telecommunications Systems Journal*. In press, published online June 2010.

International congresses:

- J. Hernández Pablo, J. Chóliz Muniesa, I. Alastruey Benedé, M. Gimeno Martín, B. Molinete Cuezva, R. Giuliano, "End-to-End Coexistence Tests in an Interworking UWB-UMTS Platform", *16th IST Mobile and Wireless Communications Summit*, Budapest (Hungary), July 2007.
- R. Badorrey, A. Hernández, J. Chóliz, A. Valdovinos, I. Alastruey, "Evaluation of TOA estimation algorithms in UWB receivers", *14th European Wireless Conference (European Wireless 2008)*, Prague (Czech Republic), June 2008.
- J. Chóliz, I. Alastruey, A. Hernández, A. Sierra, A. Valdovinos, "Study and assessment of cooperative techniques for MB-OFDM UWB", *17th ICT Mobile and Wireless Communications Summit (ICT-MobileSummit 2008)*, Stockholm (Sweden), June 2008.
- A. Sierra, J. Chóliz, I. Bucaille, A. Villanúa, A. Hernández, I. Alastruey, "UWB in Heterogeneous Access Networks", *17th ICT Mobile and Wireless Communications Summit (ICT-MobileSummit 2008)*, Stockholm (Sweden), June 2008.
- J. Chóliz, I. Alastruey, A. Hernández, A. Sierra, A. Valdovinos, "Evaluation of cooperative techniques in an interworking UWB-UMTS Platform", *2008 IEEE*

International Conference on Ultra-Wideband (ICUWB 2008), Hannover (Germany), September 2008.

- A. Sierra, J. Chóliz, I. Bucaille, A. Villanúa, A. Hernández, I. Alastruey, "UWB in Heterogeneous Access Networks", *2008 IEEE International Conference on Ultra-Wideband (ICUWB 2008)*, Hannover (Germany), September 2008.

- J. Chóliz, A. Hernández, A. Valdovinos, "Evaluation of architectures and strategies for tracking mobile devices in UWB networks", *6th Workshop on Positioning, Navigation and Communication 2009 (WPNC'09)*, Hannover (Germany), March 2009.

- A. Sierra, J. Chóliz, I. Bucaille, B. Selva, J. Campos, A. Hernández, "UWB in Heterogeneous Access Networks: EUWB proposal for application scenarios", *6th Workshop on Positioning, Navigation and Communication 2009 (WPNC'09)*, Hannover (Germany), March 2009.

- A. Sierra, I. Bucaille, B. Selva, P. Cluzeaud, J. Chóliz, J. Campos, R. Llorente, "Heterogeneous Access Networks: Study and evaluation of coexistence", *18th ICT Mobile and Wireless Communications Summit (ICT-MobileSummit 2009)*, Santander (Spain), June 2009.

- J. Chóliz, A. Hernández, A. Valdovinos, "Architectures for Location Data Acquisition and Distribution in UWB Indoor Tracking Systems", *7th Workshop on Positioning, Navigation and Communication 2010 (WPNC'10)*, Dresden (Germany), March 2010.

- I. Guío, A. Hernández, J. Chóliz, V. Montero, J. Lafuente, A. Valdovinos. "Radio resource management in OFDMA systems for strong frequency reuse in sectorized deployments", *7th International Symposium on Wireless Communication Systems (ISWCS'10)*, York (United Kingdom), September 2010.

- J. Chóliz, A. Hernández, A. Valdovinos, "Strategies for Optimizing Latency and Resource Utilization in Multiple Target UWB-based Tracking", *IEEE Wireless Communications & Networking Conference 2011 (WCNC 2011)*, Cancun (Mexico), March 2011.

- J. Chóliz, A. Hernández, A. Valdovinos, "Evaluation of Algorithms for UWB Indoor Tracking", *8th Workshop on Positioning, Navigation and Communication 2011 (WPNC'11)*, Dresden (Germany), April 2011.

- J. Chóliz, M. Eguizábal, A. Hernández, A. Valdovinos, "Comparison of Algorithms for UWB Indoor Location and Tracking Systems", *IEEE 73rd Vehicular Technology Conference (VTC2011-Spring)*, Budapest (Hungary), May 2011.
- A. Sierra, J. Chóliz, P. Cluzeaud, E. Slusanschi, "UWB Integration into Heterogeneous Access Networks", *20th ICT Future Network and Mobile Summit 2011*, Warsaw (Poland), June 2011.

Conclusiones

Debido a su elevado ancho de banda, la tecnología Ultra-Wideband presenta unas características especiales que posibilitan una variedad de aplicaciones específicas. Por un lado, aprovechando su gran ancho de banda, pueden desarrollarse aplicaciones de muy elevada capacidad de transmisión (hasta 1 Gb/s) para sistemas inalámbricos de transmisión de datos de corto alcance. Por otro lado, pueden utilizarse modulaciones pulsadas en soluciones de baja capacidad de transmisión con baja complejidad, bajo consumo de potencia y, gracias a la corta duración de los pulsos, muy alta resolución en la estimación del tiempo de llegada y en consecuencia de la distancia (del orden de unos pocos centímetros) para aplicaciones de localización y seguimiento en entornos de interiores.

Una de las principales propiedades de UWB es que permite la reutilización del espectro dado que la potencia transmitida se distribuye en una banda frecuencial muy ancha, causando una mínima interferencia en los sistemas existentes de banda estrecha. Así, UWB puede operar sin licencia compartiendo el espectro con otros servicios licenciados. Sin embargo, de cara a garantizar que UWB no perjudica a los servicios licenciados existentes o futuros,, se han llevado a cabo multitud de estudios de coexistencia en el marco del proceso regulatorio. Como resultado de estos estudios, se han definido unas máscaras espectrales muy estrictas que limitan la densidad espectral emitida por los sistemas UWB en diferentes bandas frecuenciales. También se han desarrollado técnicas de mitigación de cara a incrementar la protección sobre el resto de tecnologías radio. Aunque estos límites aseguran la coexistencia libre de interferencias, también limitan el ámbito de UWB a entornos interiores y su alcance a unos pocos metros.

De cara a extender el ámbito de las aplicaciones UWB, la integración de UWB con tecnologías de acceso WAN (Wide Area Networks) como UMTS o LTE surge como una solución prometedora. Sin embargo, la integración de UWB y otra tecnología radio en un mismo dispositivo implica que la distancia entre ellas puede reducirse a unos pocos centímetros. En estas condiciones, la coexistencia se convierte en un aspecto crítico, e incluso en el caso de que ambas tecnologías operen en bandas frecuenciales diferentes las emisiones fuera de banda podrían causar degradación. En esta tesis se ha propuesto una plataforma de interoperabilidad entre UWB y UMTS/HSPA, y se ha mostrado que no existe degradación incluso si las antenas se encuentran a 3 centímetros de distancia. La ventaja de

las plataformas de interoperabilidad es que es posible la cooperación entre los diferentes interfaces radio. Así, se han propuesto técnicas de mitigación basadas en la cooperación entre ambos interfaces de cara a garantizar la coexistencia inocua, aplicando mecanismos de protección en caso de que se detecte alguna degradación.

Centrándonos en las aplicaciones de localización y seguimiento, UWB proporciona una resolución muy elevada en la estimación del tiempo de llegada (TOA) y de la distancia. Por lo general, la estimación de la distancia supone un compromiso entre precisión y complejidad, con los receptores basados en detección de energía de gran simplicidad y menor precisión en contraste con los receptores basados en correlación, que proporcionan una elevada precisión pero conllevan una mayor complejidad y requieren una elevada tasa de muestreo. A la salida del receptor, se aplican algoritmos de estimación del TOA para estimar la primera componente de la señal. Mientras que existen algoritmos de estimación del TOA suficientemente robustos para limitar el efecto del ruido y el efecto multicamino, las estimaciones en condiciones de falta de visión directa (NLOS) presentan un elevado error debido a la ausencia de la primera componente, con lo que la distancia estimada se corresponde a una componente secundaria.

Por otro lado, existen una gran variedad de algoritmos de localización y seguimiento para obtener la posición de un nodo en base a la distancia estimada a varios nodos de referencia con distintos niveles de precisión, complejidad y conocimiento de las estadísticas del proceso. Los algoritmos geométricos, como la trilateración, son simples y proporcionan una solución cerrada, pero su precisión no puede mejorarse utilizando un mayor número de medidas, por lo que únicamente presentan buenas prestaciones para estimaciones de distancias muy precisas. Los métodos basados en optimización se basan en la minimización de una determinada función de coste. El error cuadrático de las distancias estimadas y las distancias de la posición calculada puede minimizarse mediante métodos no lineales de mínimos cuadrados, que proporcionan buenos resultados sin ningún tipo de conocimiento adicional. Por otro lado, los estimadores de máxima verosimilitud minimizan la probabilidad de las distancias estimadas de acuerdo a la posición calculada, lo que requiere el conocimiento del modelo estadístico de las medidas. Dentro de los estimadores de máxima verosimilitud, las técnicas Bayesianas, como el filtro de Kalman o el filtro de partículas, calculan la posición en base a las medidas actuales y pasadas, por lo que también requieren el conocimiento del modelo de movilidad. Su precisión depende en gran medida del conocimiento exacto de los modeles, y por ejemplo el filtro de Kalman con un simple modelo de error de medida Gaussiano presenta malos resultados, mientras que el filtro de partículas con un modelo de error de medida de 3 componentes optimizado mediante simulaciones presenta las mejores prestaciones. Sin embargo, la caracterización precisa del

modelo requeriría una costosa calibración previa del escenario, por lo que los métodos no paramétricos como la optimización por mínimos cuadrados son por lo general más adecuados.

De cualquier manera, las prestaciones de los distintos algoritmos de localización y seguimiento se ven reducidas en caso de medidas en condiciones de falta de visión directa debido a su elevado nivel de error. Diferentes mejoras a los algoritmos básicos se han propuesto con el objeto de mitigar el efecto de las medidas NLOS, incluyendo la ponderación de las medidas, la contracción de distancias y la identificación de medias NLOS en base a diversos parámetros de la señal. En esta tesis se ha propuesto el uso de información geográfica para el desarrollo de algoritmos de localización y seguimiento mejorados. Los sistemas de información geográfica están cada vez más extendidos y por lo general se combinan con sistemas de localización y seguimiento para la visualización de los resultados. En concreto, en el caso de entornos interiores es común disponer de un plano del edificio y por lo general es posible definir una serie de zonas de interés donde localizar al usuario. Esta información puede incorporarse en los modelos de los algoritmos paramétricos de cara a mejorar sus prestaciones. Los algoritmos no paramétricos también pueden mejorarse utilizando el plano para la identificación y consecuente mitigación de las medidas NLOS.

Una de las principales limitaciones de los sistemas de localización UWB comerciales existentes en la actualidad es que utilizan UWB únicamente para la localización, mientras que la comunicación entre los distintos elementos del sistema es por lo general cableada. El uso de UWB para proporcionar localización y comunicación de manera simultánea, por ejemplo en el marco del estándar IEEE 802.15.4a, es un aspecto clave de cara a reducir el coste y la complejidad de los sistemas de localización UWB e incrementar su flexibilidad. Además, esto permitiría la reutilización de una red inalámbrica de sensores existente (p.ej. sensores de detección de incendios, de temperatura, etc.) para proporcionar localización y seguimiento. En este contexto, la precisión no es el único requisito de los sistemas de localización, sino también la cantidad de recursos utilizados, ya que ello impacta tanto en la capacidad del sistema de localización como en la tasa disponible para la transmisión de datos. Por ello, en esta tesis se han analizado aspectos relativos a la implementación real tales como la arquitectura funcional, la adquisición y distribución de la información de localización. En particular, la arquitectura centralizada en los nodos móviles es la óptima en términos de uso de recursos, mientras que en el caso de arquitecturas centradas en la red la agregación de todas las medidas en un único paquete es recomendable de cara a reducir el uso de recursos.

Por otro lado, también se han tenido en cuenta las implicaciones de un sistema real, en particular de una capa MAC basada en 802.15.4a. La latencia asociada al proceso de

actualización de posición, en concreto a la adquisición y distribución de las distancias, tiene un efecto negativo en la precisión de la localización. De cara a evitar esta degradación, los procedimientos de adquisición y distribución deben diseñarse de forma que puedan completarse en una única supertrama MAC. También la limitada disponibilidad de recursos, y en particular el número de slots dedicados a ranging y a transmisión de datos en cada supertrama, conlleva una limitación del número de nodos a localizar que pueden seguirse de manera simultánea (entre 5 y 10 nodos a localizar por picocelda). En caso de que se necesitara una mayor capacidad de seguimiento, sería preferible un diseño del sistema específicamente optimizado para localización en lugar de un sistema basado en 802.15.4, cuyo objetivo son las redes inalámbricas de sensores autoconfigurables y de baja capacidad de transmisión.

Además de la aplicación directa de los sistemas de localización y seguimiento UWB en los sectores industrial, médico o domótico, la integración de UWB con tecnologías de acceso celular como UMTS, LTE o WiMAX permitiría utilizar la localización en un amplio rango de aplicaciones y servicios. De hecho, la popularidad de los servicios basados en localización está en aumento y se considera una de las aplicaciones de Internet móvil con mayor potencial. Con el sistema GPS ampliamente extendido pero limitado en entornos interiores y las redes celulares proporcionando localización con una precisión limitada, UWB permitiría extender el ámbito de los servicios basados en localización en escenarios de interiores tales como centros comerciales, distritos de negocios, centros de congresos y exhibiciones, aeropuertos, etc. Además, con la creciente demanda de capacidad debido a la popularización del acceso móvil a Internet, la información de localización podría ser utilizada también por los operadores en la gestión de recursos de sus redes. De hecho, el diseño de estrategias eficientes de gestión de recursos radio mejoradas mediante el uso de la información de localización es un tema de interés hoy en día.

De cualquier manera, el éxito comercial de la tecnología Ultra-Wideband depende de muchos más factores además de las prestaciones de la tecnología. Mientras que el estándar de WiMedia basado en MB-OFDM para aplicaciones de alta capacidad de transmisión ha sido seleccionado por el USB Implementers Forum como base de Wireless USB y algunos otros productos para la transmisión de video en alta definición ya están disponibles comercialmente, el futuro de los sistemas UWB basados en modulaciones pulsadas no está claro. El mercado potencial de los sistemas de localización y seguimiento disponibles actualmente es muy limitado a causa de su elevado precio y complejidad. Por otro lado, las aplicaciones de redes de sensores inalámbricos tienen un mayor mercado potencial, aunque los primeros chips acaban de aparecer y no hay productos finales disponibles comercialmente, mientras que ZigBee se está posicionando como la tecnología dominante en

esta área. Dado que estas aplicaciones no requieren una alta capacidad de transmisión, el bajo coste y consumo energético serán probablemente los requisitos clave, pero el coste no depende únicamente de la complejidad, sino también del nivel de penetración de la tecnología y de la cantidad de dispositivos fabricados. Sin embargo, el mercado de las redes inalámbricas de sensores todavía es incipiente y por ejemplo la domótica, que hace unos años era considerada una industria muy prometedora, presenta todavía unos niveles de penetración muy reducidos.

Annex I. Location and Tracking Algorithms

I.1 Trilateration.

Spherical trilateration is a geometric method to determine the position of a target node from a set of range measurements. A range measurement (obtained from a TOA or an RSS measurement) determines a line of position for the target's location as a sphere around the reference node. Then, the intersection of three spheres, obtained from three TOA or RSS measurements, can be used to solve for the position of the target.

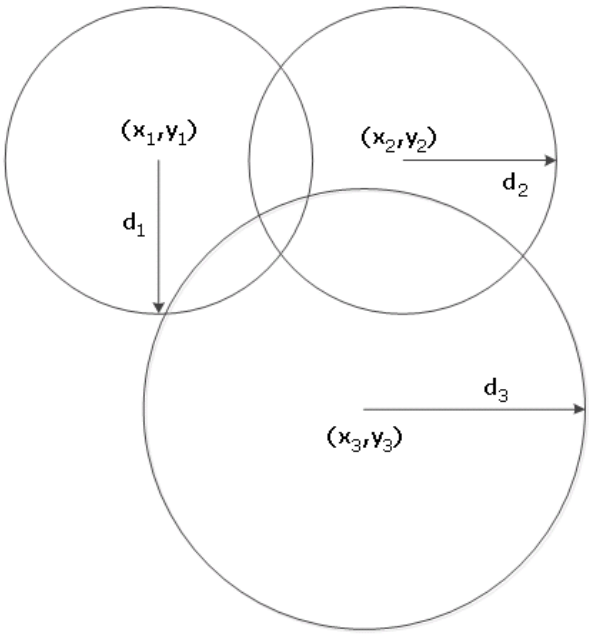

Figure I.1. Example of trilateration

Let d_1, d_2 and d_3 represent the range measurements obtained from three TOA or RSS measurements. Then, the following three equations must be solved jointly in order to estimate the position of the target via trilateration:

$$d_i = \sqrt{(x_i - x)^2 + (y_i - y)^2} \quad , i=1, 2, 3 \tag{I.1}$$

where (x_i, y_i) is the known position of the i-th reference node, and (x, y) is the position of the target node. The position (x, y) can be solved from (3.1) as

$$x = \frac{(y_2 - y_1)\gamma_1 + (y_2 - y_3)\gamma_2}{2\left[(x_2 - x_3)(y_2 - y_1) + (x_1 - x_2)(y_2 - y_3)\right]} \tag{I.2}$$

$$y = \frac{(x_2 - x_1)\gamma_1 + (x_2 - x_3)\gamma_2}{2\left[(x_2 - x_1)(y_2 - y_3) + (x_2 - x_3)(y_1 - y_2)\right]} \tag{I.3}$$

where

$$\gamma_1 = x_2^2 - x_3^2 + y_2^2 - y_3^2 + d_3^2 - d_2^2 \tag{I.4}$$

$$\gamma_2 = x_1^2 - x_2^2 + y_1^2 - y_2^2 + d_2^2 - d_1^2 \tag{I.5}$$

In order to determine the relative position of a target in a bi-dimensional plane, three measurements are required. If less than three measurements are available, there are multiple solutions and the position cannot be computed univocally. On the other hand, if more than three measurements are available, there may be no valid solution. In that case, the three measurements providing the shortest estimated distance are selected to compute the position.

I.2 Multidimensional Scaling

Multidimensional scaling (MDS) is a multivariate data analysis technique used to map "proximities" into a low-dimensional space. These "proximities" can be either dissimilarities (distance-like quantities) or similarities (inversely related to distances). Given n points and the corresponding dissimilarities δ_{ij}, MDS finds a set of points in a space such that the difference between δ_{ij} and the relative distances between the points d_{ij} is minimum and a one-to-one mapping between the original configuration and the reconstructed one exists. Then it is possible to map back the solution to the absolute reference system used by Procrustes transformation.

The objective is to find the matrix $\mathbf{X}$ of dimensions [n x η] containing the coordinates of n objects in a η-dimensional space. Defining $\mathbf{x}_i$ (i = 1,...,n) as the vectors containing the coordinates for the n points in a η dimensional space, then the dissimilarities are expressed by $d_{ij}^2 = (\mathbf{x}_i\text{-}\mathbf{x}_j)(\mathbf{x}_i\text{-}\mathbf{x}_j)^T$. Therefore the inner product between two objects $\mathbf{x}_i$, $\mathbf{x}_j$, belonging to

the original configuration of points can be written as $\mathbf{[B]}_{i,j} = b_{i,j} = \mathbf{x}_i \cdot \mathbf{x}_j^T$. Defining $\{\delta_{i,j}\}$ as the set of all inter-distances, then for the Classical scaling $\{\delta_{i,j}\}=\{d_{i,j}\}$ holds.

The Classical scaling solution, once that the set of all inter-distances $\{\delta_{i,j}\}$ is provided, constructs **B** before, and then recovers the unknown objects coordinates as the least square solution on the inner product matrix **B**. To overcome the indeterminacy of the solution due to translation, the centroid of the configuration is placed at the origin ($\Sigma_i \mathbf{x}_i = \mathbf{0}$, $i = 1,...,n$).

The Euclidean Distance Matrix (EDM) $\mathbf{D}_{[n\times n]}$ is defined as the matrix containing the set of Euclidean distances between the points $\{\delta_{i,j}\}$, $[\mathbf{D}]_{ij}=\delta_{ij}$. Then $\mathbf{B} = \mathbf{X}\cdot\mathbf{X}^T$ can be written using the objects inter-distances as

$$\mathbf{B} = -\frac{1}{2}\mathbf{J}\cdot\mathbf{D}^2\cdot\mathbf{J} \tag{I.6}$$

with $\mathbf{D}^2$ as the matrix of the squared distances, the "centering matrix" **J** defined as $\mathbf{J} = \mathbf{I} - n^{-1}\mathbf{e}\cdot\mathbf{e}^T$, **e** as the $[n\times 1]$ unitary vector, and $\mathbf{I}_{[n\times n]}$ the identity matrix. It should be noticed that **J** defines a linear transformation and it is characterized by the orthogonal property $\mathbf{J}\cdot\mathbf{J}^T = \mathbf{I}$. Now, since **B** is a symmetric, positive semi-definite matrix of rank(**B**) = η , its eigen-decomposition is expressed by:

$$\mathbf{B} = \mathbf{V}\cdot\mathbf{L}\cdot\mathbf{V}^T \tag{I.7}$$

with **V** and **L** as the eigenvectors and the diagonal-eigenvalue matrix of **B**. Indeed, due to rank(**B**) = rank($\mathbf{X}\cdot\mathbf{X}^T$) = rank(**X**) = η , and assuming both eigenvectors and eigenvalues ordered in descending order, **B** can be rewritten as

$$\mathbf{B} = \mathbf{V}_\eta\cdot\mathbf{L}_\eta\cdot\mathbf{V}_\eta^T \tag{I.8}$$

with $\mathbf{L}_\eta$ = diag ($l_1,...,l_\eta$) and $\mathbf{V}_\eta$ ($[n\times\eta]$) containing the first η eigenvalues and eigenvectors respectively. Therefore, it follows that **X**, which includes the recovered coordinates for the *n* objects, is given by

$$\mathbf{X} = \mathbf{V}_\eta\cdot\mathbf{L}_\eta^T \tag{I.9}$$

X corresponds to the original configuration up to rigid transformations (translation, rotation and reflections) on the axes. If the coordinates $\mathbf{X}_A$ of $\eta + 1$ reference points, or more, are known, then it is possible to map back the solution to the absolute reference system used by Procrustes transformation. Procrustes transformation is a linear geometric transformation involving translation, orthogonal rotation and scaling.

I.3 SMACOF

Classical scaling is based on the assumption that the dissimilarities are precisely Euclidean distances without any additional transformation. Nevertheless, in typical wireless network localization problems, ranging information is often imperfect and incomplete. Consequently, the result obtained using MDS must be optimized. Specifically, the objective is to optimize the coordinate matrix **X** resulting from MDS in a way that the set of Euclidean distances derived from **X** is as similar as possible to the set of measured distances, $d_{ij}(\mathbf{X})\approx\delta_{ij}$, where:

$$d_{ij}(\mathbf{X}) = \sqrt{\sum_{s=1}^{\eta}(x_{is} - x_{js})^2} \tag{I.10}$$

where s=1,…, η are the dimensions of the space.

Metric Least Squares MDS solves the aforementioned problem by minimizing an objective function (stress function). An example of stress function, corresponding to the least squares on the distance is

$$\sigma(\mathbf{X}) = \sum_{i=1}^{n}\sum_{j=1}^{n} w_{i,j}(\delta_{i,j} - d_{i,j}(\mathbf{X}))^2 \tag{I.11}$$

where $w_{i,j}$ are the weights of the estimated distances between the nodes i and j. Without loss of generality, it is assumed that

$$\sum_{i=1}^{n}\sum_{j=1}^{n} w_{ij}\delta_{ij}^2 = 1 \tag{I.12}$$

Nevertheless, such a stress function is proven to be non-convex in the **X** variable; therefore, either a global optimization technique or a reliable starting point is required to avoid local minima. In order to solve this problem, a majorization technique known as SMACOF (Scaling by MAjorizing a COmplicated Function) is proposed to minimize the stress function. The principle of majorization is to construct a surrogate function which majorizes a particular objective function. SMACOF consists of an iterative procedure that attempts to find the minimum of a non-convex function by tracking the global minimum of the so-called majored convex function successively constructed from the original objective and basis on the previous solution.

In order to minimize the stress function, it is derived and equaled to zero. Then, the coordinate matrix **X** that minimizes the stress function is obtained as:

$$\mathbf{X} = \mathbf{V}^{\dagger}\mathbf{B}(\mathbf{Y})\mathbf{Y} \tag{I.13}$$

where **Y** is the previous coordinate matrix, $\mathbf{V}^{\dagger}$ is the Moore-Penrose pseudo-inverse and the elements of $\mathbf{B}(\mathbf{Y})$ are given by

$$b_{ij} = \begin{cases} -w_{ij}\delta_{ij}d_{ij}^{-1}(Y) & i \neq j \text{ and } d_{ij}(\mathbf{Y}) \neq 0 \\ 0 & i \neq j \text{ and } d_{ij}(\mathbf{Y}) = 0 \\ -\sum_{k \neq i} b_{ik} & i = j \end{cases} \tag{I.14}$$

In the initial step t=0, $\mathbf{Y}=\mathbf{X}^{(0)}$, where $\mathbf{X}^{(0)}$ is the initial solution obtained from MDS. On each iteration, $\mathbf{Y}^{(t)}=\mathbf{X}^{(t-1)}$ and $\mathbf{X}^{(t)}$ is computed. Then $\sigma(\mathbf{X}^{(t)})$ is computed and iteration finishes when the stop condition $\sigma(\mathbf{X}^{(t)})-\sigma(\mathbf{X}^{(t-1)})<\varepsilon$ is met.

The strength of the algorithm is given by the usage of the weights; indeed, they have to modify the cost function in a way that the minimization is driven to the solution by those measurements that are considered more reliable (important). Therefore, it is understood that the weights needs to indicate the confidence of the measured distances.

I.4 Distance Contraction

Due to multipath and NLOS propagation, the error in distance estimation has a positive bias and range estimates are in general greater than the true ranges. Based on the fact that the range error is always positive, the Distance Contraction algorithm aims to correct the distance measurements by subtracting a certain value. Then the solution is computed with an optimization method using the contracted distances instead of the measured ones.

The implemented algorithm has 3 major steps:

1) The measured distances $\{\delta_i\}$ from the target to the anchor i are available. First the existence of a feasibility region, defined as the area formed by the intersection of the circles with centre at the anchors and radio equal to the estimated distance, is checked.

$$I = \{\mathbf{x} \mid d_i \leq \delta_i \forall i\} \tag{I.15}$$

where d_i is the distance from the point $\mathbf{x}$ to the anchor i. If the feasibility region does not exist, distance contraction cannot be applied, and the optimization algorithm is executed using the measured distances.

2) An initial point $\mathbf{x}_0$ in the feasibility region is computed using the following expression.

$$\mathbf{x}_0 = \arg\min_{\mathbf{x}\in R^n} \sum_{i=1}^{N_A} \max\left(0, d_i - \delta_i\right)^2 \tag{I.16}$$

where N_A is the number of anchors used to compute the position.

Then the contracted distances $\bar{d}_i$ are computed as the shortest distance from each anchor to the feasibility region. With this purpose, the point of tangency $\bar{x}_i$ between the feasibility region and a circle with centre at the anchor i and radius $\bar{d}_i$, which is the distance from the anchor to $\bar{x}_i$, is computed for every anchor i.

$$\bar{\mathbf{x}}_i = \arg\max_{\mathbf{x}\in I} (\delta_i - d_i)^2 \tag{I.17}$$

Figure I.2 shows graphically an example of the distance contraction algorithm, where the feasibility region is marked with a black line.

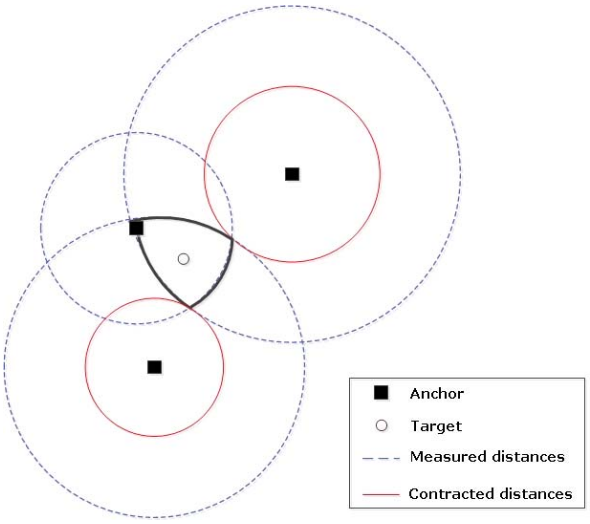

Figure I.2. Example of the distance contraction algorithm

3) Finally an optimization algorithm is run using this contracted distances $\bar{d}_i$ instead of the measurements δ_i. As the contracted distances are used, the LS-objective function is

generally convex, and any optimization method (i.e. global distance continuation, steepest descent) can be used to find the global minimum, thus reducing complexity.

I.5 Extended Kalman Filter

The Kalman Filter is a well-understood Bayesian technique known for its low-complexity, performance and stability as a tracking algorithm. The Kalman filter addresses the general problem of trying to estimate the state $\mathbf{x} \in R_n$ of a discrete-time controlled process that is governed by a linear stochastic difference equation. When the difference equation is not linear, the Extended Kalman Filter (EKF) linearizes about the current mean and covariance. The Kalman-based tracking algorithm has two major stages, namely, the update and the correction stages, which are iterated *k* times for every observation occurring at a given time *t*.

Let us assume that our process has a state vector **x** and is governed by the non-linear stochastic difference equation:

$$\mathbf{x}_t = f(\mathbf{x}_{t-1}, \mathbf{u}_{t-1}, \mathbf{a}_{t-1}) \tag{I.18}$$

with a measurement $\mathbf{z} \in R_m$ that is

$$\mathbf{z}_t = h(\mathbf{x}_t, \mathbf{e}_t) \tag{I.19}$$

where the random variables $\mathbf{a}_t$ and $\mathbf{e}_t$ represent the process and measurement noise respectively. They are assumed to be independent, white, and with normal probability distributions $p(\mathbf{a}) \in N(0,\mathbf{Q})$ and $p(\mathbf{e}) \in N(0,\mathbf{R})$. The process noise covariance **Q** and measurement noise covariance **R** matrixes might change with each time step or measurement. The non-linear function *f* in the difference equation (I.18) relates the state at the previous time step *t-1* to the state at the current time step *t*. It includes as parameters any driving function $\mathbf{u}_{t-1}$ and the zero-mean process noise $\mathbf{a}_t$. The non-linear function *h* in the measurement equation (I.19) relates the state $\mathbf{x}_t$ to the measurement $\mathbf{z}_t$ and includes as parameter the measurement noise $\mathbf{e}_t$.

In practice of course one does not know the individual values of the noise $\mathbf{a_t}$ and $\mathbf{n}_t$ at each time step. However, one can approximate the state and measurement vector without them as

$$\tilde{\mathbf{x}}_t = f(\hat{\mathbf{x}}_{t-1}, u_{t-1}, 0) \tag{I.20}$$

$$\tilde{\mathbf{z}}_t = h(\tilde{\mathbf{x}}_t, 0) \tag{I.21}$$

where $\hat{\mathbf{x}}_t$ is some a posteriori estimate of the state (from a previous time step *t*) and $\tilde{\mathbf{x}}_t$ and $\tilde{\mathbf{z}}_t$ are the approximate state and measurement vectors.

To estimate a process with non-linear difference and measurement relationships, we begin by writing new governing equations that linearize an estimate about (I.20) and (I.21),

$$\mathbf{x}_t \approx \tilde{\mathbf{x}}_t + \mathbf{F}(\mathbf{x}_{t-1} - \hat{\mathbf{x}}_{t-1}) + \mathbf{A}\mathbf{a}_{t-1} \tag{I.22}$$

$$\mathbf{z}_t \approx \tilde{\mathbf{z}}_t + \mathbf{H}(\mathbf{x}_t - \tilde{\mathbf{x}}_t) + \mathbf{E}\mathbf{e}_t \tag{I.23}$$

where

- $\mathbf{x}_t$ and $\mathbf{z}_t$ are the actual state and measurement vectors,
- $\tilde{\mathbf{x}}_t$ and $\tilde{\mathbf{z}}_t$ are the approximate state and measurement vectors from (I.20) and (I.21),
- $\hat{\mathbf{x}}_t$ is an a posteriori estimate of the state at time step *t*,
- the random variables $\mathbf{a}_t$ and $\mathbf{e}_t$ represent the process and measurement noise
- **F** is the Jacobian matrix of partial derivatives of *f* with respect to **x**, that is

$$\mathbf{F}_{[i,j]} = \frac{\partial f_{[i]}}{\partial \mathbf{x}_{[j]}}(\hat{\mathbf{x}}_{t-1}, \mathbf{u}_{t-1}, 0) \tag{I.24}$$

- **A** is the Jacobian matrix of partial derivatives of *f* with respect to **a**,

$$\mathbf{A}_{[i,j]} = \frac{\partial f_{[i]}}{\partial \mathbf{a}_{[j]}}(\hat{\mathbf{x}}_{t-1}, \mathbf{u}_{t-1}, 0) \tag{I.25}$$

- **H** is the Jacobian matrix of partial derivatives of *h* with respect to **x**,

$$\mathbf{H}_{[i,j]} = \frac{\partial h_{[i]}}{\partial \mathbf{x}_{[j]}}(\tilde{\mathbf{x}}_t, 0) \tag{I.26}$$

- **E** is the Jacobian matrix of partial derivatives of *h* with respect to **e**,

$$\mathbf{E}_{[i,j]} = \frac{\partial h_{[i]}}{\partial \mathbf{e}_{[j]}}(\tilde{\mathbf{x}}_t, 0) \tag{I.27}$$

Note that for simplicity in the notation we do not use the time step subscript t with the Jacobians **F**, **A**, **H** and **E**, even though they are in fact different at each time step.

Now we define a new notation for the prediction error, and the measurement residual,

$$\tilde{\boldsymbol{\varepsilon}}_{\mathbf{x}_t} \equiv \mathbf{x}_t - \tilde{\mathbf{x}}_t \tag{I.28}$$

$$\tilde{\boldsymbol{\varepsilon}}_{\mathbf{z}_t} \equiv \mathbf{z}_t - \tilde{\mathbf{z}}_t \tag{I.29}$$

Remember that in practice one does not have access to $\mathbf{x}_t$ in (I.28), it is the actual state vector one is trying to estimate. On the other hand, one does have access to $\mathbf{z}_t$ in (I.29), it is the actual measurement that one is using to estimate $\mathbf{x}_t$. Using (I.28) and (I.29) we can write governing equations for an error process as

$$\tilde{\boldsymbol{\varepsilon}}_{\mathbf{x}_t} \approx \mathbf{F}(\mathbf{x}_{t-1} - \hat{\mathbf{x}}_{t-1}) + \boldsymbol{\alpha}_t \tag{I.30}$$

$$\tilde{\boldsymbol{\varepsilon}}_{\mathbf{z}_t} \approx \mathbf{H}\tilde{\boldsymbol{\varepsilon}}_{\mathbf{x}_t} + \boldsymbol{\eta}_t \tag{I.31}$$

where α_t and η_t represent new independent random variables having zero mean and covariance matrices $\mathbf{AQA}^{\mathrm{T}}$ and $\mathbf{ERE}^{\mathrm{T}}$ respectively. The actual measurement residual $\tilde{\boldsymbol{\varepsilon}}_{\mathbf{z}_t}$ in (I.29) can be used in a second (hypothetical) Kalman filter to estimate the prediction error $\tilde{\boldsymbol{\varepsilon}}_{\mathbf{x}_t}$ given by (I.30). This estimate $\hat{\boldsymbol{\varepsilon}}_{\mathbf{x}_t}$ could then be used along with (I.28) to obtain the a posteriori state estimates for the original non-linear process as

$$\hat{\mathbf{x}}_t = \tilde{\mathbf{x}}_t + \hat{\boldsymbol{\varepsilon}}_t \tag{I.32}$$

Given these approximations and letting the predicted value of $\hat{\boldsymbol{\varepsilon}}_t$ be zero, the Kalman filter equation used to estimate $\hat{\boldsymbol{\varepsilon}}_t$ is

$$\hat{\boldsymbol{\varepsilon}}_t = \mathbf{K}_t\tilde{\boldsymbol{\varepsilon}}_{\mathbf{z}_t} \tag{I.33}$$

By substituting (I.33) back into (I.32) and making use of (I.29) we see that we do not actually need the second (hypothetical) Kalman filter:

$$\hat{\mathbf{x}}_t = \tilde{\mathbf{x}}_t + \mathbf{K}_t\tilde{\boldsymbol{\varepsilon}}_{\mathbf{z}_t} = \tilde{\mathbf{x}}_t + \mathbf{K}_t(\mathbf{z}_t - \tilde{\mathbf{z}}_t) \tag{I.34}$$

Equation (I.34) can now be used for the measurement update in the extended Kalman filter, with $\tilde{\mathbf{x}}_t$ and $\tilde{\mathbf{z}}_t$ coming from (I.20) and (I.21), and the Kalman gain $\mathbf{K}_t$ chosen to be the

gain that minimizes the a posteriori error covariance. The complete set of EKF equations is shown below.

- EKF time update equations:

$$\hat{\mathbf{x}}_t^- = f(\hat{\mathbf{x}}_{t-1}, \mathbf{u}_{t-1}, 0) \tag{I.35}$$

$$\mathbf{P}_t^- = \mathbf{F}_t \mathbf{P}_{t-1} \mathbf{F}_t^T + \mathbf{A}_t \mathbf{Q}_{t-1} \mathbf{A}_t^T \tag{I.36}$$

- EKF measurement update equations:

$$\mathbf{K}_t = \mathbf{P}_t^- \mathbf{H}_t^T (\mathbf{H}_t \mathbf{P}_t^- \mathbf{H}_t^T + \mathbf{E}_t \mathbf{R}_t \mathbf{E}_t^T)^{-1} \tag{I.37}$$

$$\hat{\mathbf{x}}_t = \hat{\mathbf{x}}_t^- + \mathbf{K}_t (\mathbf{z}_t - h(\hat{\mathbf{x}}_t^-, 0)) \tag{I.38}$$

$$\mathbf{P}_t = (\mathbf{I} - \mathbf{K}_t \mathbf{H}_t) \mathbf{P}_t^- \tag{I.39}$$

$\hat{\mathbf{x}}_t^-$ and $\mathbf{P}_t^-$ are a priori estimations and $\mathbf{P}_t$ is the estimation error covariance matrix:

$$\boldsymbol{\varepsilon}_t^- \equiv \mathbf{x}_t - \hat{\mathbf{x}}_t^- \tag{I.40}$$

$$\boldsymbol{\varepsilon}_t \equiv \mathbf{x}_t - \hat{\mathbf{x}}_t \tag{I.41}$$

$$\mathbf{P}_t^- = E[\boldsymbol{\varepsilon}_t^- \boldsymbol{\varepsilon}_t^{-T}] \tag{I.42}$$

$$\mathbf{P}_t = E[\boldsymbol{\varepsilon}_t \boldsymbol{\varepsilon}_t^T] \tag{I.43}$$

The time update equations project the state and covariance estimates from the previous time step *t-1* to the current time step *t*. The measurement update equations correct the state and covariance estimates with the measurement $\mathbf{z}_t$.

Focusing on the specific implementation of the EKF for our tracking application, we have defined the state vector $\mathbf{x}$ to contain target's position $\mathbf{p}_t$ and speed $\mathbf{v}_t$ as variables of our process. The measure vector $\mathbf{z}$ is defined containing the n process observations, namely the estimated distances between the target and the anchors, where n is the number of anchors used for location. The functions that describe the evolution of the state vector through time and the relation between the state vector and the measure vector are:

$$\begin{pmatrix} \tilde{\mathbf{p}}_t \\ \tilde{\mathbf{v}}_t \end{pmatrix} = \begin{pmatrix} \mathbf{I} & T_s \cdot \mathbf{I} \\ 0 & \mathbf{I} \end{pmatrix} \begin{pmatrix} \hat{\mathbf{p}}_{t-1} \\ \hat{\mathbf{v}}_{t-1} \end{pmatrix} + \begin{pmatrix} T_s^2 / 2 \cdot \mathbf{I} \\ T_s \cdot \mathbf{I} \end{pmatrix} \mathbf{a}_t \tag{I.44}$$

$$\tilde{\mathbf{z}}_t(i) = \mid \mathbf{p}_i - \tilde{\mathbf{p}}_t \mid + \mathbf{e}_t \tag{I.45}$$

Then, the different covariance and Jacobian (partial derivatives) matrixes were built. The covariance matrixes **Q** and **R** are defined by different parameters, namely the variance of process noise (acceleration) σ_a^2 and the variance of measurement noise (ranging error) σ_e^2.

I.6 Particle Filter

Particle filters are recursive implementations of Monte Carlo based statistical signal processing and are used to estimate recursive Bayesian models. The advantage of the particle filters over other parametric solutions such as the Kalman filter is that it allows using non-Gaussian noise and non-linear models, although their computational complexity is higher, so these solutions are only suitable in applications where computational power is rather cheap and the sampling rate slow.

The particle filter is based on a high number of samples of the state vector or particles, which are weighted according to their importance (likelihood) in order to provide an estimation of the state vector. On each step, the particles are moved according to the dynamic model and the weights are updated according to the likelihood of the observations (estimated distances) using the measurement error model.

Central for all navigation and tracking applications is the motion model to which various kind of model based filters can be applied. Models that are linear in the state dynamics and nonlinear in the measurements are considered:

$$\mathbf{x}_{t+1} = \mathbf{B}_x \mathbf{x}_t + \mathbf{B}_u \mathbf{u}_t + \mathbf{B}_a \mathbf{a}_t \tag{I.46}$$

$$\mathbf{z}_t = h(\mathbf{x}_t) + \mathbf{e}_t \tag{I.47}$$

where

- $\mathbf{x}_t$ is the state vector
- $\mathbf{u}_t$ are the measured inputs
- $\mathbf{a}_t$ are the unmeasured forces or faults
- $\mathbf{z}_t$ are the measurements

- $\mathbf{e}_t$ are the measurement errors

We assume independent distributions for $\boldsymbol{a}_t$, $\boldsymbol{e}_t$ and $\boldsymbol{x}_0$ with known probability densities $p_{\mathbf{a}_t}$, $p_{\mathbf{e}_t}$ and $p_{\mathbf{x}_0}$ respectively, not necessarily Gaussian.

A numerical approximation to the optimal Bayesian filter for the generic state model is given in the following algorithm.

1) Initialization

Generate $x_0^i \in p_{\mathbf{x}_0}$, i = 1,..., N. Each sample of the state vector is referred to as a particle.

2) Measurement update

Update the weights by the likelihood $w_t^i = w_{t-1}^i p(\mathbf{z}_t \mid \mathbf{x}_t^i)$, i = 1,..., N where $\mathbf{y}_t$ is the observation available at time t. The probability $p(\mathbf{z}_t \mid \mathbf{x}_t^i)$ is equivalent to the probability $p_e(\mathbf{z}_t - h(\mathbf{x}_t^i))$ according to the distribution of the measurement error e.

Weights are normalized to:

$$w_t^i = w_t^i / \sum_i w_t^i \tag{I.48}$$

Then the estimated position can be approximated:

$$\hat{\mathbf{x}}_t \approx \sum_{i=1}^{N} w_t^i \mathbf{x}_t^i \tag{I.49}$$

3) Resampling

Take N samples with replacement from the set $\left\{\mathbf{x}_t^i\right\}_{i=1}^N$, where the probability to take sample i is w_t^i. Let $w_t^i = 1/N$. This step is also called sampling importance resampling. Resampling is only done when the effective number of samples is less than a threshold

$$N_{eff} = \frac{1}{\sum_i (w_t^i)^2} < N_{th} \tag{I.50}$$

Here $1 \le N_{eff} \le N$, where the upper bound is attained when all particles have the same weight, and the lower bound when all probability mass is at one particle. The threshold can be chosen as $N_{th} = 2N/3$. The key point with resampling is to prevent high concentration of probability mass at a few particles.

4) Prediction

Simulate $\mathbf{x}_{t+1}^{i} = \mathbf{B}_x \mathbf{x}_t^{i} + \mathbf{B}_u \mathbf{u}_t + \mathbf{B}_a \mathbf{a}_t^{i}$, $i = 1,..., N$.

5) Let $t = t+1$ and iterate to item 2).

Focusing on the specific implementation of the particle filter for our tracking application, we have defined the state vector $\mathbf{x}$ to contain target's position $\mathbf{p}_t$ and speed $\mathbf{v}_t$ as variables of our process that are subject to an unknown acceleration. The motion model can be expressed as:

$$\begin{pmatrix} \mathbf{p}_{t+1} \\ \mathbf{v}_{t+1} \end{pmatrix} = \begin{pmatrix} \mathbf{I} & T_s \cdot \mathbf{I} \\ 0 & \mathbf{I} \end{pmatrix} \begin{pmatrix} \mathbf{p}_t \\ \mathbf{v}_t \end{pmatrix} + \begin{pmatrix} T_s^2 / 2 \cdot \mathbf{I} \\ T_s \cdot \mathbf{I} \end{pmatrix} \mathbf{a}_t \tag{I.51}$$

According to the model the following relations are obtained:

$$\mathbf{p}_t = \mathbf{p}_{t-1} + \mathbf{v}_{t-1} T_s + \mathbf{a}_{t-1} T_s^2 / 2 \tag{I.52}$$

$$\mathbf{v}_t = \mathbf{v}_{t-1} + \mathbf{a}_{t-1} T_s \tag{I.53}$$

Acceleration is modeled as a random variable with normal distribution, zero-mean and variance σ_a^2.

The observations are distance measurements of the target's position relative to anchors of known positions $\mathbf{p}_i$, $i=1,...,M$ where M is the number of anchors used for location, which yield M measurement equations with:

$$h_i(\mathbf{p}_t) = \| \mathbf{p}_i - \mathbf{p}_t \| \tag{I.54}$$

The measurement error distribution is not necessarily considered Gaussian. Instead, three different measurement error models have been defined:

- Simple Gaussian error model
- Two components error model: defined as a weighted sum of two Gaussian components for the different channel configurations (LOS/NLOS). The weights of each component are also Gaussian-like functions as it was defined in the ranging model.
- Three components error model: defined as a weighted sum of three Gaussian components for the different channel configurations (LOS/NLOS/NLOS2). The

weights of each component are also Gaussian-like functions as it was defined in the ranging model.

Consequently the filter is defined by different parameters, namely the variance of initial position, the variance of initial speed, the variance of process noise (acceleration) and the parameters of the measurement error model (mean and variance of the weights and mean and variance of each Gaussian component).

References

[3GPP, 2008] 3GPP "Location Services (LCS); Service description; Stage 1", *TS 22.071*, Release 8, 2008

[Alcatel, 2006] Alcatel, "Comparison of efficiency of DL Interference Coordination schemes and view on measurements on intra-frequency neighbour cells", *3GPP TSG RAN WG1 #46 Meeting*, R1-062365, 2006.

[Al-Jazzar, 2002] S. Al-Jazzar, J. J. Caffery, H.-R. You, "A scattering model based approach to NLOS mitigation in TOA location systems", in *Proceedings of 55th IEEE Vehicular Technology Conference (VTC Spring 2002)*, pp. 861-865, Birmingham (AL, USA), 2002.

[Bahl, 2000] P. Bahl, V. Padmanabhan, "RADAR: An In-Building RF-based User Location and Tracking System", in *Proceedings of 19th Annual Joint conference of the IEEE Computer and Communications Societies (INFOCOM 2000)*, pp. 775-784, Tel-Aviv (Israel), 2000.

[Bai, 2006] F. Bai, A. Helmy, "A Survey of Mobility Modeling and Analysis in Wireless Adhoc Networks", Book Chapter in *Wireless Ad Hoc and Sensor Networks*, Springer, 2006

[Bellorado, 2003] J. Bellorado, S. S. Ghassemzadeh, L. J. Greenstein, T. Sveinsson, V. Tarokh, "Coexistence of ultra-wideband systems with IEEE 802.11a wireless LANs", in *Proceedings of IEEE Global Telecommunications Conference 2003 (GLOBECOM'03)*, vol. 1, pp. 410-414, San Francisco (CA, USA), 2003.

[Beveridge, 1970] G. Beveridge, R. Schechter. *Optimization: Theory and Practice*. McGraw-Hill, New-York, 1970.

[Brunato, 2005] M. Brunato, R. Battiti, "Statistical learning theory for location fingerprinting in wireless LANs", *Computer Networks*, vol. 47, no. 6, pp. 825-845, 2005.

[Bucaille, 2007] I. Bucaille, A. Tonnerre, L. Ouvry, B. Denis, "MAC Layer Design for UWB Low Data Rate Systems: PULSERS proposal", in *Proceedings of 4th IEEE Workshop on Positioning, Navigation and Communication (WPNC)*, Hannover (Germany), pp. 277-283, 2007.

[Caffery, 1998] J. Caffery, G. L. Stuber, “Subscriber location in CDMA cellular networks”, *IEEE Transactions on Vehicular Technology*, vol. 47, no. 2, pp. 406-416, 1998.

[Caffery, 2000] J. Caffery, “A new approach to the geometry of TOA location”, in *Proceedings of 52nd IEEE Vehicular Technology Conference (VTC 2000-Fall)*, vol. 4, pp. 1943-1949, Boston (MA, USA), 2000.

[Cano, 2010] E. Cano, A. Rabbachin, D. Fuehrer, J. Fortuny, "On the Evaluation of MB-OFDM UWB Interference Effects on a WiMAX Receiver", *EURASIP Journal on Wireless Communications and Networking*, vol. 2010, 2010

[Cassioli, 2005] D. Cassioli, S. Persia, V. Bernasconi, A. Valent, “Measurements of the performance degradation of UMTS receivers due to UWB emissions”, *IEEE Communications Letters*, vol. 9, pp. 441-443, 2005.

[Chen, 2009] C. S. Chen, S. L. Su, Y. F. Huang, "Hybrid TOA/AOA Geometrical Positioning Schemes for Mobile Location", *IEICE Transactions on Communications*, vol. E92-B, no. 2, pp.396-402, 2009.

[Cheung, 2004] K. W. Cheung, H. C. So, W. K. Ma, Y. T. Chan, “Least squares algorithms for time-of-arrival-based mobile location”, *IEEE Transactions on Signal Processing*, vol. 52, no. 4, pp. 1121-1130, 2004.

[Cheung, 2005] K. W. Cheung, H. C. So, “A multidimensional scaling framework for mobile location using time-of-arrival measurements,” *IEEE Transactions on Signal Processing*, vol. 53, no. 4, pp. 460-470, 2005.

[Chiani, 2009] M. Chiani, A. Giorgetti, “Coexistence between UWB and narrowband wireless communication systems”, *Proceedings IEEE, special issue on Ultra-Wide Bandwidth*, vol. 97, no. 2, pp. 231-254, 2009.

[Chiu, 2000] M. H. Chiu, M. A. Bassiouni, "Predictive Schemes for Handover Prioritization in Cellular Networks Based on Mobile Positioning", *IEEE Journal on Selected Areas in Communications*, vol. 18, no. 3, pp. 510-522, 2000.

[Chu, 2005] Y. Chu, A Ganz, “A UWB-based 3D Location System for Indoor Environments”, *in Proceedings of 2nd International Conference on Broadband Networks (BroadNets 2005)*, pp. 1147, Boston (MA, USA), 2005.

[Cong, 2005] L. Cong, W. Zhuang, “Nonline-of-sight error mitigation in mobile location”, *IEEE Transactions on Wireless Communications*, vol. 4, no. 2, pp. 560-573, 2005.

[Dardari, 2009] D. Dardari, A. Conti, U. J. Ferner, A. Giorgetti, M. Z. Win, "Ranging with ultrawide bandwidth signals in multipath environments," *Proceedings IEEE, special issue on Ultra-Wide Bandwidth (UWB) Technology & Emerging Applications*, vol. 97, no. 2, pp. 404-426, 2009.

[Dashti, 2008] M. Dashti, M. Ghoraishi, K. Haneda, J. Takada, K. Takizawa, "Analysis of Ranging Accuracy for UWB Localization", *IEICE Technical Report*, vol. 107, no. 543, AP2007-174, pp. 7-12, 2008.

[Daum, 2005] F. Daum, ‘’Nonlinear filters: beyond the Kalman filter’’, *IEEE Aerospace and Electronic Systems Magazine*, vol. 20, no. 8, pp. 57-69, 2005.

[de Leeuw, 2009] J. de Leeuw, P. Mair, “Multidimensional scaling using majorization: SMACOF in R”, *Journal of Statistical Software*, vol. 31, no.3, pp. 1-30, 2009.

[Denis, 2004] B. Denis, N. Daniele, “NLOS Ranging Error Mitigation in a Distributed Positioning Algorithm for Indoor UWB Ad Hoc Networks”, in *Proceedings of 2004 International Workshop on Wireless Ad-Hoc Networks (IWWAN’04)*, pp. 356-360, Oulu (Finland), 2004.

[Destino, 2006] G. Destino, G.T.F. de Abreu, “Localization from imperfect and incomplete ranging”, in *Proceedings of 17th IEEE International Symposium on Personal, Indoor and Mobile Radio Communications (PIMRC’06)*, pp. 1-5, 2006.

[Destino, 2009] G. Destino, G. Abreu “Weighting strategy for network localization under scarce ranging information”, *IEEE Transactions on Wireless Communications*, vol. 8, no. 7, pp. 3668-3678, 2009.

[Destino, 2010] G. Destino, G. Abreu, “Improving Source Localization in NLOS Conditions via Ranging Contraction”, in *Proceedings of 7th Workshop on Positioning, Navigation and Communication (WPNC’10)*, pp. 56-61, Dresden (Germany), 2010.

[Du, 2003] L. Du, J. Bigham, L. Cuthbert, “Towards intelligent geographic load balancing for mobile cellular networks”, *IEEE Transactions on Systems, Man and Cybernetics*, Part C, vol. 33, no. 4, pp. 480-491, 2003.

[ECC, 2005a] Electronic Communications Committee (ECC), “ECC Report 64 on The Protection Requirements Of Radiocommunication Systems Below 10.6 GHz From Generic UWB Applications”, 2005.

[ECC, 2005b] Measurement ad hoc group chairman, “Summary Report: UWB – Mobile services measurements”, *ECC TG3 10th Meeting Contribution*, 2005

[ECC, 2006a] Electronic Communications Committee (ECC), "ECC decision of 24 March 2006 on the harmonised conditions for devices using Ultra-Wideband (UWB) technology in bands below 10.6 GHz", *ECC/DEC/(06)04*, 2006.

[ECC, 2006b] Electronic Communications Committee (ECC), "ECC Decision of 1 December 2006 on the harmonised conditions for devices using Ultra-Wideband (UWB) technology with Low Duty Cycle (LDC) in the frequency band 3.4-4.8 GHz", *ECC/DEC/(06)12*, 2006.

[ECC, 2006c] Electronic Communications Committee (ECC), "ECC Report 94 on Technical Requirements for UWB LDC Devices to ensure the protection of FWA systems", 2006.

[ECC, 2007] Electronic Communications Committee (ECC), "ECC decision of 24 March 2006 amended 6 July 2007 at Constanta on the harmonised conditions for devices using Ultra-Wideband (UWB) technology in bands below 10.6 GHz", *amended ECC/DEC/(06)04*, 2007.

[ECC, 2008a] Electronic Communications Committee (ECC), "ECC Decision of 1 December 2006 amended 31 October 2008 on supplementary regulatory provisions to Decision ECC/DEC/(06)04 for UWB devices using mitigation techniques", *amended ECC/DEC/(06)12*, 2008.

[ECC, 2008b] Electronic Communications Committee (ECC), "ECC Report 120 on Technical requirements for UWB DAA (Detect And Avoid) devices to ensure the protection of Radiolocation in the bands 3.1 - 3.4 GHz and 8.5 - 9 GHz and BWA terminals in the band 3.4 - 4.2 GHz", 2008.

[ECMA, 2005] ECMA International, "High Rate Ultra Wideband PHY and MAC standard", *Standard ECMA-368*, 2005.

[Facchini, 2009] F. Facchini, R. Giuliano, F. Mazzenga, "Ultra-wideband detect and avoid procedure for WiMAX victims", *IET Communications*, vol. 3, no. 2, pp. 268-278, 2009.

[Fang, 2008] S.-H. Fang, T.-N. Lin, "Indoor location system based on discriminant-adaptive neural network in IEEE 802.11 environments", *IEEE Transactions on Neural Networks*, vol. 19, no. 11, pp. 1973-1978, 2008.

[FCC, 2002] Federal Communications Commission (FCC), "Revision of Part 15 of the Commission's Rules Regarding Ultra-Wideband Transmission Systems", First Report and Order, ET Docket 98-153, FCC 02-48, 2002.

[Fletcher, 1963] R. Fletcher, M.J.D. Powell, "A rapidly convergent descent method for minimization", *The Computer Journal*, vol. 6, no. 2, pp. 163-168, 1963.

[Fletcher, 1987] R. Fletcher. *Practical Methods of Optimization*. Wiley, Chichester, 1987.

[Fox, 2003] D. Fox, J. Hightower, L. Liao, D. Schulz, G. Borriello, "Bayesian filtering for location estimation", *Pervasive computing*, vol. 2, no. 3, pp. 24-33, 2003.

[Foy, 1976] W.H. Foy, "Position-location solutions by Taylor-series estimation", *IEEE Transactions on Aerospace and Electronic Systems*, vol. AES-12, no. 2, pp. 187-194, 1976.

[French, 1989] R. French, "Map matching origins, approaches and applications", in *Proceedings of 2nd International Symposium on Land Vehicle Navigation*, Munster (Germany), 1989.

[Gezici, 2005] S. Gezici, Z. Sahinoğlu, A.F. Molisch, H. Kobayashi, H. V. Poor, "A two-step Time of Arrival estimation algorithm for impulse radio Ultra WideBand systems", in *Proceedings of 13th European Signal Processing Conference (EUSIPCO'05)*, pp. 4-8, Antalya (Turkey), 2005.

[Gezici, 2005b] S. Gezici, Z. Tian, G. B. Giannakis, H. Kobayashi, A.F. Molisch, H. V. Poor, Z. Sahinoğlu, "Localization via Ultra-Wideband Radios. A look at positioning aspects of future sensor networks", *IEEE Signal Processing Magazine*, vol. 22, no. 4, pp. 70-84, 2005.

[Giancola, 2005] G. Giancola, L. Blazevic, I. Bucaille, L. De Nardis, M.-G. Di Benedetto, Y. Durand, G. Froc, B.M. Cuezva, J. Pierrot, P. Pirinen, N. Rinaldi, "UWB MAC and Network Solutions for Low Data Rate with Location and Tracking Applications", in *Proceedings of 2005 IEEE International Conference on UWB (ICUWB 2005)*, pp.758-763, Zurich (Switzerland), 2005.

[Giuliano, 2005] R. Giuliano, F. Mazzenga, "On the Coexistence of Power-Controlled Ultrawide-Band Systems with UMTS, GPS, DCS1800, and Fixed Wireless Systems", *IEEE Transactions on Vehicular Technologies*, vol.54, no.1, pp.62-81, 2005.

[Gu, 2009] Y. Gu, A. Lo, I. Niemegeers, "A survey of indoor positioning systems for wireless personal networks", *IEEE Communications Surveys and Tutorials*, vol. 11, no. 1, pp. 13-32, 2009.

[Gustafsson, 2002] F. Gustafsson, F. Gunnarsson, N. Bergman, U. Forssell, J. Jansson, R. Karlsson, P.-J. Nordlund, "Particle filters for positioning, navigation and tracking", *IEEE Transactions on Signal Processing*, vol. 50, no. 2, pp. 425-437, 2002.

[Güvenç, 2005a] I. Güvenç, Z. Sahinoglu, "Threshold-based TOA estimation for impulse radio UWB systems" in *Proceedings of 2005 IEEE International Conference on Ultra-Wideband (ICUWB 2005)*, pp. 420-425, Zurich (Switzerland), 2005.

[Güvenç, 2005b] I. Güvenç, Z. Sahinoğlu, "Multiscale energy products for TOA estimation in IR-UWB systems", in *Proceedings of IEEE Global Telecommunications Conference 2005 (GLOBECOM'05)*, St. Louis (MO, USA), 2005.

[Güvenç, 2005c] I. Güvenç, Z. Sahinoğlu, "Low complexity TOA estimation for Impulse Radio UWB systems", Mitsubishi Electric Research Labs, 2005.

[Güvenç, 2005d] I. Güvenç, Z. Sahinoglu, "Threshold selection for UWB TOA estimation based on kurtosis analysis", *IEEE Communications Letters*, vol. 9, pp. 1025-1027, 2005.

[Güvenç, 2006] I. Güvenç, Z. Sahinoğlu, P. Orlik, "TOA estimation for IR-UWB systems with different transceiver types", *IEEE Transactions on Microwave Theory and Techniques, Special Issue on UWB*, vol. 54, no. 4, pp. 1876-1886, 2006.

[Güvenç, 2008] I. Güvenç, C.-C. Chong, F. Watanabe, H. Inamura, "NLOS identification and weighted least-squares localization for UWB systems using multipath channel statistics". *EURASIP Journal on Advanced Signal Processing*, vol. 2008, 2008.

[Güvenç, 2009] I. Güvenç, Z. Sahinoglu, P. Orlik, H. Arslan, "Searchback Algorithms for TOA estimation in Non-Coherent Low-Rate IR-UWB Systems", *Wireless Personal Communications*, vol. 48 no. 4, pp. 585-603, 2009.

[Hämäläinen, 2002] M. Hämäläinen, V. Hovinen, R. Tesi, J. H. J. Iinatti, M. Latva-Aho, "On the UWB system coexistence with GSM900, UMTS/WCDMA, and GPS", *IEEE Journal on Selected Areas in Communications*, vol. 20, pp. 1712-1721, 2002.

[Hämäläinen, 2006] M. Hämäläinen, J. Iinatti, I. Oppermann, M. Latva-aho, J. Saloranta, A. Isola, "Co-existence measurements between UMTS and UWB systems", *IEE Proceedings Communications*, vol. 153, pp. 153-158, 2006.

[IEEE, 2006] IEEE 802.15 Working Group, "Part 15.4: Wireless Medium Access Control (MAC) and Physical Layer (PHY) Specifications for Low-Rate Wireless Personal Area Networks (LR-WPANs)", *IEEE Standard 802.15.4-2006*, 2006.

[IEEE, 2007] IEEE 802.15 Working Group, "Wireless Medium Access Control (MAC) and Physical Layer (PHY) Specifications for Low-Rate Wireless Personal Area Networks (WPANs): Alternate PHYs", *IEEE Standard 802.15.a4-2007*, 2007.

[Intel, 2005] Intel, “Technical feasibility of dynamic frequency selective (DFS) active interference mitigation techniques”, *ECC TG3 9th Meeting Contribution*, 2005.

[ITU-R, 2006] ITU-R Task Group 1/8, “Studies Related To The Impact Of Devices Using Ultra-Wideband Technology On Radiocommunication Services”, *Annex 5 to TG 1/8 Chairman’s Report DRAFT NEW REPORT ITU-R SM.[UWB.XYZ]*, 2006.

[Kaemarungsi, 2004] K. Kaemarungsi, P. Krishnamurthy, “Modeling of indoor positioning systems based on location fingerprinting”, in *Proceedings of 23rd Annual Joint Conference of the IEEE Computer and Communications Societies (INFOCOM 2004),* vol. 2, pp. 1012-1022, Hong Kong, 2004.

[Khider, 2009] M. Khider, S. Kaiser, P. Robertson, M. Angermann, “Maps And Floor Plans Enhanced 3D Movement Model For Pedestrian Navigation”, in *Proceeding of the ION GNSS 2009*, Savannah (GA, USA), 2009

[Khodjaev, 2009] J. Khodjaev, Y. Park, A. S. Malik, “Survey of NLOS identification and error mitigation problems in UWB-based positioning algorithms for dense environments”, *Annals of Telecommunications*, vol. 65, no. 5, pp. 301-311, 2009.

[Kong, 2009] Y. Kong, Y. Kwon, G. Park, "Robust localization over obstructed interferences for inbuilding wireless applications", *IEEE Transactions on Consumer Electronics*, vol.55, no.1, pp.105-111, 2009.

[Küpper, 2005] A. Küpper. *Location-based Services: Fundamentals and Operation*. John Wiley & Sons Ltd., 2005.

[Lee, 2002] J.-Y. Lee, R. A. Scholtz, "Ranging in a dense multipath environment using an UWB radio link", *IEEE Journal on Selected Areas in Communications*, vol. 20, pp. 1677-1683, 2002.

[Lei, 2007] H. Lei, X. Zhang, D. Yang, "A novel frequency reuse scheme for multi-cell OFDMA systems", in *Proceedings of 66th IEEE Vehicular Technology Conference (VTC-2007 Fall)*, pp. 347-351, Baltimore (MD, USA), 2007.

[Li, 2007] F. Li, S. Liu, Y.S. Kim, J.W. Chong, "ANC-Based TOA Estimation with Lower Sampling Rates for UWB Systems", in *Proceedings of International Conference on Communications, Circuits and Systems (ICCCAS)*, Fukuoka (Japan), 2007.

[Liu, 2007] H. Liu, H. Darabi, P. Banerjee, J. Liu, “Survey of wireless indoor positioning techniques and systems”, *IEEE Transactions on Systems, Man, and Cybernetics Part C*, vol. 37, no. 6, pp. 1067-1080, 2007.

[Liu, 2007b] L. Liu, J. Zhu, X. Tao, Y. Wang, P. Zhang, “A novel scheme for OFDMA based E-UTRA Uplink”, in *Proceedings of IEEE Wireless Communications and Networking Conference 2007 (WCNC 2007)*, pp. 1373-1377, Hong Kong, 2007.

[Lo, 2008] A. Lo, L. Xia, I. Niemegeers, T. Bauge, M. Russell, D. Harmer, “Europcom - An ultra-wideband (UWB)-based ad hoc network for emergency applications”, in *Proceedings of 67th IEEE Vehicular Technology Conference (VTC2008-Spring)*, pp. 6-10, Singapore, 2008.

[Lu, 2006] L.L. Lu, J.L.C. Wu, H.H. Liu, "Mobility-aided adaptive resource reservation schemes in wireless multimedia networks", *Computers and Electrical Engineering*, vol.32, no.1-3, pp.102-117, 2006.

[Macagnano, 2007] D. Macagnano, G. Destino, F. Esposito, G. T. F. de Abreu, “MAC Performances for Localization and Tracking in Wireless Sensor Networks”, in *Proceedings of 4th IEEE Workshop on Positioning, Navigation and Communication (WPNC’07)*, pp. 297-302, Hannover (Germany), 2007.

[Macagnano, 2008] D. Macagnano, G. Abreu, “Tracking Multiple Dynamic Targets in LOS-NLOS Condition with Multidimensional Scaling”, in *Proceedings of 5th IEEE Workshop on Positioning, Navigation and Communication (WPNC’08)*, pp. 251-257, Hannover (Germany), 2008.

[Mallat, 1992] A. Mallat, S. Zhong, “Characterization of signals from multiscale edges”, *IEEE Transactions on Pattern Analysis and Machine Intelligence*, vol. 14, no. 2, pp. 710-732, 1992.

[Mishra, 2007] S. M. Mishra, S. ten Brink, R. Mahadevappa, R. W.Brodersen “Detect and Avoid: An Ultra-Wideband/WiMax Coexistence Mechanism”, *IEEE Communications Magazine*, vol. 45, no.6, pp. 68-75, 2007.

[Molisch, 2004] A.F. Molisch, K. Balakrishnan, C.C. Chong, S. Emami, A. Fort, J. Kaderal, J. Kunisch, H. Schantz, U. Schuster, K. Siwiak, “IEEE 802.15.4a channel model – final report”, *IEEE 802.15 TG4a Technical Report*, 2004.

[Mollfulleda, 2005] A. Mollfulleda, M. Najar, P. Miskovsky, C. Ibars, J. Mateu, M. Navarro, “Ultra-wideband testbed for reduced data-rates and location”, in *Proceedings of 2005 IEEE International Conference on Ultra-Wideband (ICUWB 2005)*, pp. 769-774, Zurich (Switzerland), 2005.

[Morley, 1995] G. D. Morley, W. D. Grover, “Improved location estimation with pulse-ranging in presence of shadowing and multipath excess-delay effects”, *IET Electronics Letters*, vol. 31, no. 18, pp. 1609-1610, 1995.

[Nasri, 2007] A. Nasri, R. Schober, L. Lampe, “Analysis of Narrowband Communication System Impaired by MB-OFDM UWB Interference”, *IEEE Transactions on Wireless Communications*, vol. 6, no. 11, pp. 4090-4100, 2007.

[Navarro, 2006] M. Navarro, S. Prior, M. Najar, “Low Complexity frequency domain TOA Estimation for IR-UWB Communications”, in *Proceedings of 64th IEEE Vehicular Technology Conference (VTC-2006 Fall)*, pp. 1-5, Montreal (Canada), 2006.

[Nortel, 2006] Nortel, “Adaptive fractional frequency reuse”, *3GPP TSG RAN WG1#44bis Meeting*, R1-060905, 2006.

[OGC, 2005] Open Geospatial Consortium (OGC), “Open Location Services 1.1”, 2005.

[Pezzin, 2007] M. Pezzin, D. Lachartre, “A Fully Integrated LDR IR-UWB CMOS Transceiver Based on "1.5-bit" Direct Sampling”, in *Proceedings of 2007 IEEE International Conference on Ultra-Wideband (ICUWB 2007)*, pp. 642-647, Singapore, 2007

[Pezzin, 2009] M. Pezzin, I. Bucaille, T. Schulze, A.V. Pato, L. De Celis, "An open IR-UWB platform for LDR-LT applications prototyping", in *Proceedings of 6th IEEE Workshop on Positioning, Navigation and Communication (WPNC’09)*, pp.285-293, Hannover (Germany), 2009.

[Porcino, 2003] D. Porcino, W. Hirt, “Ultra-Wideband Radio Technology: Potential and Challenges Ahead”, *IEEE Communications Magazine*, vol.41, no.7, pp. 66-74, 2003.

[Priggouris, 2006] I. Priggouris, E. Zervas, S. Hadjiefthymiades, "Location Based Network Resource Management", Book Chapter in *Handbook of Research on Mobile Multimedia*, Idea Group Reference, 2006.

[Qi, 2004] Y. Qi. *Wireless geolocation in a non-line-of-sight environment*. Ph.D. Dissertation, Princeton University, 2004.

[Quijano, 2005] B. Quijano, A. Alvarez, M. Lobeira, J. L. García, “Compatibility Measurement Campaign between IR-UWB and UMTS”, in *Proceedings of 14th IST Mobile and Wireless Communications Summit*, Dresden (Germany), 2005.

[Rahim, 2009] I.Rahim, ”Design and Regulatory Issues for Collocated Transceivers", *Conformity Magazine*, 2009.

[Roos, 2002] T. Roos, P. Myllymaki, H. Tirri, P. Misikangas, J. Sievanen, "A probabilistic approach to WLAN user location estimation", *International Journal of Wireless Information Networks*, vol. 9, no. 3, pp. 155-164, 2002.

[Sadler, 1999] B.M. Sadler, A. Swami, "Analysis of multiscale products for step detection and estimation", *IEEE Transactions on Information Theory*, vol. 45, no. 3, pp. 1043-1051, 1999.

[Sahinoglu, 2008] Z. Sahinoglu, S. Gezici, I. Güvenç. *Ultra-wideband Positioning Systems*. Cambridge University Press, 2008.

[Sarfaraz, 2005] K. Sarfaraz, S.A. Ghorashi, M. Ghavami, A.H. Aghvami, "Performance of WiMax receiver in presence of DS-UWB systems", *IEEE Electronics Letters*, vol. 41, no. 25, pp. 423-427, 2005.

[Schau, 1987] H. C. Schau, A. Z. Robinson, "Passive source localization employing intersecting spherical surfaces from time-of-arrival differences", *IEEE Transactions on Acoustics, Speech and Signal Processing*, vol. ASSP-35, pp. 1223-1225, 1987.

[Schiller, 2004] J. Schiller, A. Voisard. *Location-Based Services*. Morgan Kaufmann, 2004.

[Schroeder, 2007] J. Schroeder, S. Galler, K. Kyamakya, K. Jobmann, "NLOS detection algorithms for ultra-wideband localization", in *Proceedings of 4th IEEE Workshop on Positioning, Navigation and Communication (WPNC'07)*, pp. 159-166, Hannover (Germany), 2007.

[Seco, 2009] F. Seco, A.R. Jimenez, C. Prieto, J. Roa, K. Koutsou, "A survey of mathematical methods for indoor localization", in *Proceedings of 6th IEEE International Symposium on Intelligent Signal Processing (WISP 2009)*, Budapest (Hungary), pp. 26-28, 2009.

[Shen, 2009] S. Shen, T. J. Hart, N. Ingelbrecht, A. Zimmermann, J. Ekholm, N. Jones, J. Edwards, A. Frank. *Dataquest Insight: The Top 10 Consumer Mobile Applications in 2012*. Gartner Inc., 2009

[Shen, 2010] G. Shen, R. Zetik, O. Hirsch, R. S. Thomä, "Range-Based Localization for UWB Sensor Networks in Realistic Environments", *EURASIP Journal on Wireless Communications and Networking*, vol. 2010, 2010.

[Shiode, 2004] N. Shiode, C. Li, M. Batty, P. Longley, D. Maguire, "The impact and penetration of Location Based Services", Book Chapter in *Telegeoinformatics: Location-based computing and services*, CRC Press, pp. 349-366, 2004

[Sibso, 1978] R. Sibso, “Studies in the robustness of multidimensional scaling: Procrustes statistics”, *Journal of Royal Statistical Society*, Series B, vol. 40, no.2, pp. 234-238, 1978.

[Smith, 1987] J. O. Smith, J. S. Abel, “Closed-form least-squares source location estimation from range-difference measurements”, *IEEE Transactions on Acoustics, Speech and Signal Processing*, vol. ASSP-35, pp. 1661-1669, 1987.

[Sodeyama, 2010] K. Sodeyama, K. Ishibashi, R. Kohno, "An Analysis of Interference Mitigation Capability of Low Duty-Cycle UWB Communications in the Presence of Wideband OFDM System", *Wireless Personal Communications*, vol. 54, no. 1, pp. 39-52, 2010.

[Soh, 2004] W.-S. Soh, H. S. Kim, “Dynamic Bandwidth Reservation in Cellular Networks using Road Topology based Mobility Predictions”, in *Proceedings of 23rd Annual Joint Conference of the IEEE Computer and Communications Societies (INFOCOM 2004)*, vol. 4, pp. 2766-2777, Hong Kong, 2004.

[Somayazulu, 2006] V. S. Somayazulu, J. R. Foerster, R. D. Roberts, “Detect and Avoid (DAA) Mechanisms for UWB Interference Mitigation”, in *Proceedings of* 2006 *IEEE International Conference on UWB (ICUWB 2006)*, Waltham (MA, USA), pp. 513-518, 2006.

[Steiniger, 2006] S. Steiniger, M. Neun, A. Edwardes. *Foundations of Location Based Services*. University of Zürich, 2006.

[Swami, 2001] A. Swami, B. Sadler, J. Turner, “On the coexistence of ultra-wideband and narrowband radio systems”, in *Proceedings of 2001 IEEE Military Communications Conference (MILCOM 2001)*, vol. 1, pp. 16-19, McLean (VA, USA), 2001.

[Teerapabkajorndet, 2001] W. Teerapabkajorndet, P. Krishnamurthy, “Comparison of Performance of Location-Aware and Traditional Handover-Decision Algorithms in CDPD Networks”, in *Proceedings of 54th IEEE Vehicular Technology Conference (VTC 2001-Fall)*, vol.1, pp. 212-216, Atlantic City (NJ, USA), 2001.

[Texas Instruments, 2005] Texas Instruments, “UWB Interference Detection Technology”, *ECC TG3 10th Meeting Contribution*, 2005.

[USB-IF, 2005] USB Implementers Forum, “Wireless Universal Serial Bus Specification, Revision 1.0”, 2005.

[Venkatesh, 2006] S. Venkatesh, R. M. Buehrer, “Multiple-access design for Ad Hoc UWB position-location networks”, in *Proceedings of IEEE Wireless Communications and*

Networking Conference 2006 (WCNC 2006), vol. 4, pp. 1866-1873, Las Vegas (NV, USA), 2006.

[Venkatesh, 2007] S. Venkatesh, R.M. Buehrer, "Non-line-of-sight identification in ultra-wideband systems based on received signal statistics", *IET Microwaves, Antennas & Propagation*, vol.1, no.6, pp.1120-1130, 2007

[Venkatraman, 2004] S. Venkatraman, J. Caffery, H. R. You, "A novel TOA location algorithm using LOS range estimation for NLOS environments", *IEEE Transactions on Vehicular Technology*, vol. 53, no. 5, pp. 1515-1524, 2004.

[Viruete, 2005] E. A. Viruete Navarro, J. Ruiz Mas, J. Fernández Navajas, C. Peña Alcega, ”Enhanced 3G-based m-health system", in *Proceedings of the International Conference on Computer as a Tool 2005 (EUROCON 2005)*, vol. 2, pp. 1332-1335, Belgrade (Serbia), 2005.

[Widyawan, 2008] Widyawan, M. Klepal, S. Beauregard, “A novel backtracking particle filter for pattern matching indoor localization”, in *Proceedings of ACM international workshop on Mobile entity localization and tracking in GPS-less environments 2008 (MELT '08)*, pp. 79-84, New York (USA), 2008.

[Win, 2002] M. Z. Win, R. A. Scholtz, "Characterization of ultra-wide bandwidth wireless indoor communications channel: A communication theoretic view", *IEEE Journal on Selected Areas in Communications*, vol. 20, pp. 1613-1627, 2002.

[Wisair, 2005] Wisair. *Detect and Avoid Technology for UWB Spectrum usage*. White paper, 2005.

[Wu, 2009] D. Wu, L. Bao, R. Li, "UWB-Based Localization in Wireless Sensor Networks", *International Journal of Communications, Network and System Sciences*, vol. 2, no. 5, pp. 407-421, 2009.

[Xiang, 2007] Y. Xiang, J. Luo, C. Hartmann, “Inter-cell Interference Mitigation through Flexible Resource Reuse in OFDMA based Communications Networks”, in *Proceedings of 13th European Wireless Conference (EW 2007)*, pp. 1-7, Paris (France), 2007.

[Xiaochen, 2008] C. Xiaochen, “UWB Regulatory Status in East Asia”, presentation at *WALTER UWB workshop,* European Commission Joint Research Centre*,* Ispra (Italy), 2008.

[Xu, 2002] Z. Xu, Z. Ye, S.V. Kirshnamurthy, S.K. Tripathi, M. Molle, “A new adaptive channel reservation scheme for handoff calls in wireless cellular networks”, *Lecture Notes on Computer Science*, vol. 2345, pp. 672-684, 2002.

[Xu, 2008] C. Xu, C. L. Law, "Delay-dependent threshold selection for UWB TOA estimation", *IEEE Communications Letters*, vol. 12, no. 5, pp. 380-382, 2008.

[Yang, 2004] L. Yang, G.B. Giannakis, "Timing Ultra-Wideband signals with dirty templates", *IEEE Transactions on Communications*, vol. 53, no. 11, pp. 1952-1963, 2004.

[Yang, 2004] L.Yang, G.B. Giannakis, "Ultra-Wideband communications, an idea whose time has come", *IEEE Signal Processing Magazine*, vol. 21, no. 6, pp. 26-54, 2004.

[Yim, 2008] J. Yim, "Introducing a decision tree-based indoor positioning technique", *Expert Systems with Applications*, vol. 34, no. 2, pp. 1296- 1302, 2008.

[Yu, 2006] K. Yu, J.P. Montillet, A. Rabbachin, P. Cheong, I. Oppermann, "UWB location and tracking for wireless embedded networks", *Signal Processing*, vol. 86, no. 9, Special Section: Signal Processing in UWB Communications, pp. 2153-2171, 2006

[Zimmerman, 2009] A. Zimmerman. *Consumer Location-Based Services, Subscribers and Revenue Forecast, 2007-2013*. Gartner Inc., 2009